AD NUMBER

AD450151

NEW LIMITATION CHANGE

TO

Approved for public release, distribution unlimited

FROM

Distribution authorized to U.S. Gov't. agencies and their contractors; Administrative/Operational Use; Mar 1964. Other requests shall be referred to U.S. Army Tank-Automotive Center, Warren, MI.

AUTHORITY

USATAC ltr, 16 Apr 1969

UNCLASSIFIED

AD **450151L**

DEFENSE DOCUMENTATION CENTER

FOR

SCIENTIFIC AND TECHNICAL INFORMATION

CAMERON STATION ALEXANDRIA, VIRGINIA

UNCLASSIFIED

AD 450151

1769

COMPONENTS R&D LABORATORIES

LAND LOCOMOTION LABORATORY

Report No. 8470

LL No. 97

Copy No. 389

PROBLEMS OF SOIL VEHICLE MECHANICS

by

Alan R. Reece

March 1964

20040108133

Project No: 5022.11.82200

Reviewed: ~~Ronald A. Liston~~
RONALD A. LISTON
Chief, Land Locomotion
Laboratory
Components R&D Laboratories

D/A Project: 1-D-0-21701-A-045

Approved: ~~John W. Wiss~~
JOHN W. WISS
Lt. Colonel, Ordnance Corps
Chief, Components R&D
Laboratories

U.S. ARMY TANK-AUTOMOTIVE CENTER

WARREN, MICHIGAN

DDC AVAILABILITY NOTICE

OBJECTIVE

Develop the theory of soil vehicle mechanics into a more accurate tool for the design and evaluation of cross country vehicles.

RESULTS

Several suggestions for improving the basic soil mechanics are made, including a new sinkage equation and a method for dealing with slip sinkage.

CONCLUSIONS

Soil vehicle mechanics theory must be based on the static equilibrium theory for incompressible soils that is used in foundation engineering.

ADMINISTRATIVE INFORMATION

This project was supervised and conducted by the Land Locomotion Laboratory of ATAC under D/A Project No. 1-D-0-21701-A-045.

ACKNOWLEDGEMENT

TABLE OF CONTENTS

ABSTRACT

A proposal is made that the Land Locomotion Laboratory approach to soil vehicle mechanics be modified so that all the curve-fitting equations used are based on theoretical analyses approximately valid for incompressible rigid soils. The equations would have to be chosen to include the effect of compressibility also, and they would therefore be partially empirical but each would have a definite theoretical basis.

This concept has been applied to several outstanding problems and leads to new solutions. The importance of curve-fitting procedures is emphasized and a new non-statistical method proposed. It is shown that the current pressure sinkage equation $p = kz^n$ should be replaced by one of the form $p = f(\frac{z}{b})$ and this is justified experimentally. It is concluded that the results from circular plates cannot in general be applied to vehicles, long rectangular plates being necessary.

Considerations of plastic equilibrium lead to a new equation for the traction from the sides of a grousered track. A detailed analysis of the excavating effect of lugs has been made and a new conclusion is reached. Some efforts were devoted to a study of surface shear devices for measuring shear strength and it was found that in frictional soils they give a lower value of ϕ than confined tests. Suggestions for their modified design and use are made.

It is shown that current methods of determining soil deformation by superposition of the effects of horizontal and vertical loads taken separately, are wrong and can lead to serious over estimates of vehicle performance. The additional factor is called slip sinkage and it was found to be important in sand but less so in clay. An analysis is made which explains this, gives some insight into the physical nature of the phenomenum and may provide the basis for a theoretical study of equilibrium sinkage under combined loads. A method is proposed whereby data from existing Bevameters may be used to predict slip sinkage.

KEY TO SYMBOLS

a	Area	$in.^2$
b	Track or wheel or plate width	in.
c	Cohesion	$lb.in.^{-2}$
c_a	Adhesion	$lb.in.^{-2}$
e	Sum of exponential series	Dimensionless
	error	Dimensionless
	Track greuser pitch	in.
h	Track greuser height	in.
i	Slip	Dimensionless
j	Soil deformation, horizontal	in.
k	Soil sinkage modulus	$lb.in.^{-2-n}$
k'	Soil sinkage modulus	$lb.in.^{-2}$
k_c	Cohesive modulus of sinkage	$lb.in.^{-1-n}$
k_ϕ	Frictional modulus of sinkage	$lb.in.^{-2-n}$
k'_c	Cohesive modulus of sinkage	Dimensionless
k'_ϕ	Frictional modulus of sinkage	Dimensionless
l	Track or plate length	in.
n	Sinkage exponent	Dimensionless
p	Pressure	$lb.in.^{-2}$
q	Surface bearing capacity	$lb.in.-2$
r	Radius	in.
s	Shear stress or strength	$lb.in.^{-2}$
t	Moisture tension	$lb.in.^{-2}$
w	Weight of soil entrained in track	lb.

x	Co-ordinate parallel to soil surface in the direction of motion.	in.
y	Co-ordinate parallel to soil surface perpendicular to the direction of motion	in.
z	Co-ordinate perpendicular to soil surface sinkage	in.
B	Angle	Degrees
H	Horizontal force	lb.
K	Soil horizontal deformation modulus	in.
L	Horizontal force	lb.
P	Force	lb.
W	Vertical force	lb.
γ	Soil density	lb.in.$^{-3}$
μ	Angle of soil-metal (or rubber) friction	Degrees
θ	Angle	Degrees
σ	Contact pressure	lb.in.$^{-2}$
ϕ	Angle of shearing resistance	Degrees
ξ	Earth pressure coefficient	Dimensionless

1. INTRODUCTION

The use of vehicles for off the road transport is growing rapidly. Agriculture is becoming mechanised all over the world and farm tractors are being used in more and more difficult soils, even in such extreme conditions as rice paddies and peat bogs. Timber is now being sought in more remote places and the extraction of wood from such areas as the Canadian Muskeg poses a very difficult transport problem. Exploration together with the subsequent exploitation of areas rich in oil and other minerals is also proceeding in the more inaccessible regions and vehicles to carry men and machinery for these purposes over the snows, tundras and deserts of the world are growing in number. The development of atomic weapons has required a great increase in emphasis on military mobility. The enormous destructiveness of modern weapons requires that armies be able to operate in small units capable of rapid dispersal and equally rapid combination in order to avoid or mount an offensive quite independently of the normal static means of transport which must be assumed to be destroyed. Recent applications for off the road vehicles have resulted in a steady growth in the production of such machines and an equally continuous proliferation of vehicle forms. The more difficult the proposed environment and the more exotic the vehicle, the more interest there is in the relation between the vehicle and the surface over which it moves.

1

The study of the general relationship between a vehicle and its physical environment is quite novel and has no generally accepted name but has recently been called Terramechanics. It is concerned with the performance of the vehicle in relation to soft soil, obstacles, vibrations due to rough surfaces and water crossing. The major problem is undoubtedly soft soil and the detailed analytical study of the relation between vehicle tractive performance, vehicle dimensions and soil properties is now generally called soil-vehicle mechanics. This study is in its infancy and as will be shown later is at present incapable of dealing adequately with even a wide range of deep uniform soils. Claims have been made that particular theoretical systems are capable of general application to any real soil in the field, including for example layered conditions. It is the writer's opinion that such claims are unjustified, particularly when the theoretical mechanics is based on data from instruments which are smaller than the vehicle and in a sense models of its action. The true objective of soil-vehicle mechanics research today is the quantitative understanding of the performance of simple vehicle running gear in deep uniform soils (usually in the laboratory). This will provide guiding principles for more rational design, evaluation and test procedures and an intellectual framework into which field experience can be fitted to make a comprehensible picture.

The study of soil vehicle mechanics can be traced back 120 years to the work of Morin[1] on the rolling of rigid wheels on

soft and hard surfaces. Apart from the work of Reynolds[2], Bernstein[3] and Goriachkin[4] little real progress was made until the Second World War and its major mechanised campaigns. The experience of the Germans in the mud and snow of Russia and of the British in the wet clay of the North German Plains focused attention on the mobility problem. Since then considerable efforts have been put into the study of soil vehicle mechanics and some progress has been made. The approaches to the problems involved have been remarkably diverse and can perhaps be listed in the following groups.

(a) A theoretical approach based on civil engineering soil mechanics.

(b) An analytical approach using semi-empirical soil stress deformation relationships.

(c) Index systems based on attempting to describe soil characteristics by means of a single simple measuring device.

(d) Model experiments using dimensional analysis to systematize the results.

(e) A rigorous mathematical approach based on the theory of plasticity.

The first approach utilising civil engineering soil mechanics has been developed in England by the F.V.R.D.E. and its predecessors. The work originated from the decisions of the Mud Committee which was set up when the tanks, which had been so successful in the North African Desert, became immobilized in mud

3

first encountered in Italy in the winter and later on a much larger scale in North Germany. Micklethwaite[5] made the first brilliant application of Coulomb's equation to predict the maximum possible tractive effort of a vehicle. He was followed by Evans[5], Sherratt and Uffelman[7] who concerned themselves only with frictionless saturated clay soil. They were able to describe the pressure sinkage relationship for such a soil by the simple equation $p = k$ (i.e. independent of sinkage) and the shear stress-deformation relation by $s = c$ (i.e. independent of slip above a certain low value). Because these relationships were so simple they were able to apply them to quite complicated vehicle forms such as resilient tracks, smooth wheels and wheels with large lugs. The theoretical work was supported by adequate experiments and it can be concluded that a reasonably accurate scientific theory has been developed for clay soils.

Bekker, working first for the Canadian Army and later for the U. S. Army, initially followed this approach and made some outstanding contributions to what he called the stability problem.[8] This work led him to the conclusion that no general theory was possible without the use of stress-strain or stress-deformation relationships. He therefore developed a comprehensive analytical approach that would cater for frictional and compressible soils as well as clay.[9][10] This made quite explicit the basic proposition that vehicle behaviour would be interpreted in terms of the reaction of soil to simple plate loading tests. This had always been implicit in the British

4

approach. He proposed that the relation between pressure and sinkage in a plate penetration test could be described by:

$$p = \left[\frac{k_c}{b} + k_\phi\right] z^n \qquad \dots \quad \dots \quad \dots \quad 1.1.$$

where b is a dimension describing the plate size and k_c, k_ϕ and n are soil stress deformation parameters. Janosi and he further proposed that the results of horizontal shear plate tests should be described by:

$$s = (c + \sigma \tan \phi)(1 - e^{-\frac{K}{j}}) \qquad \dots \quad \dots \quad 1.2.$$

in which c and ϕ are the Coulomb soil constants and k is a stress deformation parameter. These equations were then applied to certain simple vehicle forms such as rigid tracks and rigid wheels and theoretical relationships obtained between drawbar pull and slip.

Index Systems using various forms of penetrometers have been tried out in both Civil and Agricultural Engineering. The most serious effort, however, has been made by the U. S. Army Engineer Waterways Experiment Station, who have developed the Cone Index. This system uses a standard Cone Penetrometer which was originally developed as a simple tool suitable for trafficability studies and for use by troops in the field for making tactical decisions during combat. It has been developed to serve this purpose well. Soils have first to be classified into types and so far, fine-grained soils and sands have been thoroughly investigated and muskegs and snows less

comprehensively. In the case of clay it can be assumed that the
force required to push the penetrometer in the ground is constant
and therefore a single number called the Cone Index is obtainable.
In sands, by assuming that the force will grow linearly with
sinkage, once again a single number representing the increase in
pressure per unit of depth can be used as the Cone Index.

The use of the Cone Index system in trafficability and
other military field situations seems to have been very
successful. Its use as a basis for studies of soil vehicle
mechanics appears to have been a matter of political expediency
rather than scientific judgement. Even allowing for the fact
that classifying the soil type avoided the attempt at a general
system, it is obvious that the Cone Index combines together too
many separate soil properties in proportions quite different to
those of the vehicle situations. Recent work[40] has shown that the
forces on a soil cutting blade can be accurately defined in
terms of c, ϕ, γ, c_α and μ, but they cannot be defined in terms
of any particular combination of these. The vehicle problem is
very similar to that of the blade and the same principle will
apply. The use of the Cone Index in soil vehicle mechanics is
analagous to an attempt to base fluid mechanics on a single
constant combining both viscosity and density. Now, apparently,
this approach is being abandoned.

Model experiments were first undertaken by Nuttall[12] who
attempted to use similitude principles as they are used in naval
architecture. He noted that the selection of suitable parameters

6

to define the properties of the soil was a major difficulty. His
work extending over a long period has recently tried to use
either the Cone Index or another single constant derived from
plate penetration tests to describe the soil and some success
has been achieved. M°Ewen and Willetts, Newcastle, England,
attempted to define soil properties in terms of c, $\emptyset$ and γ.
Vincent & Hicks[13] tried to use Bekker's empirical parameters to
describe the results of their model experiments.

It has become perfectly clear that the model work will
never be entirely satisfactory until a firm theoretical basis
is available which will provide the correct soil-describing
constants. It is often not appreciated that the dimensionless
groups in fluid mechanics are not curve-fitting parameters that
happen to collapse experimental data. The Reynolds number for
example was proposed by Osborne Reynolds as the consequence of
an unsuccessful attempt to solve the Navier Stokes equations for
friction in pipe flow. The importance of the number he confirmed
by subsequent experiments. The writer has recently been
concerned with work on[40] soil-cutting blades where it was possible
to develop an accurate theory in terms of c, $\emptyset, \gamma, \mu$ and c_γ.
Dimensional analysis was then used to reduce the number of
variables. Because the soil parameters involved were part of a
theory shown to be accurate by adequate experiments there can be
no doubt that the dimensional analysis is correct. It seems
clear then that model techniques will not be applied
successfully to the soil vehicle situation until a firm

theoretical foundation is available.

Attempts to solve soil vehicle problems by means of plasticity theory have failed because soils do not behave as ideal plastic materials. The development of suitable stress-strain relationships for soils is a perfectly proper field of endeavour for the applied mathematicians. However, it has become perfectly clear that they are primarily concerned with the construction of logically correct systems of ever increasing complexity rather than the solution of engineering problems. There is a danger that this approach will obscure the possibility of advance on a simplified and non-rigorous but perfectly adequate engineering basis.

Perhaps in order to complete this review some mention of Russian work should be made. Based on the work of Goriachkin it assumes that soil resists deformation by stresses in the opposite direction to the deformation and of magnitude proportional to the deformation. Numerous theoretical papers on this basis have been translated but they appear to contain little experimental support. The assumption used seems so unsophisticated that one can only assume the serious Soviet effort is reported elsewhere.

It seems clear from this brief summary of the work that has been done so far that the immediate task is to develop a general theoretical approach comparable to the British but applicable to frictional and compressible soils. Bekker's approach, which is the only one that offers any chance of such generality, must therefore be considered in more detail.

Does the system in fact actually work? This question could be answered by means of experiments in which the tractive effort of rigid wheels and tracks as a function of slip is investigated in controlled and measured soil conditions. In fact very few such experiments were carried out during the development of the system. It can therefore be stated at the outset that Bekker's system is not a scientific theory but a hypothesis.

Probably the most comprehensive independent attempt to investigate the validity of the Bekker system has been made by the Department of Agricultural Engineering, University of Newcastle upon Tyne, England. This work was supported by the Fighting Vehicles Research and Development Establishment and a summary of the results of the first four years work up to the Summer of 1962 has been described in a F.V.R.D.E. Report.[14] Most of the contents of this report have been published in references 15 and 16. Bekker soil values in sandy soils were measured and applied to the prediction of the performance of full sized rigid tracks in the field, and small model sized tracks in laboratory conditions. Since the Report was written, further work has been conducted on the rolling resistance of rigid wheels.

The Bekker equations were applied to the results of many shear plate and footing tests on a variety of sandy soils. Equation 1.2 was found to describe the results reasonably well although it may require some slight modification in order to allow for the size of the loading area and its mean contact

pressure. Equation 1.1 was not so satisfactory; the experimental pressure-sinkage curves were never quite straight when plotted on logarithmic coordinates. A technique is therefore needed to select the best fitting straight line and to measure the error involved in using it instead of the actual curve. Nevertheless it appears that the equation $p = k'z^n$ and certainly the modified form $p = p_0 + k'z^n$ do fit the facts reasonably well, with n a soil constant, and k' a function of soil and the strip width b. The main deficiency in equation 1.1 was found to be in the relation between k' and b expressed by

$$k' = \frac{k_c}{b} + k_\phi.$$

Wills showed that equation 1.2 works well in predicting the slip-pull relationship for full sized rigid tracks operating without large sinkages. Reece and Adams demonstrated by means of experiments with a model tracklayer that this agreement deteriorated as the soil became weaker and sinkage increased. This was explained as being the result of an interaction between the vertical and horizontal loadings. It was concluded that equations 1.1 and 1.2 cannot be applied to a vehicle by simple vector addition, making use of the principle of superposition. Additional sinkage was found to occur because the horizontal loads reduced the capacity of the soil to support vertical loads. This phenomenon was called slip sinkage.

In the unpublished rolling resistance work the Bekker prediction was generally less than the measured value. It was

encouraging to observe, however, that the theoretical curves
differed from the actual curves in a very systematic way.
Analysis has shown that the Bekker theory generally underestimates
the sinkage and therefore gives too low a value for the work done
in making the rut. When the measured sinkage is used in
computing energy losses, there is still a deficit; and this can
be attributed to horizontal deformation of the soil due to the
slip or skid of the wheel.

The general conclusion was that the usual concept of
rolling resistance of a towed wheel (as being due to the work
done in deforming soil vertically) is greatly oversimplified,
and only applies to very small sinkages. In fact work is also
put into horizontal soil deformation which results in slip and
slip sinkage. Even at small sinkages the theory is inadequate
as it does not correctly describe the magnitude of the sinkage
or the resulting pressure distribution.

The preceeding survey of the field of soil vehicle
mechanics in general and the Bekker (or Land Locomotion
Laboratory) system in particular represents the overall view
of the author when commencing a year's Sabbatical work in the
Land Locomotion Laboratory. It was clear that there was no lack
of technical problems to investigate, and of these the mechanics
of the slip-sinkage phenomenon was perhaps the most interesting.
However, it appeared more important to try to find a general
approach that could possibly unite the conflicting schools of
thought in this field. For this reason an effort was made to

involve as many aspects of soil-vehicle mechanics as possible. The slip sinkage question is very suitable in this respect because it involves the relation between the two fundamental Bekker tests and therefore the whole of the underlying soil mechanics.

There finally emerged a general point of view that may well provide the necessary unification. It is based upon the premise that the relation between vehicles and soil can be explained in terms of the reaction of soil to simple plate loading situations. This may not be true, but there seems no alternative at the moment, and it is certainly a proposition common to the British, Bekker, Cone Index and Model approaches. It is then agreed that the results of the plate tests must be described in terms of empirical curve-fitting equations as in the Land Locomotion Laboratory System. It is proposed, however, that these equations be chosen so as to fit theoretical solutions based upon the normal Coulomb plastic equilibrium approach which assumes the soil to be incompressible and to require zero shear strain to reach shear failure. Such theoretical solutions are supported by the considerable achievement in the field of soil mechanics of foundations, based on the work of Terzhagi. These theoretical approaches yield answers either in the form of very long equations (for example Osman worked out the equation for the force on a cutting blade and it occupies a closely typed page)[40] or more usually computed numerical relationships. These are both unsuitable for use in a general soil vehicle mechanics, but

12

can be described by Bekker-type curve fitting equations which
can be of simple form without excessive inaccuracy. The curve-
fitting equations will be chosen so as to accommodate the
additional factor of compressibility, by a mixture of experiment
and intuition. Ideally then, the new Bekker-type soil parameters
will be computed functions of c, ϕ and γ for soils at maximum
density, but empirical constants for loose soils. A further
development may later become possible in which new approaches to
soil mechanics, emphasizing the particulate nature of soils, as
in the work of P. W. Rowe[17] at Manchester and K. H. Roscoe and
A. N. Schofield[18] at Cambridge, are used to obtain theoretical
solutions allowing for compressibility as well.

The horizontal shear-deformation equation 1.2 is already
of the proposed form. If K is zero then it reduces to
$s = c + \sigma \tan \phi$, the normal Coulomb equation, and this condition
of shear failure at zero shear strain is a basic assumption of
classical plastic equilibrium soil mechanics. The effect of
deformation is introduced in such a way as to lead to a
parameter K of constant dimension in.$^{-1}$. At first sight it
appears odd that the stress is a function of deformation rather
than deformation divided by a characteristic dimension of the
zone of soil stressed by the shear plate, which would result in
a dimensionless K. Some of the work at the University of
Newcastle[16] suggests that this may be so, at least for sand if
not clay. The main point at the moment, however, is that this
equation is firmly based on soil mechanics theory, that it can

include the usual simple ideal case, and that it is dimensionally simple. Wills' experiments lend strong support to it as a useful tool. It would be interesting to investigate the shear stress-deformation relationship in an attempt to determine k as a function of more basic soil parameters, and here the stress-dilatancy theories of P. W. Rowe may be particularly relevant. This would probably clarify the relation between k, b and σ.

The pressure sinkage relationship in equation 1.1

$$p = \left[\frac{k_c}{b} + k_\phi \right] z^n$$ however, is not so satisfactory. It has no connection with the pressure sinkage relationships that can be derived on the basis of incompressible Coulomb materials. It is dimensionally faulty because both k_c and k_ϕ have dimensions that are a function of n and are not constant, and it has not stood up well to experimental test. It is shown later that this situation can easily be rectified by the use of an equation of the form $p = f\left(\frac{z}{b}\right)$ instead of $p = f(z)$. Values of the modified Bekker constants can then be computed for incompressible materials in terms of c, ϕ and γ using the bearing capacity theory developed from Terzaghi[19] by Meyerhof.[20] The validity of this approach has been demonstrated in the following pages by pressure sinkage experiments in dry sand, wet sand, and clay.

The slip sinkage problem has been approached by constructing a suitable apparatus for applying first vertical loads and then horizontal deformations or loads axially along a narrow strip footing. The apparatus has been used so far for a preliminary

reconnaissance in the dry and wet compact sand and saturated
clay. The results could be described in terms of a third Bekker-
type equation, but in accordance with the previously advocated
principle, priority has been given to trying to develop a theory
for incompressible soils, which could be used as a basis for a
suitable equation. An attempt to apply the results of the slip
sinkage rig experiments to the prediction of the sinkage of a
model tracklayer was unsuccessful, but at least a likely
procedure has been described.

This proposed method then, neatly combines the Bekker and
the British approach. It also offers considerable promise of
providing definite soil parameters for use in dimensional
analysis. The application of this principle should provide
better functions with which to describe the results of plate
penetration and shear tests. There is reason to believe,
however, that this will not be sufficient and that it is
necessary to modify the way in which the simple plate load test
data is fitted into the vehicle situation. This is done at
present in a very simple manner by making use of several
assumptions, none of which have been clearly stated, let alone
experimentally justified. It is possible that improvements in
the theory can be made by a critical investigation of these
assumptions.

The basis of the Bekker approach is the assumption that
the pressure on an element of a plate that has been pushed down
to a depth z is the same as that of an element of a wheel or a

15

track. In the principal references to the Land Locomotion Laboratory system this assumption is presented implicitly in the form that the pressure under an element of the vehicle at a depth z is the same as the mean pressure under a flat plate of any shape (whether a circle, rectangle or infinite strip) at the same depth. Once it is stated explicitly, this principle can be seen to be untenable and this is confirmed in a later section of this report. A little reflection will show that the basic assumption of the Land Locomotion Laboratory method can only be that a crosswise element of area of a wheel or track of very small width δx at a depth z corresponds to a similarly narrow element running right across a strip footing of sufficiently high aspect ratio to be taken as infinite. This correspondence is illustrated in Fig. 1.1. On this basis the principle assumptions can be listed as follows:

Assumption 1. The main difference between a crosswise element of a wheel or track and that of a strip footing is that neighbouring elements are not at the same depth and that the element itself is at an angle θ to the soil surface. Assumption 1 is that this does not affect the pressure on the element and does not give rise to a shear stress along its face. There must clearly be a limit which can be expressed in terms of θ, the trim angle of a track or the angle of inclination of the tangent to the rim of a wheel. The nature of this limitation needs to be elucidated by means of experimental and possibly theoretical investigations.

Assumption 2 is that the pressure on the element is unaffected

16

by its proximity to the beginning or end of the contact patch. This may be stated in another way as the assumption that it does not matter what the aspect ratio of the contact patch is. Assumption 3 is that there is no recovery of deformation in the soil in the bottom of the rut. This means that normal stresses and shear stresses cease abruptly vertically below the axle of a wheel.

Assumption 4 is that when a succession of wheels follow each other in the same rut, each wheel sees exactly the same soil as that preceding it. This assumption is made by the Land Locomotion Laboratory in its current evaluation procedures but it is not one made by Bekker. In his first book he assumes that the pressure required to initiate the sinkage of the nth wheel is the same as that reached at the maximum sinkage of the preceding one.

Assumption 5 is that the principle of superposition can be used so that the results of the two basic soil-plate tests can be simply applied to the vehicle situation. In particular it is assumed that the pressure beneath a vehicle element at a depth z is the same as that below a vertically loaded plate at the same depth, even though the vehicle may be applying considerable horizontal loads as well. It is this assumption that results in the division of the drawbar pull into two separate parts, the gross tractive effort and the rolling resistance. Its replacement will necessitate the use of a more complex scheme in which both gross tractive effort and rolling resistance are

continuous functions of slip.

Assumption 6 is that the sinkage of a wheel is small relative to its diameter, but many soils will permit a wheel to operate at considerable sinkages and it is very doubtful if such an assumption is really acceptable. It probably covers most situations relevant to agricultural tractors but certainly not the extreme limits of performance that concern the military.

All of these assumptions are clearly reasonable in certain circumstances, but by now it has become apparent that in conditions which often exist beneath vehicles some or all of them may not be applicable. This is probably one of the main reasons why the theory based on these assumptions has been supported by some experiments but not by others.

Careful examination of these assumptions, and the development of methods of dealing with the situations in which they do not apply, cannot fail to result in progress towards a better understanding of soil vehicle mechanics.

The report that follows is concerned basically with the slip sinkage problem and the attempt to replace assumption 5 by a more sophisticated concept. At every opportunity side issues were explored in an attempt to relate the Bekker - Land Locomotion - method to traditional soil mechanics. A certain amount of success may have been achieved and although the report raises more questions than it answers, it is felt that at least it suggests avenues of possible advance. Many of the questions discussed are left abruptly in mid-argument. This has happened

because this report is concerned with the writer's ideas at the end of a year's effort in Detroit rather than a particular finished piece of work. The main lines of investigation continuted the previous work in Newcastle and are being actively pursued there now. The year in Detroit was a most enjoyable and stimulating opportunity to carry on the work in the company of an expert group with a very different history, environment and purpose.

In this thesis a great deal of effort is devoted to detailed criticism of the work of Bekker and his colleagues at the Land Locomotion Laboratory. It should be made clear that in the writer's opinion Dr. Bekker has been responsible not only for laying the firm theoretical foundation upon which any system of soil-vehicle mechanics must rest, but also for the creation of most of the current interest in the subject throughout the world. It is not to be expected that the details of any theories in this field will survive more than a few years of use, but instead will be steadily changed and improved. It is hoped that the suggestions made here will be accepted as just such proposals for improvement within the limits of the Bekker - Land Locomotion Laboratory approach.

2. APPARATUS AND SOILS

2.1. Linear Shear Apparatus

In order to investigate slip sinkage in the simplest possible circumstances it is necessary to use a straight shear plate long enough to represent an infinite strip, to be able to load it with dead weights to beyond its bearing capacity and to force it to move horizontally without restricting its freedom to sink. The apparatus shown in Figs. 2.1.1. and 2.1.2. meets these requirements in a satisfactory manner.

The counter balanced double parallelogram allows the shear plate to move freely in a vertical plane but forces it to remain horizontal. It is moved by a hydraulic ram acting through a ball bearing roller to ensure that no extraneous vertical loads are applied. The linkage joints utilize needle roller bearings which are friction free and set wide apart so that the shear plate is prevented from falling over sideways. The double parallelogram can apply a torque to the shear plate in a vertical plane to neutralize the couple Hh, and it ensures that the longitudinal distribution of soil pressure beneath the plate is independant of W and H. This distribution is therefore only dependant upon the soil beneath the plate and will be uniform if the plate is long enough to minimize end effects. The dead weight loading was hung by a spring from a crane and could be lowered on to the shear plate without shock.

The horizontal load H_t was measured with a strain gauge load cell, horizontal movement with a potentiometer, the two producing a load displacement record on an X-Y plotter. The slip sinkage trajectory was plotted directly on a sheet of paper held vertically beside the shear plate by means of spring loaded pencils just below the weight carrier. This trajectory was later traced on to the X-Y plotter record to produce records such as are shown in Figs. 7.2.1. to 7.2.8.

The apparatus was intended for shear plates 30" long (but 90" is possible) and up to 4" wide with vertical and horizontal loads of up to 1000 lb. It could move the plate a horizontal distance of 16" while permitting a sinkage of 8". A check on the accuracy was made by placing the shear plate on rollers and making the apparatus lift a heavy weight via a cable and pulley; friction was found to be negligible.

2.2. Modified Bevameter

An existing Bevameter was modified to increase its vertical load capacity from 1000 lb. to 2000 lb. This only required the repositioning of the penetration cylinder in the centre of the frame to minimize distortion and the resetting of the hydraulic relief valve.

The shear head was modified so that sinkage could be recorded as it was rotated. This was achieved by fitting a coffee can of the mean radius of the annulus to the torque shaft. A pen on the frame traced out the slip sinkage trajectory

21

as the annulus shaft and can rotated and sank. Torque-against-twist and load-against-sinkage were plotted on the X-Y plotter using strain gauge load cells and potentiometers. The Bevameter is shown in Fig. 2.2.1. where it is set up for very slow speeds using a triaxial machine electric drive to force oil out of a ram into the Bevameter ram.

2.3. Model Tracklayer

An existing model of a D.4 tractor was modified to provide a much higher clearance so that experiments could be conducted under conditions of considerable slip sinkage. A 1½" double-pitch conveyor chain was used to provide a closely scaled model of a tractor track. It proved impossible to drive this smoothly and the track vibrations were later thought to have caused considerable additional sinkage. The replacement of the track rollers by a skid along which the chain bushes ran was very successful. The tracklayer weighed 142 lb. and the track area was 2 x 16" x 2", giving a mean contact pressure of 2.22 lb.in.$^{-2}$

The tracklayer is shown in Fig. 2.3.1. ready for an experimental run in sand. The associated gadgets are similar to those made previously in England. The drawbar pull was applied by hauling weights up a tower via thin wire rope running round large diameter ball bearing pulleys. The load transfer from the drawbar pull and movement of centre of gravity as the tractor tilted was cancelled out by means of a sliding balance weight. Sinkage at the front and rear of the track was recorded by two pencils that traced on to a long sheet of paper. Slip, or

rather distance travelled per revolution of the drive sprocket, was obtained from marks made on the paper by a pencil actuated by a solenoid switched on and off by a micro switch on the sprocket.

A simple track link dynamometer to measure the normal pressure on a track plate as it passed under the tractor was made and is shown in Fig. 2.3.2. The gauges are arranged to respond to the moment vV but to ignore Hh and the torque Hv. Static tests showed that they were satisfactory in this respect. The device will therefore measure track pressure as long as it is uniformly distributed across the track, which it will be if the soil is uniform. The results shown in Fig. 7.4.3. are disappointing in that they suggest a serious cross sensitivity; unfortunately there was not time before leaving Detroit to find out why this happened. A potentiometer connected to a point on the track chain by a thin wire provided the input to the 'X' axis and the pressure was shown on the 'Y' axis of the X-Y plotter, providing direct diagrams of pressure against position along the track.

2.4. Soil Tanks and Processing Methods

A minimum of three soils should be used in any soil vehicle mechanics investigation that is intended to be comprehensive. A dry coarse round-grained sand and a saturated clay provide the two extremes and a loamy farm soil will enable work to be done in a c – ∅ soil at a wide range of compressibilities. Because of the limited time available the loam was left out, but instead

23

some work was carried out in the sand in a saturated condition. This had the same ϕ as the dry sand plus $\frac{1}{10}$ lb.in.$^{-2}$ cohesion, which gives it the great advantage of clearly showing failure planes where they break out on to the surface.

At the University of Newcastle upon Tyne it has become standard practice to measure the strength of each soil in as many ways as possible in an effort to achieve really reliable values for the basic soil mechanical constants c, ϕ, and γ. This had not been the tradition of the Land Locomotion Laboratory, who had considered that the Bevameter adequately measured "soil values" relevant to the vehicle situation. There was, therefore, only a 6 cm. square shear box available. However, a "commercial grade" triaxial machine was quickly obtained and a first class machine placed on order. A small shear vane (1½" deep x 1½" dia.) was made and also a 5" dia. N.I.A.E. shear box; both of these were twisted by hand, using torque wrenches. As many as possible of these devices were used in each soil as well as the Bevameter and the linear shear apparatus itself.

The minimum quantity of each soil was determined by the size of the slip sinkage rig and model tractor. A single test of the rig needed a length of 5', a width of 2' and an absolute minimum depth of 12". The tracklayer needed a longer run than this, and also more width and some existing 10' x 3' x 2' deep steel tanks seemed ideal, giving the possibility of two slip sinkage runs in each preparation.

In order to ensure a uniform moisture content in the wet sand it was decided to flood the tank and drain it as part of each preparation. (This excellent idea was proposed by E. Hegedus). The tank was flooded and drained from the bottom using a longitudinal perforated pipe in the centre of a 6" deep layer of gravel. The gravel was prevented from rising under the action of the considerable hydrodynamic forces by a cotton cloth secured to a wooden frame. The gravel layer was put into all three tanks, leaving an 18" depth of sand of which 12" was cultivated. A 13" depth of clay was used.

The marks of a test were removed by pulling a vibrating cultivator through the two sand tanks. The cultivator had ½" square backward raked tines, 2" apart and was vibrated by a 2000 lb. capacity 60 c.p.s. electric vibrator; it worked 12" deep. The raking action loosened the soil and removed the voids made by preceeding tests while the vibration reduced the draught and compacted the soil. The towing speed was therefore critical, as the slower it went the more compact the soil became; and it was finally hauled along by an overhead crane via a wire rope and a pulley block fixed to a fork lift truck. The rake was used in the wet sand while it was flooded. After some weeks' effort satisfactorily reproducible experiments could be carried out in the two sands, as shown by the typical pressure sinkage curves of Figs. 4.8.1 and 4.8.2.

The clay was obtained in saturated condition from a 30' deep excavation being made just outside the Arsenal. It was

allowed to partially dry out, and most of the large stones were removed by hand. It was then mixed with water in 1000 lb. lots in a large kneading machine, water being added until the cohesion measured with the vane fell to 1 lb.in.$^{-2}$ Just before the final set of pressure-sinkage and slip sinkage tests it was remixed to ensure uniformity. The holes made by sinkage tests were removed by stamping in the clay in bare feet, an energetic but effective technique. The surface was levelled with a trowel and between experiments was covered with water to prevent evaporation.

2.5. Dry Sand

This was a sieved medium sized Ottawa sand. The shear box showed that at the maximum density of γ = .0705 lb.in.$^{-3}$ ϕ = 36°, at γ = .066 as obtained from the vibrating rake in the tank ϕ = 32° and at the minimum density γ = .059, ϕ = 28° 36'.

2.6. Wet Sand

This was the same Ottawa sand as in the dry sand tank but contained rather more dirt and a little clay that must have got in during its long life in the Laboratory. When saturated its density after cultivating was slightly less than that of the dry sand at .064 lb.in.$^{-3}$, its ϕ the same 32° but there was about $\frac{1}{10}$ lb.in.$^{-2}$ cohesion. The average moisture content was 2.3%.

2.7. Clay

This was obtained at a depth of 30' from the subsoil beneath the Arsenal. It contained some stones and a little sand

26

but not enough to give it appreciable friction. When wet it was dark grey but became very light in colour when dried. Shear strength was measured with the vane, N.I.A.E. shear box, triaxial machine and slip sinkage rig. This resulted in an average value of c of about 1 lb.in.$^{-2}$ and a negligible value for $\emptyset$ of about 8° - checked at up to 75 lb.in.$^{-2}$ water pressure in the triaxial machine.

2.8. Comment

The getting together of the soils and apparatus just described occupied a considerable part of the year available, and the major proportion was concerned with the soil, the soil tanks and developing the vibrating rake technique for the sand and the kneading-stomping for the clay. It is characteristic of this type of work in most research laboratories that more effort goes into preparation than into the actual experiments. This may not be the most efficient way of doing land locomotion research.

The situation can only be remedied by providing several soils (at least four: dry sand, wet sand, loam and saturated clay) in suitable quantities, with proper equipment for powered processing to give complete control of density and moisture content. The processing and measuring of physical properties should then become a matter of routine carried out by regular laboratory staff. The same principle would apply to the provision of obviously desirable apparatus for the supporting and driving of single wheels and tracks (at both model and full

27

scale) and instrumentation for measuring forces, torques and soil stresses.

The main obstacle to producing this Utopian situation is that it requires a major effort which for quite a long period would detract from the output of research. A second obstacle is that there are not at present available any completely satisfactory soil processing techniques.

3. CURVE FITTING TECHNIQUE

3.1. Introduction

The theory of soil-vehicle mechanics developed at the Land Locomotion Laboratory depends entirely upon the fitting of actual soil stress - deformation curves with the nearest possible curve that is described by an arbitrarily chosen simple type of equation. The simple equation can then be used to develop further equations describing vehicle performance, which tend to become complicated, even with a simple starting point. The justification for this procedure is purely one of expediency. The actual equations describing pressure sinkage relationships in compact soils, for example, are so complicated that using them in the additionally complex vehicle situation would be impossible. The only alternative to the use of a particular equation would appear to be the use of a series, a possibility that does not seem to have been adequately investigated. For example, it may be mathematically convenient to replace

$$p = \left[\frac{k_c}{b} + k_\phi \right] z^n \text{ by } p = (A + Cb + Db^2....)(a + cz + dz^2....)$$

The curve-fitting process is an explicit part of the Bekker system which it has inherited from the work of Bernstein. Other attempts at interpreting vehicle behaviour always involve the same idea although they do not usually make this very clear. For example, the work of Uffelman in clay is based on an assumed relation $p = k$ and that of the Waterways Experiment Station at

Vicksburg on p = k for clay and p = kz for sand. It is note-worthy that both of these are special cases of the Bekker equation.

The curve-fitting process necessarily introduces an error into prediction just because the simple equation will not fit the actual observations exactly. It also introduces a major intellectual difficulty in the choice of equation constants which will give the best fit and the measurement of error introduced because the fit is not exact. There are two separate problems involved in the curve fitting. One is due to the variability of the soil which will yield a set of curves for a single test arrangement. Fig. 3.1.1a shows the sort of results that may be expected from a plate penetration test in the field or in a poorly set up laboratory experiment. The second problem arises in good laboratory conditions where a single curve results from a set of tests, but this curve does not exactly fit the chosen equation. This situation is shown in Fig. 3.1.1b where the family of curves is sufficiently close to a single line, but this is not straight when plotted on logarithmic axes. It should be noted that these are separate problems that do not occur together. The variability in the field will entirely obscure the fact that individual curves are not quite the right shape as long as the soil is reasonably suitable for application of the particular system of soil vehicle mechanics (not layered for example). In the laboratory the whole object of setting up the artificial conditions of a soil tank is to make it possible to

achieve accurately repeatable results which provide the
opportunity to investigate the effect of small changes in the
condition of the test. Figs. 4.8.1. to 4. show the sort of
results that can be obtained from a reasonably well organized
laboratory test and it is plain that the groups of curves can be
accurately represented by mean curves drawn by eye. The problem
is then to fit the mean curve to the equation.

The field problem is really one for the future since it is
not yet possible to apply soil-vehicle mechanics to the general
case in the laboratory. However it is clear that it will be
necessary to plot all of the results for each plate size
together and represent them by a single line, rather than to fit
each experimental curve with a line and then work with the
resulting empirical constants. Probably it will be possible to
put in a mean line by eye as in Fig. 3.1.1a and use this to
predict vehicle performance adequately, hoping that the greater
areas covered by each vehicle running gear element, the wide
spread of the separate elements and the machine's momentum will
suffice to average local differences.

The other problem of finding the best constants in a
given equation to describe a particular curve is one of
considerable current importance. It is involved in basic
experiments to find suitable characteristic equations and in
attempts to use these equations to predict performance.

3.2. Current Methods

The first curve-fitting technique consisted of plotting

31

the curves on to log-log or semi-log axes and then fitting a straight line by eye. While fitting a set of points by a straight line by skilled eyes can give excellent results on linear axes, the method falls down due to the distortion produced by the logarithmic axes. A better method than this was proposed by the late S. J. Weiss[21] of the Land Locomotion Laboratory but fell into disuse and was reintroduced by Dr. B. M. D. Wills.[15] It consists of comparing the experimental curves with a family of the selected simple form and choosing by eye the best fit. It is not really satisfactory in that it involves a subjective decision and therefore does not give a unique answer, and also it does not give a measure of the error involved. It is also not convenient for use with equations involving more than one arbitrary constant. It can be used with

$$s = (c + \sigma \tan \phi)(1 - e^{-\frac{i}{K}}) \quad \ldots \quad \ldots \quad \ldots \quad \text{by rewriting}$$

this in the form $\frac{s}{s}_{max} = (1 - e^{-\frac{i}{K}}) \quad \ldots \quad \ldots \quad$ but is not

applicable to $p = \left[\frac{k_c}{b} + k_\phi \right] z^n \quad \ldots \quad \ldots \quad$ because

of the three constants involved.

A common suggestion that is often made is that if the experimental curve does not fit the chosen equation very well then it can be broken up into lengths and the separate pieces fitted. This is a useless notion, because it loses sight of

the object of the exercise, which is to provide soil stress-
deformation data which can be put into the vehicle situation.
It is hard enough to put in the single equation. For example,
in the wheel rolling resistance equation, gross approximations
are already necessary, without making integrations across
discontinuities. If one is forced to go in this direction, then
it is better to go the whole way and use the actual soil strength-
deformation curves and a digital, graphical or analog technique.
This is incidentally a worthwhile research exercise to enable
errors due to basic assumptions to be separated from those due
to curve fitting. It can also be a useful teaching method.
The main objection to this is that it makes it impossible to
develop general equations of vehicle performance from which
general conclusions can be drawn. If ever soil-vehicle mechanics
gets away from the limitations of ideal laboratory soils,it will
of course be very much easier to handle field soil-pressure-
sinkage data if each soil can be described by three numbers
instead of two families of graphs. If the existing equations
are found not to give a good enough fit which seems very likely,
then a great deal more can be done in the direction of using
better equations. For example, it is now well known that

$$p = p_0 + \left[\frac{k_c}{b} + k_\phi \right] z^n$$

affords a much better fit in many cases and the use of the
single extra constant is much preferable to doubling the number.
It is shown later that $p = (k_c' \, \mathfrak{C} + \gamma k_\rho' \frac{b}{2})(\frac{z}{b})^n$ gives an overall

33

better fit without any extra complication at all.

A serious attack on the curve fitting problem was made by Hanamoto and Jebe[22] in a paper describing an experiment to investigate the effect of aspect ratio on the pressure-sinkage relationship for rectangular plates in sand. The method used lumped the two problems of soil variability and curve fitting together. Six replications of each test were made and very closely repeatable results obtained over the very small depth range considered (variation was a maximum of $\pm$ 6%). The six curves for each plate size were converted to digital form and then a linear regression used to obtain the "best fitting" straight line on log-log paper, treating pressure as the dependent variable.

In order to facilitate discussion of the technique used, let it be assumed that no variation between replications occurred; but that the actual curves differed from $p = kz^n$ by an appreciable amount. The method suffers from the following theoretical and practical objections.

1. The justification in using a minimum sum of deviations squared criterion for selecting the "best" fitting line is questionable in this case. The normal least squares regression follows from a situation in which the true relation is <u>known</u> to be linear; the variations are due to genuine errors in the 'Y' measurement only; and the distribution of these errors is normal or Gaussian. These conditions are not met in this case.

34

2. There is questionable justification for applying the least squares principle to the logarithms of the deviations. This gives excessive weight to deviations at low pressures which are in fact probably the least significant.

3. The regression technique gives a different best fitting line if p is considered the controlled variable and z the dependent. There seems to be something wrong with a technique that gives a different answer as a result of making an equally justifiable alternative decision. In fact, it may be more justifiable to consider z the dependent variable since it is a fact that it is much harder to measure the sinkage accurately than the pressure. This point seems valid even if the suggestion of Dr. Joseph Berkson is followed and for the term "independent variable" we substitute the term "control variable".

4. The method used was laborious, requiring conversion of each curve to digital form and then the use of a digital computer to calculate the "best fitting" line.

5. The use of statistical methods tends to obscure the soil mechanics, by introducing many unfamiliar and rather complex words and techniques into the experiments. Unless the engineer concerned is conversant with the statistical methods used, he will have his attention distracted from his real task - one of soil mechanics which is difficult enough by itself.

A statistical method could be logically applied to determine the best curve with which to fit a set of experimental curves. It is now possible to do this using a high speed

computer without greatly restricting the form of the curve used. When this has been done the problem of choosing the best fitting version of a particular equation would remain. It is not necessary to do this with the results of laboratory experiments just because the variability can be kept very small. It is a matter of sound judgement to appreciate that a curve representing each of the sets of curves in Figs. 4.8.1. and 2, for example, can easily be drawn in by eye. The criterion here is that the uncontrolled variability in the curves should be small relative to the changes caused by controlled variables.

3.3. The minimum error method

A simple curve-fitting technique will be described with reference to the pressure-sinkage relationship. The basis of any curve fitting must be the selection of suitable limits; the closer these are the better the fit, but the narrower the range of application. Convenient limits for the pressure-sinkage relationship for use with full-sized vehicles are probably a minimum of 1" sinkage and a maximum of 10" or a maximum pressure of 30 lb. per sq. in., whichever is reached first. These have been chosen because below 1" the pressures are not going to contribute greatly to the rolling resistance unless the sinkage is small and the rolling resistance low - in which case quite large percentage errors in rolling resistance will have only a small effect on total performance. If sinkage is great enough to give a significant rolling resistance, then even for the smallest jeep-sized tire an error in pressure distribution below the 1"

36

sinkage will not constitute a large error in the total. The upper limit was chosen because a sinkage of $10''$ will immobilize most vehicles while a mean pressure of 30 lb. per sq. in. is the maximum likely to be applied by any cross-country vehicle. These limits are suggested as being generally suitable for full scale work; for model experiments lower pressures would be appropriate.

Fig. 3.3.1. shows the problem to be solved; the actual curve is shown in full and it is necessary to fit the best curve described by the chosen equation which is represented by the dotted line. This will usually intersect the full line in two places and the error e will be given by $e = \dfrac{p_a - p_t}{p_a}$. The distribution of error as a function of z is shown and it is clear that there are three peak values - e_1 at $z = 1$ inch, e_{30} at z corresponding to 30 p.s.i. (or $10''$) and e_m in between. The maximum error can be minimized by making these three errors equal and this can easily be done for equations like $p = kz^n$ which are represented by straight lines on log-log paper. The limit lines $z = 1$ and z at $p = 30$ p.s.i. or $10''$ are drawn in and a straight line drawn between the intersections of the experimental curve and the limit lines on log-log paper. Another straight line is drawn tangential to the curve and parallel to the first line and a third is drawn parallel to these two and midway between them (that is, midway taking account of the logarithm scale - not geometrically midway). The best fitting curve is then described by the centre line; the three

37

peak errors are equal and simply given by -

$$e_m = \delta p_{30} / p_{30}$$

The justification lies in the following:

Consider $p = kz^n$

Taking logs we have

$$\log p = \log k + n \log z$$

and similarly from $(1 \overset{+}{-} e) p = (1 \overset{+}{-} e) kz^n$

We have $\log p (1 \overset{+}{-} e) = \log k + n \log z + \log (1 \overset{+}{-} e)$

which is a straight line parallel to the line representing $p = kz^n$ Therefore, parallel lines on either side of a particular straight line define zones of constant maximum error.

The Land Locomotion Laboratory soil value system allows that k is a function of plate width but assumes that n is a constant independent of width. This requires that a family of curves such as those shown plotted on logarithmic axes in Fig. 3.3.2. are fitted by a family of straight lines of the same slope. There does not seem to be any logical way of doing this, because once the slope is changed from that obtained by the minimum error method, then the errors at the two ends and the middle become different and can be distributed in any number of arbitrary ways.

The curves on Fig. 3.3.2. have been drawn with maximum errors of 5, 10, 15 and 20% respectively, in order to illustrate how far the curves can depart from straight lines before they cannot reasonably be described by $p = kz^n$.

38

An important point here is that the main use of the pressure-sinkage relation is the computation of sinkage and rolling resistance and this involves the use of $\int p dz$. The operation of integration averages out the errors involved and use of a p - z relation that is nowhere more than e% from the actual can be expected to yield a $\int p dz$ figure that is within roughly $\frac{e\%}{2}$ of the correct figure. This would suggest that a maximum error in p of 20% is acceptable, and as can be seen in Fig. 3.3.2. this is very far from straight. It can be concluded that a lot of the despondency that has arisen at the sight of curves like those of Fig. 3.3.2. has been unnecessary.

The method described, allowing n to vary with b, is suitable for work that is concerned with comparison of actual pressure sinkage curves with chosen equations and will permit examination of the factors which control k and n, for example. In order to describe the k value as a function of plate width, however, it is necessary to consider at least two plate widths. When it is appreciated that this soil-mechanics system is in an early stage of development and is at present used almost entirely as a research tool, it is rather clear that it is best to treat each curve separately and to plot n and k as functions of b. It also follows that a clearer picture will result if at least four plate widths are chosen. Figs. 4.8.6 - 9. show the data from the dry sand and wet sand tests and illustrate the way in which k_c, k_ϕ and n can be chosen in a manner which will permit optimum extrapolation to wider plates than those actually tested.

3.4. Application of the Minimum Error Method to Linear Function

It may not be possible to apply the principal of equal errors minimizing the maximum error to curve-fitting functions in general. However, in the case of one other particular function of interest in soil vehicle mechanics it can be done easily enough. For the linear relationship $p = A + Cz$ an equal positive and negative error gives $p(1 \overset{+}{\underset{-}{}} e) = A(1 \overset{-}{\underset{+}{}} e) + C(1 \overset{+}{\underset{-}{}} e)z$. These are two straight lines that intersect when $Cz + A = 0$ or when $z = \dfrac{A}{C}$.

This application of the method is illustrated in Fig. 3.4.1. which shows the mean pressure sinkage curve for a 2" x 18" plate in compact Ottawa sand on linear axes. P and Q are the intercepts of the curve on the arbitrary upper and lower limits of 30 lb.in.$^{-2}$ and 1 in. A line is drawn through P and Q to cut the z axis at R. A tangent from R is drawn to touch the curve at S and the 30 lb.per.in.$^{-2}$ line at T. The best fitting straight line is RU where U is midway between R and T. A is the intercept of this line on the pressure axis and C the slope. The maximum error involved in describing the experimental curve by $p = A + Cz$ is then e, where $e = \dfrac{PV}{VW}$. This error occurs equally at Q where it is also negative and at S where it is positive.

3.5. A Possible Refinement

The method described in section 3.4 gives a best curve of a chosen family with which to represent pressure as a function of depth. However, ultimately the pressure-sinkage curve will be

used to predict rolling resistance as a function of contact pressure. The rolling resistance depends upon the work done in compressing unit area of soil down to a sinkage at which it can support the contact pressure p_0. That is for a track

$$R \propto \int_0^{P_0} p.dz$$

It is possible to choose the best fitting curve so that the error in $\int p\, dz$ as a function of p is minimized and this will yield the most accurate values of rolling resistance.

The data from a $p - z$ curve can be transformed to give the corresponding $\int p\, dz - p$ curve using Simpson's rule and a computer say; or it could be plotted directly from the Bevameter using an integrating circuit. The constants n and k can be obtained in the following way:

$$\int_0^z p\, dz = \int_0^z k\, z^n\, dz = \frac{k}{n+1}\, z^{n+1}$$

from $p = kz^n$ we have $z^{n+1} = \left[\frac{p}{k}\right]^{\frac{n+1}{n}}$

$$\therefore \int_0^z p\, dz = \frac{p^{\frac{n+1}{n}}}{k^{\frac{1}{n}}(n+1)}$$

Taking logarithms of both sides gives

$$\log \int_0^z p\, dz = \log \frac{1}{(n+1)\, k^{\frac{1}{n}}} + \frac{n+1}{n} \log p$$

so that the slope of a straight line on the log

$p\, dz - \log p$ curve gives $\frac{n+1}{n}$

and the intercept gives

$$\dfrac{1}{(n+1)\,k^{\frac{1}{n}}}$$

$\int p\,dz$ is plotted as a function of p between the limits of pressure corresponding to $z = 1"$ and $z = 10"$ or $p = 30$ lb.in.$^{-2}$. The best fitting straight line is drawn in following the same procedure as previously described, so that an equal maximum error occurs at the chosen limits and around midway between them.

It is not recommended that this method be used at present, since the immediate task is to describe pressure-sinkage relationships adequately. The scheme also suffers from inaccuracies due to the extra operation involved (particularly the integration) and is laborious to use. However, at some later date the principle may be applicable.

4. PRESSURE SINKAGE AND BEARING CAPACITY

4.1. Introduction

All present day theories of soil-vehicle mechanics are based upon the assumption that the pressures beneath an element of a vehicle running gear are equal to those below an appropriately sized and shaped flat plate at the same sinkage. This is a major assumption requiring a great deal of theoretical and experimental support before it can be accepted as an important part of any genuinely scientific theory. Uffelman[7] has shown that it applies quite well to the measured pressures beneath a rigid wheel in a purely cohesive saturated clay and Hegedus[23] has shown that it definitely does not apply to rigid wheels in sands and sandy loam. From a theoretical viewpoint it would be surprising if it were generally true because the contact areas involved in the case of wheels are so small that edge effects are important. It would therefore, seem likely that it is necessary to bring the pressure distribution beneath the flat plate into the picture in a suitable way.

However, the more basic proposition that the only feasible approach to an understanding of soil vehicle mechanics lies through the use of parameters obtained from tests involving simple plates remains true. For this reason the vehicle engineer and the civil engineer have a common interest in the pressures developed beneath small flat plates as they are forced into soil in laboratory soil tanks. To the civil engineer this

43

type of test appears as an excellent model of a foundation but at an excessively small scale, while to the vehicle engineer the scale is reasonable but the similarity of the model is suspect.

It is the very essence of the Land Locomotion Laboratory system that it is a model system. Vehicle performance is not to be predicted from data obtained from simple plate tests of the same order of magnitude as the vehicle (although this in itself would be an important achievement), but from tests using small plates in the same soil. This limits the application of the system to uniform soil conditions that are homogeneous to depths below the zones influenced by the vehicle, that is, to a depth equal to at least the width of the tire or track plus the sinkage. This limitation is serious because layered soils are very widespread; for example, most farm fields are relatively loose for a few inches on a firm subsoil.

It is a surprising thing, but pressure-sinkage data using plates of reasonable size and shape in uniform constant soil conditions are not readily available. Tests were therefore carried out on a family of circular plates of 1", 2", 3", 4" and 6" diameter, and rectangular plates of 1/2", 1", 2", 3" and 4" widths, all 18" long, on the three soils. The soils were uniform in condition to the depth of the vibratory rake (12") in the case of the sands, and to the gravel layer (13") in the case of the clay. The load sinkage curves could be repeated very closely; examples are shown in Fig. 4.8.1. and 4.8.2. and mean curves were drawn through 2 or 3 actual curves to represent the results

and are shown in Figs. 4.1.1., 4.1.2. and 4.1.3. and in tabular form in Tables 4.1.1. to 4.1.7.. The results were used to investigate the relation between slip sinkage and ordinary vertical sinkage and also to provide a set of results against which current ideas could be examined.

4.2. Plate Shape

It has been pointed out in Chapter I and Figure 1.1. that a lateral element of contact area corresponds to a similar crosswise element of an infinitely long strip footing. At present, there are no theories available for any type of wheel or track, other than those that make a rut of width independent of depth - this is luckily the great majority of real cases. There is similarly no theoretical way of relating the pressure beneath a square, circular or elliptical plate, with that beneath a wheel or track. Despite this fact, the practice has grown up of using circular plates to obtain sinkage data. This has been justified by Land Locomotion Laboratory Report No. 57[24], which attempts to show that pressure beneath a circular plate of radius b are in fact and theory equal to those beneath a strip of width b. The theory in this report is questionable since it consists of a circular argument that starts (in L.L.L. Report No. 46[25]) with the assumption of equivalence. The experimental justification is not adequate, being based on two soil types and there is a considerable amount of unexplained variation in the results. One set of careful tests in a uniform soil which show that pressures beneath circular and rectangular plates are not

equal - such as those illustrated in Fig. 4.1.1. is quite sufficient to demolish this proposition. Incidentally the curves of this figure are entirely in agreement with both theoretical and experimental observations of the bearing capacity of foundations below the surface.

Meyerhof points out that the relationships between pressure and sinkage and plate shape are very complex, changing completely with variation in the depth and the soil type. His theory predicts that in clay the bearing capacity of a circular footing will range from 10 to 20% greater than that of a strip of width equal to the diameter as the depth increases. In sand the surface bearing capacity may be as low as half that of a strip rising to double as the depth increases. It must therefore be concluded that plate pressure-sinkage relationships relevant to vehicle sinkage, can at present only be obtained from rectangular strip plates of aspect ratio greater than 4:1.

4.3. Plate Size

The curves for the wet and dry sand show in Figs. 4.1.1. and 4.1.2. and Tables 4.8.1. - 4.8.4. a systematic effect of width over the range 2, 3, 4", but the 1/2" and 1" plates show a different trend. This has been emphasized by plotting pressures at a particular sinkage as a function of plate width in Figs. 4.3.1. and 4.3.2. The explanation is probably that the narrow plates caused mainly lateral compression rather than general shear failure. A similar phenomena has been pointed out by Payne[26] and Zelenin[27] in their experiments on narrow cutting

46

blades. This makes it clear that there is a minimum size below which the small Bevameter plates will not represent the behaviour of the large plate which itself is hopefully representative of some aspects of a wheel on track. If the explanation involving soil compressibility is correct, it would seem possible that the minimum width will go up with compressibility.

These experiments would have been better if the plates had all been of aspect ratio 4½:1. This was realized during the course of the work but time did not allow the use of a set of constant aspect ratio plates except in the clay. However according to Meyerhof (Ref. 20 Page 328) aspect ratio has negligible effect on the pressure-sinkage relationship in sand when $\emptyset$ is less than 35° so that for these experiments with $\emptyset = 32^o$ it is reasonable to treat the plates as if they are all strip footings.

4.4. Minimum Plate Sizes and Loads

The considerations of the previous two sections would suggest a minimum plate width of 2" and the wider plate would then have to be at least 4" if the extrapolation to vehicle widths of up to 20" is not to be too inaccurate. Incidentally, it would appear to be well worthwhile to make at least a limited number of tests with very large plates to check that such extrapolation does in fact work. Since the subsequent theoretical treatment requires at present that the sinkage data be representative of infinite strips, an aspect ratio of 4 to 1 is a bare minimum. This leads

to areas of 16 and 64 sq.in., and a reasonable practical
pressure minimum is 30 lb. per sq. in., giving a minimum load of
1920 lb.

This load requirement demands that any field measurement
be made from a vehicle weighing at least a ton. It makes the use
of the "hand Bevameter" quite valueless unless this instrument is
to be used as a sophisticated cone penetrometer, making records
of cone index against depth and identifying the nature of the
soil by measurements of C and $\emptyset$. This would appear to be a
useful concept.

4.5. Repetitive Loading

The case of the multi-wheeled vehicle in which a succession
of tires follow each other is important in practice. Bekker
proposed that the rolling resistance of a wheel following
another in the same rut could be determined, using the assumption
that the pressure-sinkage relation was unaffected by the
intermittent nature of the loading. That is, the pressure-
sinkage relation for the soil at the bottom of a rut of depth z,
would start from a pressure p_1, as shown in Fig. 4.5.1. This
means that each wheel meets soil with a different set of soil
values. If the soil-pressure-sinkage relation is described by
$p = kz^n$, the second wheel running in the rut of the first wheel
sees soil described by

$$p = k (z_1 + z)^n = kz_1^n + k_2 z^m$$

$$= p_1 + k_2 z^m \qquad \cdots \qquad \cdots \qquad \cdots \qquad 4.5.1.$$

48

This gives rise to a radically different pressure distribution beneath succeeding wheels with greatly diminished rolling resistance (and also probably increased thrust as shown in Fig. 4.5.1). Bekker avoided the use of equation 4.5.1. by integrating $p = kz^n$ between limits p_1 and p_2, but only at the cost of a small sinkage approximation. Equation 4.5.1. has been shown to often give better fit to measured $p - z$ relationships and since it seems necessary to use it for the nth wheel, this is a powerful reason for using it as the general pressure-sinkage relationship. In this case p_1 is theoretically the surface bearing capacity of the soil.

The current Land Locomotion Laboratory evaluation process ignores this work of Bekker's and assumes that the soil in the rut is unaffected by the passage of the preceding wheel and that all wheels meet soil described by $p = kz^n$. It also ignores any strengthening and resulting extra thrust, and is therefore a scheme which will not give adequate advantage to multi-wheeled vehicles if Bekker's assumption is true.

It would seem that Bekker's assumption can be easily checked by a Bevameter pressure-sinkage test carried out in a discontinuous manner. The sinkage is made in, say, one inch steps with the load being reduced to zero before each additional increment of sinkage. Fig. 4.5.2. shows the possible results in the two cases that have been discussed. These represent the two extremes that are possible and either is relatively simple to incorporate into the mathematics describing the vehicle-soil

relationship.

Figs. 4.5.3. and 4.5.4. show the results of repetitive loading tests carried out in wet sand and the clay. It is clear that both are very much closer to the Bekker assumption. It would be interesting to carry out such tests and also measure pressure distribution beneath a succession of wheels to see if they do behave as shown in Fig. 4.5.1. In the meantime it would seem advisable to use Bekker's theory in the Land Locomotion Laboratory's evaluation procedure.

4.6. Pressure-Sinkage and Bearing Capacity

A theory of pressure-sinkage relations has long been in the process of development in the form of bearing capacity theory. Until recently reference to this theory has been a hindrance causing much confusion, due to its limitation to the case of surface footings, with only token regard to sinkage in the form of surcharge. Meyerhof[20] has recently made a major step forward with his theory of the bearing capacity of foundations, treating the depth of the foundation as a variable of prime importance.

A major limitation to the application of this theory to pressure-sinkage relations in top soils is that it does not take into account compressibility - and perhaps it may be doubted whether this will ever be possible. However, any equation describing pressure sinkage over the whole range of C, ϕ, γ and compressibility, must certainly deal with the incompressible case and it would seem that Meyerhof's theory makes an excellent starting point for the development of such an equation. This is

50

particularly so in view of the inadequacy of the present equation disclosed in section 4.8., and the fact that there are no pressure-sinkage data available for compressible soils.

Mayerhof's theory is based on assumed plastic failure zones which perhaps would be rigorously correct for an imaginary plastic material, but which are a basic assumption for real soil. The assumed patterns can be justified by reference to experimental observations of the actual zones and by measurements of the surface deformations and finally by showing that the theory gives correct answers over a range including purely c, c - $\emptyset$ and purely $\emptyset$ soils. This experimental basis is perhaps rather inadequate particularly as far as c - $\emptyset$ soils and the shallow sinkages of relevance to vehicles are concerned.

The theory assumes that an elastic wedge with sides inclined at $45^{\circ} + \frac{\emptyset}{2}$ to the horizontal is formed beneath the base if it is rough, and it is suggested that the bearing capacity of a "smooth" footing is very much less. However, this seems an unnecessary complication because if the state of stress within the wedge is uniform and the sides which are failure planes are inclined at $45 + \frac{\emptyset}{2}$ then horizontal planes are principal planes and therefore no lateral shear stresses act on the base of the wedge. This implies that it doesn't matter whether the base of the footing is rough or smooth. This was checked by comparing load versus sinkage of an 18" x 2" wide footing covered with sand paper with another covered with glass. The results for dry sand are shown in Fig. 4.6.1. at two widely different speeds and they

51

seem conclusive enough. It is interesting to note the following quotation from Meyerhof, "Trial computations have shown that in practice the base can always be taken as perfectly rough".

Meyerhof's theory divides the problem into two parts and separately considers the pressure due to forces acting on a cohesive weightless mass shown on the left of Fig. 4.6.2. and a frictional body with weight shown on the right. There is a zone of radial shear ACD and BCD, and plane shear AED and BED on each side. The logarithmic spirals for the cohesive zone are centred at A. For the frictional zone a centre at any point is chosen such that the spiral passes through the points C and E determined from the cohesive zone, and the resulting passive pressure on BC is a minimum. The soil above the planes AE and BE is treated as a surcharge but the force obtained from it depends upon the conditions on the foundation wall FB. Meyerhof points out that the wall FB considerably increases the bearing capacity if it is rough. This is a point which has been overlooked in the study of soil vehicle mechanics, where footing tests are made without the wall at all corresponding to a tracked vehicle, and the presence of the side walls on wheeled vehicles has been neglected.

The calculation of the bearing pressure from this assumed pair of failure patterns is a matter of considerable complexity, but the answer can be expressed in the familiar form –

$$p = q = cN_c + \gamma \frac{b}{2} N_\gamma + p_o N_q \quad \ldots \quad \ldots \quad \ldots \quad \ldots \ 4.6.1.$$

where the first term represents the influence of the cohesion and

the second, the weight of the material and its frictional
strength and the third, the effect of the over-burden pressure
on the line AE.

The factors N_c, N_γ and N_q are all functions of $\emptyset$ and the
geometry of the figure which is defined by the angle B. Meyerhof
has computed values of these factors as functions of $\emptyset$ for various
values of B. The angle B, however, is a function of $\emptyset$ and z/b
and it is therefore in principle possible to plot the bearing
capacity factors as functions of z/b for varying $\emptyset$, a form which
would be of the most interest. Meyerhof has in fact done this
for the two special cases of purely cohesive and purely
frictional soils. It therefore follows that the factors N_c,
N_γ and N_q are dimensionless and functions of $\emptyset$ and $\frac{z}{b}$, the two
factors that govern the geometry of the strip footing situation
shown in Fig. 4.6.2. According to Meyerhof equation 4.6.1. can
be written –

$$p = q = cN_{cq} + \frac{b}{z} N_{\gamma q} \quad \ldots \quad \ldots \quad \ldots \quad \ldots \quad 4.6.2.$$

where N_{cq} is a function representing the influence of the
cohesion and depends upon N_c and N_q; $N_{\gamma q}$ represents the influence
of the weight of the material and depends upon N_γ and Nq.
Comparison of equation 4.6.2. with the Land Locomotion Laboratory
equation rewritten into two separate terms as –

$$p = \frac{k_c z^n}{b} + k_\emptyset z^n \quad \ldots \quad \ldots \quad \ldots \quad \ldots \quad 4.6.3.$$

shows that there is very little similarity and that the two terms
cannot correspond to those of equation 4.6.3. because b does not

occur in each term in the proper way. Karafiath was able to show
a certain relationship between equation 4.6.3. and bearing
capacity theory but only for purely frictional soils, and then
only by making a fairly radical change to equation 4.6.3. so
that it becomes

$$p = \frac{\gamma}{2} \, b \, N_\gamma + \left[\frac{k_c}{b} + k_\phi \right] z^n \qquad \ldots \quad \ldots \quad \ldots \quad \ldots \quad 4.6.4.$$

This was then shown to fit roughly an approximate bearing
capacity theory suggested by Terzhagi in which

$$p = \frac{\gamma}{2} \, b \, N_\gamma + \gamma z \, N_q + \frac{\gamma}{b} z^2 \, N_D \qquad \ldots \quad \ldots \quad \ldots \quad 4.6.5.$$

Unfortunately, this rough scheme of Terzhagi's has now been
abandoned as unsatisfactory because it assumed that the lateral
extent of the failure zones was not a function of depth.
Nevertheless it does seem a pity that this excellent initiative
by Karafiath was not followed up with the aim of finding a
general agreement between pressure, sinkage, and bearing capacity
for c $-\phi$ soils.

Once this goal is desired and the simple Meyerhof equation
is accepted then it becomes clear that the Land Locomotion
Laboratory equation must be rejected and replaced by one of the
form -

$$p = (k_c' + k_\phi' \, b) \, \left(\frac{z}{b}\right)^n \qquad \ldots \quad \ldots \quad \ldots \quad \ldots \quad 4.6.6.$$

or perhaps better still

$$p = (c \, k_c' + \gamma \frac{b}{2} k_\phi') \, \left(\frac{z}{b}\right)^n \qquad \ldots \quad \ldots \quad \ldots \quad \ldots \quad 4.6.7.$$

in which $k_c' \left(\frac{z}{b}\right)^n = N_{cq}$

and $k_\phi' \left(\frac{z}{b}\right)^n = N_{\gamma q}$

This equation fits the bearing capacity theory to the extent that $N = k' \left(\frac{z}{b}\right)^n$ is capable of describing the functional relation between __both__ N_{cq} and $N_{\gamma q}$ with only a change in the k' value to give the difference between the two (i.e. the same n has to be used). Unfortunately Meyerhof only provides values of N_{cq} and N_q for the cases of $\phi = 0$ and $c = 0$ and for the general case he provides graphs of N_c N_q and N_γ.

For the particular case of saturated clays ($\phi = 0$) Meyerhof gives a graph of N_{cq} against $\frac{z}{b}$ which is reproduced in Fig. 4.6.3. Points taken from this figure for the theoretical capacity of a strip have been replotted on logarithmic axes in Fig. 4.6.4. and a best fitting straight line drawn in by eye. It will be seen that this line fits very well indeed between $\frac{1}{4} < \frac{z}{b} < 2.2$. The equation of this straight line is $N_{cq} = 7.2 \left(\frac{z}{b}\right)^{.172}$ so that $k_c' = 7.2$ and $n = .172$.

At $\frac{z}{b} = 3$ the error involved in using this equation is about 3% but it rapidly increases for higher values of $\frac{z}{b}$. If high values of $\frac{z}{b}$ are to be used (as for example with the Cone Penetrometer) then the dotted line is the best fit and $n = 0$ and $k_c' = N_{cq} = 8.3$. It is clear that for purely cohesive soils the best fit would be achieved by an exponential equation such as

$$p = 8.3 \, c \, (1 - e^{-w\frac{z}{b}}) \qquad \ldots \quad \ldots \quad \ldots \quad \ldots \quad 4.6.8.$$

This was proposed by Evans[6], but is only applicable to this particular case of clay soil. Meyerhof includes two curves showing the results of his experiments in soft and stiff clay and the mean of these is drawn on Fig. 4.6.3. As would be expected this is a rounding off of the experimental curves with a slightly higher maximum (8.5 instead of 8.3) that is not reached until higher values of $\frac{z}{b}$ ($\frac{z}{b} = 5$ instead of 2.2). It is probably reasonable to use this curve as a general representation of frictionless soil and if this is so, then n = .14 and $k_c' =$ 6.75 and a close fit is achieved from $\frac{z}{b} = 0.3$ right up to $\frac{z}{b} = 5$.

For the particular case of dry sand (c = 0) Meyerhof also provides curves of $N_{\gamma q}$ against $\frac{z}{b}$ but unfortunately the $\frac{z}{b}$ axis extends from $\frac{z}{b} = 0$ to $\frac{z}{b} = 40$ and in the region between $\frac{z}{b} = 0$ and 3 the diagram is too small to permit values of $N_{\gamma q}$ to be extracted with any accuracy.

For the general case of a c, ϕ soil separate graphs are given for N_c, N_q and N_γ as functions of ϕ for various values of the equivalent free surface angle B, and m the degree of mobilization of the shear stresses on the equivalent free surface. It is evidently necessary to compute values of N_{cq} and $N_{\gamma q}$ as functions of $\frac{z}{b}$ for various values of ϕ. A start has been made on this task but it involves a great deal of work and there are certain theoretical problems to overcome. Indeed if it were not a formidable task Meyerhof would have done it as it yields results in a much more readily usable form. Once these results are available it will be possible to evaluate the

usefulness of $N = k' (\frac{z}{b})^n$ to represent the bearing capacity factors. However in the meantime some conclusions can be drawn from the shape of the families of curves for the three factors. These were roughly transformed into N as a function of $\frac{z}{b}$ for various values of $\emptyset$ assuming $m = 0$ and simplifying the relation between B and $\frac{z}{b}$. The results are shown in Figs. 4.6.5., 4.6.6. and 4.6.7. The values of N_c, N_q and N_γ as functions of $\frac{z}{b}$ for $\emptyset = 30^o$ are plotted on log-log axes in 4.6.8. These are obviously anything but straight and the errors involved in representing them so are about $\pm$ 14% for N_c, $\pm$ 20% for N and $\pm$ 16% for N_q. If a single slope had to be used for all three then the error would grow to about $\pm$ 25%. The reason for this is obviously the large N value at $\frac{z}{b} = 0$. In practice some small sinkages are necessary to develop any pressure and the curves may be expected to round off as indicated for N at $\emptyset = 30^o$ in Fig. 4.6.5. However this does not straighten the log-log line very much. It appears that for reasonably accurate representation it is necessary to use equations of the form

$$N_{cq} = A + k_c' (\frac{z}{b})^n \quad \ldots \quad \ldots \quad \ldots \quad \ldots \quad 4.6.9.$$

$$N_{\gamma q} = B + k_\emptyset' (\frac{z}{b})^n \quad \ldots \quad \ldots \quad \ldots \quad \ldots \quad 4.6.10.$$

leading to a final pressure sinkage relation

$$p = A c + \frac{B\gamma}{2} b + (k_c' c + k_\emptyset' \gamma \frac{b}{2}) (\frac{z}{b})^n \quad \ldots \quad 4.6.11.$$

This is so complicated that it almost precludes its use for analyses leading to general conclusions. It is possible that

once the initial surface bearing capacity constants A and B have been accepted then the n could be dropped leaving a simple linear relation between p and $\frac{z}{b}$. This would certainly fit the theoretical N factors of Figs. 4.6.5., 6, and 7 with acceptable accuracy, and would involve 4 constants instead of 3. It would have the tremendous advantage of giving a linear pressure-sinkage relation capable of integration around a circular wheel without gross approximations.

The final choice of a pressure-sinkage relationship must await further research. What is clear at this stage is that $p = f(z)$ must be replaced by $p = f(\frac{z}{b})$ and that bearing capacity theory must form the basis of the work.

Equation 4.6.7. represents a major improvement over the existing Land Locomtoion Laboratory equation for several reasons. First, it fits in with any conceivable theoretical approach. Second, it allows the use of computed k and n values for compact soils. Third, it is dimensionally attractive, the k and n values all being dimensionless - the old equation was open to serious criticism on this account. Fourth, it reduces to an equation very similar to the old one for the special case of n = 1 which is roughly true for sands, which is the soil type in which most work with the old equation was carried out. Sixth, it gives a better overall fit to experimental results in sand, wet sand and clay as will be discussed in the next section.

This new equation should enable the three principal approaches to the problem of soil vehicle mechanics to be unified.

The British school studying clay only are using the special case of equation 4.6.7. in which $n = 0$ and $k_c' = 8.3$, or a smaller value if only small sinkages are used. (It should be noted that the Bekker equation could only accommodate this special case by making $k_{\phi} = 8.3$ and $k_c = 0$. Thus, the subscripts selected were incorrect). The cone penetrometer becomes a particular form of a Bevameter footing using very high $\frac{z}{b}$ ratios, which preclude its use as a model of vehicle action, but enable it to accurately indicate stratification.

It is worth noting that it is the consensus of opinion from Terzhagi to Meyerhof that the best way to accommodate the compressible soils into the bearing capacity picture, is to reduce the value of ϕ used to predict their strength. This implies that the form of the pressure-sinkage relation will not change with increasing compressibility and that therefore the form of equations used will apply to all uniform soils.

4.7. A Comparison of the Two Equations

Equation 4.6.7. can be rewritten to read

$$p = \left[\frac{c\, k_c'}{b^n} + \frac{k_{\phi}'\gamma}{2\, b^{n-1}} \right] z^n$$

or

$$p = k'\, z^n \text{ or } k'' \left(\frac{z}{b}\right)^n$$

as compared to

$$p = \left(\frac{k_c}{b} + k_{\phi}\right) z^n \text{ or } p = kz^n$$

This makes it clear that the two only differ in the relation between k, k' or k" and b. Any particular pressure-sinkage curve will have the same n value whichever equation is used and furthermore k = k'.

The constants in the new equation can be evaluated by plotting log p against either log z or log $\frac{z}{b}$, and fitting the best straight line by the minimum-pressure-error method described in Chapter 3. The slope gives n in each case and k" can be obtained as the intercept with z = b or $\frac{z}{b}$ axis is used.

The new equation does nothing whatsoever to help with the basic problem described in Chapter 3, that is that real pressure-sinkage relations do not closely approximate to straight lines when plotted as log p against log z. This is because it uses the same basic relation $p = k z^n$. The curve fitting error for a single curve will be exactly the same for the old and new equations.

However, the relation between k' or k" and b can be expected to be much better than k and b due to the dimensional correctness and sound theoretical physical basis of the new equation.

4.8. Experimental Results and the Two Equations

Pressure-sinkage tests as constant speed were carried out in the dry sand, wet sand and clay, using rectangular and circular plates. The circular plates were of 1", 2", 3", 4" and 6" diameter and at first a set of 18" x 4", 18" x 3", 18" x 2" and 18" x 1" rectangular plates were used. These were originally

chosen on the assumption that an aspect ratio of 4½:1 was near enough to a strip to be comparable with the aspect ratio of 18:1 and for the practical reason that this gave reasonably large forces for the narrow plates enabling the same recorder amplification to be used. The development of the new sinkage equation with its emphasis on dimensionless ratios made it clear that the experiments should be carried out with plates of constant aspect ratio and a new series of rectangular plates, 1" x 4½", 2" x 9", 3" x 13½" and 4" x 18" were used in the clay.

Load was measured as a function of sinkage and a continuous curve plotted on the x - y plotter. Three or four of these curves were represented by a mean curve drawn through them by eye and they were converted to digital form with the results shown in Tables 4.1.1. to 4.1.7.

Very good repeatability was obtained in the two sands using the circular plates. The rectangular plates showed markedly more scatter but were still adequately close. Typical results are shown in Figs. 4.8.1. and 4.8.2. The clay was, of course, harder to deal with, it being difficult to fill in the large holes made by the sinkage tests. Typical results are shown in Figs. 4.8.3. and 4.8.4. Better results in the clay could probably have been achieved if more time had been available.

Fig. 4.8.6. shows the results of a test in which pressure was plotted directly instead of load. This can be done by altering the amplifier gain so that it is inversely proportional to plate area. This is easy to do and if possible this is the

best way to run the tests. It was not adopted because the amplifier gain could not cover sufficient range to deal with the tremendous change in area from 1" dia. to 4" x 18".

The sand results were converted to straight lines on log-log paper using the minimum-pressure-error techniques described in Chapter 3. This yields n, k or k" and e and these have been plotted for the rectangular plates in the two sands in Figs. 4.8.6. to 4.8.9. The e and n values as a function of b are of course the same for the two equations. The k" should be a linear function of b if a good fit to the new equation is desired and it clearly is. k should be a rectangular hyperbola to fit the Bekker equation and it obviously is not. These results therefore show a better fit to the new equation than the old, although they are not entirely satisfactory because the n value was not constant.

The results for the similar rectangular and circular plates in the clay shown in 4.8.10. and 11. are very close together when plotted against $\frac{z}{b}$, and each set can reasonably be represented by a single curve. They therefore fit in with Meyerhof's theory in that they show that $p = f(\frac{z}{b})$.

Bekker's equation has no possibility of accommodating these results because it makes pressure a function of sinkage and not sinkage-width ratio. Given that $\frac{1}{10} < n < \frac{2}{10}$ there is no way of getting the correct answer for clay, the nearest is to fit the rough representation that pressure is independent of sinkage, i.e. $p = 8.3 c$ and $n = 0$. This can only be done by making $8.3 = k_\emptyset$ and $k_c = 0$.

4.9. Experimental Results and Meyerhof's Theory

Meyerhof's theory was applied to the 2" and 4" wide rectangular plates in the dry and wet sand, using the curves for N_γ, N_q and N_c as a function of $\frac{z}{b}$ from 0 to 4 shown in Figs. 4.6.5., 4.6.6. and 4.6.7. p_0 was taken as $\gamma z \cos^2 B$ and an allowance made for m increasing with B. The results are shown in Fig. 4.9.1. From 0 to 3" the agreement between theory and experiment is excellent, particularly impressive is the way the theory allows for the effect of cohesion and plate width. The divergence above 3" is probably due to the approximate method used to calculate the N values from Meyerhof's data, the simplifications necessary being such as to reduce the N values. It may also be possible that the upward curve in the experimental results is a bottom effect because the total depth of the sand was only about 15" and the cultivated layer 12".

The clay results are shown in 4.9.2. and it is clear that theoretical predictions are correctly shaped and as is shown by Fig. 4.8.10. the effect of width is very well accounted for. It is not clear why the experimental results are lower than the theoretical which were based on a value of 1 p.s.i. for the cohesion. It may be that all the voids in the clay from the previous penetrations were not filled in. This is quite likely since the method of removing the holes was quite inadequate.

Fig. 4.8.13. shows the 18" long plates in the clay and the decreasing aspect ratio is clearly shown to cause an increasing maximum pressure reached at decreasing $\frac{z}{b}$ ratio. The limit of

this process is reached when circular plates are used and this is well shown by the results in Fig. 4.8.12. That this fits well with the Meyerhof theory is shown by reference to the theoretical curves for circular and strip footings shown in Fig. 4.6.3.

The agreement between Meyerhof's theory and the rather rough and ready experiments is good enough to justify the conclusion that this theory should form the basis for future thinking and research into pressure-sinkage relationships.

5. THE EFFECT OF GROUSERS ON VEHICLE PERFORMANCE

5.1. Introduction

Traction on hard surfaces is produced by friction, between the vehicle running gear and road, and grousers are unnecessary, except in a vestigial form to permit drainage of water in an effort to prevent hydrodynamic lubrication. While no gain in performance can be expected from providing grousers some drawbacks ensue; vibrations are caused, particularly at speed, forces on the tire carcase or track increase and damage to the road surface is possible. Off-the-road, however, grousers are necessary and since most vehicles operate partly on and partly off the road a difficult compromise is necessary.

The following sections attempt to contribute to the understanding of the action of grousers, when these are simple minor projections on the surfaces of continuous running gear. Grousers can be enlarged until they alter the whole relation between soil and vehicle, but this is a different subject.

5.2. Grousers and Effective Contact Conditions

Grousers help to insure that failure occurs between soil and soil and not between soil and rubber or metal. Lugs will therefore improve traction by an amount depending on the ratio of soil to soil and soil to metal or rubber areas in the total contact area. From the point of view of soft ground performance the lug tip area should be minimized and for vehicles which rarely travel on roads the lug tips can constitute as little as

4% of the contact area for a steel tracked tractor or 24% for an agricultural tractor tire. The lugs on the steel track are as thin as can be from a strength point of view but the tractor tire lugs are a compromise with hard road wear requirements.

The gain in maximum traction will also depend on the difference between soil-soil shear strength depending on c and ϕ and soil-metal or rubber shear depending on c_α and μ. These factors are fairly well understood for soil to steel but not so for rubber. While μ can be as low as 8^0 for a highly polished chromimum plated steel surface it is usually equal to or only two or three degrees below ϕ for the normal rough (steel or rubber) surface beneath a vehicle. Any tread pattern can therefore be assumed to give full frictional traction that the surface of the soil will permit.

The nature of the adhesive forces between soil and steel have been studied by Fountaine.[28] He found that no equivalent of soil internal cohesion exists between steel and soil but that a tensile force can exist if the soil pore pressure is negative. That is, a moisture tension, t, can exist between metal and soil and this can give rise to a shear stress t tan μ independent of applied normal pressure. Payne and Fountaine[29] report that in agricultural soils which are usually frictional with some cohesion, and are rarely saturated, adhesion has been found to be very low or zero. In saturated clays pore pressure, under a vehicle, is likely to be positive rather than negative. It therefore seems reasonable to conclude that negligible cohesive

shear stresses will act between lug tip and soil and that maximum
tractive effort will be given by

$$H = c (a - a_t) + W \tan \emptyset \qquad \dots \qquad \dots \qquad \dots \qquad \dots \qquad 5.2.1.$$

where a_t is the lug tip area. This would imply a very serious
loss of tractive effort in cohesive soil for vehicles such as a
Centurion tank or industrial tracked loader where the lug tip
area is about 1/3 and 1/2 respectively of the total. Such a
loss in traction does not appear to have been investigated
experimentally and this needs to be done.

The nature of the adhesive forces between rubber and soil
has not been investigated and it is not possible to say how much
traction is lost by a large rubber contact area. If c_α for
rubber is as low as it is for steel then the typical American
Military tire and track would indeed be a poor cross-country
device. It seems that a straightforward research effort here
may yield very interesting and useful results.

5.3. Penetration of Hard Ground

If the surface is hard then the contact pressure beneath
wide lugs may be insufficient to cause penetration and the
vehicle will stand on its lug tips. Under these conditions
rolling resistance will be low and the traction due to $W \tan \mu$
is usually entirely adequate. However, in the case of packed
snow and vegetation covered hard clay μ can be very small and
traction insufficient to climb a hill or to pull a tillage tool
whose draft will be high just because the clay is hard. Under
these circumstances narrow lugs can give penetration and

therefore some mobilization of the considerable cohesive strengths available. This is the principal reason for the use of chains around rubber tires and the development of snow tires with aggressive tread. Track laying tractors are often submitted to official performance tests on hard grass-covered clay and it is alleged that sometimes additional performance is obtained by fitting the test tractor with special machined thin lugs.

5.4. Penetration of Weak Surface Layers

Probably the most commonly encountered mobility problem is due to the existence of a weak surface layer on top of a strong soil. Examples are a wet layer on a clay soil due to recent rain where the increased moisture content has lowered the cohesion; or another version of the same situation in which previous traffic has broken down the structure of a clay soil diminishing its internal friction and water holding capacity and turning it from a strong structured c - $\emptyset$ soil into a very weak remolded purely cohesive soil.

A surface cover of succulent vegetation or of farm yard manure can give a similar effect where traction is drastically reduced by simultaneous reduction in both $c_\propto$ and μ . A loose tilled agricultural soil can be made difficult to traverse by the opposite effect in which drying of the surface layer reduces its cohesion, leaving only the frictional component to overcome the high rolling resistance due to the looseness of the soil.

These situations can be greatly mitigated by the use of deep narrow lugs capable of penetrating the surface layer to the

68

firmer soil beneath. It is in these situations that the necessity
for self-cleaning of the tread arises.

5.5. The Effect of Vertical Contact Area

Long lugs on a wheel or track have the effect of giving a
considerable increase in contact areas because of the additional
vertical surfaces on each side. It can be assumed that in soft
ground the cohesion will act along the whole of these surfaces
giving a useful increase in tractive effort in cohesive soils.
The frictional stresses along this surface will depend upon the
lateral pressures and it is not at all obvious what these are.
Bekker[9] made an interesting approach to this problem by
considering the lateral pressures beneath the edges of a strip
load on a semi-infinite elastic material. This yields the result
that the additional traction is given by

$$H_{side} = W \tan \phi \ (0.64 \frac{h}{b} \cot^{-1} \frac{h}{b}) \quad \ldots \quad \ldots \quad \ldots \quad 5.5.1.$$

This equation has been generally accepted and appears in many
recent papers.

Elastic theory may be applicable to the motion of vehicles
on hard soils at low drawbar pulls but generally we are
interested in maximum drawbar pull when the soil beneath the
vehicle and at the sides of its driving gear has failed and is,
therefore, totally beyond the region of elastic stress-strain
relations. It is, therefore, reasonable to approach the problem
of maximum sidewall traction be means of an analysis of the static
equilibrium at failure along the lines of classical soil mechanics.

Fig. 5.5.1a shows a cubic element of soil with one wall in the plane of the sides of the lugs. This vertical plane is forced to be a failure plane due to the geometry of the situation and the shear stresses on this plane act horizontally because they oppose the relative shearing motion. (It is assumed that slip sinkage is negligible and that the track trim angle is small). Since there are no vertical shear stresses on this plane, there are no shear stresses in the y direction on the horizontal planes. Shear stresses in the x direction on horizontal planes are exceedingly unlikely because any shearing motion of horizontal layers is caused by rigid vertical lugs which will have the same effect on adjacent layers. It can, therefore, be assumed that horizontal planes are principal planes and the greatest normal stress on these planes is given by γ z, the hydrostatic pressure.

It, therefore, follows that the state of stress at the side of the track is described by the Mohr diagram of Fig. 5.5.1b, in which the point F represents the failure plane and A, B, and C represent the principal planes; A being horizontal, and B and C vertical. It follows from the conditions of plastic equilibrium that the planes B and C make angles of $(\frac{\pi}{4} - \frac{\phi}{2})$ and $(\frac{\pi}{4} + \frac{\phi}{2})$ with the side of the track.

The values of the principal stresses on B and C can vary between the magnitudes shown in Fig. 5.5.2a and b. The maximum is represented by 5.5.2a in which the Rankine Passive pressure is developed on plane C due to a heavy load on the track causing it

70

to sink, forcing soil out sideways beneath it. The minimum
stress condition shown in Fig. 5.5.2b corresponds to an active
state in which the soil at the sides of the lugs is collapsing
into the space between the lugs beneath the track. This situation
is conceivable at low vertical loads and high slips when it is
possible for the track to rise up on the plane P Q (Fig. 5.5.1a).
If there is any cohesion at all, the active pressure will be
negative for small values of z near the surface, and a lower
limit will be set at about $\sigma = 0$ when tensile cracks will appear
on the plane B.

The state of stress at the sides of the track is therefore
indeterminate and will depend upon the relation between the
contact pressure and the soil strength. Therefore, an analysis
of the common agricultural or earth moving situation where the
vehicle is operating with high drawbar pulls on firm soil with
negligible sinkage would be very difficult, and the best estimate
will be that in this case lateral pressure and, therefore,
frictional lug side thrust is zero. However, where the problem
is to determine performance near the point of immobilization
(as it usually is in military and cross-country transport) it can
be assumed that the bearing capacity has been exceeded with
considerable sinkage and, therefore, passive conditions exist.

At the maximum (passive) stress state the principal stress
σ_1 on the plane C can be obtained from the Mohr diagram as

$$\sigma_1 = 2 c \sqrt{N_\phi} + \gamma z N_\phi \qquad \ldots \quad \ldots \quad \ldots \quad \ldots \qquad 5.5.2.$$

71

where $N_\phi = \tan^2 (45 + \frac{\phi}{2})$

and the stress on the plane B as

$$\sigma_{111} = \gamma z \qquad \ldots \quad \ldots \quad \ldots \quad \ldots \quad \ldots \quad 5.5.3.$$

The shear stress on the failure plane F can then be obtained by considering the horizontal equilibrium of the triangular prism cut out of the unit cube by the plane of the track side. This is shown in Fig. 5.5.3. and from the condition that the resultant force in the F plane direction must be zero, and using the fact that horizontal planes are principal planes, it follows that

$$S_f = (\sigma_1 - \sigma_{111}) \sin (45 + \frac{\phi}{2}) (\cos 45 + \frac{\phi}{2}) \ldots \quad \ldots \quad 5.5.4.$$

$$= 2c \sin^2 (45 + \frac{\phi}{2}) + \gamma z [\tan^2 (45 + \frac{\phi}{2}) - 1] \sin (45 + \frac{\phi}{2})$$

$$\cos (45 + \frac{\phi}{2})$$

$$= 2c \sin^2 (45 + \frac{\phi}{2}) + \gamma z \tan (45 + \frac{\phi}{2}) \cos (90 - \phi) \ldots 5.5.5.$$

In the general case when this equation is applicable the track will have sunk until the lower surface of the track plate is at a depth z_0 and the grouser tip at a depth $z_0 + h$. Then the resultant force from the two sides of a track is given by

$$H_{side} = 2 \ell \int_{z_0}^{z_0 + h} S_f \, dz$$

from which

$$H_{side} = 4 c h \ell \sin^2 (45 + \frac{\phi}{2})$$

72

$$+ 2 \ell\, z_m\, h\, \gamma \tan (45 + \tfrac{\phi}{2}) \cos (90 - \phi) \dots \quad 5.5.6.$$

where $z_m = z_0 + \frac{h}{2}$ the mean lug depth.

It is encouraging to observe that when $\phi = 0$, this reduces to $H_{side} = 2 \ell\, c\, h$.

An interesting aspect of this equation is that the side wall traction has three components; the purely cohesive $2\,c\,h\,\ell$, the cohesive-frictional which is a frictional stress proportional to the cohesive part of the passive pressure given by $4\,ch\,\ell\,[\sin^2 (45 + \tfrac{\phi}{2}) - \tfrac{1}{2}]$ and the remainder a purely frictional term, proportional to the mean depth of the lugs below the surface.

The Mohr Circle showing the passive failure condition in Fig. 5.5.2a appears to have only one circle and two failure planes represented by the points F and E. However, the circle is actually two circles superimposed on each other, one representing the $\sigma_1\,\sigma_{11}$ plane and the other the $\sigma_1\,\sigma_{111}$ planes. There will, therefore, be four failure planes, F, E. and P. Q. of which F along the track side and Q coming up from the tips of the lugs at an angle of $B = \tan^{-1}\left[\dfrac{1}{\cos (45 - \tfrac{\phi}{2})}\right]$ may be observed under suitable conditions. These failure planes are shown in Fig. 5.5.4.

Experimental verification of this theory was attempted using the linear shear apparatus and comparing the maximum thrust on three track plates 30" long x 4" wide and with lugs

1/4", 2" and 4" long. This is a difficult comparison to make because on the long lug plates the total force is made up of the shear beneath the plate, the bulldozing force at the front and an additional frictional force due to the weight of the soil entrained between the grousers and fallen on to the top of the shear plate as it sinks, as well as the side shear.

The tests were carried out in dry sand with zero cohesion. The effective value of ϕ was obtained from the summarized results of all the small lug tests shown in Fig. 6.4.1. These results were less drag which was measured by pulling the shear plates an extra 2" at the end of each test with the whole of the weight removed.

The long lug tests were made in the usual way, measuring horizontal force against displacement and sinkage against displacement. The bulldozing effect of the front lug was measured by pulling it alone, with the weight of the apparatus supported on a long string. A movement of 6" at zero sinkage built up a surcharge in front of the blade and then it was allowed to sink rapidly to give a measure of the bulldozing force appropriate to conditions at the end of the main set of experiments.

Typical force against horizontal movement and sinkage with horizontal movement records for a single lug are shown in Fig. 5.5.5. This has curves for 1.1/4" wide x 2" deep and the 4" wide x 2" deep lugs, and a result for the 4" wide x 4" deep lugs is shown on Fig. 5.5.7. Two or three such tests were carried out and the average value of the front bulldozing force at the final

depth reached in the main test was used to provide the figures in
column 3 of Tables 5.5.1. and 5.5.2.

The experiment using the 4" wide x 30" long track plates
with a range of contact pressures produced the results shown in
Figs. 5.5.6. and 5.5.7. The forces involved at the end of the
run when the shear plates had sunk deeply are analysed in
Tables 5.5.1. and 5.5.2. The final mean sinkage was obtained
from the experimental sinkage curves (as for example are shown
on Fig. 5.5.6.) by adding half the lug height to them, and is
shown in column 2. The bulldozing force is shown in column 3,
and was obtained as described in the previous paragraph. Column
5 was obtained by multiplying column 1 by .55, the mean value of
tan ϕ obtained from the short lug tests summarized on Fig. 6.4.1.
Column 6 shows the weight of entrained soil multiplied by tan ϕ
= .55. ω was taken as being $\gamma \ell$ b ($z_m + \frac{h}{2}$), which assumes that
the sand flows over the top of the track plate like a liquid.
This was observed to be very nearly so, there being a little less
sand on the track than this at the rear but more at the front.
The side force was obtained from equation 5.5.6. taking c = 0
and $\phi = \tan^{-1}$ .55 and $\gamma = $ .06 lb.in.$^{-3}$ The calculated
horizontal force is the sum of columns 3, 5, 6 and 7 and is
shown in column 8. The agreement with the experimental figure
can be seen by comparing column 8 with column 4. This comparison
is presented graphically in Fig. 5.5.8. for the 4" wide x 2"
deep lugs and in Fig. 5.5.9. for the 4" wide x 4" deep lugs. In
order to show the contribution of side shear, the other three

components have been plotted below the horizontal axis and only side shear above. The total force points have been put in from the lowest line so that their distance above the horizontal axis indicates the experimental measure of side shear.

The agreement between theory and experiment is excellent and the results lend strong support to equation 5.5.6. The side force calculated from Bekker's elastic theory is shown above the horizontal axis and it is clear that it leads to forces greater than the limiting equilibrium theory will allow, and much greater than found in practice.

The agreement found depends upon the value of γ and ϕ used in the calculations. The value of $\tan \phi = .55$ ($\phi = 28^\circ 36'$) was the minimum obtained in the shear box tests and equal to the angle of repose and slightly above the mean of the linear shear apparatus results. The minimum density of .06 lb.in.$^{-3}$ corresponding to the minimum shear box ϕ was also used. The sand under the track plate was at a higher density than this to start with and it is assumed that it reduced to the minimum under the influence of the very large disturbances caused by the horizontal movement of up to 12" and sinkages of up to 5". The use of a higher value of ϕ in the calculations would have upset the agreement with experiment and would have made the prediction using Bekker's equation even worse. To make Bekker's equation fit the experimental results, a value of $\tan \phi = .435$ ($\phi = 23\frac{1}{2}^\circ$) would have had to be used. There is absolutely no way in which this could be justified.

It is difficult to draw any firm conclusions from the results of this analysis - other than that the equation 5.5.1. used previously is wrong and that it over-estimates the frictional tractive effort. A major indeterminancy arises due to the difficulty of deciding when full passive conditions arise, although these may be reasonably expected to occur when the contact pressure exceeds the surface bearing capacity given by

$$q = cN_c + \frac{1}{2} \gamma b \quad N_\gamma \quad \ldots \quad \ldots \quad \ldots \quad \ldots \quad \ldots \quad 5.5.7.$$

Equation 5.5.6. is dimensional and complex and this in itself precludes general conclusions. However, a few trial calculations strongly suggest that the frictional component of sidewall traction is quite small in the case of real vehicles. To illustrate the implications of the analysis consider a tractor weighing 5,000 lb. on long narrow tracks with a length of 50" and width of 6" and nominal ground pressure of 8.33 lb. per sq. in. Fig. 5.5.7. shows the tractive effort for a soil where $\phi = 30^o$ and c varies between zero and one lb. per sq. in. Because of the narrow tracks the contact pressure is always high relative to the bearing capacity, and use of the full passive state theory is justified.

It will be observed that in a purely frictional soil the practical 2" lugs gained about 2% over a rough track without lugs while even if the lugs were made 6" long the gain only rose to 11% (Note that using equation 5.5.1. this latter figure would have been 50%).

If the soil had been purely cohesive the lugs would have been vitally important. The 2" lugs would have increased traction by 67% and the 6" by 200%.

In the c - $\emptyset$ soil with c = 1 p.s.i. and $\emptyset$ = 30° the 2" lugs give a gain in traction of 19% and the 6" lugs a gain of 60%. In each case, nearly half the gain is dependent on the friction $\emptyset$.

It is clear in this example that if only the purely cohesive side traction had been included, then an appreciable error would have been made. It seems reasonable to take into account the frictional side force even if it is small because an accurate theory is not likely to result if small items are discarded here and there. The traction equation, for a single track, then becomes

$$H = b \ell c + W \tan \emptyset + H_{side} \quad \ldots \quad \ldots \quad \ldots \quad \ldots \quad 5.5.8.$$

where for $\sigma < q$

$$H_{side} = 2 \ell h c$$

and for $\sigma > q$

H_{side} is given by equation 5.5.6.

5.6. Slip and Excavation

The relation between the slip of a grousered track and its sinkage due to excavation is very widely misunderstood, due principally to an erroneous account of the phenomena in Reference 9. In this account it is proposed that this sinkage increases linearly along the track giving rise to a tail down

trim angle.

The true state of affairs can be understood by reference to Fig. 5.6.1a which shows a track with grousers of height h and spacing e operating at 50% slip on a firm cohesive soil. The grousers are placed in the soil and begin slipping backwards at half the vehicle speed and before they are lifted out of the ground they will have moved half the track length. The distance moved by each grouser from its original place is shown on the diagram. The grouser B will slip half the track link pitch e before the grouser A is placed in the soil. Therefore, half the space between A and B will have been excavated and the track plate carrying lug A will stand on a column of soil of length 1/2 e. If the strength of the clay is nicely chosen with respect to the contact pressure of the tractor, these blocks can remain intact and are moved bodily along sliding over the main body of the soil. This situation is shown in the photograph of Fig. 5.6.3. which shows the track print from a model tractor operating at 50% slip. The important point to note is that the block of soil between the lugs A and B cannot be diminished in volume due to motion after the lug A has entered the ground – because these two lugs are held at a fixed distance apart by the track chain. Therefore, all excavation is entirely concentrated at the front of the track. At first it may appear that the process described will leave a series of rectangular holes in the surface of the soil, and that, therefore, a volume of soil will have disappeared. This is not so. The hole opened up at the front of the track is

closed up again at the back when the last 1/2 track pitch of movement neatly slides the block F up against the now stationary block G, leaving a level surface once again. Normally, of course, the block of soil will collapse to fill up the space between the lugs and this will happen right at the front because if it doesn't the track plate will be above the general level and will, therefore, have a large part of the vehicle's weight concentrated on it.

The relation between the sinkage due to excavation and the slip i and lug height h can be determined by reference to Fig. 5.6.1b. The kinematics of the track motion has been simplified to a right-angled vertical then horizontal movement to clarify the situation; this does not affect the final answer. The track is assumed to have attained a level sinkage z_e due to excavation only and the middle grouser will have excavated a hole of depth $(z_e + h)$ and length (i.e.) which will be beneath the incoming track plate. If we now assume that z_e is caused by the collapse of the column of soil beneath the incoming track plate and that this sinkage is sufficient to cause the soil column to completely fill up the space beneath the track plate then it follows that

Area ABCD = Area EFGH

and: $(1 - i) e (h + z_e) = eh$

or $z_e = \dfrac{h\ i}{1 - i}$ 5.6.1

This relation is illustrated in Fig. 5.6.2a which shows that the

sinkage due to slip excavation is small at the low slips at which track layers normally operate becoming equal to the lug height "h" at 50% slip. From then on the sinkage increases rapidly to infinity at 100% slip.

Figure 5.6.2b illustrates the process of filling in that occurs behind a track which sinks due to excavation. It shows two links following each other to the end of the track and then lifting vertically upwards, and makes it clear that the second link bulldozes soil left by the former up into the rut which is thereby filled in. This is an interesting difference between excavation sinkage and sinkage due to vertical loading and slip, which compact the soil and displace it to the side of the vehicle and leave a rut. In excavation sinkage the vehicle digs a rut, gets down into it, then gets out and fills the rut back in again.

In order to verify equation 5.6.1. experimentally it would be necessary somehow to separate sinkage due to excavation from that due to vertical load and slip. This could possibly be done in a soft clay using a tracked tractor with contact pressure rather less than the bearing capacity. In this material slip sinkage would be negligible and the sinkage due to contact pressure could be assumed constant. Tests would be run at constant slip using wires wrapped around drums of different diameters fixed to the driving sprockets. The drawbar pull would be measured from the force in the slip wires and the resulting load transfer counteracted by means of the sliding weight.

5.7. Slip and Contact Area

Slip does not usually have any effect on contact area, any excavated zones being normally filled up by collapse of the remaining soil pillars. However, in the situation described in the beginning of the previous section where the tracklayer is operating on a firm plastic clay with bearing capacity considerably greater than the contact pressure, this is not so. As the slip increases, the blocks of soil between the track grousers decrease in length and the contact area diminishes in proportion to the slip, so that $A = i \, b \, \ell$. The drawbar pull slip relation becomes similar to that shown in Fig. 5.7.1a. The pull increases rapidly with slip at first in the normal way until nearly the normal maximum is reached. After that the effect of the diminishing contact area decreases the pull linearly with slip. A third phase occurs when the area of the blocks of soil is insufficient to support the weight of the tractor and they collapse so increasing the contact area again, during this phase the drawbar pull becomes constant at a low level.

This phenomena can be readily observed in the laboratory and according to a verbal communication from Mr. P. H. Bailey, it has been noticed during the standard test of crawler tractors on grassland on heavy clay at the N.I.A.E.

If the contact pressure is <u>very</u> low relative to the bearing capacity it is possible to get a reduction in contact area to below the value $i \, b \, \ell$. This is caused by the block of clay flowing beneath the lug tip as the lug pushes it along. When this

happens the blocks develop a curved leading edge (flow is greater
at the ends of the lugs) and diminish in size from front to back
of a tractor track. Fig. 5.7.1b is a photograph of the track of
a model crawler tractor operating in saturated clay showing this
effect. Fig. 5.7.2. shows the same phenomena in the same clay
but beneath a Bevameter annulus, here the motion of each grouser
is the same and therefore the flow is the same all round the ring.

This flow effect only happens at low contact pressures and
this gives rise to a change in shape of shear stress deformation
curve obtained from a Bevameter at the normal loading increases.
Typical results are shown in Fig. 5.7.3. in which the test at
$\sigma = .44$ is the one from which Fig. 5.7.2. was obtained.

5.8. The Effect of Grousers on Rolling Resistance

If grousers were placed into and taken out of the ground
by means of the rectilinear motion shown in Fig. 5.6.2. then the
only effect on rolling resistance would be due to carrying the
vehicles weight on a heavily loaded area (the lug tips) and a
lightly loaded area. This would probably lead to an increase of
work done in soil compaction, particularly in sand, although this
is a proposition that is difficult to prove. In practice, how-
ever, the lugs are placed in and taken out of the soil in a way
that involves rocking them through an angle when viewed in the
vertical plane containing the track. This rocking motion
involves both digging and horizontal compression of the soil and
consumes energy, some of which may have to come from the tractive
effort. The loss due to this effect does not appear to have been

investigated, at least in any published work, although it is
generally believed that the loss will be minimized by placing
the lugs at the front of the track plates as they enter the soil.
(i.e. the opposite way around to that shown in 5.6.2. for
convenience).

The excavation due to slip described in the previous
section obviously needs energy but this comes from sprocket
torque and does not reduce traction - until the tractor chassis
bottoms. It may, therefore, be concluded that the additional
drag due to grousers will be small and will only exceed the gain
in traction where this is a minimum, that is, in sand. It would
seem worthwhile to investigate the digging loss involved in
grouser action in order to find out how to minimize this.

6. THE MEASUREMENT OF SHEAR STRENGTH BY SURFACE SHEAR DEVICES

6.1. Introduction

Linear and annular surface shear devices have been introduced by agricultural engineers (N.I.A.E. Shear box) earthmoving engineers (sheargraph) and military engineers (Bevameter) to meet their common need for in-situ measurements. The requirement is for a test that can be made on or near the surface, under drainage and rate of shear circumstances that simulate those of a vehicle or implement. The top soils met with are unsuitable for removal to the laboratory because of their friable nature and the presence of vegetation.

Several such devices have been used extensively in the past few years, but doubts remain that they do in fact measure c and $\emptyset$. These doubts spring from a small number of attempts that have been made to compare the values obtained from the surface devices with the traditional linear shear box and triaxial machine. Such attempts have usually disclosed significant differences, but very little definite information has been published. The reason for this is quite simply that the principal conclusion from such work has been that it is extremely difficult to measure shear strength by any single method, let alone several. Researchers have not had sufficient confidence in their skill and the quality of their results to publish their findings.

It is important that the situation be clarified because c and $\emptyset$ are the foundation of all soil mechanics, and it is

intolerable that this should not be absolutely sound. One
possible explanation for the prevailing doubt is that the basic
Coulomb equation,

$$s = c + \sigma \tan \phi \qquad \ldots \quad \ldots \quad \ldots \quad \ldots \quad \ldots \quad 6.1.1.$$

is inadequate to describe soil shear strength. This inadequacy
can arise conceivably from the equation's neglect of drainage
and soil water pressure effects, the lack of a time-dependent or
speed term and the two dimensional nature of the equation
although it has to be applied to a three dimensional world.

Drainage and pore pressure effects are the principal
problem confronting civil engineers and they are indeed
formidable - at least if the volume of published work is any
guide. This fact often leads the civil engineers engaged in soil
vehicle mechanics work to take up a particularly pessimistic
attitude towards theoretical solutions based on shear strength.
However, it does not appear that any real difficulty arises with
respect to vehicles and implements in the more common soils. In
the case of saturated clays the rate of loading is so rapid that
there is no doubt full pore pressures will develop and that
friction angles will be small and that the quick undrained
triaxial test is appropriate. For saturated sands the situation
is simplified because we are interested in a free surface
condition with no possible confinement or hydraulic head to give
rise to a neutral stress. A drained test therefore is
appropriate. These two propositions would be very easy to verify
experimentally and it would be well worthwhile to do this. The

two extremes of sand and clay are opposites in that one is a drained case and the other undrained which suggests that somewhere in between, perhaps in the silts, lies a situation where the effective stresses are a function of vehicle speed, and where care would be necessary in the determination of shear strength.

The effect of speed of shearing has been treated in too casual a way by soil-vehicle mechanic workers in the past, and it has in fact usually been ignored. Evidence is accumulating that within the range between the "fast" speed of a standard triaxial machine (.001 inches per second) and the shearing speed of a wheel or implement, say 5 m.p.h. or 60 inches per second, very considerable changes occur. This is quite possibly one of the prime reasons for the variations found between the results of the various shear tests. At the very least it seems reasonable to make all shear tests at a fixed speed, say 24" per second. This would require motorization of hand-held devices like the N.I.A.E. Shear box and Sheargraph, speeding up the laboratory tests and the use of recording instrumentation.

The difference between the two dimensional and three dimensional situation is best described in terms of the magnitude of the third principal stress which is intermediate in size between the two which act to cause failure under plane strain but is equal to the minor principal stress in triaxial conditions. There is quite a lot of evidence[33, 34, 35] accumulating that ∅ at least is dependent on the value of the intermediate principal

stress and that an increase of about 10% is possible between triaxial and plane strain conditions. This is a most unpleasant possibility which would considerably complicate matters. It would seem to be necessary to make a serious effort to come to a definite conclusion on this point.

In the course of the experiments concerned with slip sinkage and side shear forces, it was necessary to determine c and ϕ for the soils used, and the opportunity was taken to make some observations regarding the behaviour of the surface shear devices.

6.2. The Effect of Side Shear

The usual form of Bevameter annulus has thin lugs in order to produce soil-soil failure and these present two vertical shear surfaces as well as the main horizontal plane. The standard Land Locomotion Laboratory procedure is to ignore the vertical shear surfaces and it would seem a good idea to see if this is justified. To simplify matters the frictional and cohesive stresses on the side will be considered separately, using the equation developed in Section 5.5.

According to equation 5.5.6. the frictional side force per unit length of one side, F_ϕ is given by

$$F_\phi = h \, z_m \gamma \, \tan \left(45 + \frac{\phi}{2} \right) \, \cos \left(90 - \phi \right) \dots \quad \dots \quad 6.2.1.$$

The greatest value of h that would be used in a measuring instrument is ¼", and the maximum sinkage about 6". Considering a value of ϕ of $30°$ as a commonly found value, we arrive at a

maximum likely value of F as

F = .078 lb. per inch

Assuming the annulus to be one inch wide and that a normal pressure of 6 p.s.i. is required to give the sinkage of 6", we have that the side force (2 sides) is .156" lb. per in. compared with the base frictional shear of 3.45 lb. per in. If the side force is ignored this gives an error of about $4\frac{1}{2}$%. The surface bearing capacity would be only about .6 lb. per sq. in. so that passive conditions at the sides can be assumed to exist for all readings and therefore equation 6.2.1. will remain valid. At lower contact pressures the sinkage will diminish roughly proportionately and therefore the error will remain about the same.

An error of $4\frac{1}{2}$% is not acceptable and one possibility would be to incorporate equation 5.5.6. into the annular ring situation and analyze the results accordingly. This is hardly practical since it would excessively complicate the reduction of the experimental data. c and ϕ would be mixed up and the sinkage would have to be measured and different equations used depending on whether or not $q < \sigma < q$

The more practicable approach is to reduce the ratio of the vertical to horizontal areas. There is no reason to believe that a grouser height of 1/10" is inadequate, and this in association with a 1" wide annulus would reduce the error due to the frictional side shear to less than 2%.

The cohesive side stresses can be divided into two parts,

one which may be termed purely cohesive and equal to the soil cohesion c, and the other the cohesive-frictional component whose magnitude depends upon the extent to which passive conditions exist at the side of the lugs. For full passive conditions this is given by $c \left[2 \sin^2 (45^{\circ} + \frac{\phi}{2}) - 1 \right]$ which gives $\frac{1}{2}c$ at $\phi = 30^{\circ}$ and zero at $\phi = 0$. It is unfortunately very clear that neither of these two cohesive stresses can be ignored because with the 1/10" lugs on the 1" wide shear plate the cohesion will be measured with an error of 20% at $\phi = 0$ and between 20 and 30% at $\phi = 30^{\circ}$ depending on whether $q < \sigma < q$

If the total cohesive stresses on the vertical surface are given by ξc where ξ is somewhere between 1 and $2 \sin^2 (45^{\circ} + \frac{\phi}{2})$ depending on whether $q < \sigma < q$, then for an annular shear ring of inside and outside radii r_i and r_0 and lug height h we have from $\Sigma M_0 = 0$

$$T = (c + \sigma \tan \phi) \frac{2 \pi}{3} (r_0^3 - r_i^3) + \xi c \, 2 \pi (r_0^2 + r_i^2) \, h$$

or rearranging

$$T = c \left[\frac{2}{3} \pi (r_0^3 - r_i^3) + 2 h \pi (r_0^2 + r_i^2) \xi \right] + \sigma \tan \phi \left[\frac{2}{3} \pi (r_0^3 - r_i^3) \right] \quad \ldots \quad 6.2.1.$$

This equation of course assumes that the full shear strength of the soil acts uniformly across the base of the annulus.

Equation 6.2.1. is a straight line relationship between T and σ which is shown plotted in Fig. 6.2.1. c and ϕ are determined from the graph in the following way.

$$\tan \phi = \frac{\tan \theta}{\frac{2}{3}\pi (r_o{}^3 - r_i{}^3)} \qquad \ldots \quad \ldots \quad \ldots \qquad 6.2.2.$$

If the annulus sank an appreciable amount, say $z > \frac{b}{2}$, then passive conditions can be assumed to exist at the sides and ξ can be taken as $2 \sin^2 (45 + \frac{\phi}{2})$, if it did not sink then $\xi = 1$.

The cohesion is then determined from the intercept value T_o at $\sigma = 0$, by the equation

$$c = \frac{T_o}{\frac{2}{3}\pi (r_o{}^3 - r_i{}^3) + 2 h (r_o{}^2 + r_i{}^2)\xi} \qquad \ldots \qquad 6.2.3.$$

The same principles can be applied to a linear surface shear device of length l, width b and lug height h, using

$$\tan \phi = \frac{\tan \theta}{bl} \qquad \ldots \quad \ldots \quad \ldots \qquad 6.2.4.$$

and

$$c = \frac{H_o}{bl + 2\xi hl} \qquad \ldots \quad \ldots \quad \ldots \qquad 6.2.5.$$

Where K is determined from the sinkage and ϕ as before.

6.3. Drag

The linear shear device is subject to excessive amounts of drag force which cannot be analysed and used in the determination of c and ϕ. This force comprises the bulldozing on the front grouser and drag on the side of the supporting member and top of the shear plate due to the soil collapsing after some sinkage. The front drag forces can only be minimized by a high $\frac{l}{b}$ ratio, but this will give high side drag forces.

In a soil like a dry sand where cohesion is known to be zero, the drag can be separated out by removing all of the

applied weight (including that of the shear plate itself) and continuing the test. This was done for all of the slip-sinkage experiments and typical results are shown in Figs. 7.2.3. to 7.2.7. from which it is seen that drag is dependent on sinkage which is roughly proportional to vertical load, giving an approximately constant value for the drag of 25% of the horizontal force. In the case of the very high aspect ratio 90" x 2" sandpaper tests shown in Fig. 7.2.9. this fell to about 15%. In the clay the drag problem is diminished because of the small sinkage and the problem was overcome by cutting a groove in the clay equal in width and depth to the shear plate, which effectively eliminated the front bulldozing force.

The Bevameter was treated the same way in the sand and the drag measured with the normal load removed. A typical result is shown in Fig. 7.2.11. from which it can be seen that the maximum drag is very much smaller than for the linear devices and that it remains fairly constant in magnitude. It constitutes 33% of the horizontal force at $\sigma = 1$ lb. per sq. in. and $z = 1"$ but falls to about 10% at $\sigma = 4$ lb. per sq. in. and $z = 4"$. The drag problem can therefore be overcome by the unloading technique in dry sand and is probably negligible in clay but presents a major problem in loose loams where sinkage is considerable and both c and $\emptyset$ have to be measured accurately. It must be concluded that the present design of Bevameter ring is unacceptably crude and that a new design is needed in which the drag is not included in the measured torque. Fig. 6.3.1. shows in principle a way in which

this can be done. The grousered ring A is supported from the main loading cylinder B by three strain gauged cantilevers. Torque on the ring is measured from the bending of the cantilevers. Rubber sealing rings D are bonded to the steel parts on their top and bottom surfaces and must be soft to accommodate relative movement without taking too much load off the strain gauged cantilevers. This design also has the advantage of minimising the inertia torques that are transmitted to the strain gauges. This will be a major difficulty if this type of instrument is to be used at vehicle speeds. It is plain that there are several problems to overcome in this design but they are not insuperable.

6.4. Kinematics of Surface Shear Devices

The constants in equation 1.2, this is c, $\emptyset$ and k, would ideally be measured using an infinitely long straight shear plate or an annular ring of infinite radius. Infinitely large measuring devices are somewhat inconvenient to use and the quite small radii and lengths used in practice will affect the values obtained for all the soil constants.

Fig. 6.4.1b shows a shear plate of length 1 that has been moved horizontally a distance j from its initial position shown at a. Imaginary vertical lines in the soil will be bent by this movement somewhat as shown at b. The soil beneath the rear portion of the plate of length 1 - j will all have been deformed horizontally a distance j but under the front portion of length j the deformations diminish linearly to zero at the front of the plate. Since the deformations at the front are less, the shear

stresses are less and the mean shear stress will be lower than would be measured by an infinitely long plate after the same deformation j. If the shear stress beneath an infinitely long footing is related to the deformation j, by

$$s = s_{max} (1 - e^{-\frac{j}{K}}) \quad \dots \quad \dots \quad \dots \quad \dots \quad \dots \quad 6.4.1.$$

then for a footing of finite length l the relation will be

$$s_m bl = b\, s_{max} (1 - e^{-\frac{j}{K}}) (1 - j) + b \int_0^j s\, dj$$

$$= b\, s_{max} \left[(1 - e^{-\frac{j}{K}}) (1 - j) + (1 + \frac{K}{j} e^{-\frac{K}{j}} - \frac{K}{j}) j \right]$$

$$\therefore s_m = s_{max} \left[1 - \frac{K}{l} - e^{-\frac{j}{K}} (1 - \frac{K}{l} - \frac{j}{l}) \right] \quad \dots \quad \dots \quad 6.4.2.$$

Whereas equation 6.4.1. is an exponential in which s tends towards s_{max}, in equation 6.4.2. s_m tends towards $s_{max} (1 - \frac{K}{l})$. H also moves towards this lower asymptote rather more slowly because of the $\frac{j}{l}$ term in $(1 - \frac{K}{l} - \frac{j}{l})$. The $\frac{s}{s_{max}}$ relation from equation 6.4.2. has been plotted in Fig. 6.4.2. for $\frac{l}{K} = \infty$ and $\frac{e}{E} = 10$. This makes it clear that if linear shear plates are to be used for measuring c and $\emptyset$ then $\frac{l}{K}$ must be at least 30 if an acceptable accuracy is to be achieved (the error here will be - 3%). In practice K is found to have a maximum value of about 1 in sandy soils. (Note that 95% of s_{max} is reached at a deformation of 3K inches, or 3 inches for sand with K = 1). Therefore it seems that 30" is a minimum length for a linear shear plate.

94

An annular shear plate is shown in Fig. 6.4.3. If it is rotated through an angle θ then an elementary ring at a radius r will move a distance θr. If the relation between the stress and deformation beneath an infinite strip is given by equation 6.4.1. (1.2) then for the elementary ring,

$$s_\theta = s_{max} (1 - e^{\frac{-r\theta}{K}}) \qquad \ldots \quad \ldots \quad \ldots \quad \ldots \qquad 6.4.3.$$

In the shear annulus therefore, the deformations and hence the stresses will not be uniformly distributed across the ring, and the relation between s and θ will be quite complex. The shear stress is obtained from measuring the torque applied to the ring which will be equal and opposite to the sum of the torques due to the shear stresses acting on annular rings. It follows therefore that,

$$T_0 = 2\pi s_{max} \int_{r_i}^{r_0} (1 - e^{-\frac{r\theta}{K}}) r^2 \, dr$$

$$= 2\pi s_{max} \left[\frac{r_0^3 - r_i^3}{3} + e^{-\frac{r_0\theta}{K}} \left(\frac{r_0^3 K}{\theta} + \frac{2K^2 r_0}{\theta^2} + \frac{2K^3}{\theta^3} \right) \right.$$

$$\left. - e^{-\frac{r_i\theta}{K}} \left(\frac{r_i^3 K}{\theta} + \frac{2K^2 r_i}{\theta^2} + \frac{2K^3}{\theta^3} \right) \right] \qquad \ldots \quad \ldots \quad \ldots \qquad 6.4.4.$$

In practice it has been assumed that the shear stress is uniformly distributed across the ring and concentrated at a hypothetical "mean radius" r_m. This uniform stress is then obtained from

$$T_\theta = 2 s \pi \int_{r_i}^{r_o} r^2 \, dr$$

$$= 2 s \pi \frac{r_o^3 - r_i^3}{3} \qquad \ldots \quad \ldots \quad \ldots \quad \ldots \quad 6.4.5.$$

and the s - j relationship is assumed to be given by

$$s = s_{max} \left(1 - e^{-\frac{r_m \theta}{K}}\right) \qquad \ldots \quad \ldots \quad \ldots \quad \ldots \quad 6.4.6.$$

where r_m is obtained from either

$$r_m = \frac{r_o + r_i}{2} \qquad \ldots \quad \ldots \quad \ldots \quad \ldots \quad 6.4.7.$$

or

$$r_m = \frac{2(r_o^3 - r_i^3)}{3(r_o^2 - r_i^2)} \qquad \ldots \quad \ldots \quad \ldots \quad \ldots \quad 6.4.8.$$

The first has no theoretical justification. The second follows logically from the assumption of uniform stress distribution since it is obtained from dividing the torque by the stress multiplied by total annulus area (or shear force) to give the effective radius.

The validity of the uniform stress assumption was checked for the case of an annulus with r_o = 3.625 and r_i = 2.625 and area of just below 20 sq. inches. The stress as a function of angle of twist was calculated from equation 6.4.4. and compared with the results from using equations 6.4.5. and 6.4.7. for the case of a soil with K = 1. No significant difference was obtained and therefore it may be concluded that this particular annulus has a sufficiently high ratio of $\frac{r_m}{r_o - r_i}$ to justify the uniform

stress assumption.

Solid circular shear devices have become popular because they offer some practical advantages in comparison with an annulus. The first was the N.I.A.E. Shear box[36] which is usually 5" in diameter and it was followed by the Sheargraph.[37] These devices are never used to obtain the deformation modulus k but only c and ϕ, and from equation 6.4.4. it is clear that ultimately as $\frac{\theta}{k} \longrightarrow \infty$ the full value of s_{max} will be approached. Fig. 6.4.4. shows the shear stress-angle of twist relationship for the 5" dia. shear box on a soil with $K = 1$, compared with the curve for the 1 inch wide annulus of the same base area previously discussed. The slow rate of growth of the curve for the circular box is very striking, and could lead to a considerable error if it is not twisted far enough. In practice using the box with a hand torquemeter it is unusual to turn it through more than 90° and this will give a value too low by about 8%. This problem will of course diminish in cohesive soils as k gets smaller. This theoretical result is borne out by practical experience in which the N.I.A.E. shear box gives the same values of c and ϕ as other methods for most soils but lower values for dry sand.

6.5. Experimental Results

In the clay the linear shear apparatus gave a value for c about the same as the triaxial and vane tests and showed little evidence of any ϕ. (See Fig. 7.2.1.) No attempt was made to use it to measure the strength of the wet sand due to the difficulty of allowing for the drag forces. In the dry sand

the drag could be easily discounted by continuing the horizontal movement for a short distance with the shear plate counter-balanced to zero normal load. The results of these tests are shown in Figs. 7.2.3. to 7.2.9. and are summarised in Table 6.5.1. which shows the maximum shear stresses obtained after the drag has been deducted. Linear shear box tests were carried out at maximum and minimum densities of .0705 lb.in.$^{-3}$ and .059 lb.in.$^{-3}$ and also at the density of .066 lb.in.$^{-3}$ which was produced in the soil bin by the action of the vibrating rake. The shear box results are shown in Fig. 6.5.1. The lower value of 28° 36' was corroborated by measurements of the angle of repose and the increase in $\emptyset$ of just over 7° due to the maximum increase in density is in accordance with general experience.[38] [39]

The points representing 28 tests using the linear shear apparatus and the Bevameter are marked on the figure. They start from the origin and move along the shear box line at corresponding density but above 1 lb.in.$^{-2}$ they fall below even the minimum shear box line and are scattered about a line corresponding to $\emptyset = 26^o$ 36' or tan $\emptyset = 0.5$. It seems therefore that the linear shear plate gives a measure of tan $\emptyset$ of 0.5 compared with .625 from the shear box at the same density. This is a reduction of 20%.

This remarkably low value of $\emptyset$ has been commonly observed in the work at Newcastle and also at the Army Mobility Research Centre at Vicksburg (verbal communication), and is characteristic of both linear and annular surface shear devices. It is usually

98

not noticed because it often happens that it is almost exactly compensated for by the drag. It is a phenomenon that needs explanation.

The preceeding section on kinematics was prompted by the search for an explanation and while it is clear that this will account for some reduction, it will only be of the order of 3% for a shear plate of $\frac{1}{h}$ ratio 30:1 as was used.

It is generally held that the change from plane strain to triaxial conditions reduces the effective value of $\emptyset$ by about 10%. Presumably conditions in a shear box approximate to plane strain, and it should therefore give a high value of $\emptyset$. The stress conditions beneath a vertically loaded plate will also be plane but it appears that as a horizontal load is added they will tend towards a triaxial condition. This would be clarified if it was possible to accurately describe the state of stress beneath a shear plate under slip sinkage conditions. So far this has not proved possible.

It was suggested that since the shear box was operated at a very slow speed (.001" per second) and the shear plate quite fast (1" per second) this might be a cause of the difference. The slip sinkage rig was therefore operated at .003" per second by means of the slow speed transmission described in Section 2. The results were opposite to what was hoped for, the value of tan $\emptyset$ falling to an even lower figure. The elasticity of the oil in the loading ram permitted the development of stick-slip vibration and separate static and dynamic values of tan $\emptyset$ = .42

and .37 were obtained.

It seems that this low value of ϕ is part of the slip sinkage phenomena because it is not observed at values of σ below the bearing capacity nor with clay soils in which slip sinkage is not so severe. It is shown in Section 7 that slip sinkage occurs because the applied horizontal force "uses up" some of the soil's available shear strength leaving less to support the vertical load. It seems likely that the converse is also true and that when the shear plate is sinking vertically less shear stress is available to overcome horizontal loads. This would imply that the horizontal soil surface across the tips of the lugs of the shear plate is not a failure surface, as is commonly assumed and as the longitudinal symmetry seems to demand.

It can be concluded that the reason for the low shear stresses will not be clear until a satisfactory stress and shear plane pattern has been discovered.

7. SLIP SINKAGE

7.1. Introduction

The Land Locomotion Laboratory soil values system is based on measuring the resistance offered to vertical and horizontal loads as functions of the resulting deformations in two separate tests. The horizontal load test is carried out by first loading the shear plate vertically and then horizontally, and is therefore an inclined load test at varying angle of inclination. Vertical deformations during this test are ignored. The information from the two tests is then fed into the vehicle situation making the assumption that the principle of superposition applies and that sinkages due to vertical loads are not influenced by the existence of horizontal loads. This is an unjustified assumption made for simplicity in the face of the fact that additional sinkage is seen to result from the shear forces in a large proportion of horizontal load-deformation tests. It is now well known that in fact horizontal loads reduce the capacity of the soil to support vertical loads and that therefore the sinkage of vehicles is a function of drawbar pull or slip and the phenomena has come to be known as slip sinkage. The drawbar pull of a tracklaying vehicle applies a longitudinal horizontal force to the soil beneath the track. The corresponding strip foundation problem is shown in Fig. 7.1.1a and there does not appear to be any published work on this situation. It is a three dimensional problem with a plane

101

of symmetry and should not be confused with the laterally loaded strip foundation problem shown in Fig. 7.1.1b. This has been the subject of much work and reasonable useful solutions are available[8,30], it is a simpler two dimensional problem. These two separate vehicle and foundation situations both tend towards the same problem as the aspect ratio diminishes and they become square corresponding roughly to the contact patch of a wheeled vehicle.

The effect of slip sinkage on the performance of a track-laying vehicle has been discussed by Reece and Adams.[16] They show that since the horizontal stresses and deformations increase from front to back of a slipping track, then so will the additional slip sinkage, causing the vehicle to take up a tail down attitude with a trim angle θ.

A theory was developed to take into account the slip sinkage angle θ assuming that it could be expressed as a function of j the linear deformation as a result of static soil tests.

Fig. 7.1.2. shows the forces acting on a tractor with trim angle θ.

From the vertical equilibrium -

$$W = \Sigma p \delta a \cos \theta + \Sigma s \delta a \sin \theta \quad \ldots \quad \ldots \quad \ldots \quad 7.1.1.$$

where δa is an element of ground contact area. From the horizontal equilibrium

$$L = \Sigma s \delta a \cos \theta - \Sigma p \delta a \sin \theta \quad \ldots \quad \ldots \quad \ldots \quad 7.1.2.$$

From equation 1.2. at a slip i

$$\Sigma s \smallint a = H_i = B\ ac + Bap_m \tan \emptyset \quad \text{...} \quad \text{...} \quad \text{...} \quad 7.1.3.$$

where $B = 1 + \dfrac{K}{i1}\ e^{-\frac{i1}{K}} - \dfrac{K}{i1}$ is a function of slip that is

obtained by integrating equation 1.2. along the track length

and $ap_m = \Sigma p \smallint a$

Substituting 7.1.3. in 7.1.1.

$$W = p_m a \cos \theta + acB \sin \theta + p_m a\ B \tan \emptyset \sin \theta$$

from which

$$ap_m = \frac{W - acB \sin \theta}{\cos \theta + B \tan \emptyset \sin \theta} \quad \text{...} \quad \text{...} \quad \text{...} \quad 7.1.4.$$

Substituting 7.1.4. and 7.1.3. in 7.1.2.

$$L = acB \cos \theta + \frac{W - acB \sin \theta}{\cos \theta + b \tan \emptyset \sin \theta} (B \tan \emptyset \cos \theta - \sin \theta)$$

$$\text{...} \quad \text{...} \quad 7.1.5.$$

when $\theta = 0$ this reduces to

$$L = acB + W \tan \emptyset\ B \quad \text{...} \quad \text{...} \quad 7.1.5a.$$

Although equation 7.1.5. is only a simple trigonometrical
function of the factors in equation 7.1.5a. it is complicated
enough to obscure the basic mechanics of the effect of the tilt
angle. This can be seen by returning to Fig. 7.1.2. from which
it is clear that there are three components to the reduction in
traction represented by the difference between equation 7.1.6.
and 7.1.5. The total normal force and therefore the frictional
traction on the contact area is reduced because part of the
tractor's weight is supported by the vertical component of the
shear stresses. The part of the shear stresses contributing to

103

traction is reduced because these shear stresses do not act in the direction of the drawbar pull. Part of the shear stress is used up overcoming the backward component of the normal stresses.

It was at first thought that the whole of the effect of the tail-down sinkage could be described as an additional rolling resistance, to be called the slip-sinkage-rolling resistance. However, it is clear now that only the last of the three components described above is in fact a force opposing motion that fits the description of a rolling resistance. It is suggested that the reduction in traction be called the slip-sihkage-loss.

For an infinitely long track at 100% slip on a cohesionless soil equation 7.1.5. simplifies to

$$L = W \frac{\tan \phi \cos \theta - \sin \theta}{\cos \theta + \tan \phi \sin \theta} \quad \ldots \quad \ldots \quad \ldots \quad \ldots \quad 7.1.6.$$

This is the Micklethwaite equation, $L = W \tan \phi$, modified to take account of the effect of the trim angle. It is useful in that it gives an impression of the magnitude of the effect. The function $\frac{\tan \phi \cos \theta - \sin \theta}{\cos \theta + \tan \phi \sin \theta}$ has been plotted against θ from 0 to 20° at various values of ϕ in Fig. 7.1.3. This shows a very drastic reduction in pull for quite small trim angles, the reduction being greater for small angles of ϕ. 10° is probably a severe trim angle for a full sized vehicle in the field and in this case traction is reduced to 70% of $W \tan \phi$ for $\phi = 45^{o}$ and 63% of $W \tan \phi$ when $\phi = 30^{o}$.

For an infinitely long track at 100% slip in a frictionless soil equation 7.1.5. reduces to

$$L = ac \left[\cos \theta + \sin \theta \tan \theta \right] - W \tan \theta \quad \ldots \quad \ldots \quad 7.1.7.$$

The function $\cos \theta + \sin \theta \tan \theta$ is only very slightly greater than 1 for θ between 0 and 20° and the equation can therefore be simplified to

$$L = ac - W \tan \theta \qquad \ldots \quad \ldots \quad \ldots \quad 7.1.7a.$$

This can be considered as the normal drawbar pull minus the component of the vehicle weight acting down the "hill" represented by the trim angle. It is interesting to note that in the purely frictional soil the reduction is considerably greater than this.

The effect of slip sinkage on a wheel will be to reduce the supporting capacity of the soil beneath the axle where the shear deformation is greatest. This will mean that the pressure distribution changes so that higher pressures exist at the front where they have greater backward components and therefore rolling resistance will be increased. Traction may be reduced because normal pressures are concentrated to the front of the contact patch where shear deformations are a minimum. Wills[15] showed that this will cause a reduction in performance in the case of very short contact patches.

The mechanics of a wheel have not been satisfactorily worked out for situations in which slip-sinkage is unimportant so it therefore seems reasonable to concentrate on the simplest possible situation concerning a rigid tracklayer. Since pressure

distribution appears to be of secondary importance, the problem will have been solved if the trim angle θ can be predicted. This could be done if the relationships between z_i and s, σ, j for various track widths could be determined in a simple test analogous to the Bevameter annular shear test.

It was therefore decided to explore these relationships using linear shear plates of varying widths. The plates could be loaded vertically with dead weights and forced to move horizontally while remaining free to sink but not tilt. Suitable arrangements were made to measure the horizontal force as a function of horizontal movement and the actual trajectory of the shear plate as a curve with x and z coordinates. The apparatus is shown in Figs. 2.1.1. and 2 and it should be noted that the pressure distribution beneath the shear plate is not affected by the external loading. The moment caused by the difference in height of the horizontal motion ram and the grouser teeth is counteracted by an equal and opposite moment in the double parallel linkage. Tests were conducted in the dry sand, wet sand, and clay.

The apparatus can be used at constant rate of horizontal deformation using the hydraulic transmission systems shown in Figs. 2.1.2. and 2.2.1. and to give different velocities. Alternately it was intended to use controlled horizontal loads by slowly increasing the pressure applied to the ram, by steadily increasing the pressure setting of the relief valve in the circuit. So far there has only been sufficient time to carry out

constant strain rate tests.

Vehicles apply a steady rate of horizontal strain to the soil corresponding to the slip velocity. The problem here is to determine the slip sinkage as a function of applied horizontal deformation. There does not at present seem to be much prospect of obtaining a theoretical solution to this problem, because there is little understanding of the relation between horizontal stress and deformation. The foundation problem is rather different in that it is usually the horizontal load which is fixed, and it should be possible to determine the resulting sinkage, at least for incompressible soils.

The aim of investigations of slip sinkage must be to evolve a suitable equation for relating slip sinkage, z_s, to the slip deformation and the length, breadth and pressure on the contact area. This would be another curve-fitting equation the constants of which would be determined from a suitably designed soil loading test. Such an equation would be most likely to succeed if it was derived from a theory relating the sinkage of strip footings to the magnitude of the vertical and longitudinal forces imposed on them. Such a theory would have considerable academic interest and it would fill a real gap in our understanding of the bearing capacity of foundations.

7.2. Observations Concerning Slip Sinkage

Typical results of the constant strain rate-slip sinkage experiments are shown in Figs. 7.2.1. to 7.2.10. Each graph shows sinkage z as a function of horizontal movement x at the top

and horizontal force as a function of x at the bottom, both for various values of the mean contact pressure σ. The upper and lower horizontal scales are different in most of the figures. The results of 28 of these experiments in the three soils are summarized in Fig. 7.2.12. where the sinkage after 3k was chosen because it is just sufficient to make the soil develop nearly its full shear strength. (95% if the soil exactly fits

$s = s_{max} (1 - e^{-\frac{i}{K}})$). K was taken as 1" for the sand and 0.33" for the clay.

The following observations can be made.

A. Rough sand paper develops full soil shear strength, in sand at least. A sandpaper covered shear plate abo has the same deformation and slip sinkage characteristics as one with small lugs, compare Fig. 7.2.4. with 7.2.6.

B. Slip sinkage can be an effect of major importance in frictional soils but is much smaller in purely cohesive soil. In studying Fig. 7.2.12. and comparing Fig. 7.2.1. with Fig. Fig. 7.2.4. it needs to be borne in mind that the clay with a cohesion of about 1 lb.in.$^{-2}$ is a very weak soil, that would not support the lightest cross-country vehicle, whereas the sand is compact and strong and would support even an ordinary road vehicle.

C. Slip sinkage can best be described as a function of shear deformation rather than shear stress. The sinkage goes on rising after the horizontal force has reached its maximum.

D. The slip sinkage curves were asymptote to lines representing a constant rate of sinkage - not as might be expected to a fixed sinkage. This is illustrated in Fig. 7.2.7. where results are shown from tests in which the shear plate was started off at a considerable depth, and also in Fig. 7.2.8. where major sinkage was prevented by a heavy surcharge on the soil surface on each side of the shear plate.

E. Slip sinkage was less for stronger soils, even the addition of 1/10 lb. per sq. in. cohesion to the sand (achieved by wetting it) was sufficient to reduce its slip sinkage appreciably.

F. In sand the additional sinkage due to slip is roughly proportional to the initial sinkage due to mean contact pressure. The ratio of the two decreases with increasing contact pressure.

In clay however the additional sinkage is more near to being constant.

G. In sand slip sinkage at a particular contact, pressure is only slightly reduced by increasing shear plate width, in accordance with observation F. This is shown by Fig. 7.2.12.

H. Slip sinkage occurs in a manner similar to sinkage under vertical load only, that is by lateral soil flow. The rupture planes break out on the surface closer to the sides of the shear plate and occur at a smaller vertical sinkage. The soil therefore behaves in a more brittle manner than it does under vertical loads.

I. The single set of results from the small annulus in dry sand fit neatly into the summarized results for the linear shear plates shown in Fig. 7.2.12. This is encouraging in that it suggests that the information necessary to predict slip sinkage can be obtained from existing Bevameters with only a slight modification to enable them to measure annulus sinkage as well as twist.

J. Theoretical approaches that assume a triangular prism of soil to exist below the shear plate are supported by tests in which a prism of wood covered with sandpaper was placed beneath the 30" x 2" sandpaper shear plate. Compare Figs. 7.2.6. and 7.2.10.

K. The 30" long shear plates showed similar slip sinkage trajectories to the 90" plates and may be considered long enough to represent infinite strips. Compare Figs. 7.2.6. and 7.2.9.

7.3. The Basis of a Slip Sinkage Theory

The physical nature of slip sinkage can be appreciated by considering the equilibrium of a triangular element of soil beneath the shear plate with sides sloping at $45^\circ + \frac{\phi}{2}$ from the horizontal, as shown in Fig. 7.3.1. It is assumed that the sides of this triangle are failure planes, once the surface bearing capacity has been exceeded. This is an assumption of most bearing capacity theory and although is not kinematically correct, it appears to give reasonably appropriate results. Its use in this particular situation is justified to some extent by

110

experiments in which the two-inch sandpaper shear plate was tested on a 2" - 60° wooden triangle with the three sides covered with sandpaper. The results of normal sinkage and slip-sinkage tests of the 30" x 2" sandpaper with and without the solid prism are shown in Figs. 7.2.6. and 7.2.10. from which it is seen that its presence makes very little difference.

To simplify matters the two cases of a purely frictional soil and a purely cohesive one will be considered. The forces acting upon a unit length of the elastic soil wedge beneath a strip footing of unit width in sand are shown in Fig. 7.3.1a. for the case of a vertical load per unit length which is greater than the surface bearing capacity, so that, from $\Sigma F_z = 0$

$$P = \frac{W}{2\left[\cos\left(45 + \frac{\phi}{2}\right) + \sin\left(45 + \frac{\phi}{2}\right)\tan\phi\right]} \quad \ldots \quad 7.3.1.$$

When the maximum horizontal load is applied to the strip footing, the forces on the wedge change to those shown in Fig. 7.3.1b. Part of the frictional force on the side of the wedge is now used up carrying the horizontal load and less is available to support the vertical load, and the normal force on the side of the wedge will have to change from P to P' and the total frictional force available will be $P'\tan\phi$, of which only $\tan\phi\sqrt{P'^2 - \frac{W^2}{4}}$ will act in the vertical plane.

From the vertical equilibrium we have:

$$\frac{W}{2} = P' \cos (45 + \frac{\phi}{2}) + \sqrt{P' - \frac{W^2}{4}} \tan \phi \sin (45 + \frac{\phi}{2})$$

which rearranges to:

$$P^2 \left[\tan^2 \phi \sin^2 (45 + \frac{\phi}{2}) - \cos^2 (45 + \frac{\phi}{2}) \right] + P' \left[W \cos (45 + \frac{\phi}{2}) \right]$$

$$- \frac{W^2}{4} \left[1 + \tan^2 \phi \sin^2 (45 + \frac{\phi}{2}) \right] = 0$$

a quadratic which yields:

$$P' = W \frac{- \cos B \pm \sqrt{\cos^2 B + \tan^2 \phi \sin^2 B - \cos^2 B \, 1 + \tan^2 \phi \sin^2 B}}{2 \left[\tan^2 \phi \sin^2 B - \cos^2 B \right]}$$

where $B = 45 + \frac{\phi}{2}$

This can be simplified to:

$$P' = W \left[\frac{\cos B \cos^2 \phi - \sin \phi \sin^2 B}{\cos 2 B + \cos 2 \phi} \right] \quad \ldots \quad \ldots \quad \ldots \quad 7.3.2.$$

In a purely cohesive soil the situation is quite different and the forces involved are shown in Fig. 7.3.2. Under vertical loads exceeding the surface bearing capacity a unit length of the wedge will be in equilibrium with a normal load P and a shear force of 2C acting upon the two wedge faces. These forces are shown in Fig. 7.3.2a. and from considering the vertical equilibrium it follows that

$$P = \frac{W}{\sqrt{2}} - \frac{C}{\sqrt{2}} \quad \ldots \quad \ldots \quad \ldots \quad 7.3.3.$$

When the full horizontal load of C lb. per unit length the forces change to those at Fig. 7.3.2b. and

$$P' = \frac{W}{\sqrt{2}} - \frac{C}{2} \quad \ldots \quad \ldots \quad \ldots \quad 7.3.4.$$

From bearing capacity theory W can be between about 5.1c at the surface and 8.3c when the footing has sunk to a depth of 3b. Considering the situation when $W = 6c$, the effect of adding the maximum possible horizontal force is to change the resultant force applied by the wedge to the soil in the vertical plane from 3.46c at 56° 18' to the horizontal to 3.77c at 52° 36'. Both the increase in magnitude and decrease in angle would require further sinkage to enable the surrounding clay to support them, but it is to be expected that this will be small since the changes are so slight.

A similar calculation was carried out for sand with $\phi = 30°$ and the results are shown in Fig. 7.3.1c. It can be seen that the applied force has increased greatly (18%) and the angle to the horizontal diminished very appreciably. It is rather obvious that if the sand were only just in equilibrium under the vertical load only, then the effect of the additional horizontal load would require considerable further sinkage in order to restore equilibrium.

It seems then that slip sinkage occurs because the effective shear strength of the soil, as far as vertical loads are concerned, is diminished because some of the shear strength is used up in supporting the horizontal load. The great difference in behaviour between cohesive and frictional soils arises from their different area dependent, versus load dependent characteristics when considered in relation to the conditions of equilibrium.

To really settle the matter, the analysis needs to be taken further to give the final equilibrium sinkage that the shear plate would reach after the maximum horizontal load was applied. Meyerhof's bearing capacity theory would have to be used as a basis, because it is the only available analysis that takes into account the growth of bearing capacity with sinkage.

An equilibrium sinkage could possibly be computed on the basis shown in Fig. 7.3.3. The upper drawing shows a wedge-shaped footing with $\delta = \emptyset$ that has come into equilibrium under the applied vertical load W at a sinkage z, that would be computed using Meyerhof's theory. The lower drawing shows the slip sinkage situation transformed from a three-dimensional problem to a two dimensional one. The footing base friction has been reduced from $\emptyset$ to λ so that the passive pressure on the wedge gives a force in accordance with equation 7.3.2. The value of $\emptyset$ for the soil in the plastic zones would have to be approximately reduced to $\emptyset'$ to allow for the effect of the horizontal stresses. It might be possible to do this by considering the three dimensional equilibrium of prisms of cross-section ABCD in the same way as it was done for the triangle ABD. This would probably suggest a varying effective $\emptyset'$, changing from λ at the side of the triangle to the full $\emptyset$ at the line B E. It may prove difficult to compute sinkages using spirals with varying $\emptyset$ and perhaps a further approximation resulting in a fixed reduced $\emptyset$ may be possible.

The discussion so far has really been concerned with a footing with a solid wedge fixed beneath it with sides sloping at $(45 + \frac{\phi}{2})$ to the horizontal and very rough surfaces. It seems likely that the soil wedge will change in shape due to the changing stress pattern beneath the shear plate. An attempt has been made to describe the stresses beneath the plate and the resulting directions of principal planes and failure surfaces, but without success. It does not seem possible to find a simple pattern that satisfies both the conditions of equilibrium of a Coulomb material at failure and the longitudinal symmetry of the system. However, it is believed that the hypothesis using the fixed section prism describes well the physical mechanism responsible for slip sinkage. The experiment with the sandpaper covered wedge suggests that it may in fact be quite near to the real situation.

The discussion of the physical nature of slip sinkage has so far been conducted in relation to incompressible soils. In loose soils the normal sinkage under vertical loads is partly due to compaction and partly due to plastic flow. Slip sinkage will presumably occur due to the reduction in effective shear strength discussed previously, but additional sinkage may be expected to be caused by additional compaction. Vandenberg[31] has shown that compaction in loose soils is described by

$$\gamma = c_s \, \sigma_m \, (1 + \bar{e}_{max.})$$

where $\bar{e}$ is the logarithmic strain (shear) and σ_m is the applied mean normal stress.

The hydrostatic pressure causes some compaction by moving together soil particles with some re-orientation, but the imposition of the shear strain moves particles relative to each other, giving more opportunity for re-orientation and consequently greater compaction. It is plain therefore that slip will cause additional compaction.

The continuing sinkage after long horizontal movements is one of the most interesting results of the experiments. It occurs even at very low contact pressures on both the sands and clays. To determine if the slip sinkage would ever finish, some tests were carried out in which the shear plate was buried deep in the soil before it was forced to move horizontally. The results are shown in Fig. 7.2.7.; test 1 is the normal run with an initial sinkage under vertical load of 0.3" increasing to 2.2" after 10" of horizontal movement. Tests 2 and 3 started at a sinkage of 2.3" and 4.4" respectively and both still show increasing sinkage although at a slow rate.

Another test was conducted in which a heavy surcharge was placed on the soil surface on each side of the shear plate, before it was loaded. The results are shown in Fig. 7.2.8. and by comparison with Fig. 7.2.5. it can be seen that the initial sinkages of .25" and .95" have been reduced to zero by the surcharge. The ensuing slip sinkage is also reduced but shows no sign of reaching an equilibrium value. It was at first thought that this was a frontend effect. As the shear plate moves forward the front is always coming on to unstressed soil which

perhaps cannot carry its share of the load. If this is so, then the shear plate should be long relative to its total horizontal movement if it is to represent an infinite strip. The plates used were only 30" long which is short relative to the 15" of horizontal motion. To check this idea a shear plate 90" long x 2" wide was used in the dry sand with a typical result shown in Fig. 7.2.9. which can be compared with Fig. 7.2.6. for the 30" x 2" plate. From these and other tests it was clear that the length made no appreciable difference to the slip sinkage (although it did affect the shape of the shear stress deformation curve). It therefore appears that the front-end effect is not important - probably because the fresh soil engaged is at a considerable depth and is preloaded by the weight of soil above it.

A more plausible explanation can be reached by considering the equilibrium of the wedge of soil which has previously been assumed to move with the shear plate. It is a fundamental characteristic of Coulomb Friction and soil - soil shear stresses that they act in a direction opposite to the shearing motion or strain. This is true of both frictional and cohesive shear stresses but is not generally true of the relation between complex stress and strain.

When a vertical load is applied to the shear plate it sinks vertically and soil slides up the faces of the wedge causing the shear stresses to act vertically. When the wedge is forced to move horizontally, then the shear stresses act horizontally;

117

some of the support is lost and the plate sinks, restoring a vertical shear force component. When the horizontal force reaches its maximum value the shear forces will act in the direction shown in Fig. 7.3.1b and 7.3.2b and the relative motion between the wedge and the layer of soil adjacent to it must be as shown. (Note. This is not the absolute direction of motion because the soil at the side of the wedge will also be moving, increasing the horizontal component of absolute motion). Presumably the shear plate cannot apply a greater force to unit length of wedge than $W \tan \emptyset$ or c and at this point the wedge may be expected to stop moving while the shear plate slides along the top of it. Sinkage would then cease and the forces would remain as shown at b in Fig. 7.3.1. and 2. This was precisely what happened when the wooden wedge was used, with no positive connection between wedge and shear plate. Typical results are shown in Fig. 7.2.9.

With a positive drive between wedge and plate however, sinkage proceeded exactly as in the tests without the wedge shown in Fig. 7.2.6. In order that sinkage may cease the wedge would have to move horizontally and the whole of the shear stresses would then be horizontal and the wedge would be supported on the normal forces only. This however, is not possible because it requires greater horizontal shear forces on the sloping sides of the wedge than can be provided on the top surface. In cohesive soil this is simply because the sloping sides have 2 times the area of the top. In a purely frictional soil with $\emptyset = 30^{o}$,

118

if the wedge is supported only by forces P' normal to the wedge sides, then $P' = W$ and $2P' \tan \phi = 2W \tan \phi$, twice the maximum force that can be applied to the top of the wedge. It therefore is clear that the force arrangements shown in Figs. 7.3.1a and b are limiting cases, and if further horizontal movement is imposed on the shear plate then it can be expected to go on sinking in approximately the same direction as when the maximum horizontal force was reached. The most unsatisfactory feature of this discussion is that it is not at all clear why the wedge is obliged to move with the shear plate once the maximum shear force is reached.

7.4. Slip Sinkage and Tracklayer Performance

A clear picture of the slip sinkage behaviour of an infinitely long strip footing can be obtained from the tests with the linear shear apparatus. The next step is to apply this information to predict the behaviour of a model tracklayer with tracks of the same width operating in the same soil. A preliminary attempt to do this was made using the model tracked vehicle set-up described in Section 2.3. It will be recalled that the principal features of this are controlled drawbar pull from weights and string, fixed location of the resultant soil force on the track surface by use of a sliding balance weight and measurement of sinkage at front and rear of the track and distance travelled in each revolution of the sprocket. A crude track link dynamometer was made to give an indication of the pressure distribution beneath the track.

The drawbar pull at a particular slip can be calculated in the usual way from the shear stress deformation curves if there is no slip sinkage. If there is, it is necessary to determine the sinkage at the front of the track and the trim angle θ. The effect of the trim angle can be taken into account by means of equation 7.1.5. and the initial sinkage by means of some suitable rolling resistance theory.

The sinkage at each end of the track can be determined graphically in the following way. Typical slip sinkage curves for an infinite strip of the same width as the track are shown in Fig. 7.4.1b. These are curves of slip sinkage z against linear shear deformation j for various uniform contact pressures $\sigma_.$, σ_2, σ_3, etc. A curve of σ_m the mean contact pressure of the tractor can be drawn in by interpolation. A vertical line cd can be drawn in at j = i 1 and this represents the shear deformation beneath the rear end of the track of length 1, at a slip i. The deformation j at the front of the track is zero. If the track is straight and rigid then it follows that deformations j must grow linearly along the track and therefore a 'j' axis is an 'x' axis to another scale (related by j_x = ix). It is also necessary that sinkages grow linearly along the track length. These two requirements are satisfied if the relation between z, j and x from x = 0 to x = 1 at a slip i is represented by any straight line such as fg or hk. The pressure distribution represented by such a line can be obtained from its intersections with the mean contact pressure "contours". The line hk for example results in

120

the pressure distribution shown at c which evidently has a mean pressure between σ_2 and σ_3. It also has a resultant normal pressure acting to the rear of the track, as could happen under normal circumstances due to load transfer from the drawbar pull. A line such as fg will represent the z, j, x, σ relation for a tracklayer with a mean contact pressure σ_m and no load transfer. The corresponding pressure distribution is shown at Fig. 7.4.1d.

The locating of the correct line 'fg' can be carried out quite accurately and very speedily using this graphical approach. However, the whole business could be treated analytically if the data of Fig. 7.4.1b could be represented by an equation of the form $z_i = z_V + f(j,\sigma)$ where z_i is the slip sinkage, z_V the sinkage due to vertical loads only and $f(j,\sigma)$ a suitable function describing the growth of sinkage with slip. The final sinkage and pressure distribution could then be obtained using

$$z_i = z_V + f(j,\sigma) \qquad \ldots \quad \ldots \quad \ldots \quad \ldots \quad 7.4.1.$$

$$z_i = A + Bj \qquad \ldots \quad \ldots \quad \ldots \quad \ldots \quad 7.4.2.$$

$$j = i\,x \qquad \ldots \quad \ldots \quad \ldots \quad \ldots \quad 7.4.3.$$

From the vertical equilibrium of the tractor

$$2b \int_{x=0}^{x=1} \sigma\,dx = W\cos\theta + L\sin\theta \qquad \ldots \quad \ldots \quad 7.4.4.$$

121

From the moment equilibrium of the tractor

$$2b \int_{x=0}^{x=1} \sigma \, x \, dx = Wm + Ln \quad \ldots \quad \ldots \quad \ldots \quad \ldots \quad 7.4.5.$$

The preceeding analysis assumes;

(a) that the pressure is uniformly distributed along the track except for the effect of slip sinkage and weight transfer, i.e. when the vehicle is self propelled without excessive sinkage or any drawbar pull.

(b) that the initial shear and excavation as the track plates are put on to the ground does not cause an undue front-end effect.

It is not necessary to know the actual pressures beneath the track to accomplish this prediction process. Preliminary experiments were carried out on the wet sand and compared with the slip sinkage curves of Fig. 7.2.2. These trials showed that the tracklayer sank about twice as deep as the theory would predict. A possible explanation would be that the pressure distribution was far from uniform with the slip sinkage being determined by the most heavily loaded point. To check this the rather rough and ready track link pressure transducer was made and a further set of experiments conducted in dry sand.

The results of a typical set of four runs at 0, 30½, 4, 50½ lb. drawbar pull are shown in Fig. 7.4.3. The slip sinkage curves of Fig. 7.2.4. are redrawn in Fig. 7.4.2. and the theoretical straight lines representing the conditions of the four test runs are marked on them. Lines representing the

measured sinkages are also shown and it is clear that they were systematically very much greater than expected. They in fact followed closely the pattern that might be expected from a contact pressure twice the actual figure.

This excessive sinkage was particularly apparent in the test at zero drawbar pull. When the tractor was carefully lowered on to the sand it sank about 1/2" which with its mean contact pressure of 2.2 lb.in.$^{-2}$ accords well with the pressure sinkage data of Fig. 4.1.2. or slip sinkage data of Fig. 7.2.4. However as soon as it started up, even though there was no drawbar pull, its sinkage increased to .85" and 1.80" at front and rear respectively. Fig. 7.4.3a shows a contact pressure record from this run; it is a good one in that it integrates to very nearly the weight of the tractor and its centre of pressure is in the right place. It shows (as did many other records) that the pressure distribution is far from uniform, being roughly parabolic in shape with a peak of 3.2 lb.in.$^{-2}$ instead of the mean of 2.2 lb.in.$^{-2}$. A pressure of 3.2 lb.in.$^{-2}$ could according to Fig. 7.4.2. cause a sinkage of about 0.9 in. at zero slip still only half the actual sinkage. A possible explanation is that the tractor vibrated vigorously due to running a 1.1/2 in. pitch track chain on a sprocket designed for standard 3/4" pitch chain; this vibration caused the negative slip of -2% at zero drawbar pull.

Four typical pressure records are shown in Fig. 7.4.3. The first integrates to the weight on one track of the tractor

but the others are far too small, even allowing for the effect
of the trim angle. No explanation was found for this; the obvious
one of interference from the shear forces on the track plate
appears to be unlikely because the dynamometer link showed
negligible cross-sensitivity in static tests. The records are
noteworthy in that they are much smoother than those published [15,32]
showing tracks using conventional track rollers instead of the
skid suspension. It is interesting to note that there is a
distinct trend towards redistribution of the pressure from the
centre of the track to the ends as predicted theoretically in
Fig. 7.4.1.

These experiments were unsatisfactory because sinkages were
much greater than expected in a consistent and systematic manner.
The next step is obviously to carry out further experiments at
various contact pressures in other soils using a more reliable
type of track link pressure dynamometer. It would probably be
advantageous to use a larger track with a smoother drive.

8. CONCLUSIONS

At the end of each conclusion, reference is made to the chapter of the report on which it is based.

1. The primary objective of soil-vehicle mechanics research today is the quantitative understanding of the performance of simple vehicles in deep uniform soils. This would provide guiding principles for more rational evaluation, design and test methods, and an intellectual framework into which field experience could be fitted to make a comprehensible picture.

<div align="right">Chapter 1.</div>

2. The approach to soil vehicle mechanics pursued by the Land Locomotion Laboratory involves explaining the reaction of soil to the complex loading imposed by vehicles in terms of its reaction to simple loading by flat plates. This is correct and is in fact the only available approach; it can give the work a firm basis in soil mechanics theory and has been responsible for all the advances in understanding made so far, including those contributed by overseas scientists.

<div align="right">Chapter 1.</div>

3. The current state of the art is difficult to judge due to the shortage of experimental results. What results there are suggest that present theories work reasonably well for rigid tracks on firm soils but deteriorate to a totally unacceptable degree for wheels on soft soils. Despite this, the current

<div align="center">125</div>

theory is a useful evaluation method if it is used by those
fully aware of its limitations; used by others, it can at best
waste time and, at worst lead to incorrect decisions.

Chapter 1.

4. The main obstacle to progress is the lack of proper
facilities for conducting research in this field. The scientific
problems involved are considerable by any standards demanding
both theoretical and experimental skill and major engineering
achievements in the design of suitable equipment.

Chapters 1 & 2

5. Future experimental work should aim at the investigation
of the assumptions on which existing theories are based.

Chapter 1

6. The experimental work described in this report was
carried out as an isolated project and the equipment, soils and
processing methods had to be developed especially for it. Most
current work is done on this basis and it is totally
unsatisfactory. A land locomotion laboratory worthy of the name
must be able to provide large quantities of a complete range of
soils covering the purely frictional, mixed frictional-cohesive
and purely cohesive types in closely controlled and accurately
repeatable condition. The density and hence compressibility of
the $\emptyset$ and c - $\emptyset$ soils must be controllable. The soils need to be
available in two sizes of container representing full size and
model conditions. Versatile equipment capable of testing wheels,
tracks and tires and various types of loading plates must be

available to work in the soil bins.

Chapter 2.

7. Soil processing techniques can and should be developed to give repeatability sufficient to make the adoption of statistical methods unnecessary.

Chapter 3.1.

8. The fitting of experimental data to selected equations is an important part of soil vehicle mechanics. Statistical methods based on minimizing the square of deviations are totally irrelevant to this process. A logical approach is described and a technique suitable for pressure sinkage is proposed.

Chapter 3.3.

9. Contemporary soil-vehicle mechanics is an analytical approach based on a mixture of elastic theory, plastic static equilibrium, empiricism and error. It needs consolidating into an analytical approach based on the static equilibrium methods of classical soil mechanics giving a theoretical basis for dense soils from which compressibility can be dealt with empirically.

Chapters 1, 4, 5, 6 and 7.

10. The pressure sinkage equation $p = (\frac{kc}{b} + k_\emptyset) z^n$ is inadequate. The k_c and $k_\emptyset$ suffixes are totally misleading. The equation fits sand quite well; it does not suit cohesive soils. The equation is diminsionally unpleasant. It does not fit bearing capacity theory for incompressible soils.

Chapter 4.6 and 4.7.

127

11. A proper pressure-sinkage equation must have the form $p = f(\frac{z}{b})$. The equation $p = (ck'_c + \gamma \frac{b}{2} k'_\emptyset) (\frac{z}{b})^n$ is shown to fit the experimental results for both sand and clay quite well. It is dimensionally attractive and accords with bearing capacity theory.

Chapter 4.6. to 4.9.

12. Present theories and approaches are only applicable to deep uniform soils. Layered soils will need special treatment.

Chapters 1 and 4.6.

13. The practice of using circular sinkage plates is shown to have neither theoretical nor experimental justification. It is concluded that it is necessary to use rectangular plates of aspect ratio greater than 5:1.

Chapter 4.2.

14. It is shown that there is a definite lower limit to the width of plate that can be used in order to extrapolate up to vehicle sizes. It follows from this and Conclusion 13 that a Bevameter must employ minimum vertical loads of 2,000 lb.

Chapters 4.3. and 4.4.

15. The performance of trains of wheels may possibly be explicable in terms of an intermittent loading test.

Chapter 4.5.

16. Meyerhof's bearing capacity theory provides an excellent basis for the understanding of pressure sinkage phenomena. It would be worthwhile to fully develop it in the sinkage range relevant to vehicles and to attempt to extend it to

cover compressible soils.

<div align="right">Chapter 4.6.</div>

17. An equation has been developed to take account of the thrust from the sides of grousers. The previous equation was suspect because it was based on elastic stress distribution. The new one is based on plastic equilibrium and is supported by experimental results.

<div align="right">Chapter 5.5.</div>

18. A new equation to describe sinkage due to excavation is proposed.

<div align="right">Chapter 5.6.</div>

19. It is shown experimentally that linear shear devices give a lower value of $\emptyset$ than confined tests. This results in having to use one value of $\emptyset$ to explain the sinkage of a towed wheel and another for the traction of a driven one. Further investigation is required.

<div align="right">Chapter 6.5.</div>

20. It is pointed out that in cohesive soils, the effect of the sides of the lugs on a Bevameter annulus needs to be taken into account. An equation is developed to do this.

<div align="right">Chapter 6.2.</div>

21. It is shown that in conditions where slip sinkage occurs, the present type of surface shear measuring device is subject to unwanted drag forces which cause an error in the results. A new design is proposed to overcome this failing.

<div align="right">Chapter 6.3.</div>

22.   Slip sinkage is shown to be of considerable magnitude
in purely frictional soils but much less in purely cohesive.
Further investigations are needed to cover c - $\emptyset$ and compressible
soils.   It is suggested that it may be possible to measure slip
sinkage using a Bevameter with large annulus and recording
sinkage as well as torque and twist.

<div style="text-align: right">Chapter 7.2.</div>

23.   The basis of a theory of slip-sinkage in
incompressible soils is described.

<div style="text-align: right">Chapter 7.3.</div>

24.   An attempt to predict slip sinkage of a small vehicle
using soil data from the linear shear rig or Bevameter failed.
The vehicle sank much further than expected.   Only very limited
experiments were carried out and further investigation is required.

<div style="text-align: right">Chapter 7.4.</div>

25.   No theory in soil-vehicle mechanics can be considered
proven unless supported by experimental results in dry sand, wet
sand, a range of c - $\emptyset$ soils of varying compressibility and a
purely cohesive soil.

Table 4.1.1. Pressure as a function of sinkage for rectangular plates in wet sand.

Sinkage	Plate Size				
	½ x 18	1 x 18	2 x 18	3 x 18	4 x 18
½	7.79	7.78	6.65	8.25	8.33
1	8.89	8.60	8.20	10.55	11.05
1½	10.55	9.72	9.43	11.85	12.80
2	11.65	11.40	11.50	13.40	14.50
2½	14.42	13.35	12.75	15.00	16.20
3	16.65	15.60	14.45	16.75	17.80
3½	19.45	17.80	16.55	18.60	19.45
4	21.70	20.30	18.30	20.60	21.10
4½	24.45	22.80	20.50	22.75	22.80
5	27.20	25.30	22.75	25.20	24.70
5½	30.00	28.10	24.95	27.80	26.50
6	32.80	30.80	27.4	31.30	30.4
6½	35.50	33.90	29.5	33.10	32.5

Table 4.1.2. Pressure as a function of sinkage for circular plates in wet
             sand.

Sinkage	Plate Size					
	1" Dia.	2" Dia.	3" Dia.	4" Dia.	5" Dia.	6" Dia.
½	10.2	7.96	7.08	9.43	9.2	8.12
1	12.75	11.15	10.6	12.75	12.0	11.8
1½	12.75	14.34	13.4	15.5	14.55	14.7
2	15.30	15.91	16.3	18.0	17.4	17.5
2½	19.1	18.45	18.4	21.1	20.2	20.5
3	23.0	20.7	21.9	24.3	23.2	23.5
3½	25.5	23.9	24.75	27.5	26.5	26.8
4	31.9	27.1	28.3	31.0	30.4	30.4
4½	38.2	31.2	31.8	35.0	34.2	34.6
5	44.6	35.0	36.1	39.4	38.8	39.4
5½	51.0	39.8	40.3	44.2	44.4	44.5
6	57.4	43.0	46.0	49.7	53.6	50.7

Table 4.1.3. Pressure as a function of sinkage for rectangular plates in dry sand.

Sinkage	Plate Size				
	½ x 18	1 x 18	2 x 18	3 x 18	4 x 18
½	1.33	1.67	2.78	3.42	4.3
1	2.78	3.06	3.9	4.8	6.1
1½	4.44	4.16	5.0	6.3	7.36
2	5.77	5.56	6.25	7.5	8.5
2½	7.21	6.68	7.5	8.9	9.9
3	8.88	8.06	8.9	10.4	11.1
3½	11.0	9.46	10.3	11.8	12.5
4	12.2	11.1	11.8	13.5	14.2
4½	14.4	12.5	13.4	15.2	15.9
5	16.6	14.5	15.3	17.0	17.8
5½	19.4	16.4	17.2	19.1	20.0
6	21.6	18.4	19.0	21.3	22.5
6½	23.9	20.3	21.7	23.9	25.6
7	26.6	22.5	24.2	26.3	

Table 4.1.4. Pressure as a function of sinkage for circular plates in dry sand.

Sinkage	Plate Size					
	1" Dia.	2" Dia.	3" Dia.	4" Dia.	5" Dia.	6" Dia.
$\frac{1}{2}$	2.546	3.18	2.86	3.42	2.8	3.53
1	3.819	4.76	4.72	4.78	4.45	5.24
$1\frac{1}{2}$	5.09	6.36	6.43	6.22	5.75	6.7
2	6.365	7.95	7.85	7.57	7.2	8.4
$2\frac{1}{2}$	7.638	9.54	9.3	8.9	8.9	10.2
3	9.55	12.2	10.7	10.4	10.65	12.15
$3\frac{1}{2}$	12.73	14.3	12.6	12.35	12.55	14.1
4	14.0	15.9	14.6	14.32	14.75	16.4
$4\frac{1}{2}$	15.3	18.4	16.85	16.72	16.9	18.7
5	19.1	21.0	19.0	19.2	19.4	21.1
$5\frac{1}{2}$	22.9	23.8	21.7	22.3	22.5	24.0
6	26.7	26.7	24.9	25.5	24.9	26.4
$6\frac{1}{2}$	31.8	30.2	28.85	28.7	28.0	29.2
7	38.19	34.4	33.0	32.8	31.2	31.8

Table 4.1.5. Pressure as a function of sinkage for rectangular plates in saturated clay.

Sinkage	Plate Size			
	1 x 18	2 x 18	3 x 18	4 x 18
½	3.61	2.86	2.27	2.57
1	5.00	4.17	2.76	3.96
1½	5.56	4.78	4.54	4.70
2	5.84	5.25	5.04	5.15
2½	6.06	5.55	5.46	5.45
3	6.10	5.78	5.61	5.68
4	6.28	5.98	5.95	6.03
6	6.67	6.40	6.34	6.60
8	6.95	6.81	6.95	7.09
10	7.55	7.79	7.87	8.04

Table 4.1.6. Pressure as a function of sinkage for similar rectangular plates in saturated clay.

Sinkage	Plate Size			
	1 x 4½	2 x 9	3 x 13½	4 x 18
½	4.23	3.00	2.86	2.81
1	5.34	4.33	3.83	3.31
1½	5.79	5.16	4.40	4.03
2	6.00	5.66	4.82	4.52
2½	6.45	6.00	5.14	4.86
3	6.90	6.23	5.39	5.15
4	7.35	6.40	5.80	5.61
6	7.79	6.56	6.30	6.32
8	9.12	6.67	6.80	7.09
10	11.77	7.40	7.90	8.34

Table 4.1.7. Pressure as a function of sinkage for circular plates in saturated clay.

Sinkage	Plate Size			
	1" Dia.	2" Dia.	4" Dia.	6" Dia.
½	5.73	4.14	3.26	2.49
1	6.50	5.42	4.86	3.85
1½	6.50	6.21	5.97	4.60
2	6.50	6.70	6.38	5.02
3	6.50	6.88	6.60	5.41
4	6.50	7.07	6.76	5.65
6	7.65	7.16	6.67	6.01
8		7.16	7.17	6.65

Table 5.5.1. Analysis of total horizontal force on 30" long track plate 4" wide with 2" deep lugs. Shown graphically as Fig.5.5.8. Columns 2 and 4 from Fig.5.5.6. Column 3 from mean of Fig.5.5.5. and other similar tests.

	Measured Values				Calculated Forces			
1	2	3	4		5	6	7	8
Vertical Load lb.	Final Mean Sinkage in.	Bulldozing Force lb.	Total Horizontal Force lb.		W tan $\emptyset$ lb.	W tan $\emptyset$ lb.	Side force lb.	Total Horizontal Force lb.
100	1 1/2	6	93		55	10	9	80
200	2	10	148		110	11	11	142
300	2 3/4	20	220		165	14	16	205
500	3 3/4	27	340		275	18	21	331
700	5 1/4	50	475		385	20	30	485

Fig.5.5.2. Analysis of total horizontal force on a 30" long track
plate, 4" wide with 4" deep lugs. Shown graphically as
Fig.5.5.9.
Column 4 from Fig.5.5.7.
Column 3 from mean of Fig.5.5.7. and other similar tests.

	Measured Values				Calculated Forces			
1	2	3	4	5	6	7	8
Vertical Load lb.	Final Mean Sinkage in.	Bulldozing Force lb.	Total Horizontal Force lb.	$W \tan \phi$ lb.	$W \tan \phi$ lb.	Side Force lb.	Total Horizontal Force lb.
100	2.2	35	133	55	16	26	131
200	2.5	40	203	110	17	29	196
300	2.85	45	258	165	18	33	263
500	3.8	60	410	275	22	44	401
700	5.0	75	522	385	27	58	545

Table 6.5.1. Summarized values of shear stress against normal pressure for dry sand from the linear shear apparatus and Bevameter.

Shear plate size	30" x 1¼" x ¼" lugs		30" x 2" x ¼" lugs		30" x 2" sandpaper		90" x 2" sandpaper		30" x 4" x ¼" lugs		5¼" - 7¼" Dia. Annulus	
Results from Figure Number	7.2.3.		7.2.4.		7.2.6.		7.2.9.		7.2.5.		7.2.11.	
Stress	σ	s	σ	s	σ	s	σ	s	σ	s	σ	s
	.85	.48	.53	.35	.53	.38	.56	.29	.83	.48	1.0	.34
	1.92	1.0	1.67	1.0	1.67	.78	2.2	1.20	1.67	.85	1.7	1.0
	2.66	1.28	3.33	1.72	3.33	1.60	3.9	1.70	2.5	1.3	3.4	1.9
	4.0	2.03	5.0	2.45	5.0	2.33			4.2	2.22	4.1	2.2
	5.34	2.40	6.67	3.17	6.67	3.17			5.83	2.9	5.1	2.7
Symbol used in Figure 6.5.1.	⋈		✕		+		△		•		○	

140
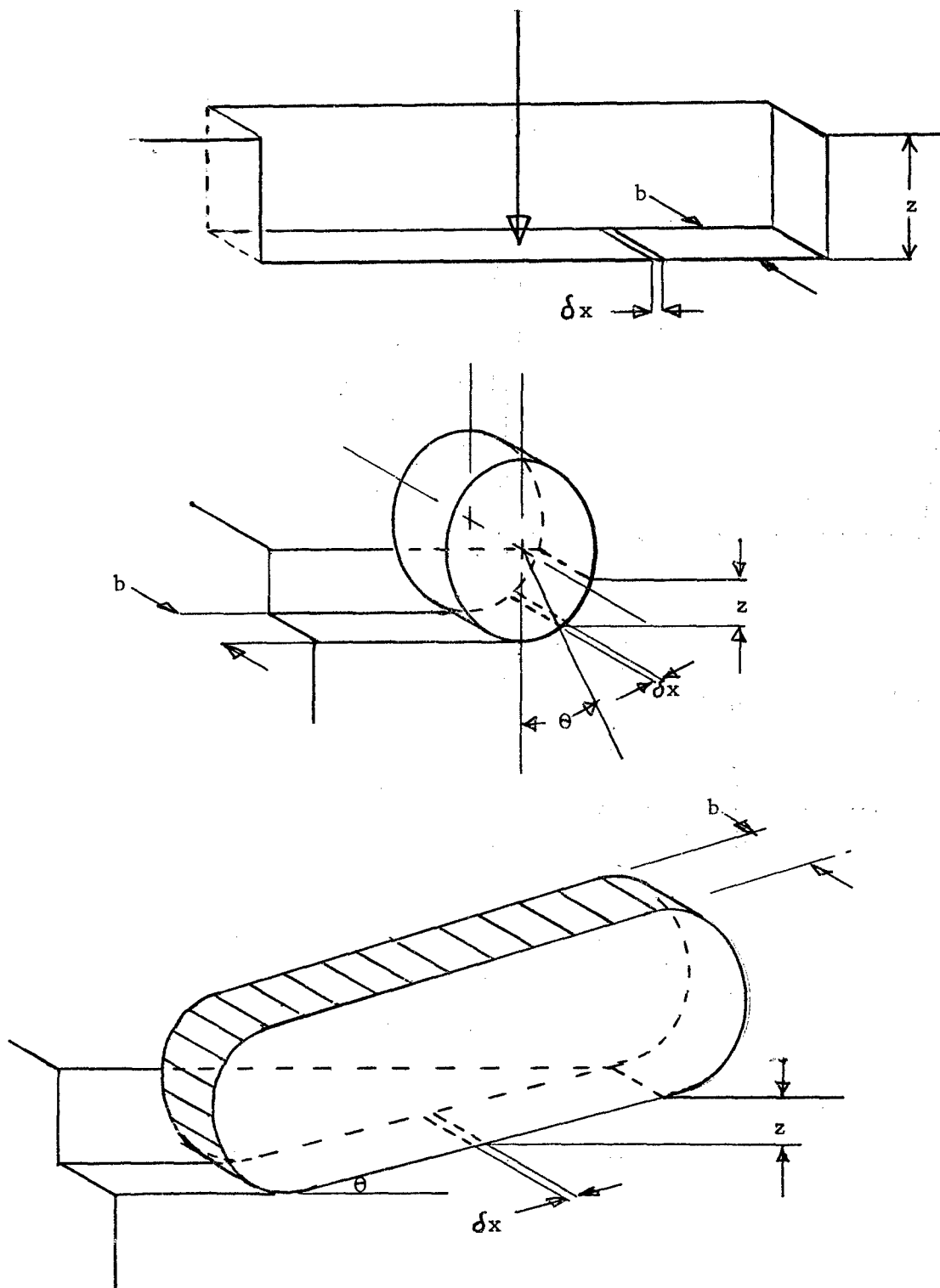
Fig.1.1. An elementary crosswise strip from an effectively infinitely-
long strip footing and the corresponding element on a wheel
and a track.

141
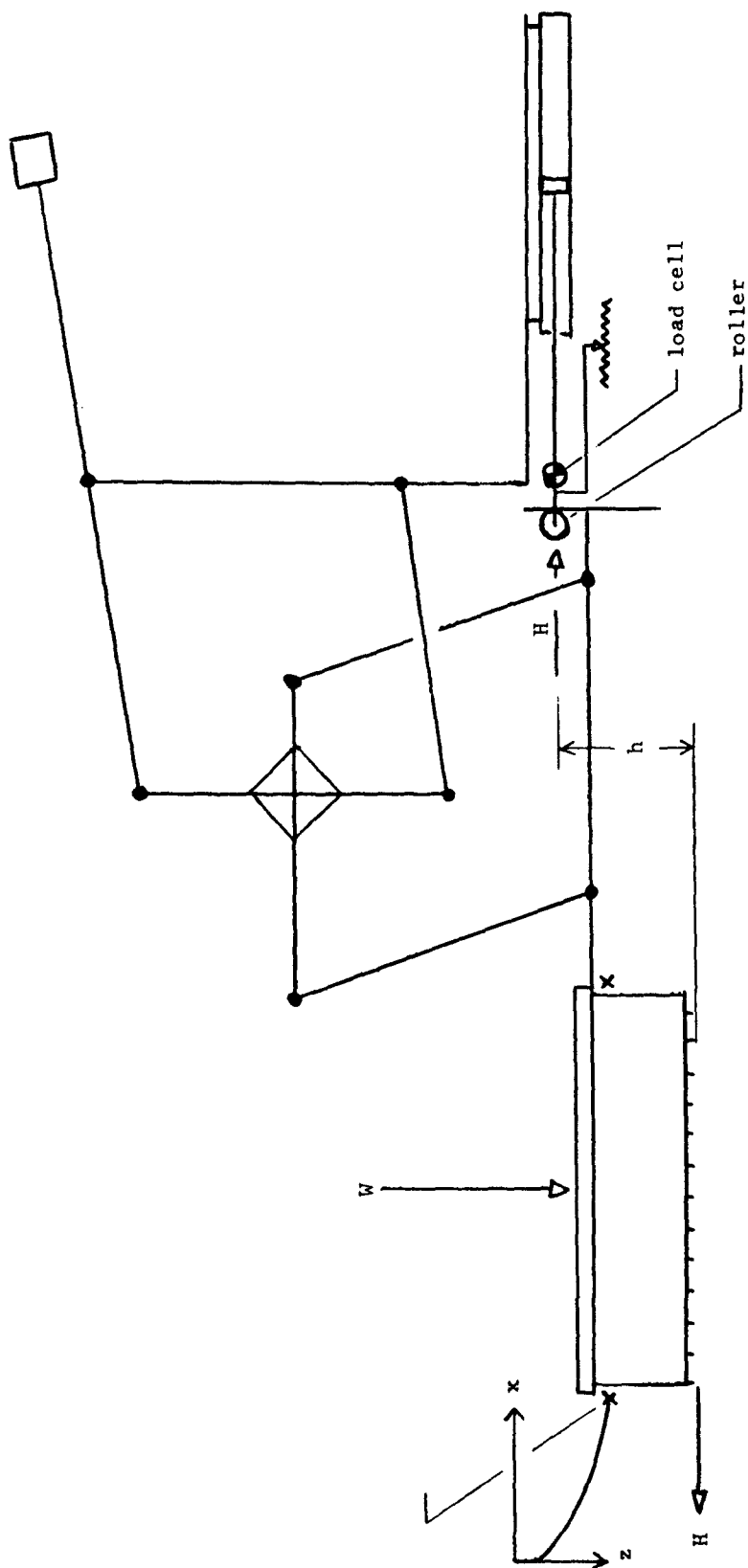
Fig.2.1.1. Diagram showing the main features of the linear shear apparatus.

load cell

roller

H

h

W

x

z

H
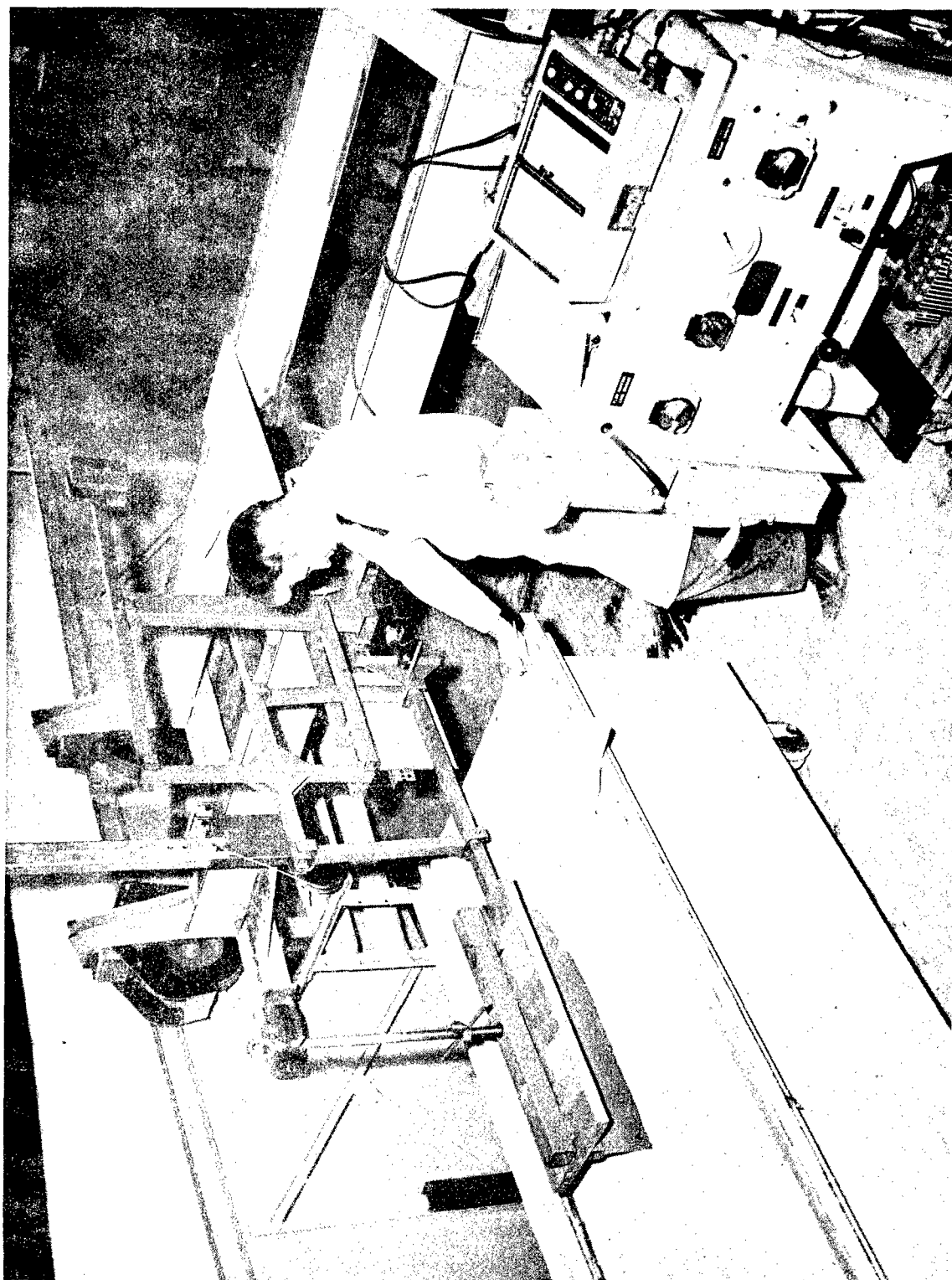
Fig.2.1.2. Linear shear apparatus showing soil tank, hydraulic power pack and X-Y plotter.
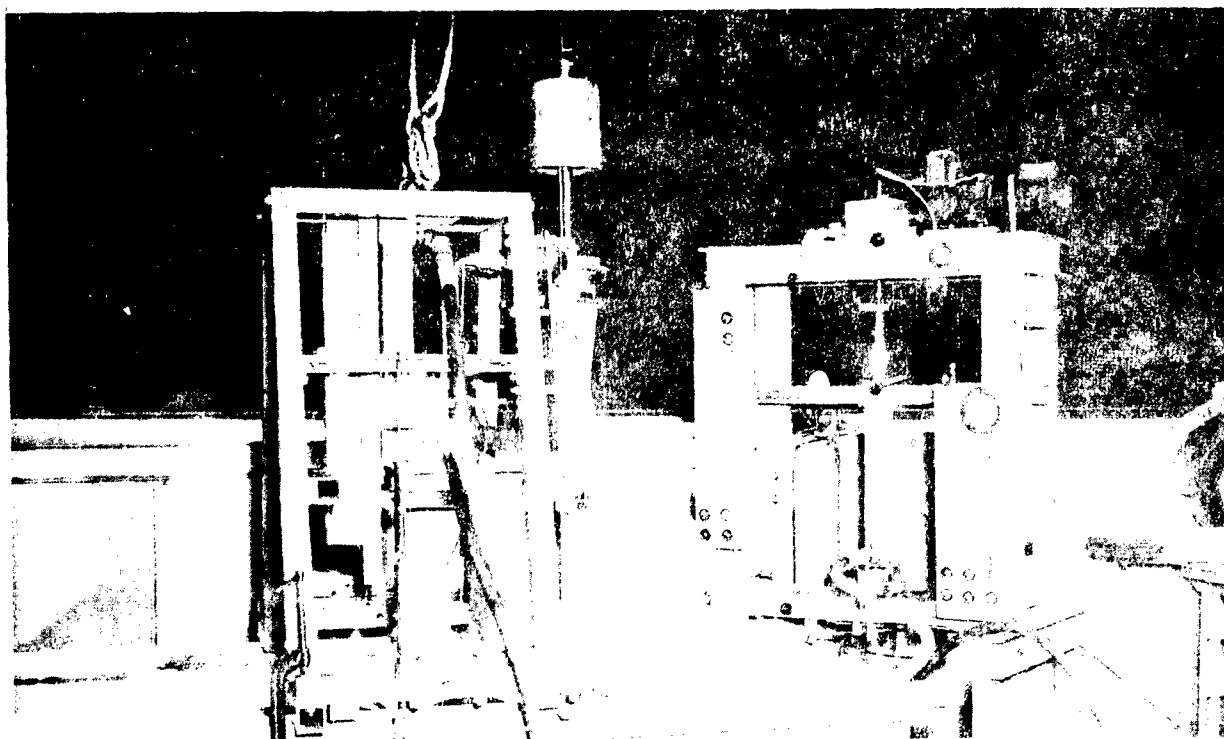
Fig.2.2.1. Modified Bevameter, showing slow speed drive from triaxial
machine via hydraulic transmission.
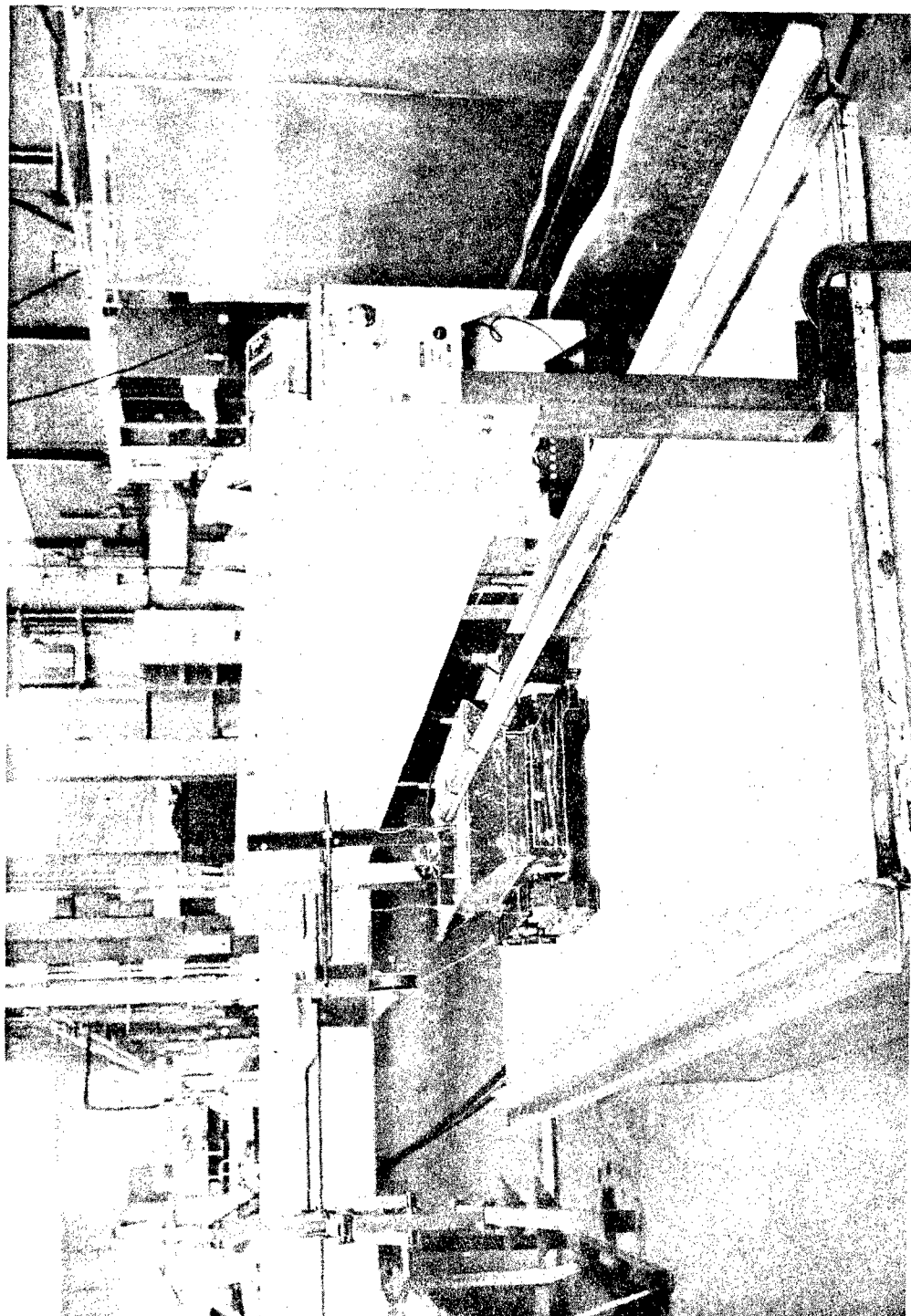
Fig.2.3.1. Model tracklayer, showing gravity dynamometer, sinkage recorders, counterbalance weight and tracklink pressure and position transducers.
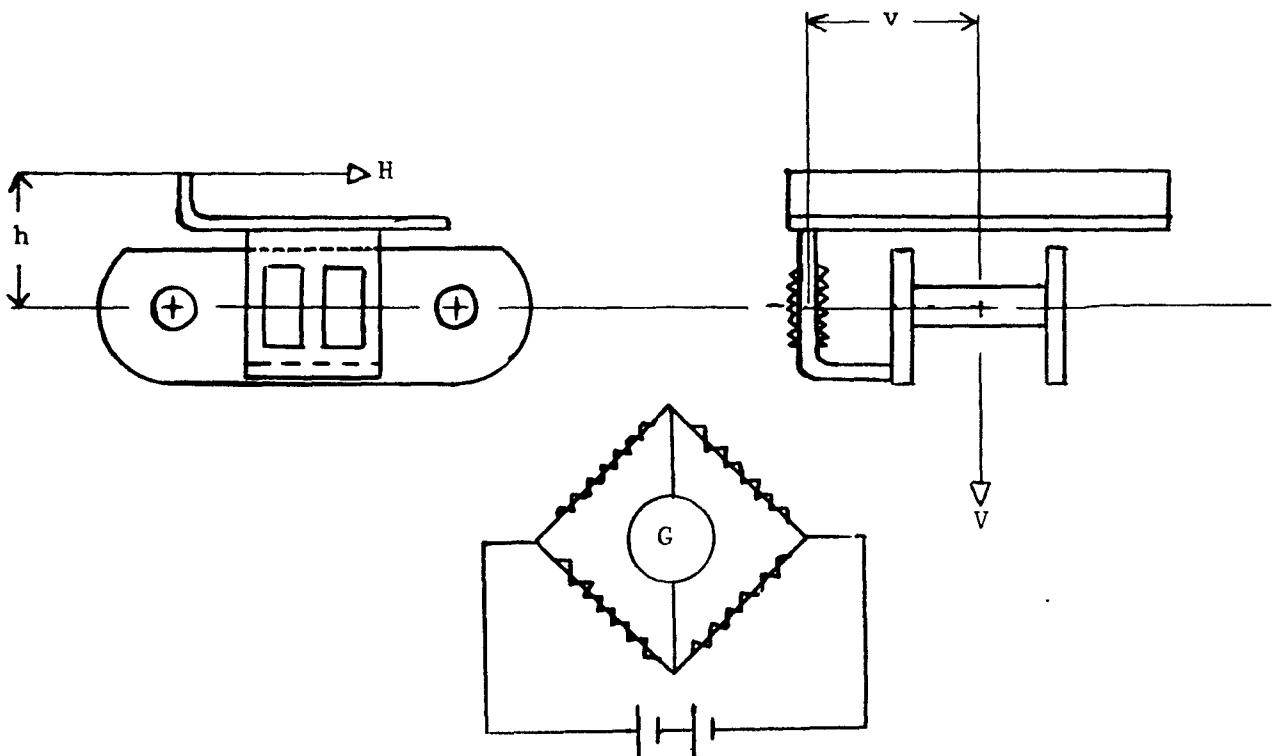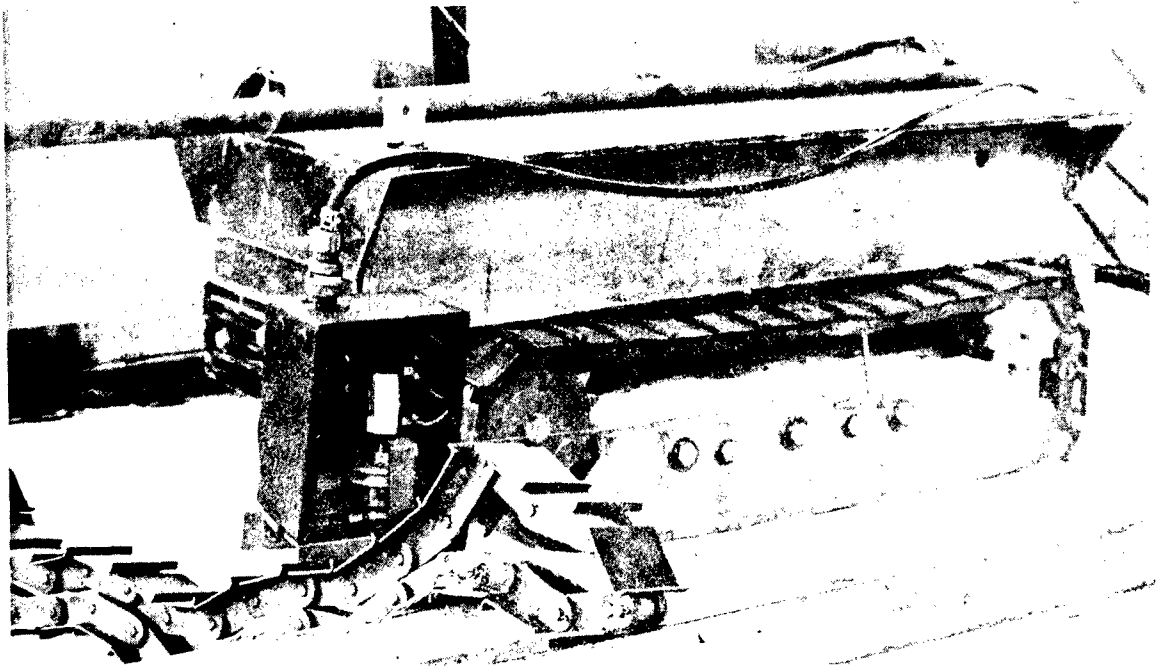
Fig.2.3.2. The photograph shows the tracklink dynamometer in the track chain and the position indicating potentiometer, which is operated from the top run of the other track. The diagram shows the arrangement of the strain gauges on the dynamometer link.

146
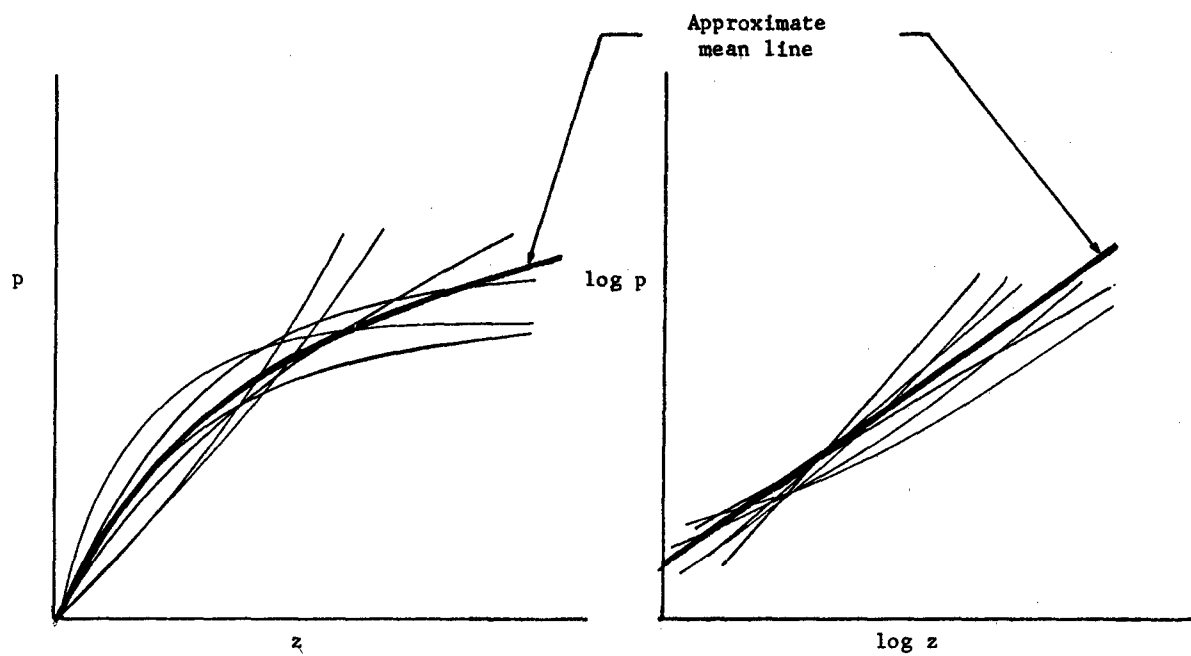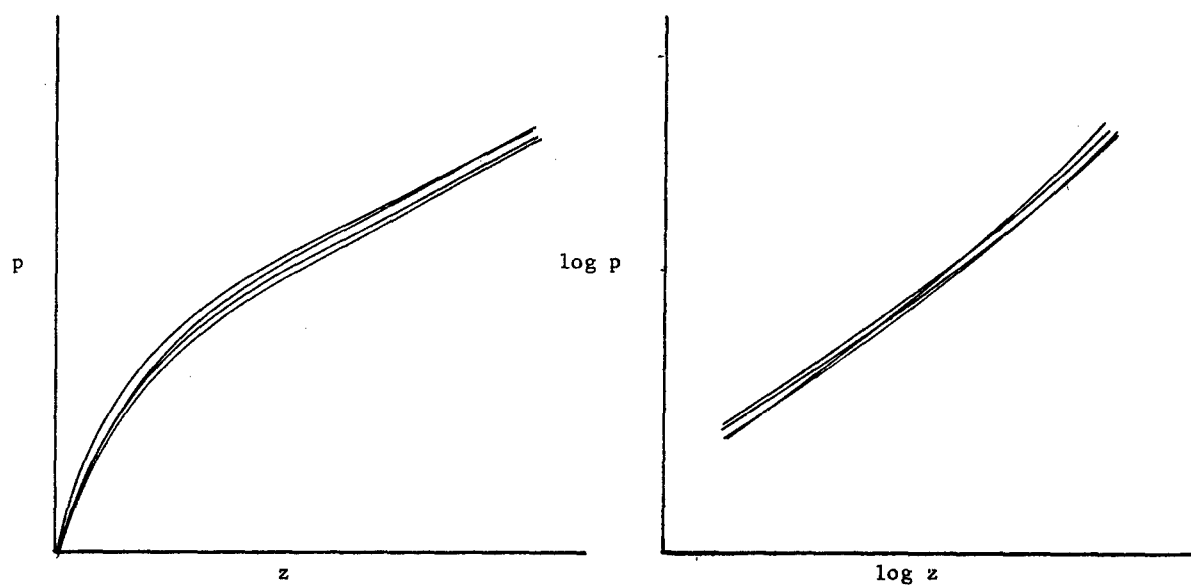
Fig.3.1.1. Typical pressure sinkage curves using one plate size.
    (a) From the field.
    (b) From the laboratory.
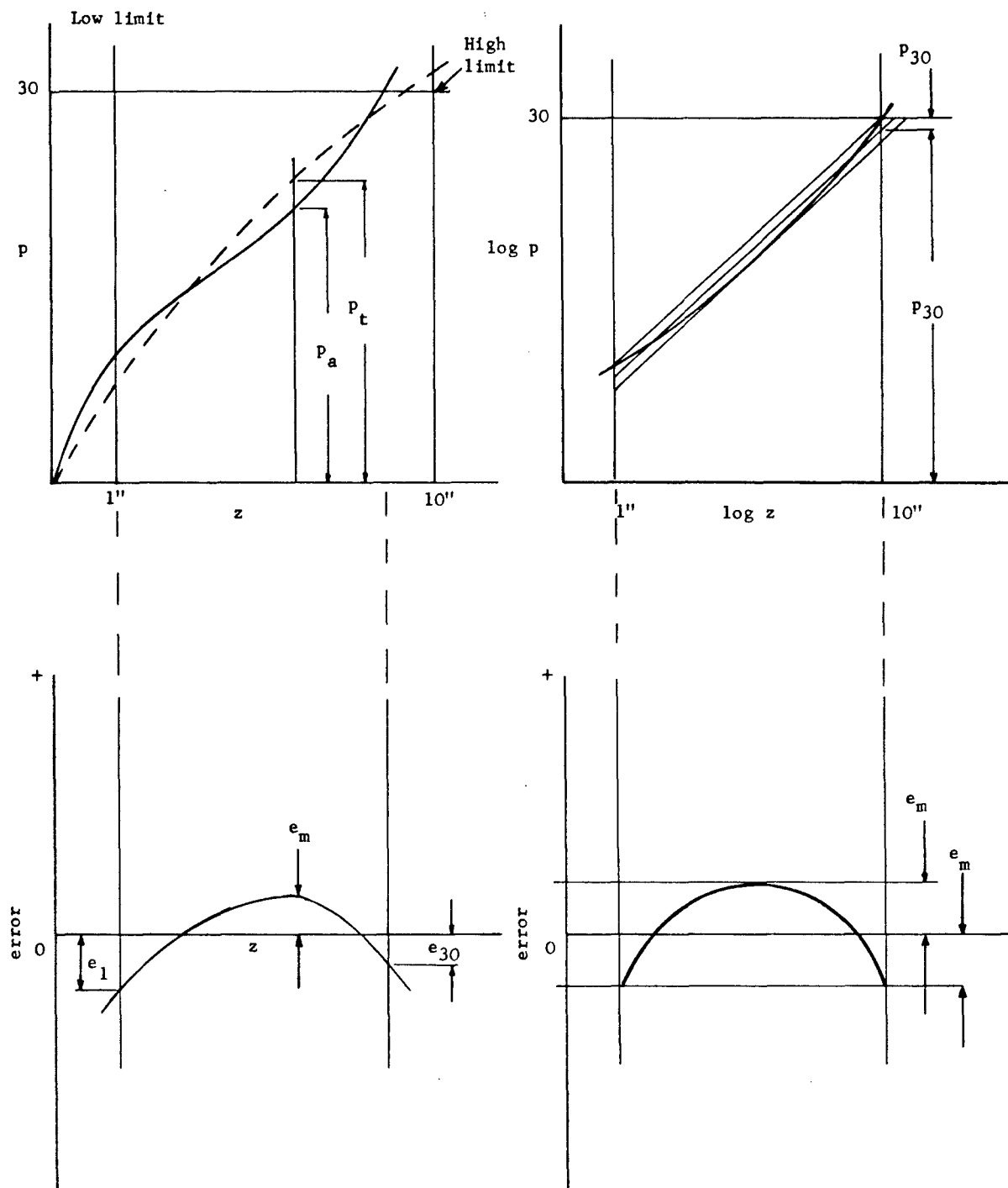
Fig.3.3.1. An illustration of the proposed curve fitting method,
applied to $p = kz^n$, showing the resulting optimum
distribution of error.

148
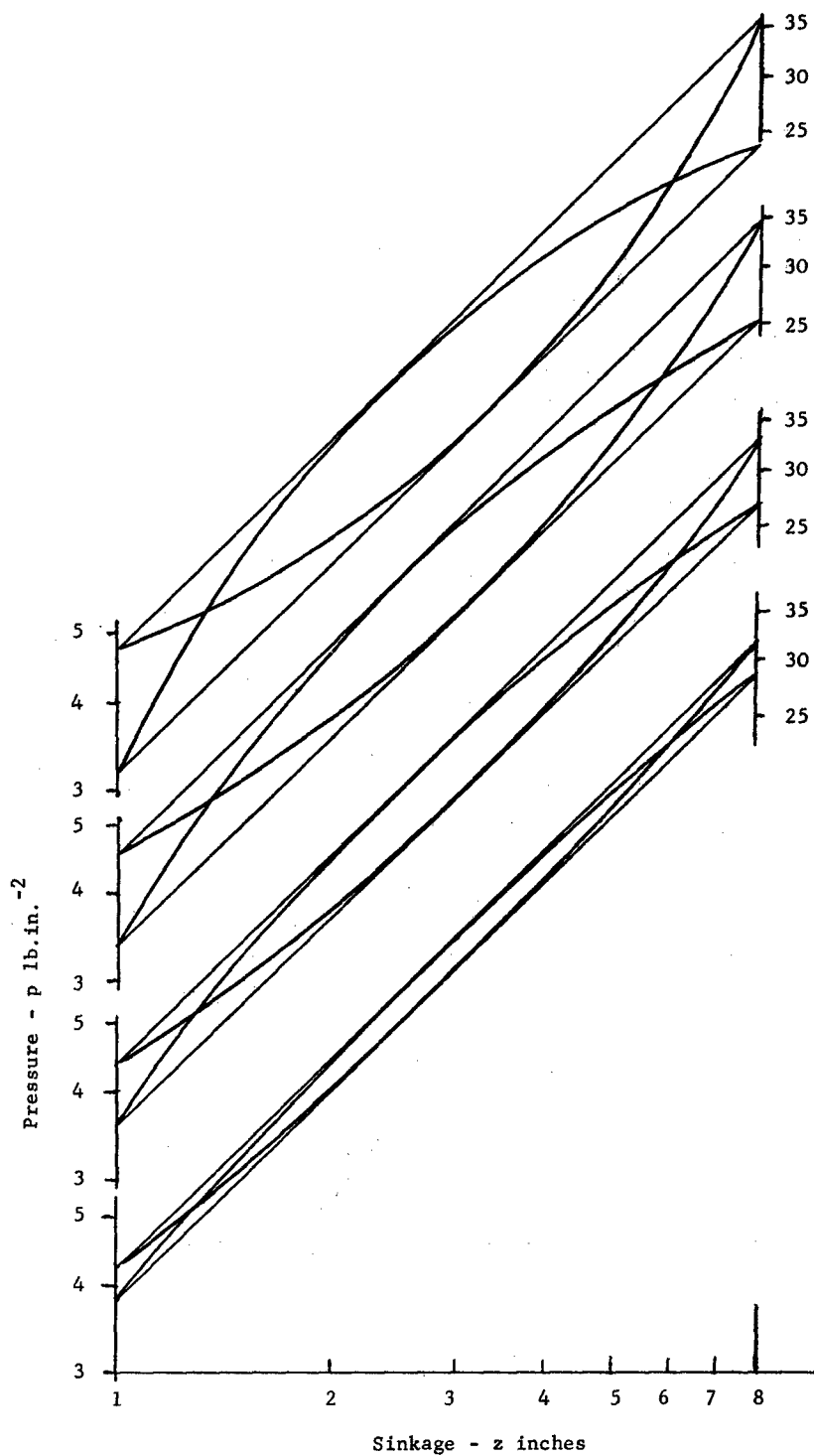
Fig.3.3.2. A family of pressure sinkage curves with the
same k and n values but with a range of misfit
to $p = kz^n$ of 5, 10, 15 and 20%.

149
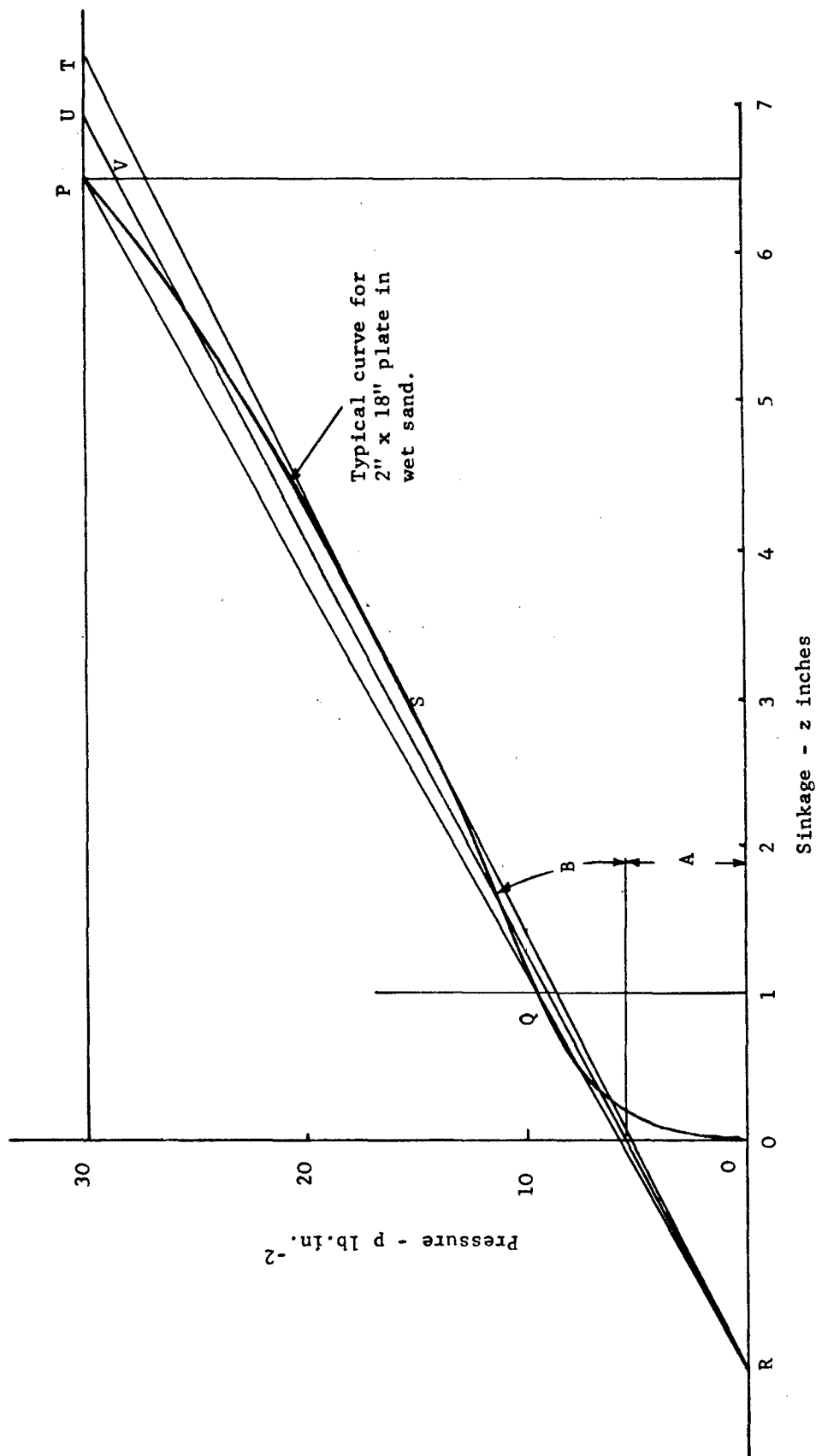
Fig.3.4.1. The application of the minimum error method to find the best fitting equation of the form p = A + Bz
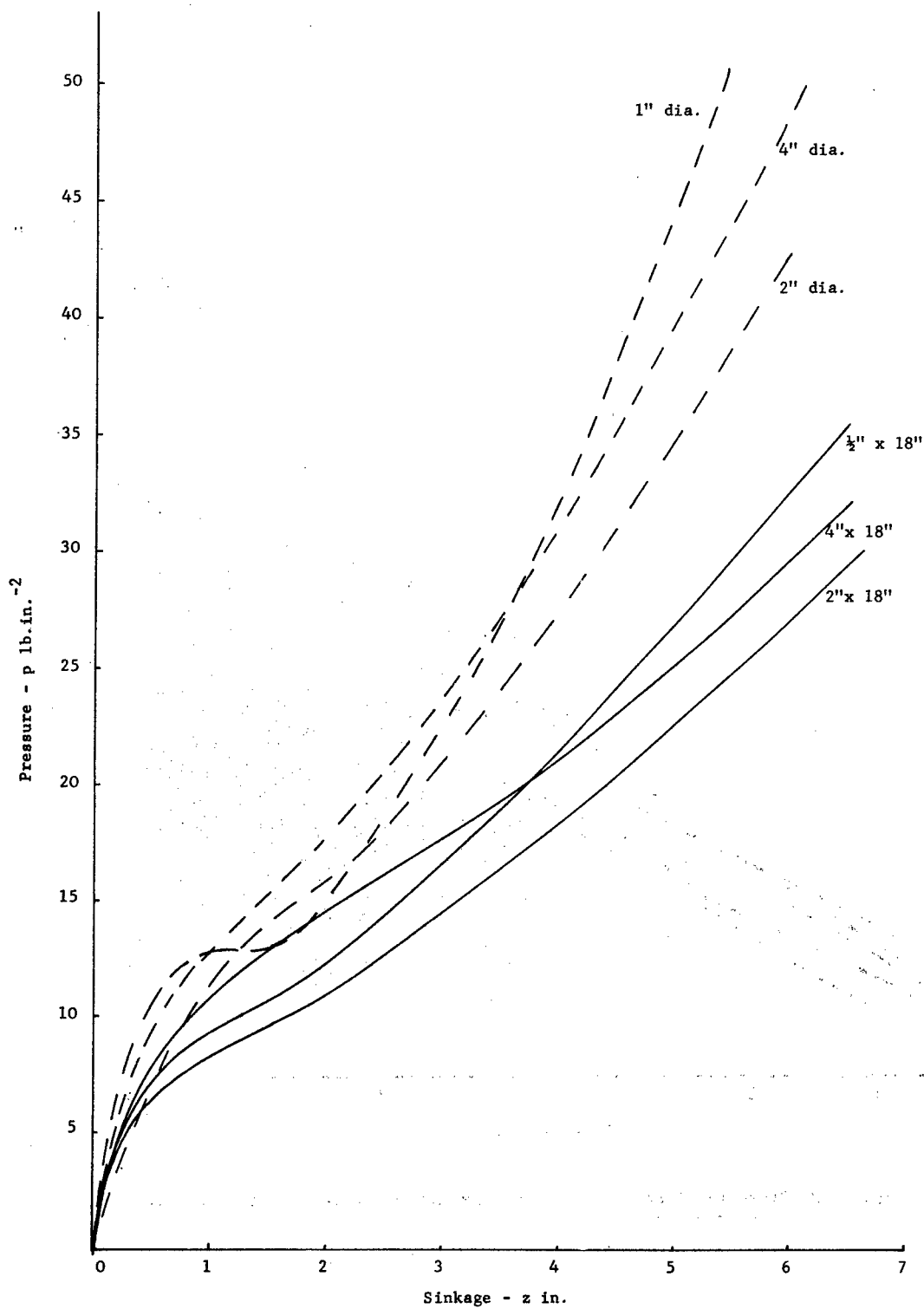
Fig.4.1.1. Pressure sinkage curves for circular and rectangular plates
in compact wet sand.

This Document Contains
Missing Page/s That Are
Unavailable In The
Original Document
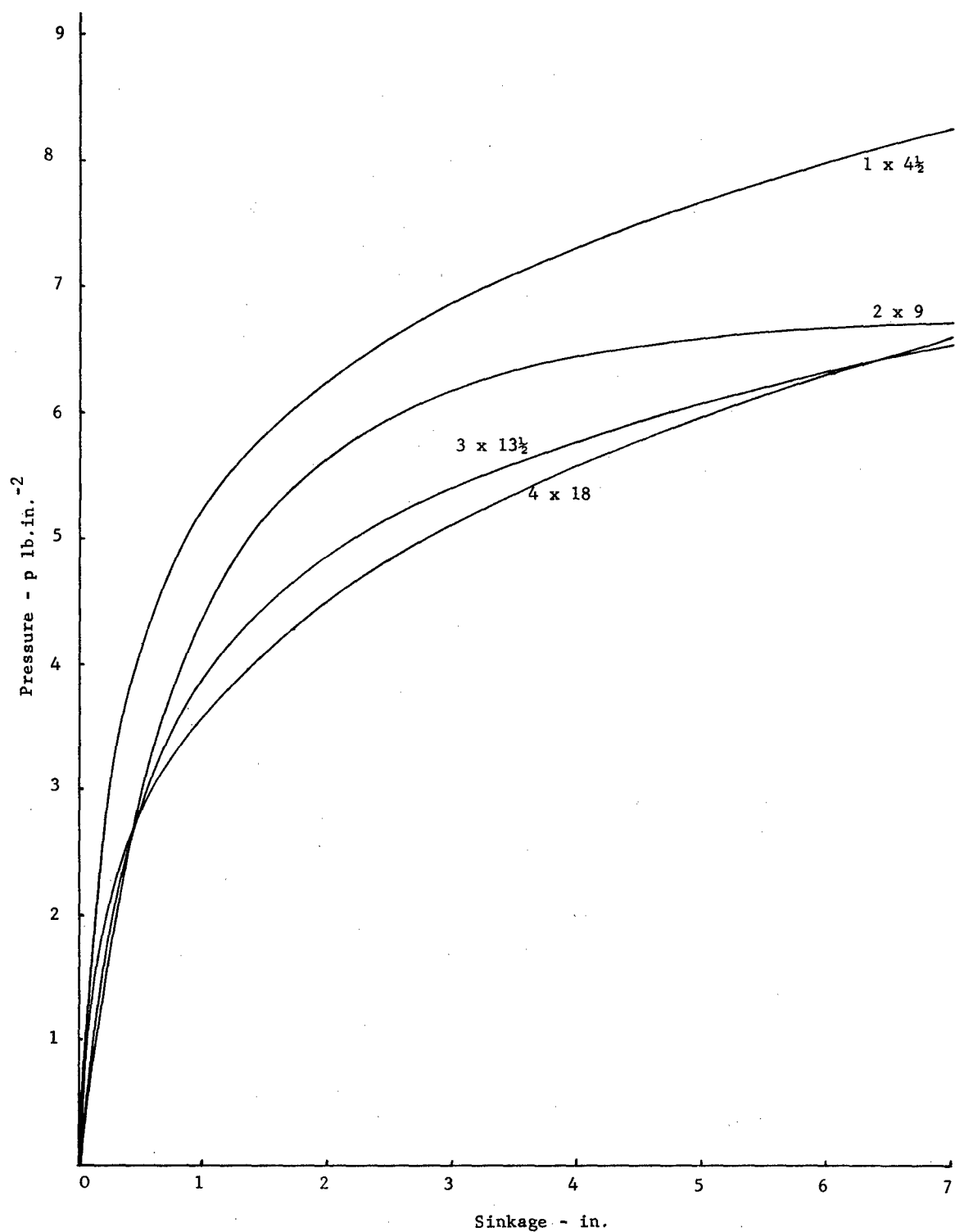
Fig.4.1.3. Pressure sinkage curves for similar rectangular plates
in saturated clay.
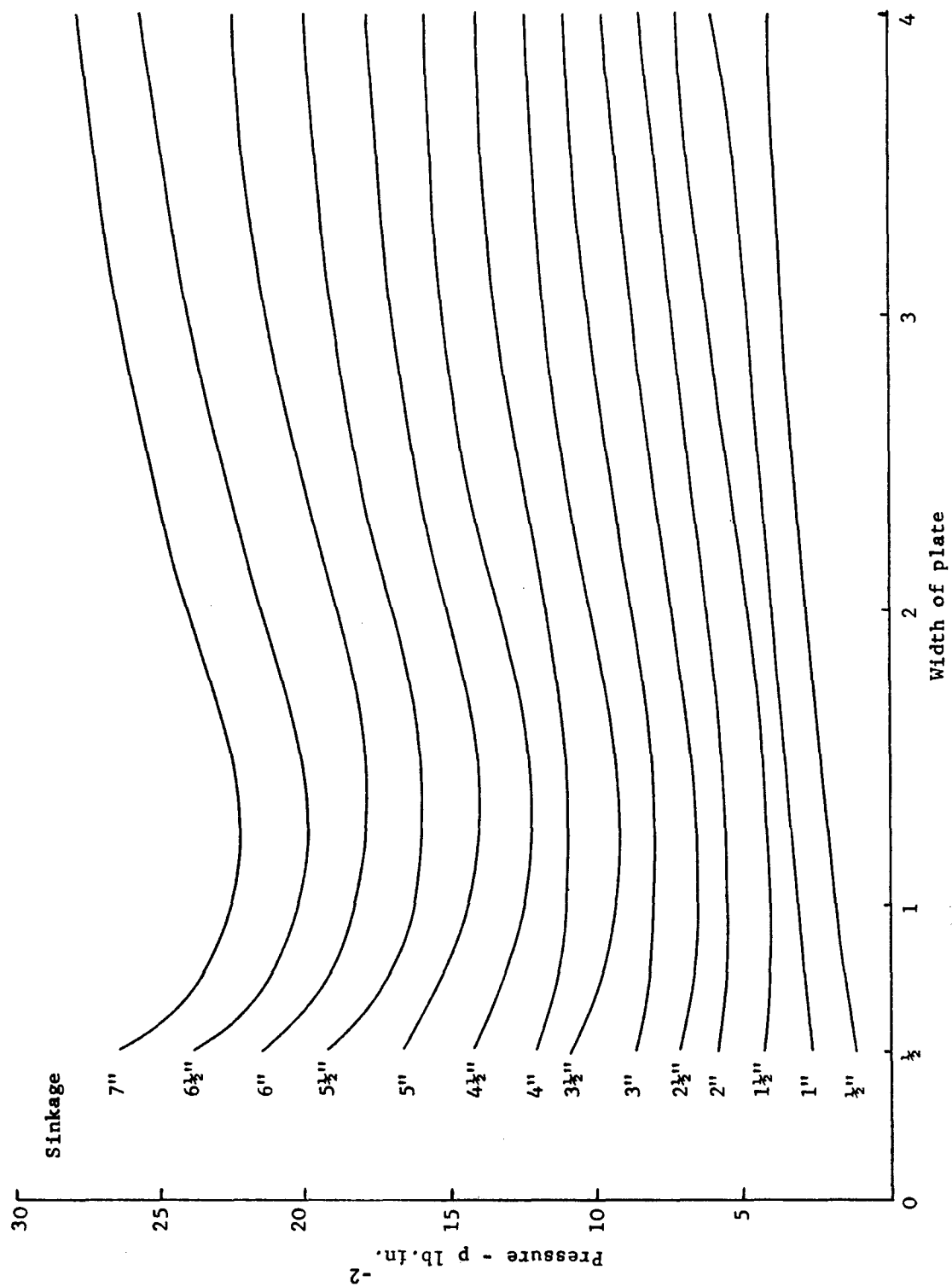
Fig.4.3.1. Pressures at particular sinkages as a function of plate width. 18" long plates in compact dry sand.
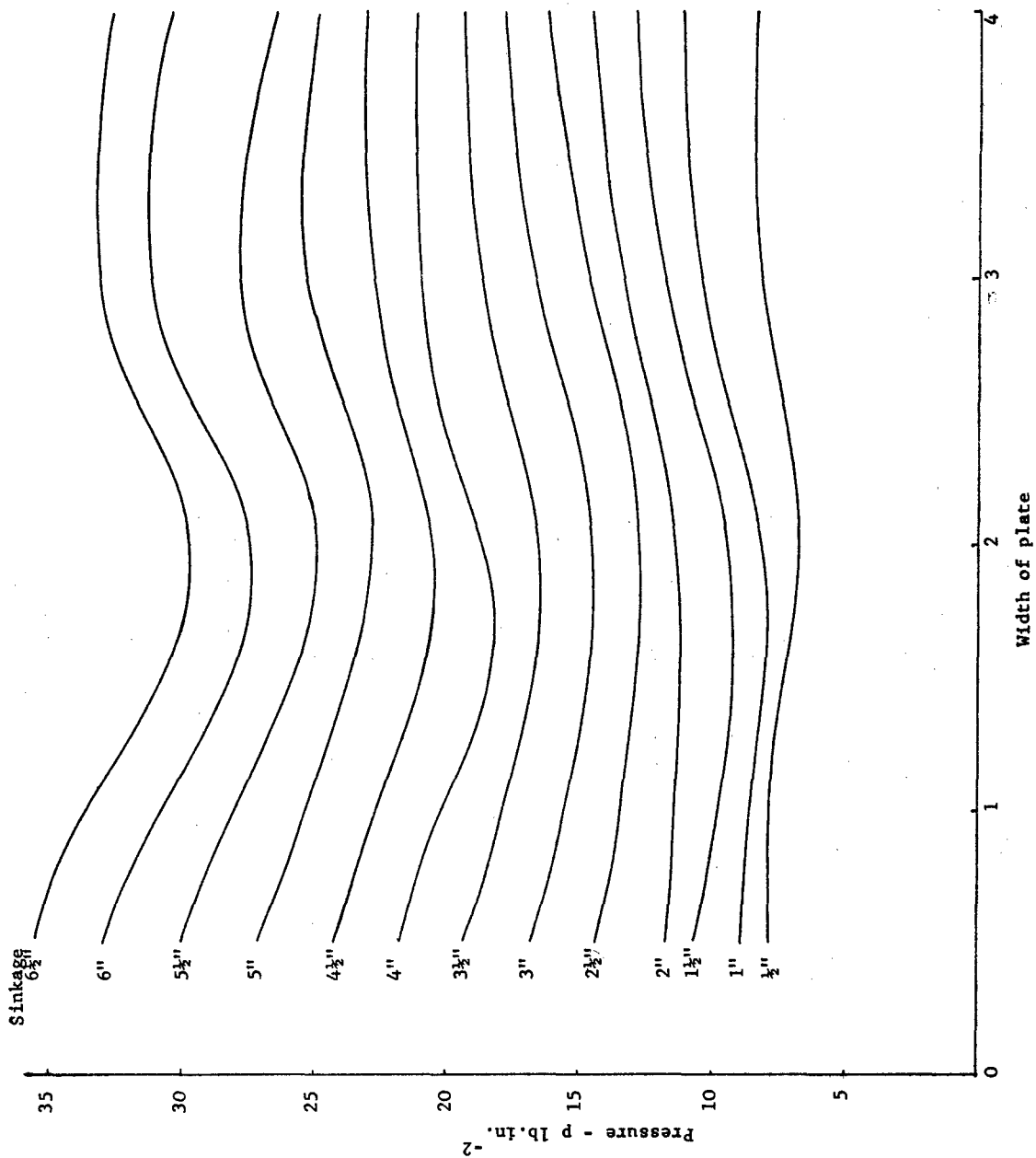
Fig.4.3.2. Pressures at particular sinkages as a function of plate width. 18" long plates in wet sand.
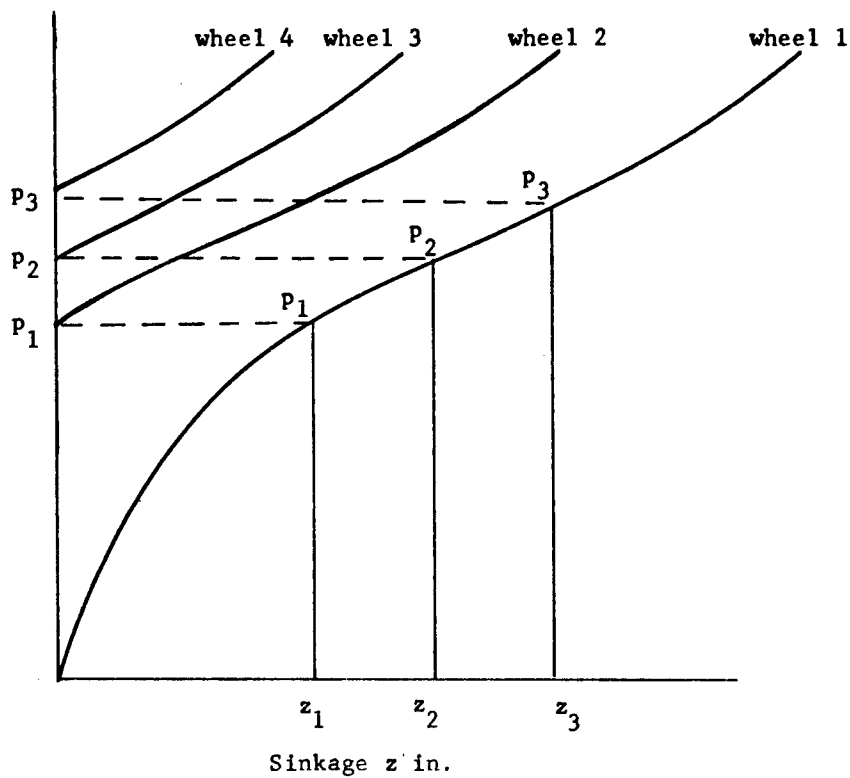
(a)
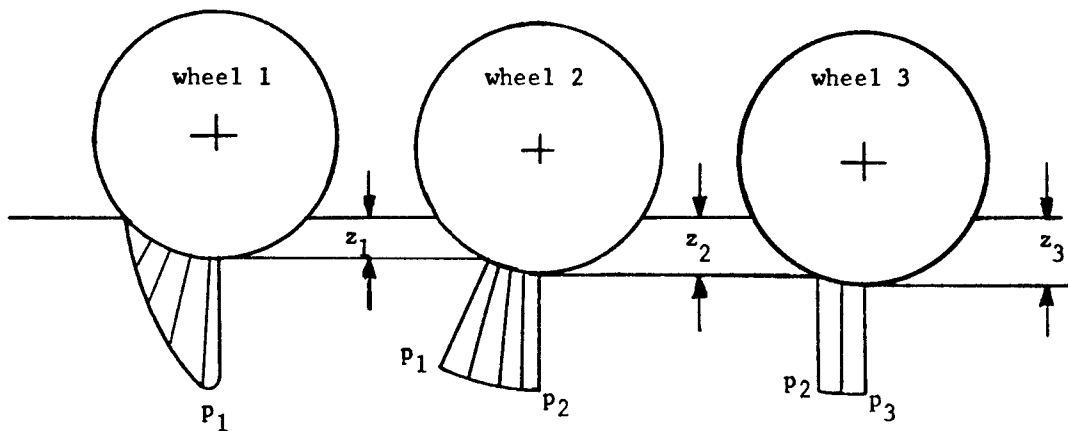
(b)

Fig.4.5.1. The pressure sinkage relation after the successive
passage of wheels in the same rut.
(a) Plate sinkage test results.
(b) Effect on wheel pressure distribution.

156
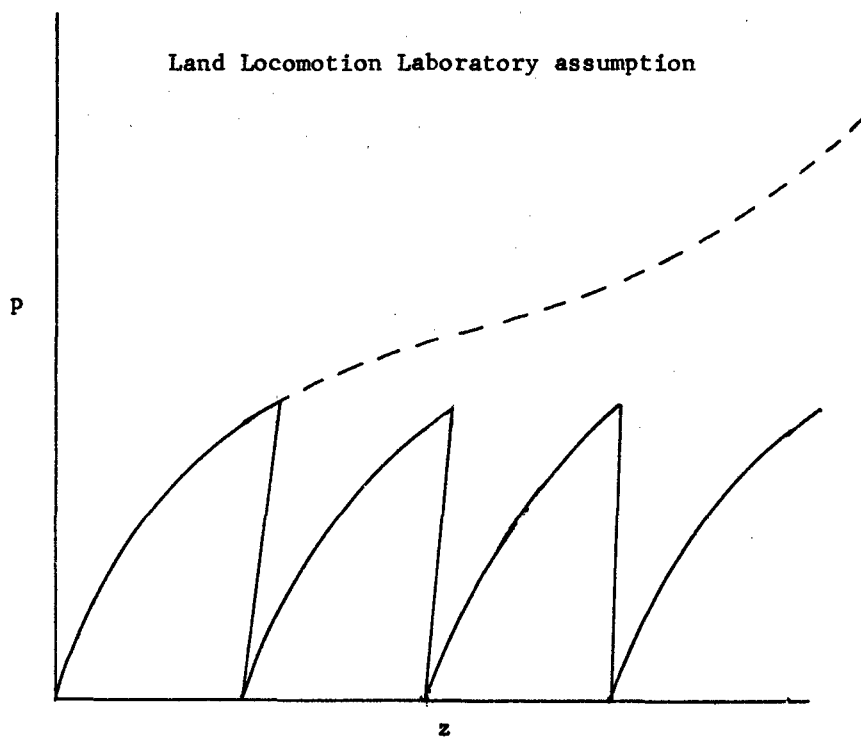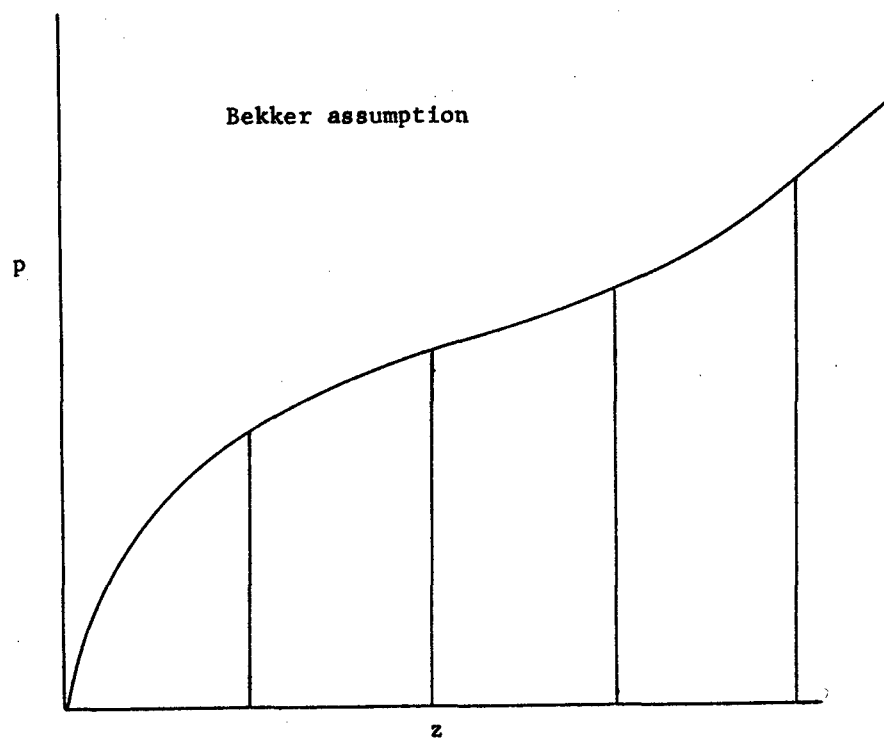
Fig.4.5.2. A comparison between the effects of repetitive loading
assumed by Bekker and the Land Locomotion Laboratory.
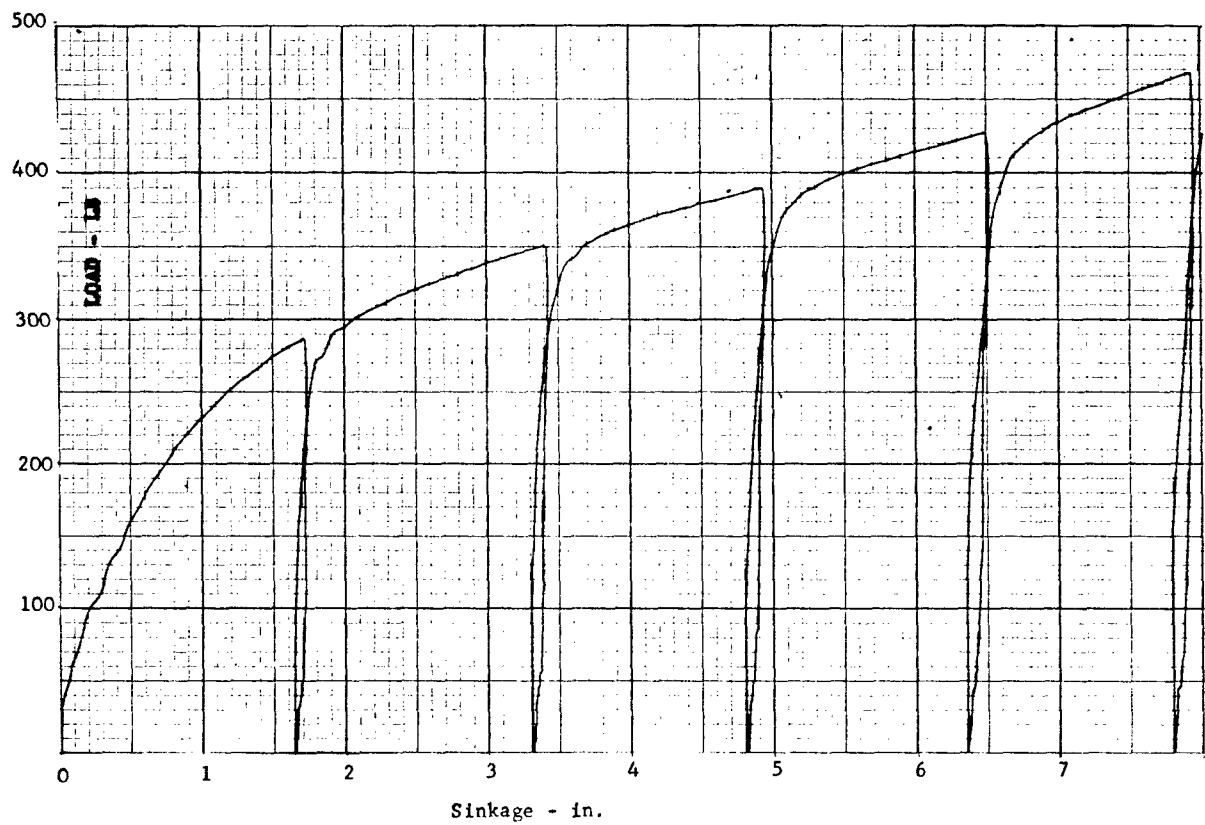
Fig.4.5.3. Results of an interrupted loading test using 4" x 18" plate in saturated clay.
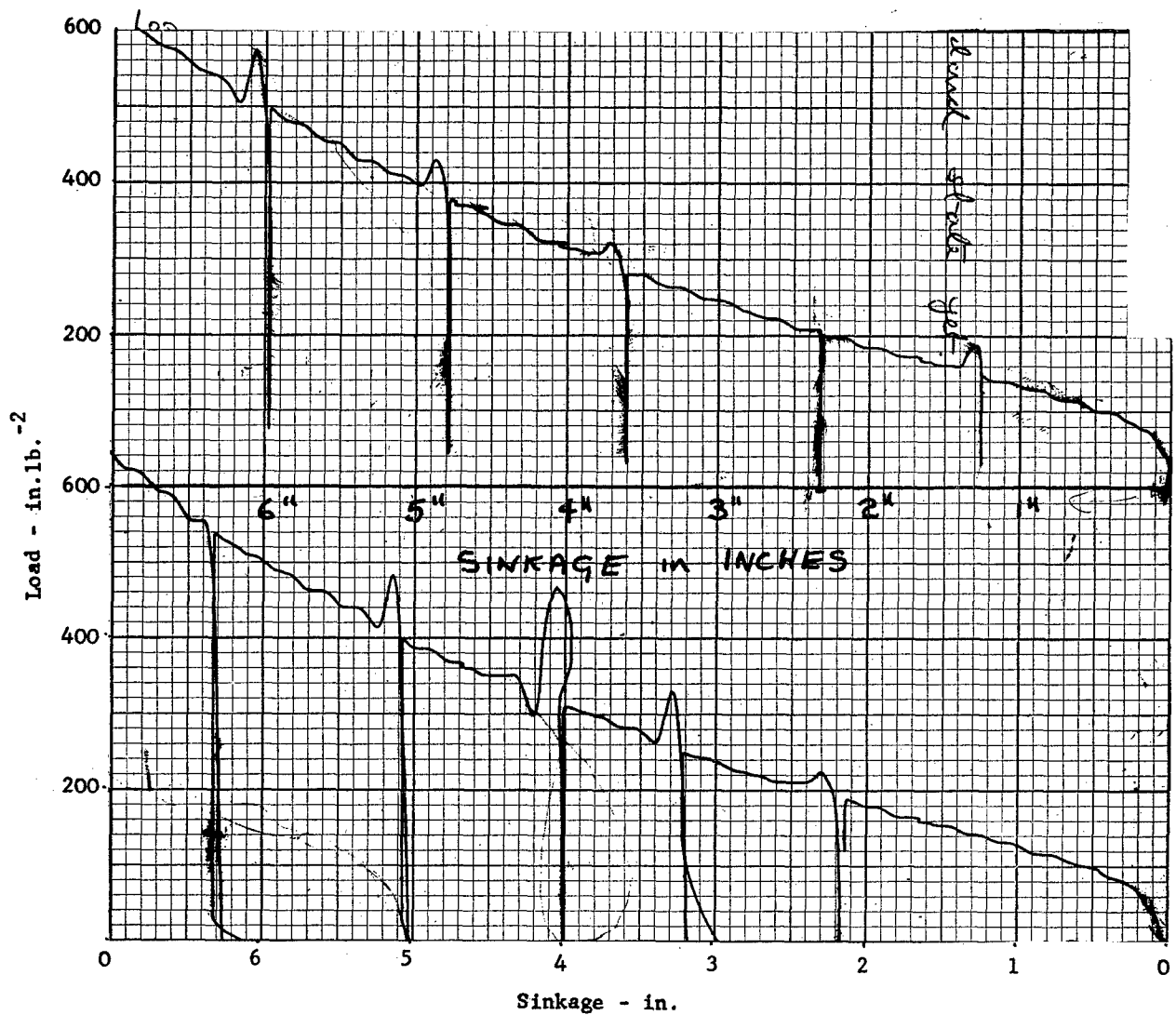
Fig.4.5.4. Results of two interrupted loading tests using a 4" dia.
plate in wet sand.

159
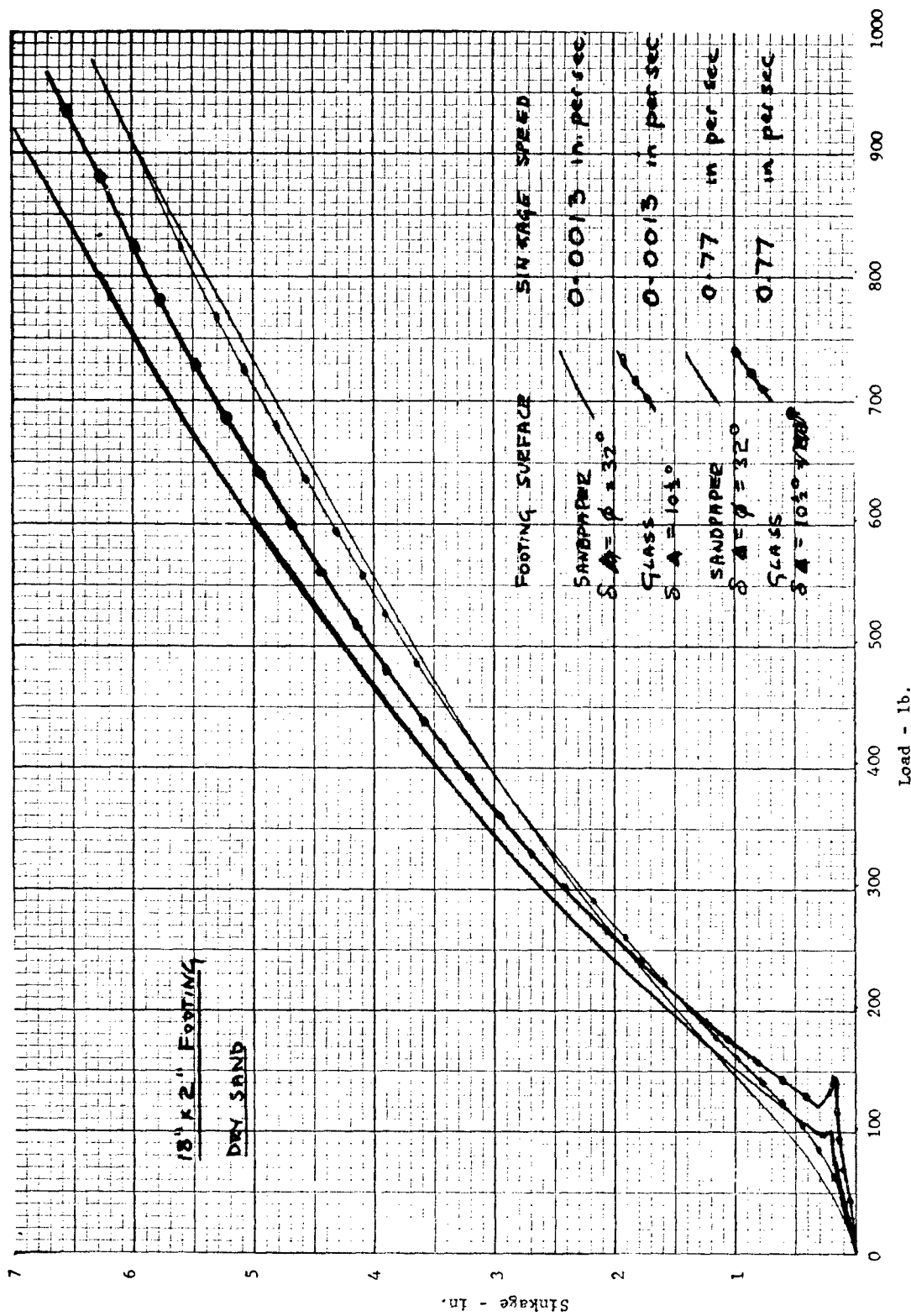
Fig.4.6.1. Results showing the effect of surface roughness and penetration speed on the pressure sinkage relationship for a 18" x 2" plate in dry sand.

160

Fig.4.6.2. Failure zones used by Meyerhof to compute the ultimate bearing capacity of foundations.
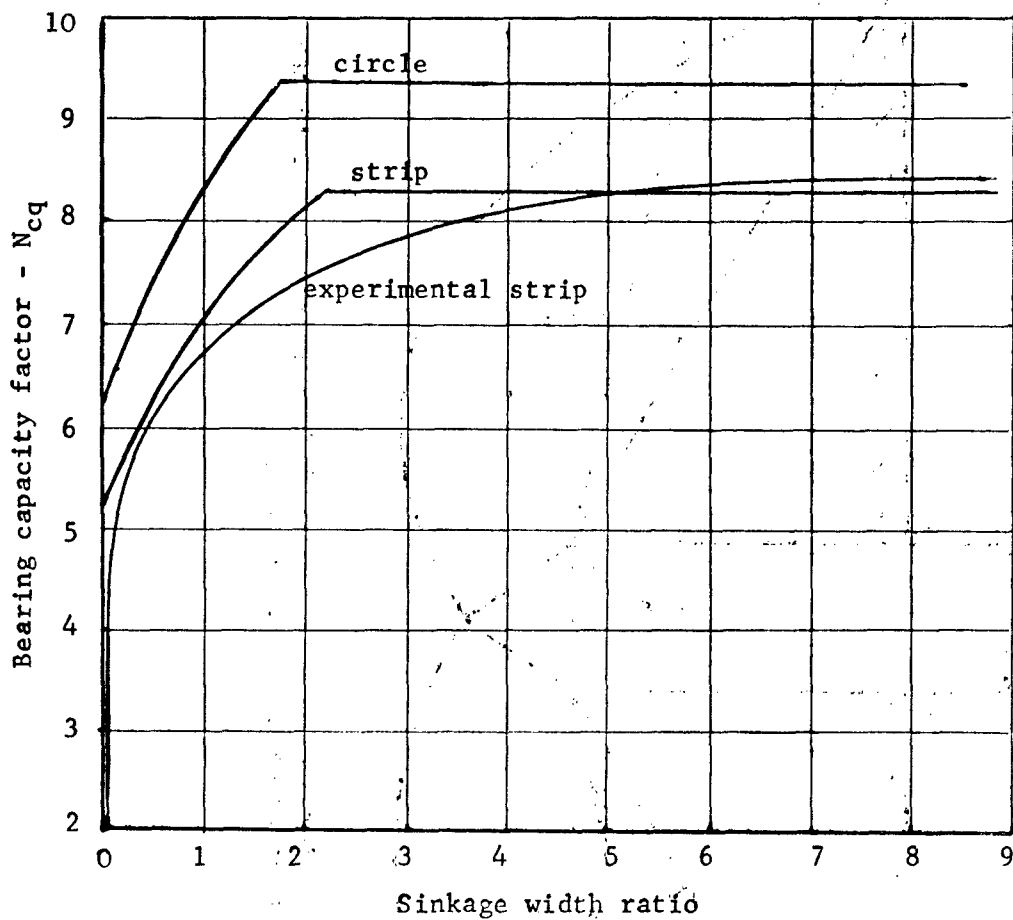
Fig.4.6.3. Theoretical and experimental bearing capacity
factor N_{cq} as a function of sinkage width ratio
for strip and circular footings in frictionless
soil. (after Meyerhof)
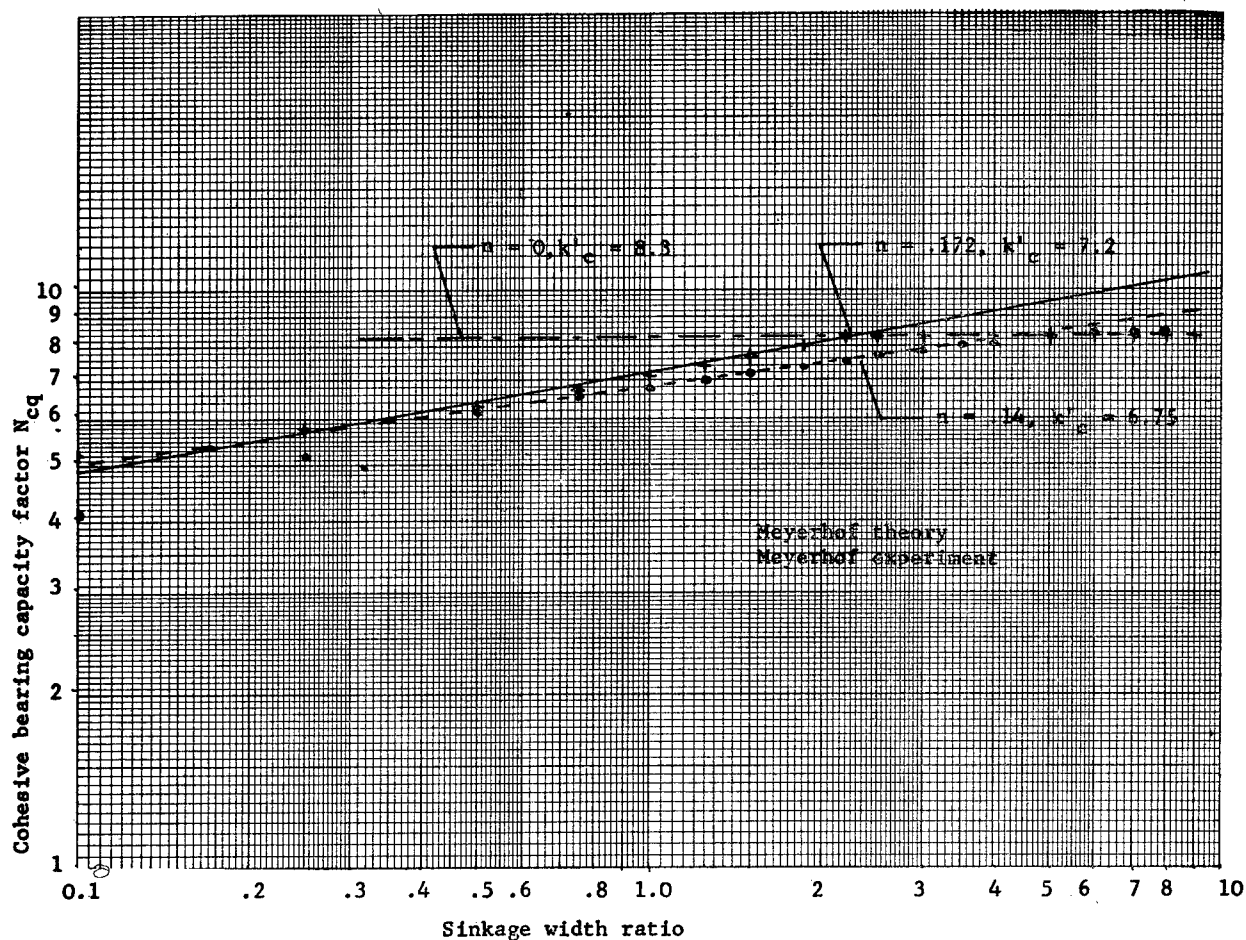
Fig.4.6.4. Theoretical and experimental bearing capacity factor N_{cq} as a function of sinkage-width ratio for frictionless soil. The points are plotted on logarithmic axes and best fitting straight lines representing equations of the form $N_{cq} = k'_c \left(\dfrac{z}{b}\right)^n$ are shown.
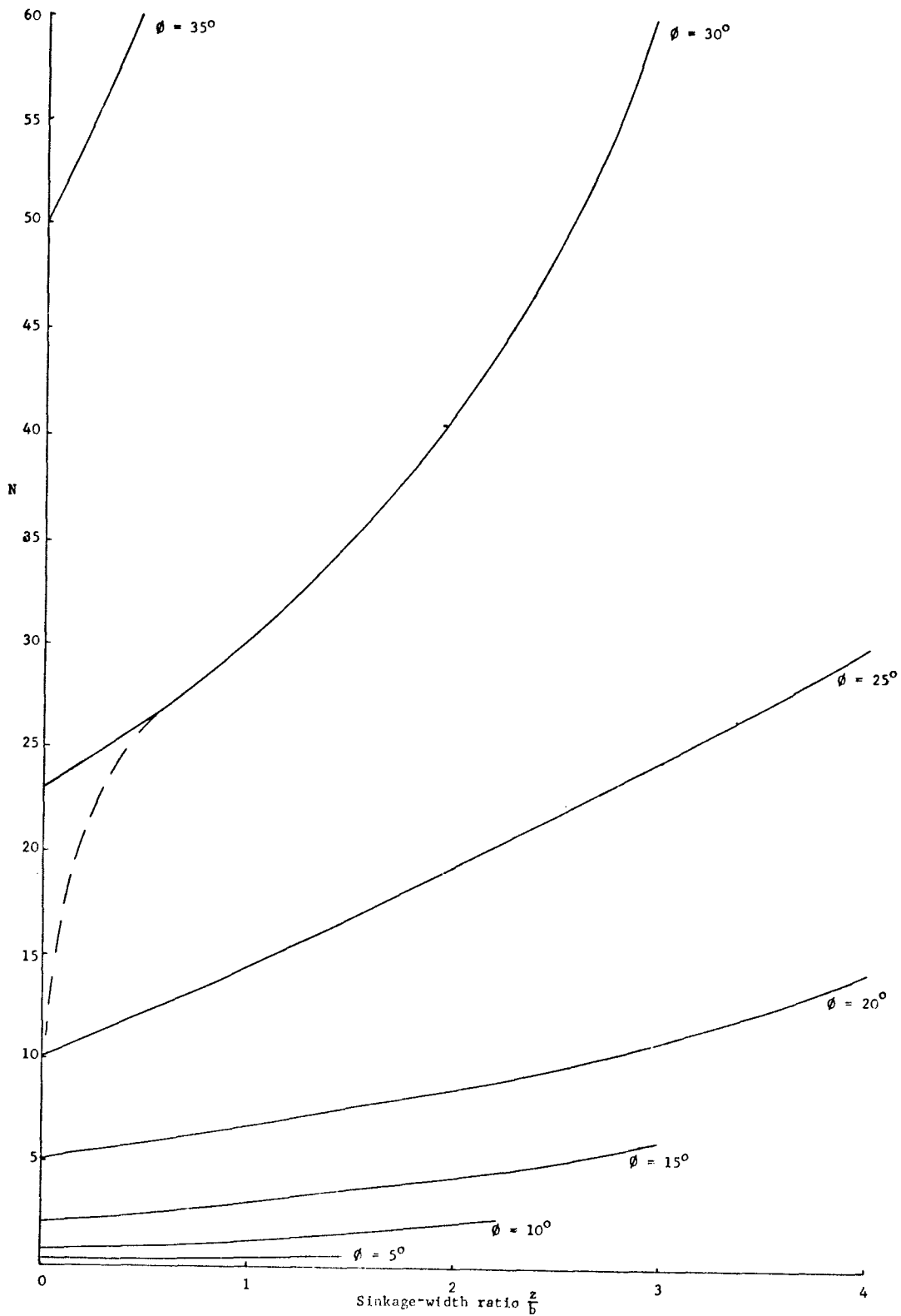
Fig.4.6.5. Bearing capacity factor N as a function of sinkage-width ratio $\frac{z}{b}$

164
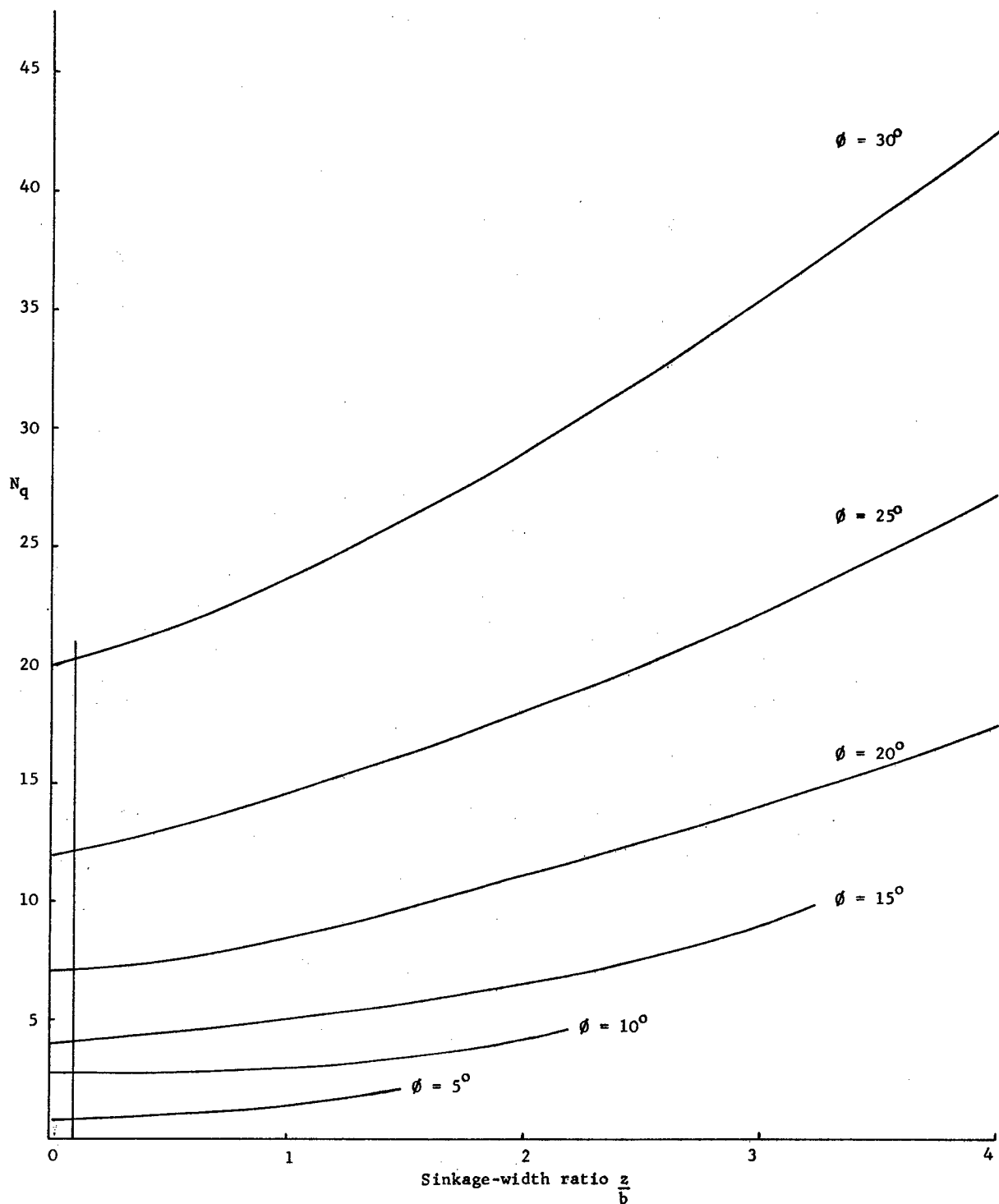
Fig.4.6.6. Bearing capacity factor N_q as a function of sinkage width ratio $\frac{z}{b}$
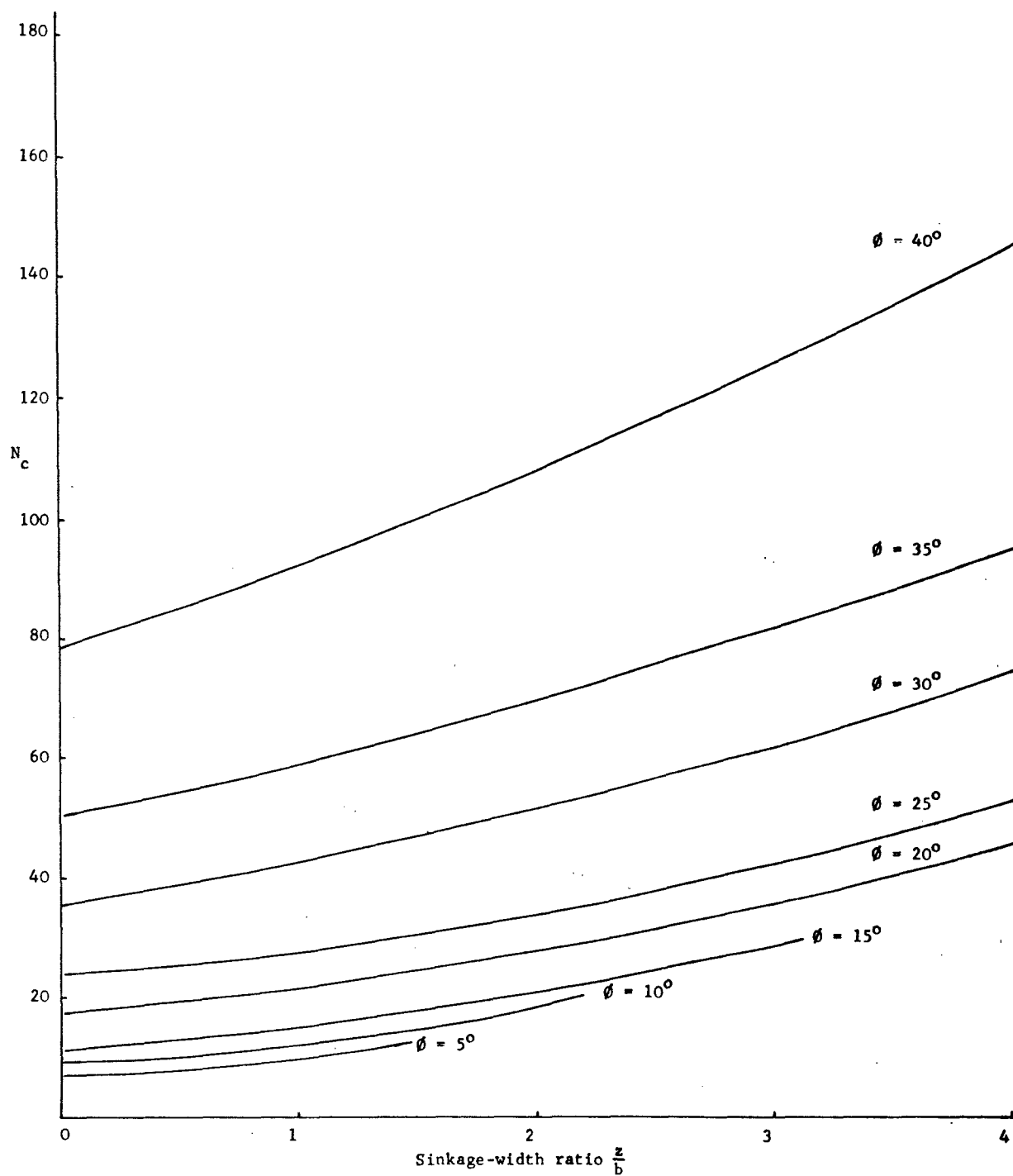
Fig.4.6.7. Bearing capacity factor N_c as a function of sinkage width ratio $\frac{z}{b}$
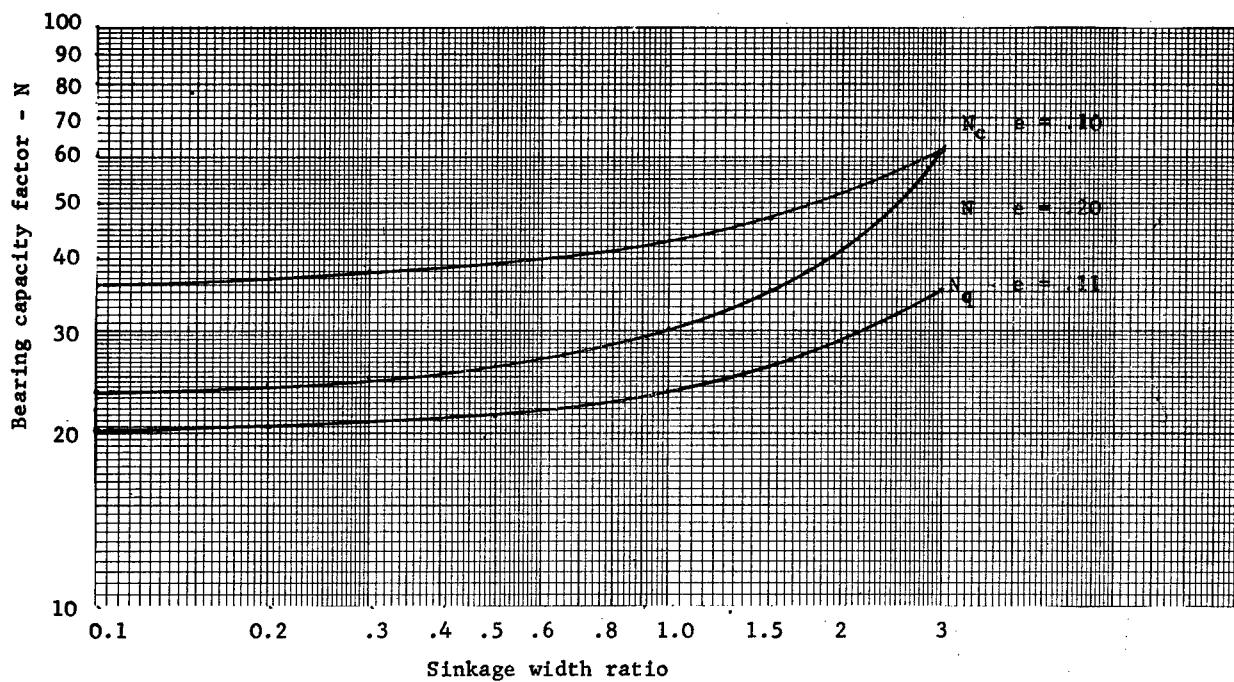
Fig.4.6.8. Bearing capacity factors N_c, N and N_q for $\emptyset = 30^o$
as functions of sinkage width ratio on logarithmic axes.
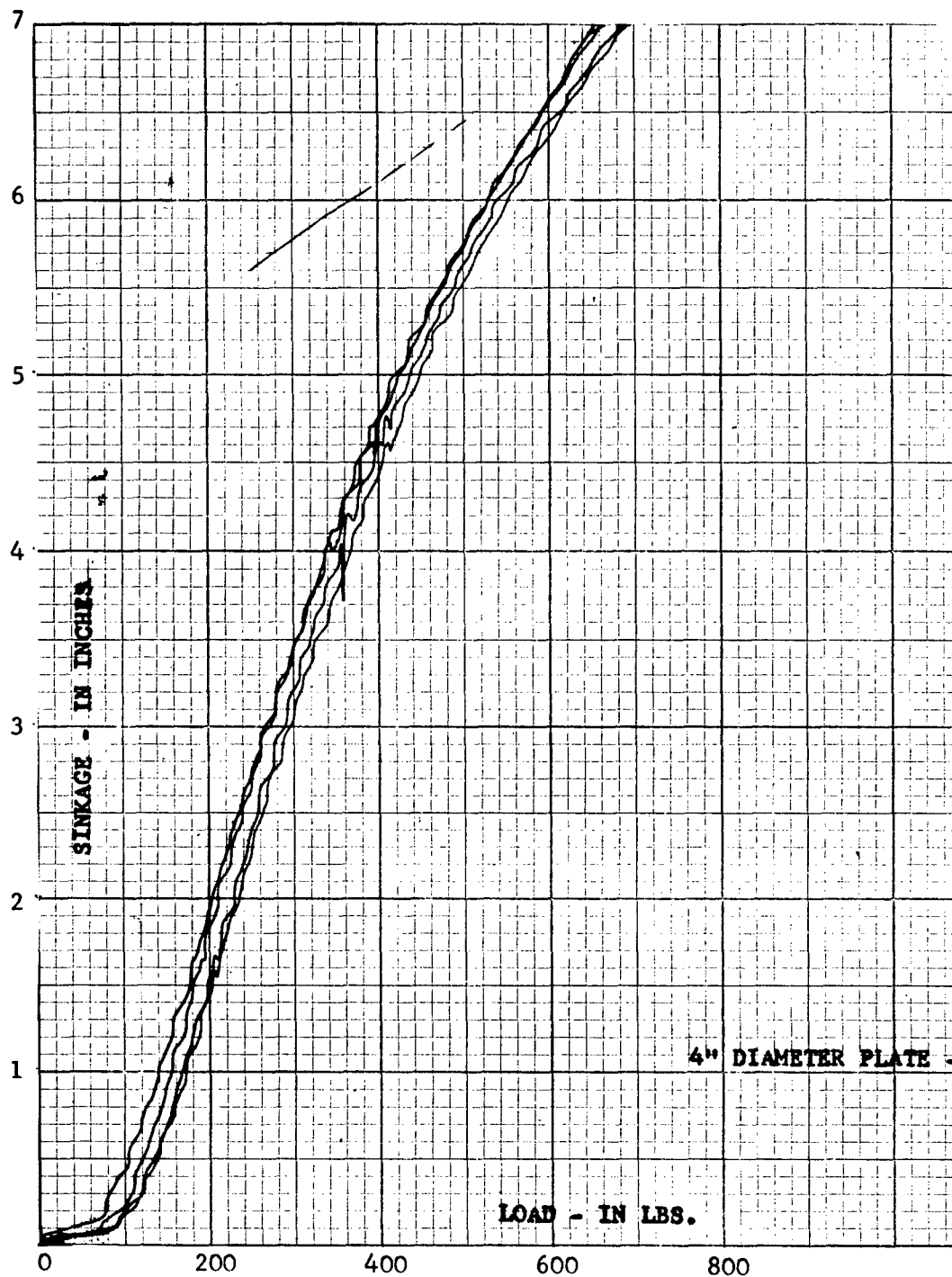
Fig.4.8.1. Typical X-Y plotter traces from four penetrations
with a 4" dia. plate into wet sand.

168
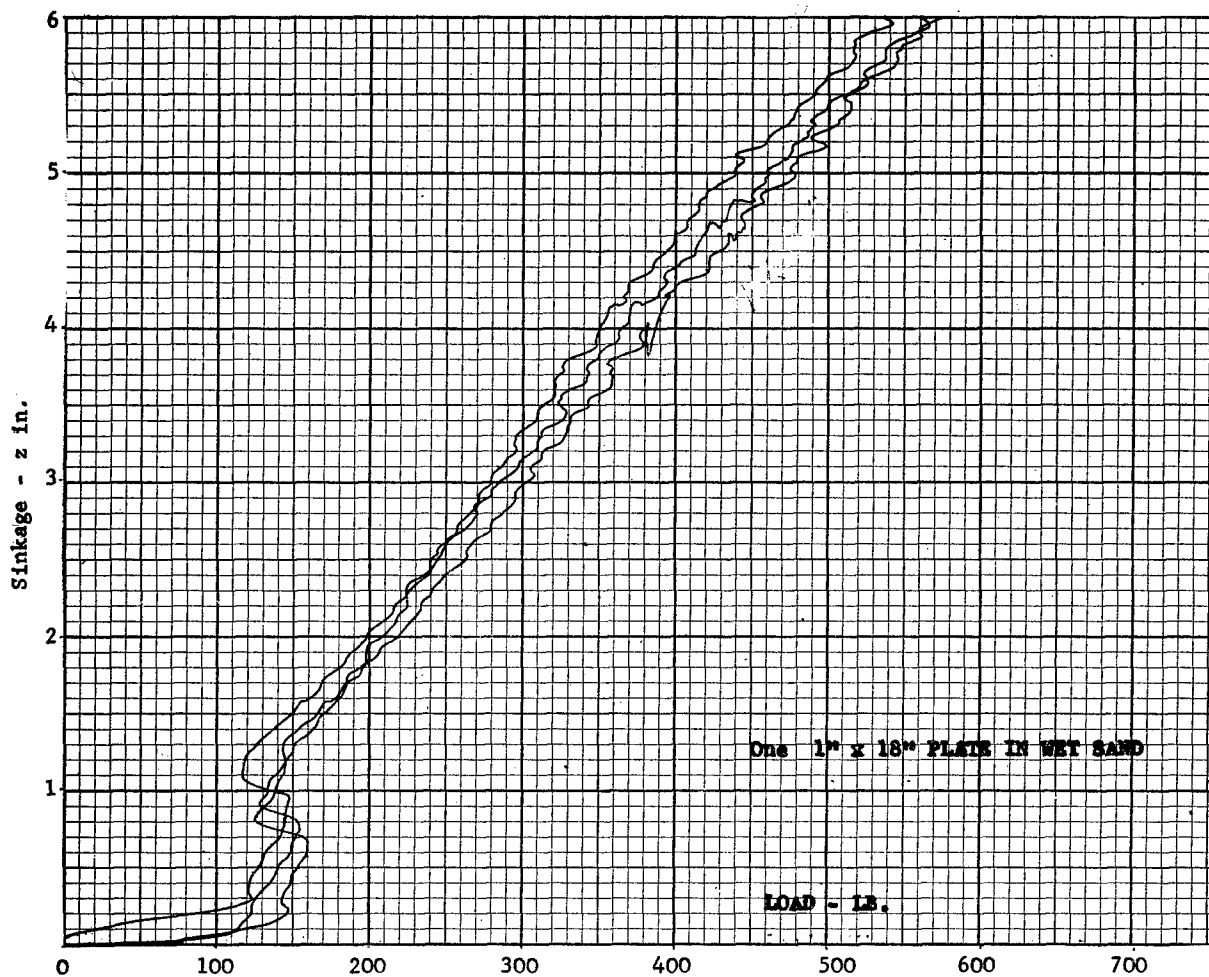
Fig.4.8.2. Typical X-Y plotter traces from four penetrations with a 18" x 1" plate into wet sand.
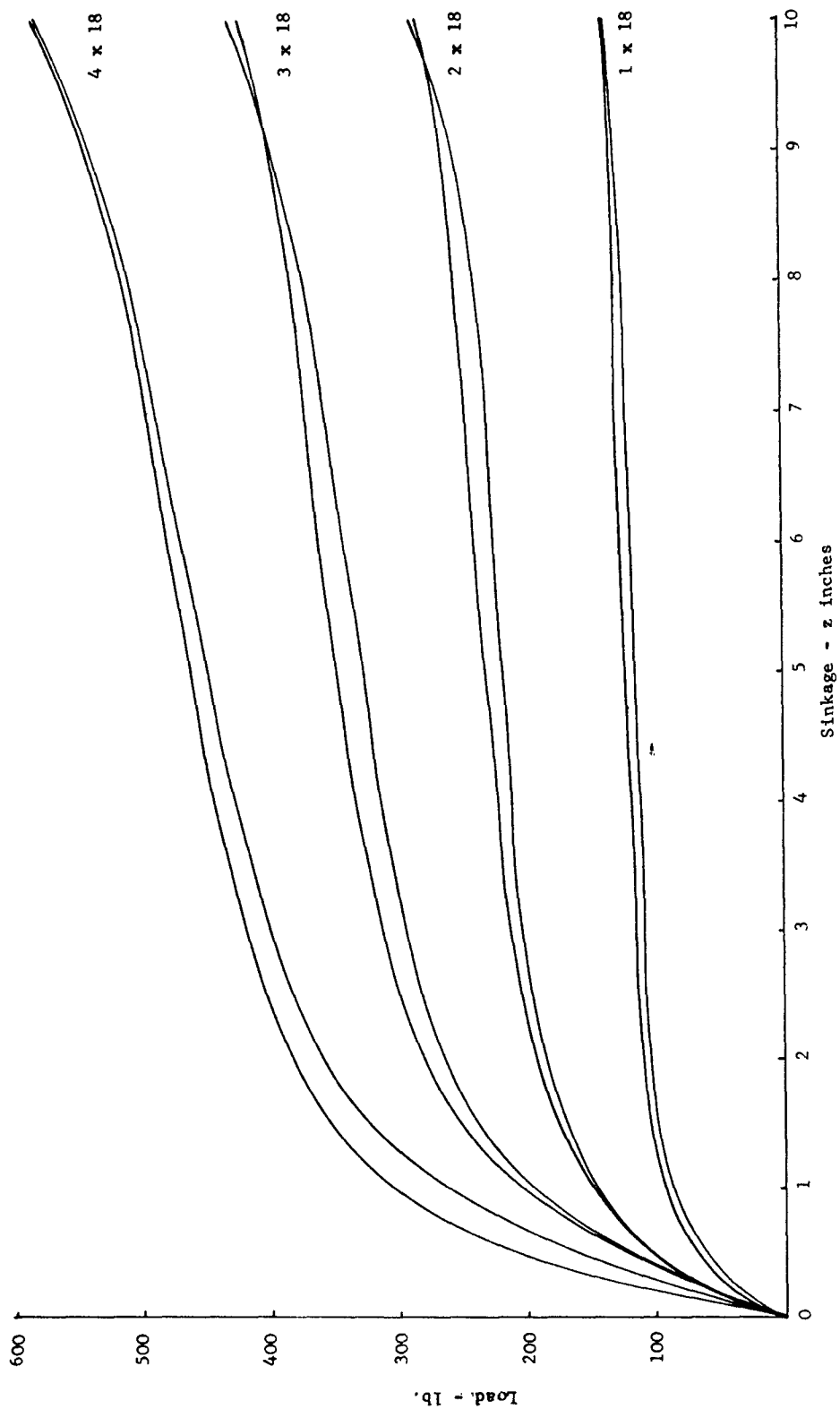
Fig.4.8.3. Pairs of typical X-Y plotter traces from four rectangular plates, in saturated clay.
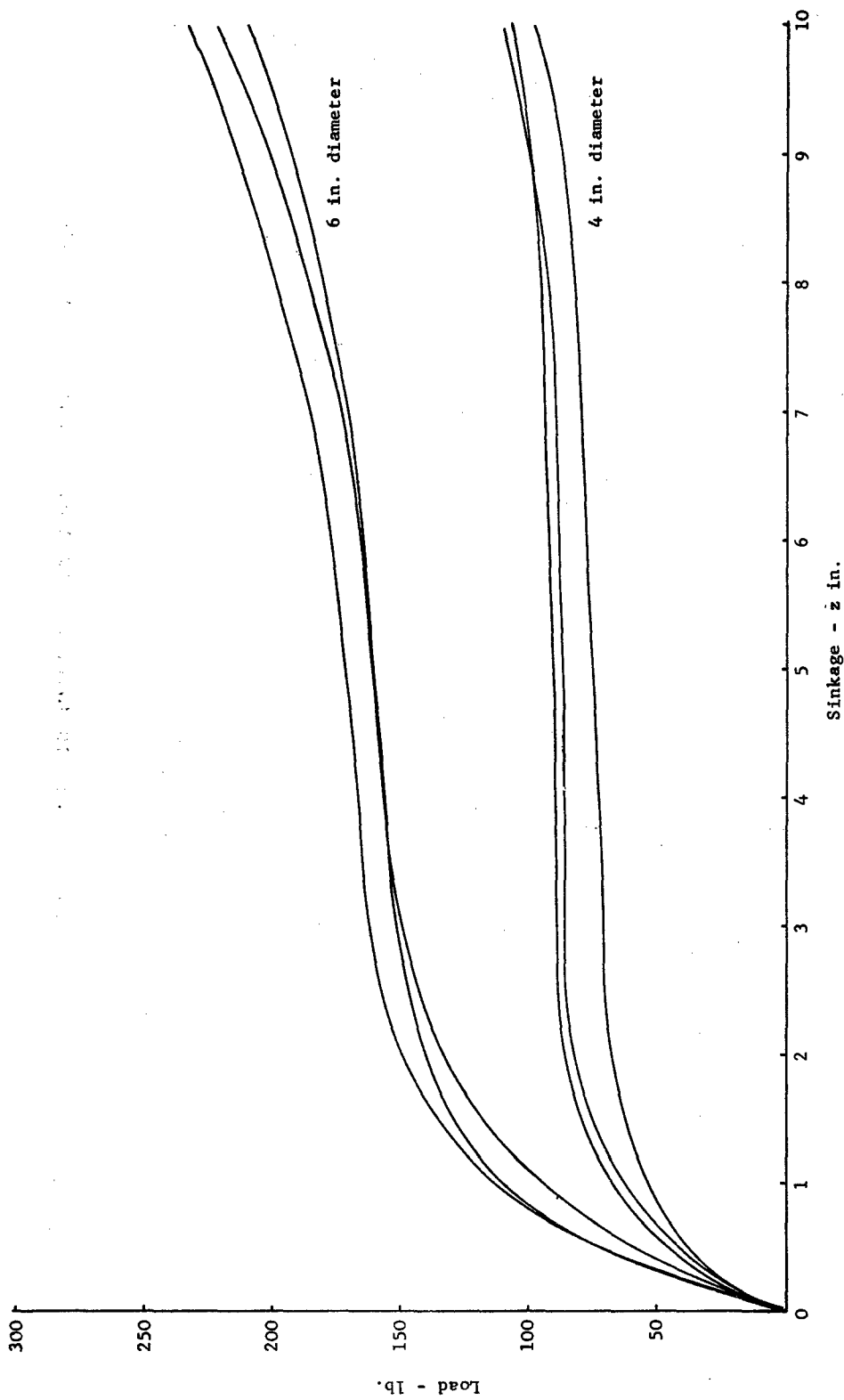
Fig.4.8.4. Typical X-Y plotter traces from three tests with two plate diameters in saturated clay.

171
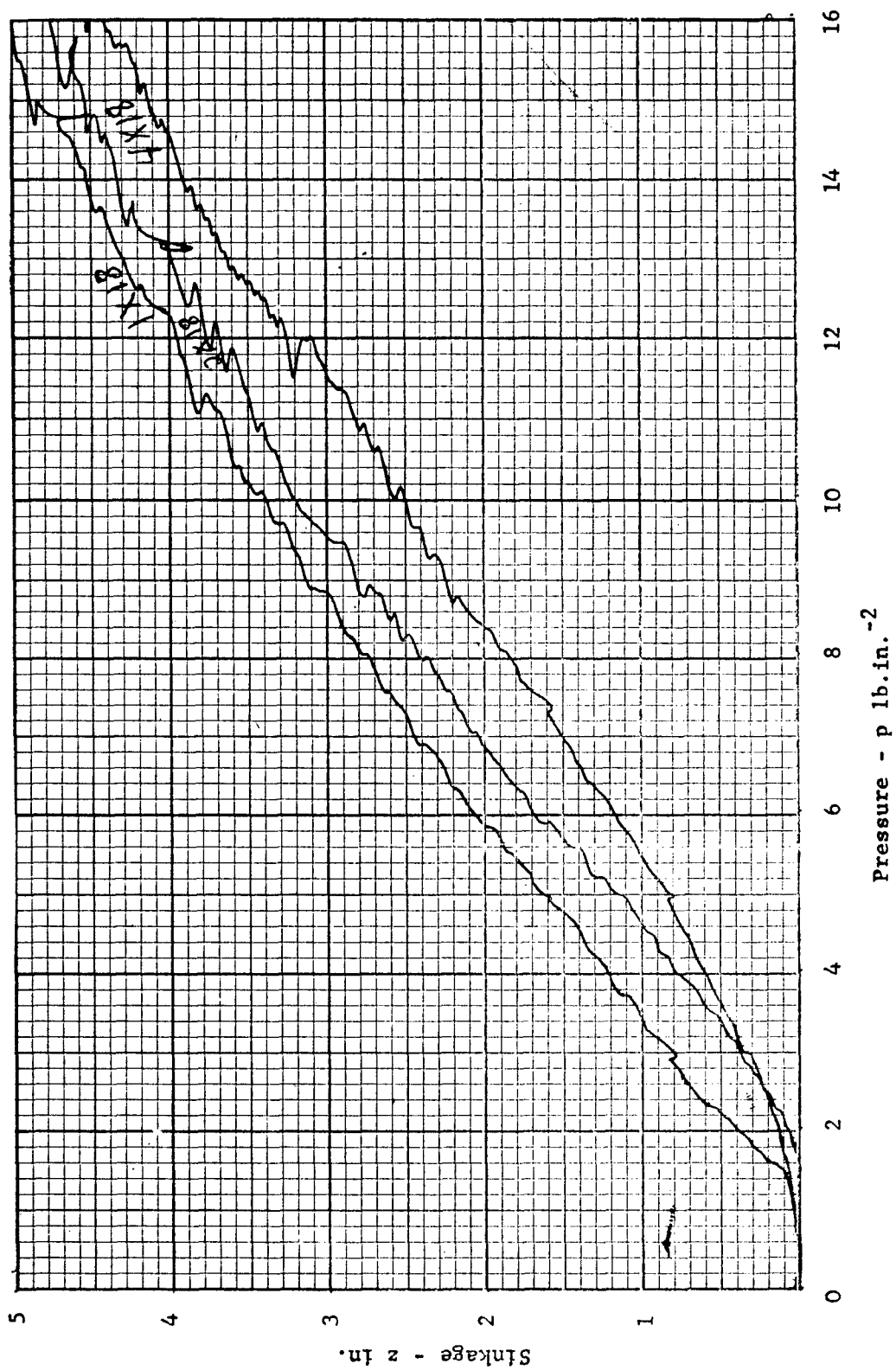
Fig.4.8.5. Trial X-Y plotter record showing direct measurement of pressure instead of load.
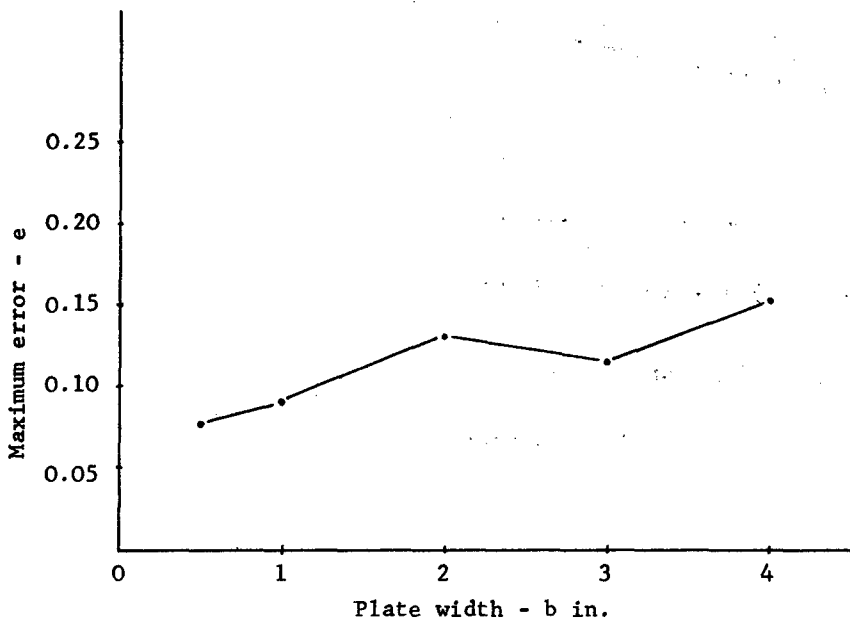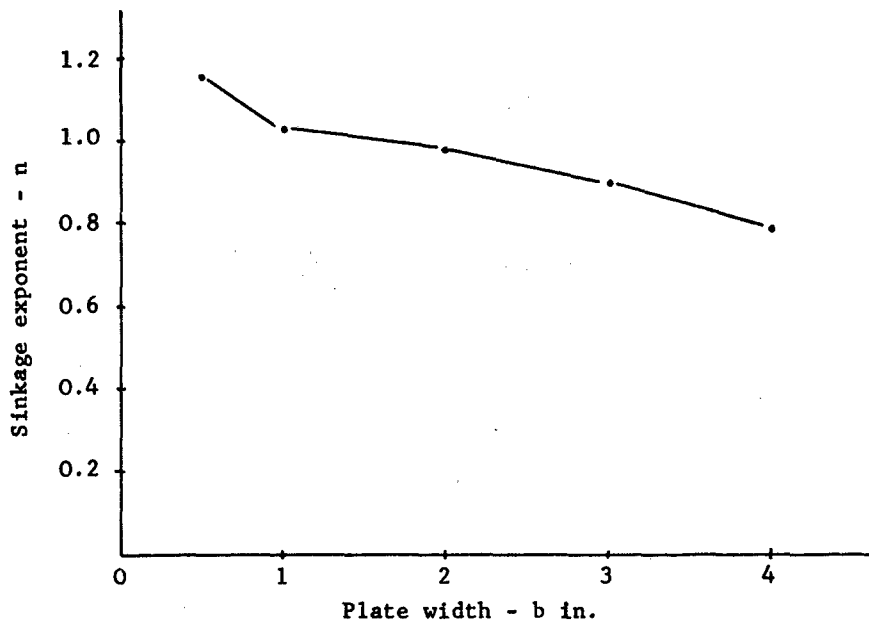
Fig.4.8.6. Analysis of mean pressure sinkage relations for rectangular strips of different widths, b, in dry sand. The exponent n and the maximum curve fitting error e using the equation $p = kz^n$ are plotted against plate width.
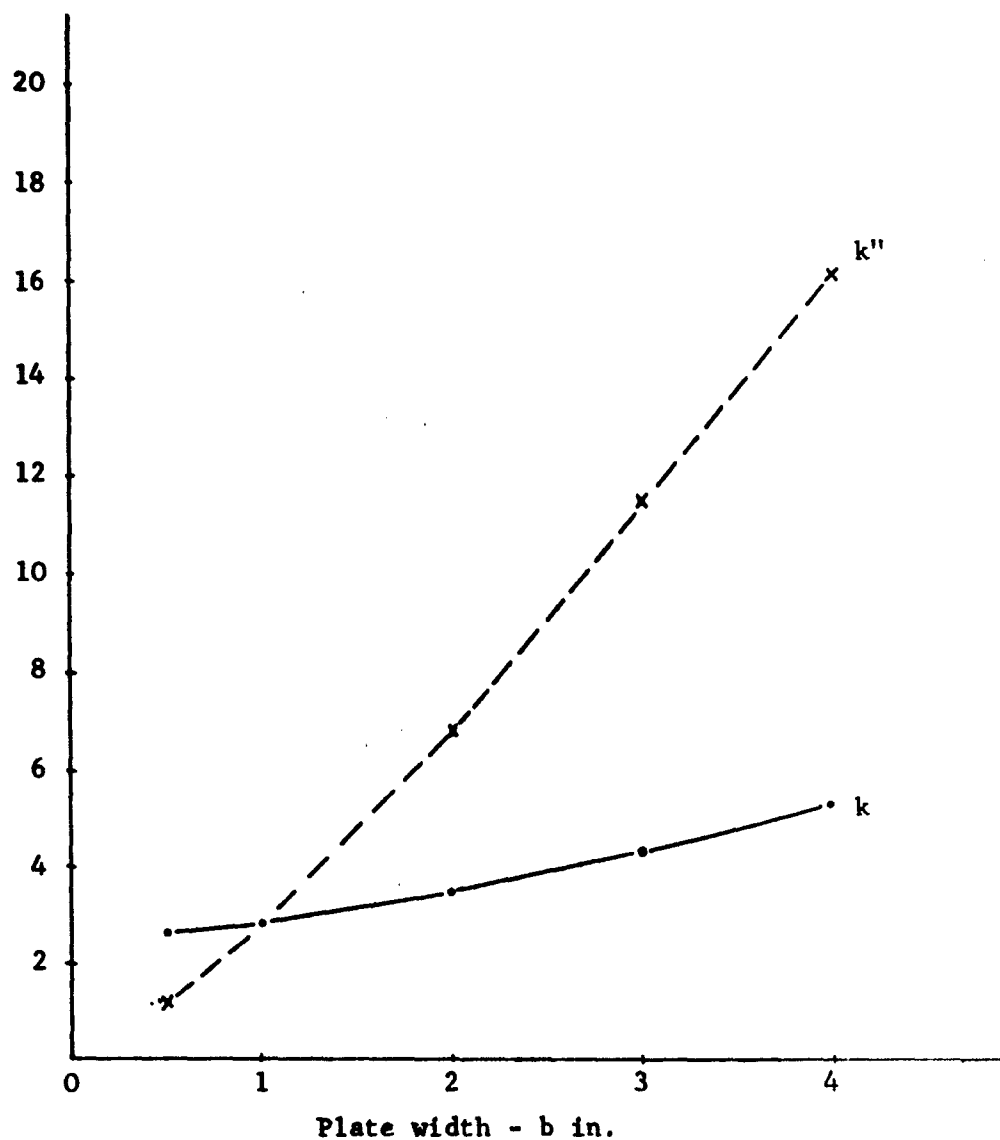
Fig.4.8.7. The relation between k in $p = kz^n$ and k" in $p = k'' \left[\dfrac{z}{b}\right]^n$

and plate width for rectangular plates in dry sand.
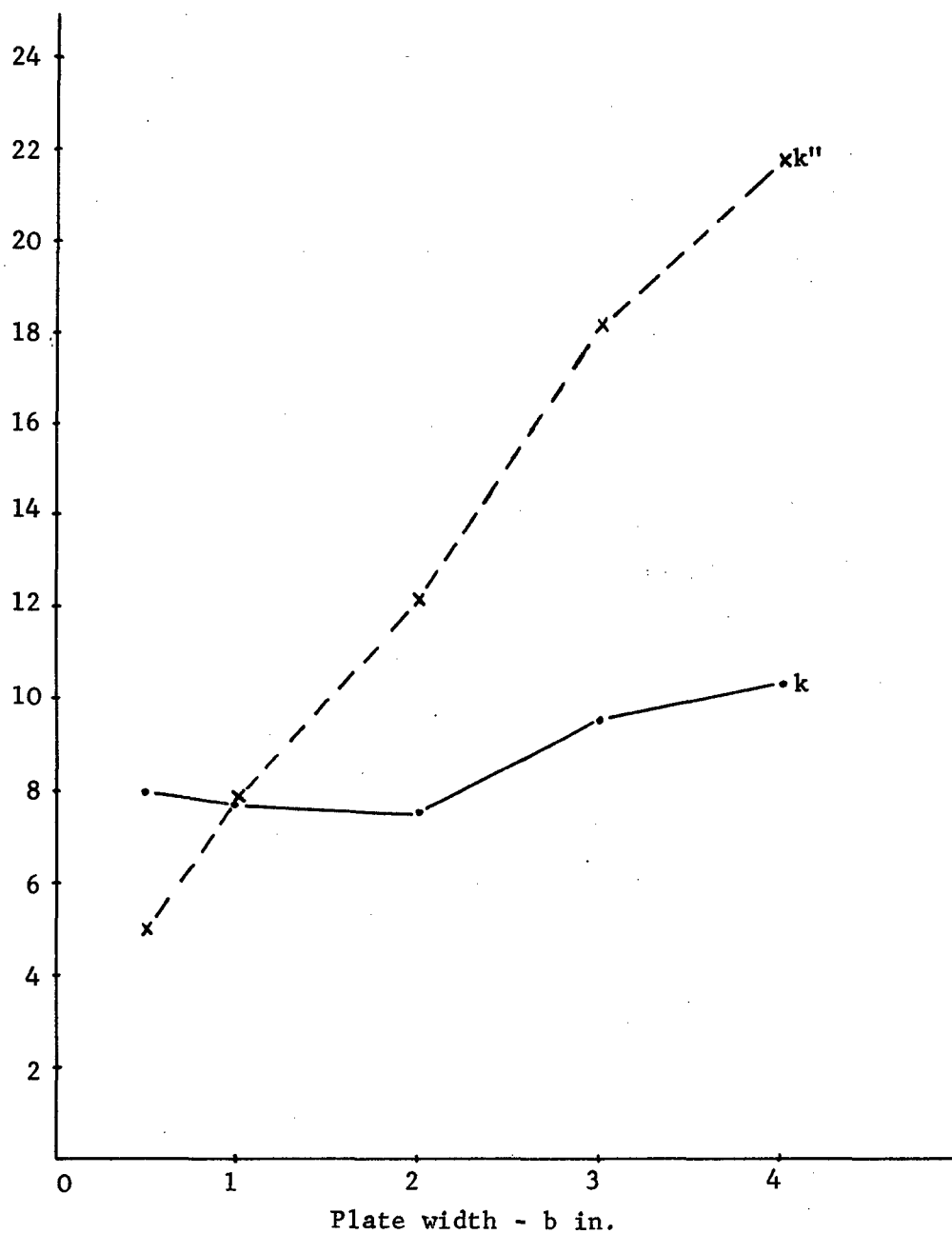
Fig.4.8.8. The relation between k in $p = kz^n$ and k" in $p = k'' \left[\dfrac{z}{b}\right]^n$

and plate width for rectangular plates in wet sand.
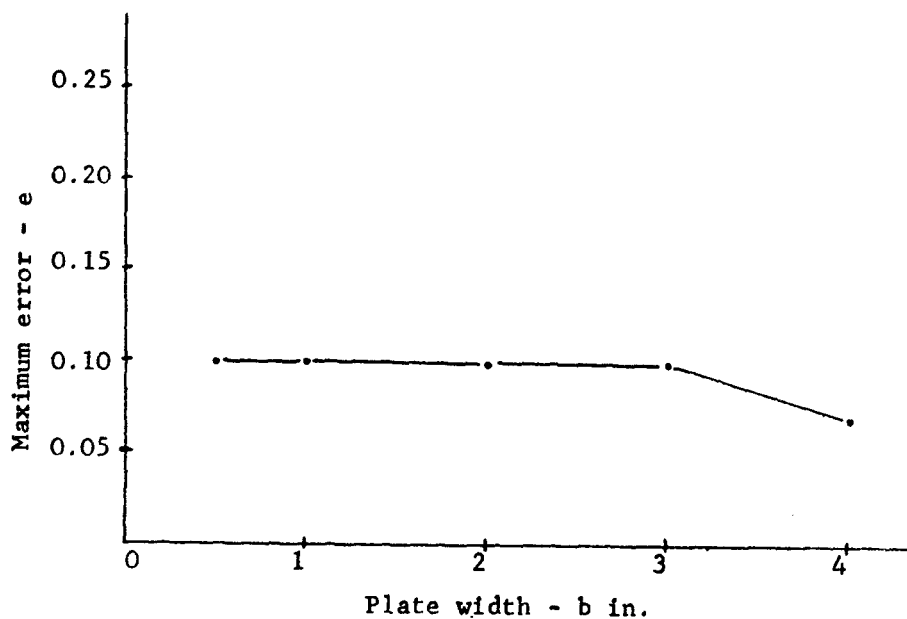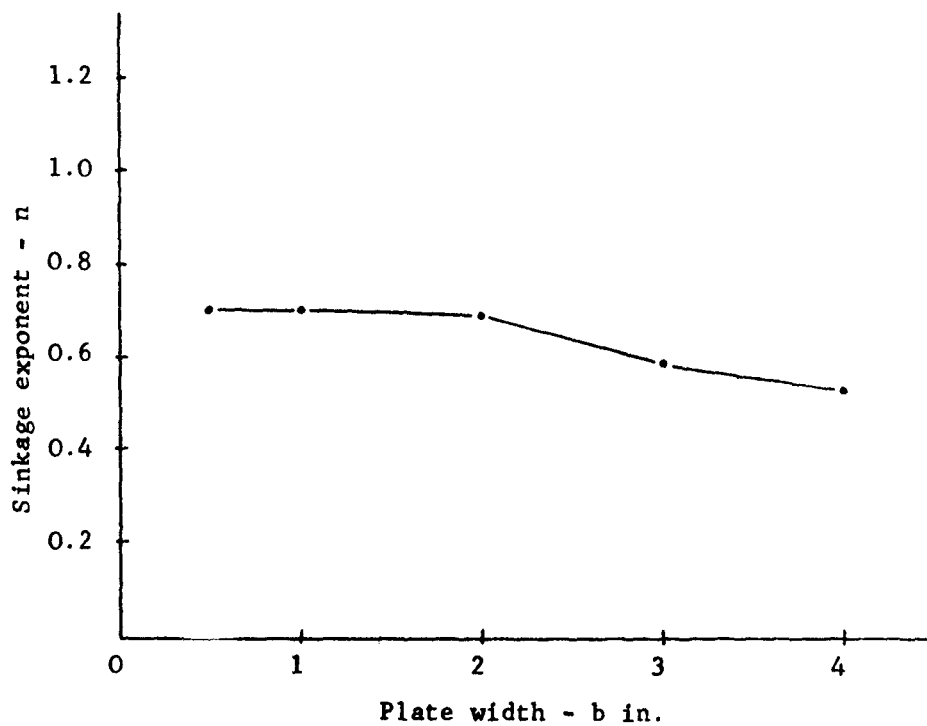
Fig.4.8.9. Analysis of mean pressure sinkage relations for rectangular strips of different widths, b, in wet sand. The exponent n and the maximum curve fitting error e using the equation $p = kz^n$ are plotted against plate width.

176
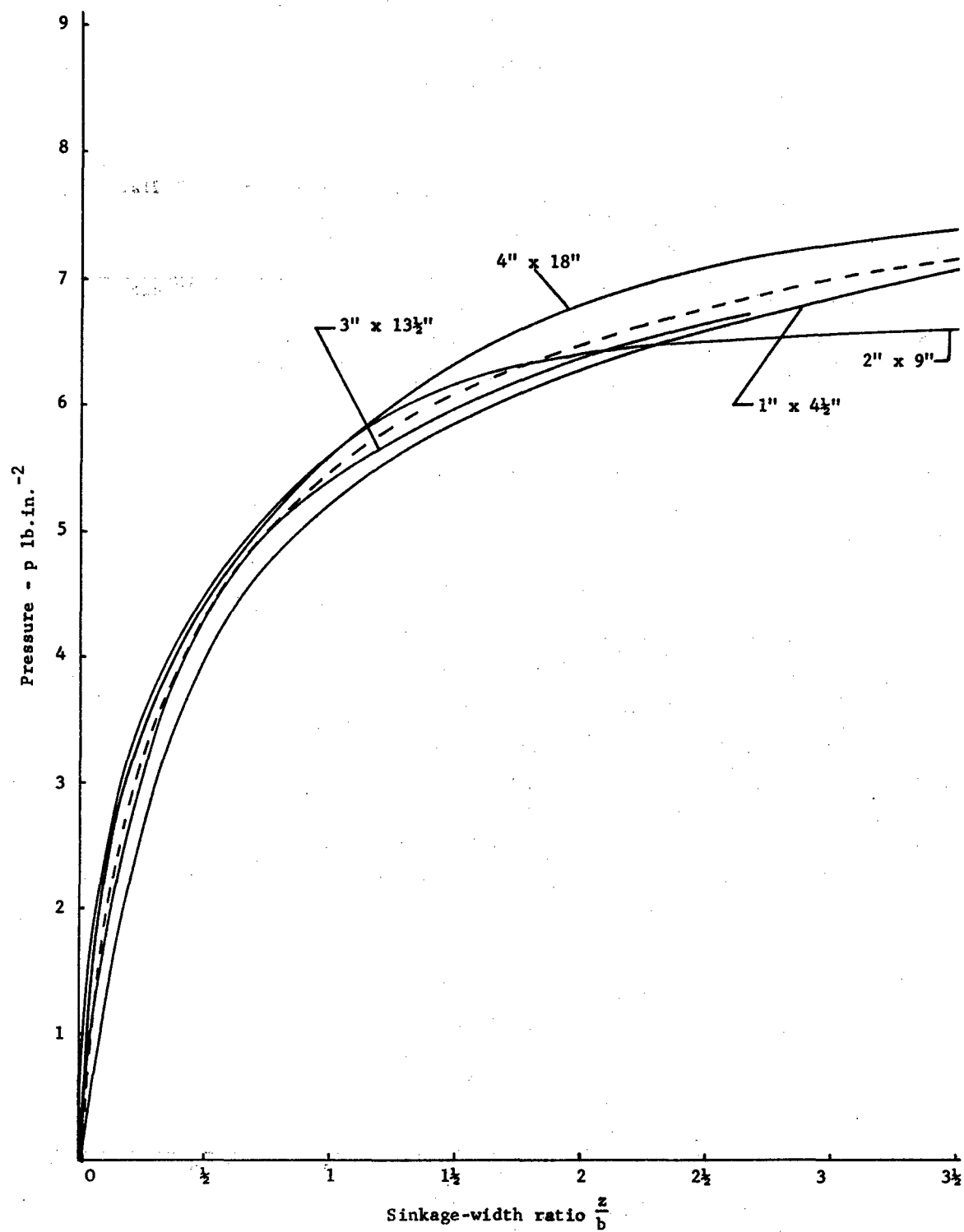
Fig.4.8.10. Pressure plotted against sinkage-width ratio for similar rectangular plates in saturated clay.

177
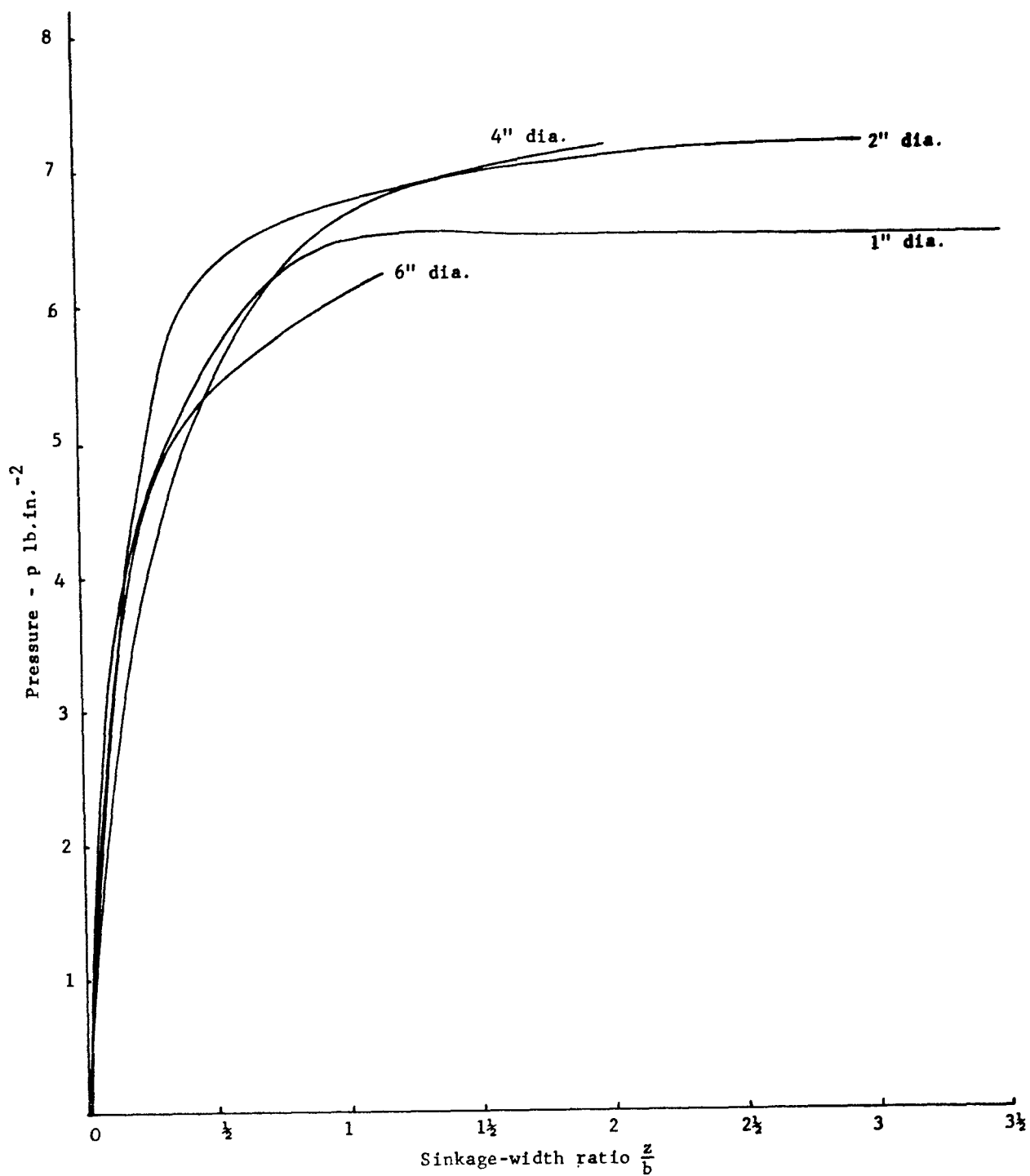
Fig.4.8.11. Pressure plotted against sinkage-width ratio for circular plates in saturated clay.
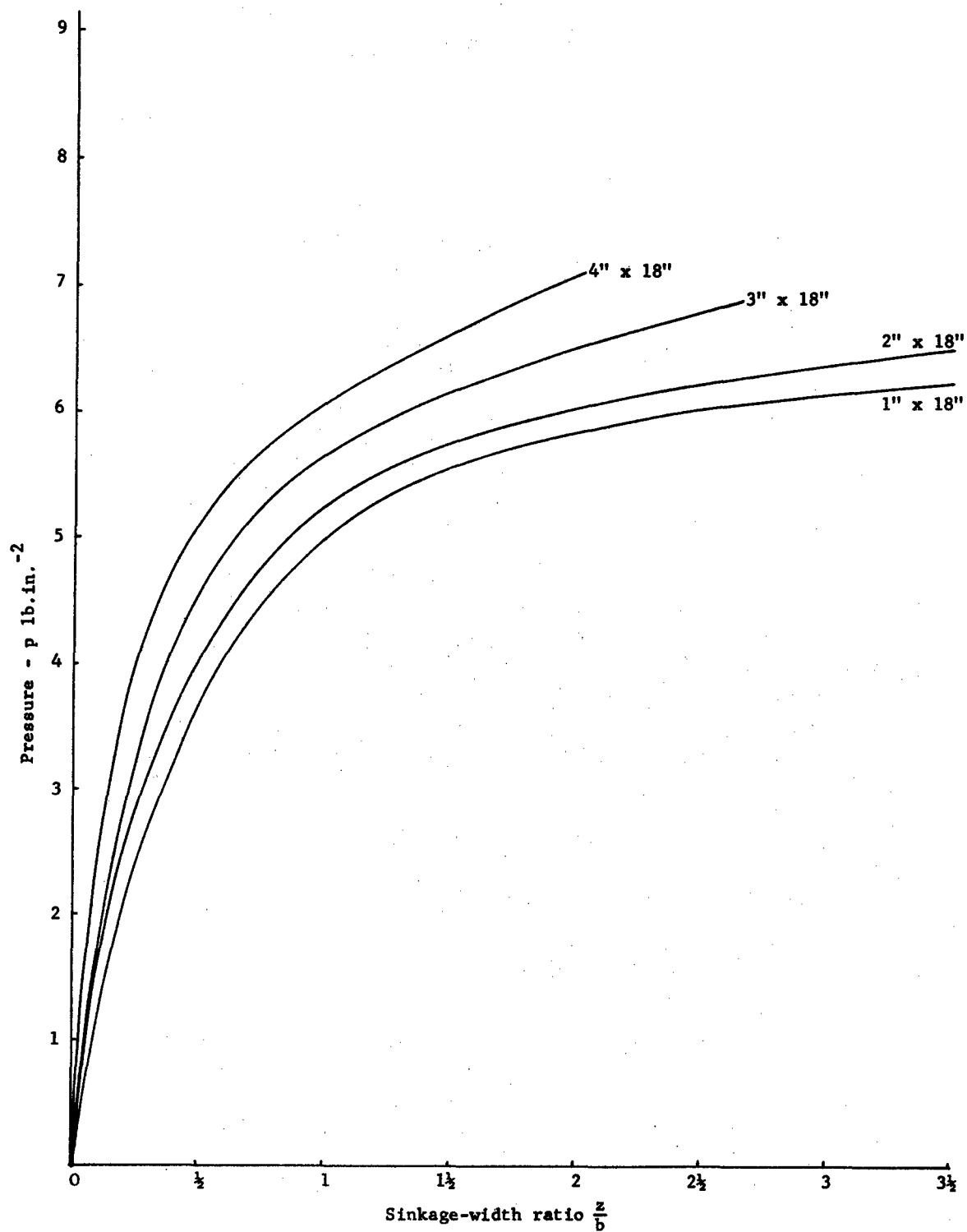
Fig.4.8.13. Pressure plotted against sinkage-width ratio for rectangular plates
in saturated clay.
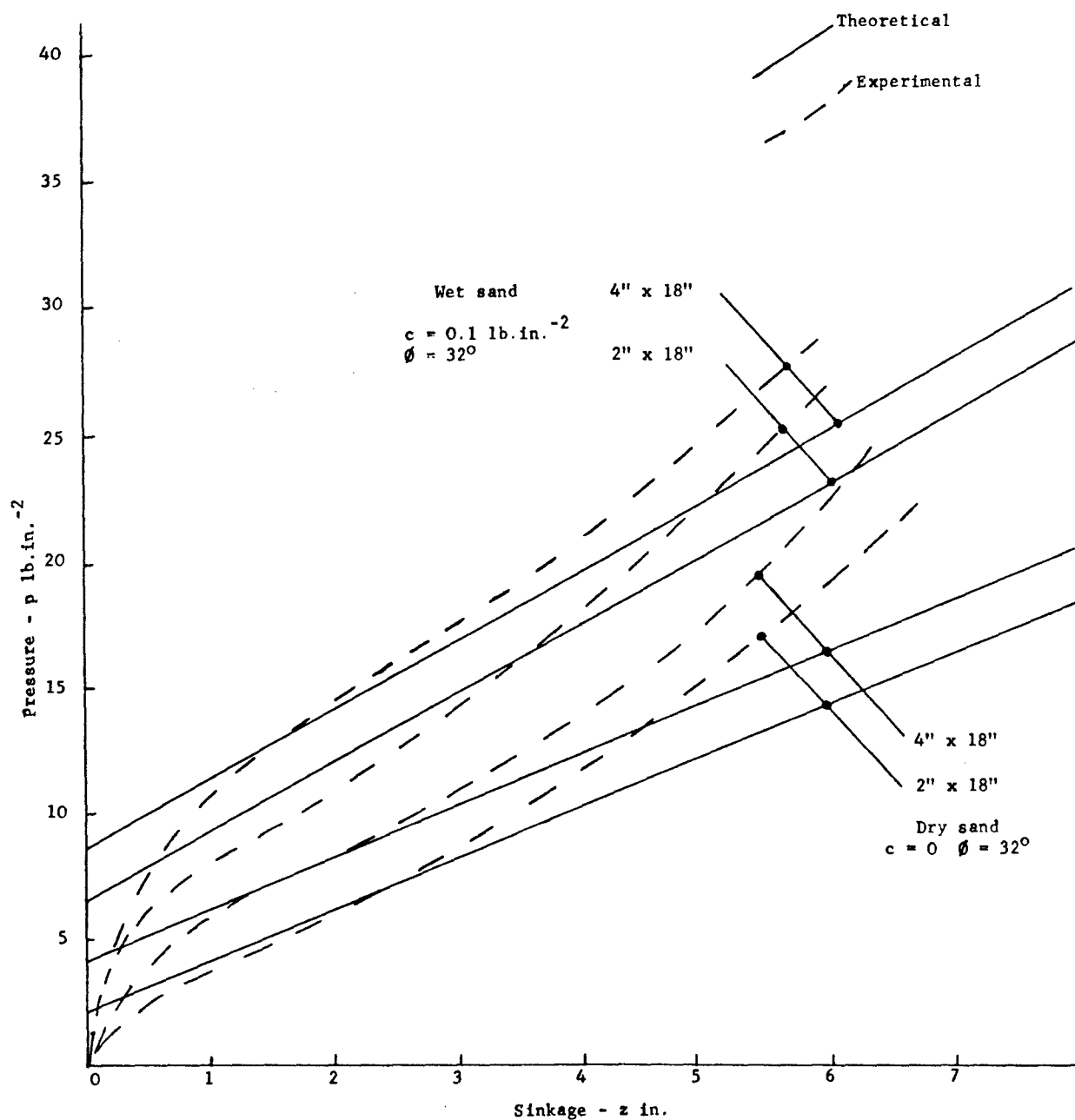
Fig.4.9.1. A comparison of experimental pressure sinkage curves in sand
with those calculated from Meyerhof's theory.
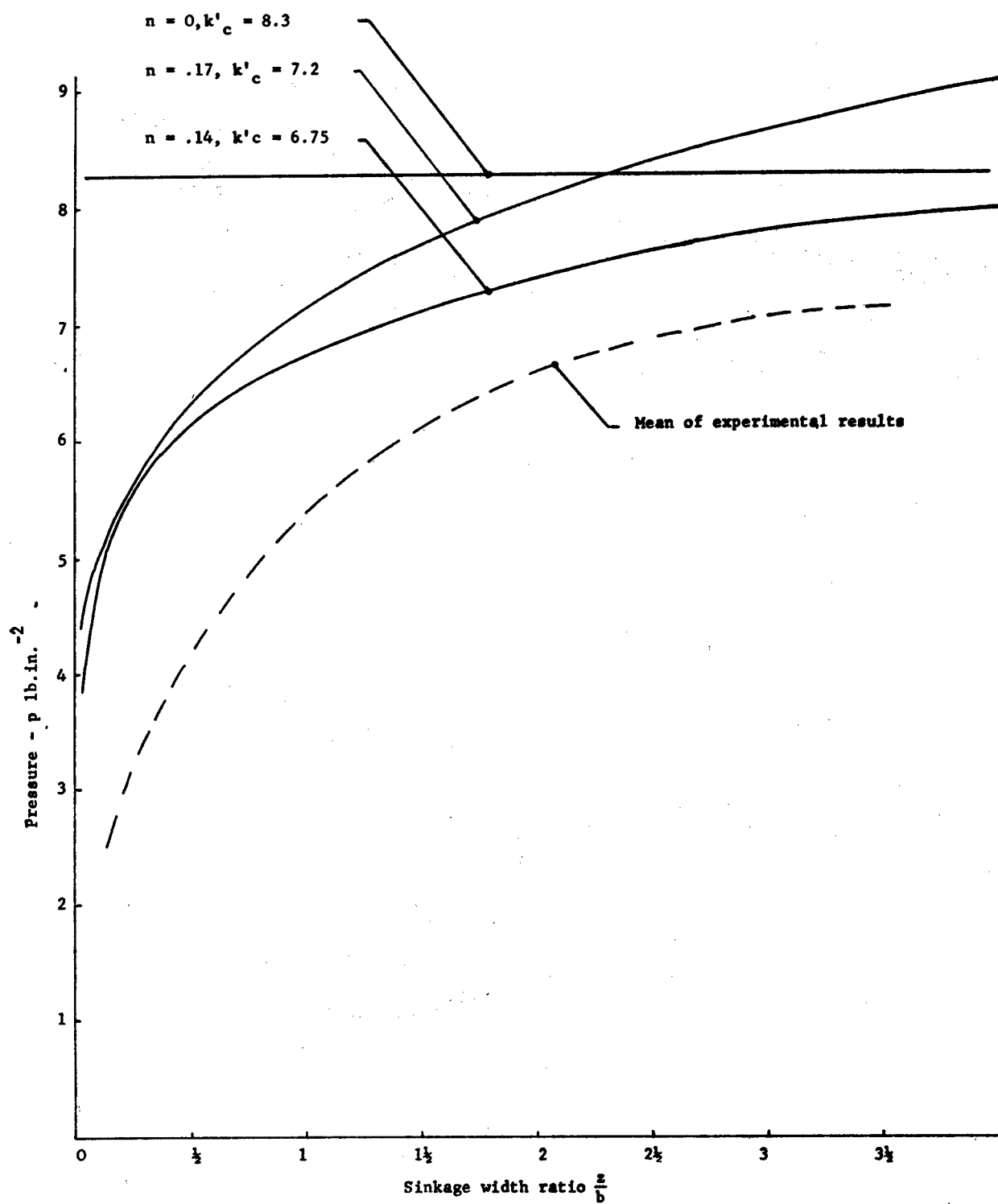
Fig.4.9.2. A comparison between theoretical and experimental pressure sinkage curves in saturated clay.

Fig.5.5.1. (a) The shear plane at the side of a track.
(b) The general state of stress at the side of a track.
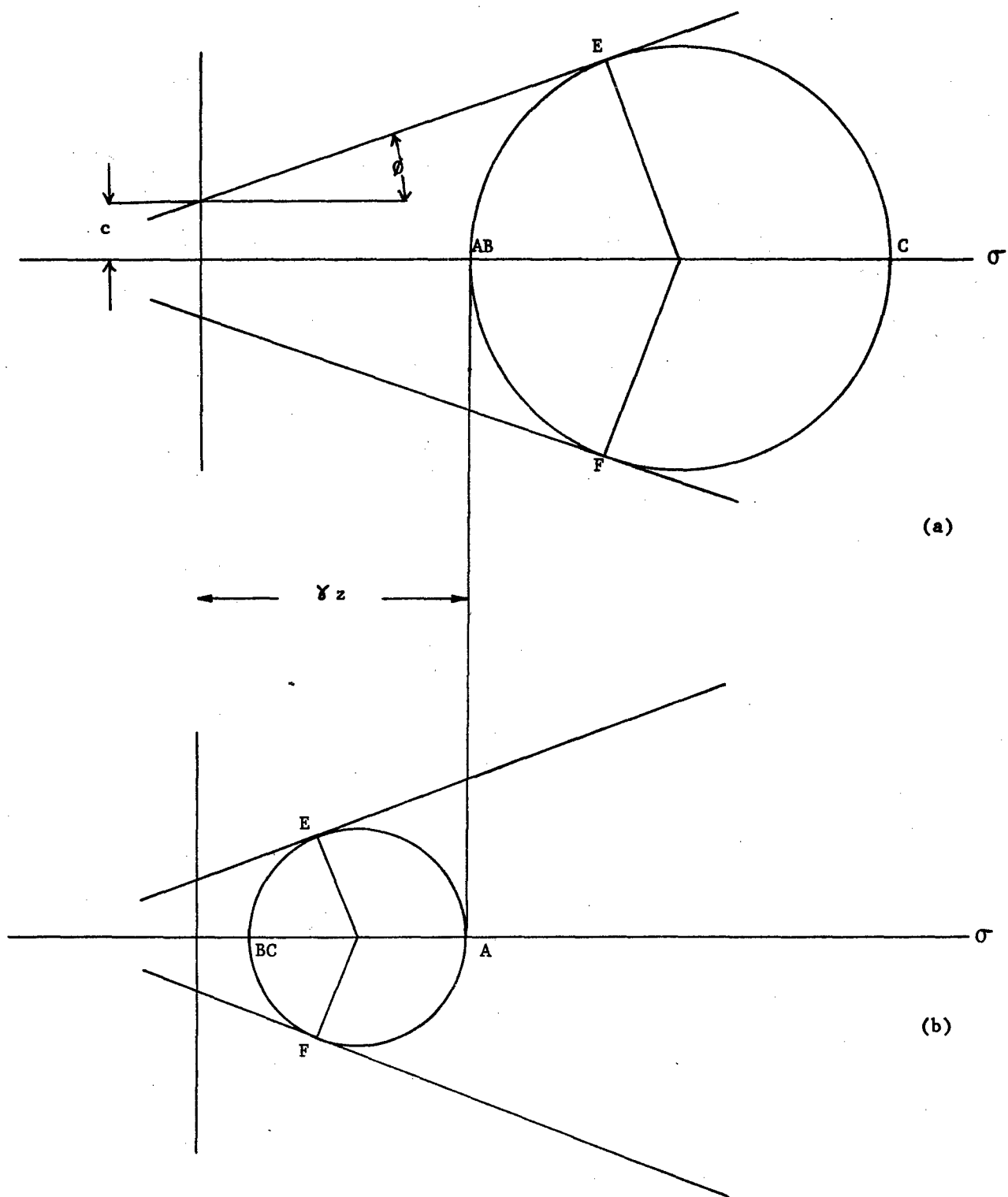
Fig.5.5.2. Stress states at the side of a track.
     (a) Maximum stresses - passive state.
     (b) Minimum stresses - active state.

183

(a)

(b)
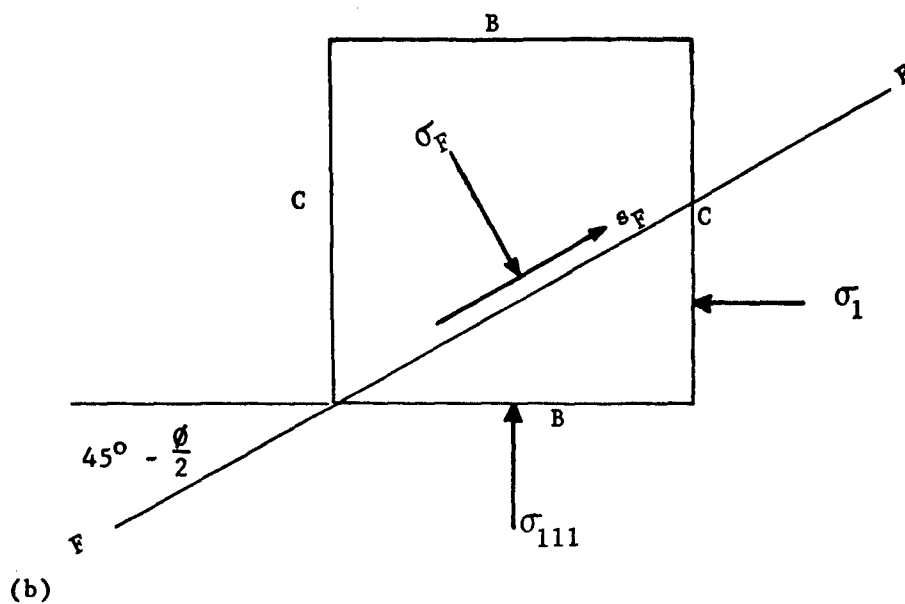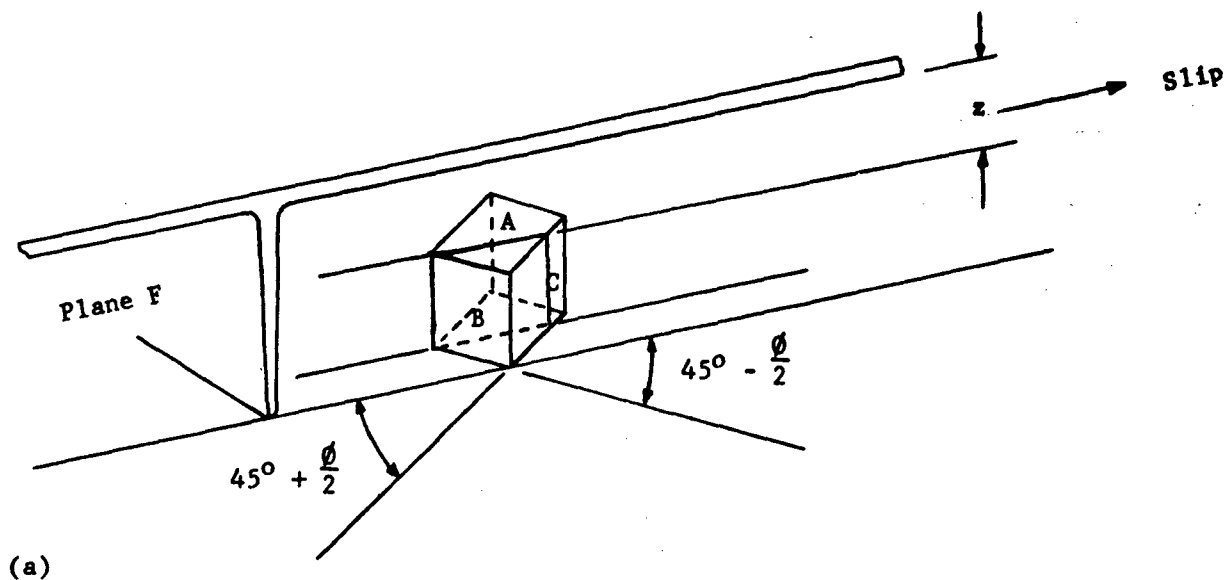
Fig.5.5.3. (a) Principle planes at the side of a track.
(b) Plan view of principle plane cube
intersected by failure plane F.

184
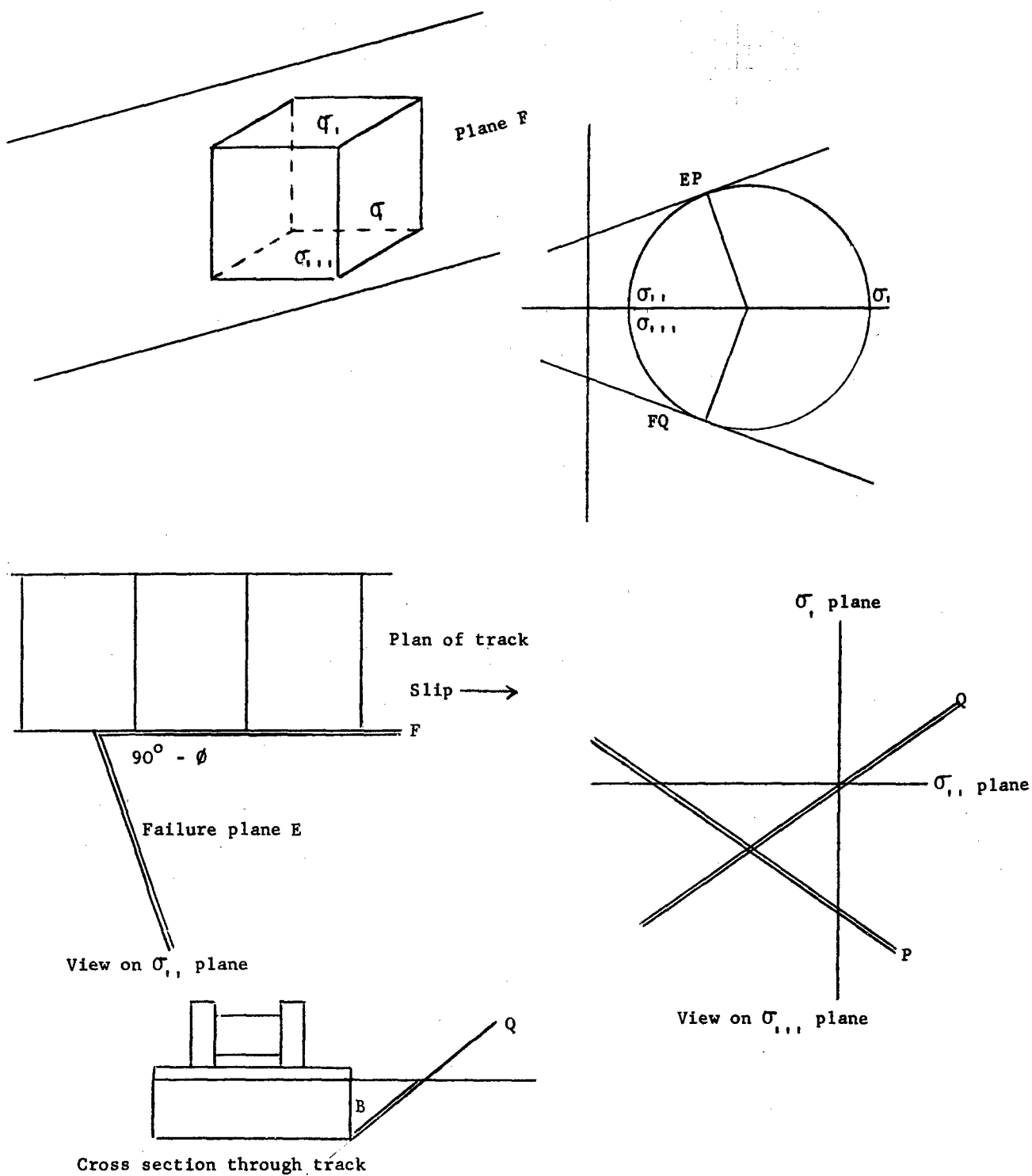
Fig.5.5.4. Orientation of failure planes relative to track side.

Plane F

EP

$\sigma_{,,}$ $\sigma_{,}$

$\sigma_{,,,}$

FQ

Plan of track

Slip →

F

$90° - \emptyset$

Failure plane E

View on $\sigma_{,,}$ plane

$\sigma_{,}$ plane

Q

$\sigma_{,,}$ plane

P

View on $\sigma_{,,,}$ plane

B

Q

Cross section through track

185
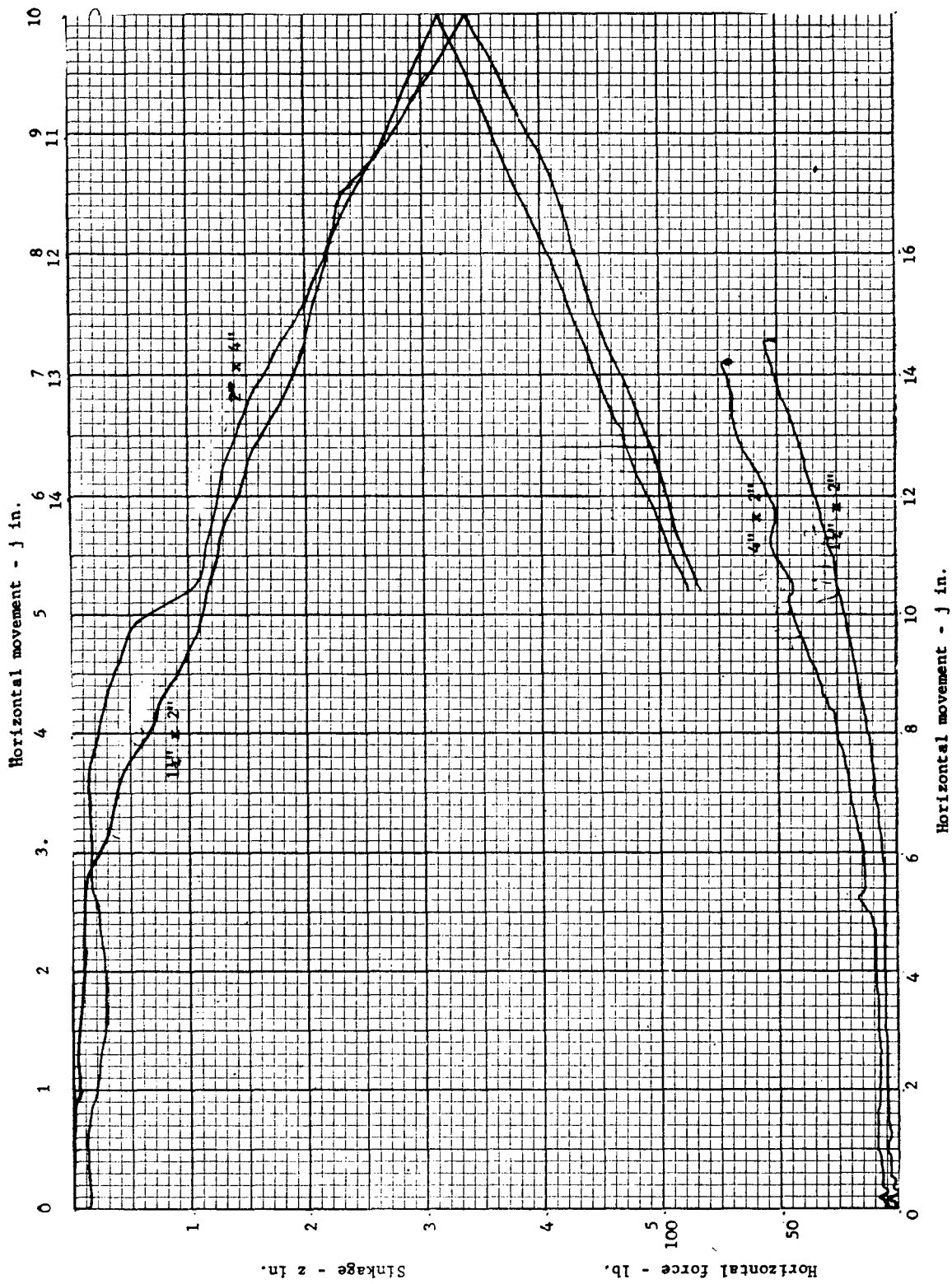
Fig.5.5.5. Bulldozing force test on a single 4" wide x 2" deep and a 1¼" wide x 2" deep shear plate. X-Y plotter traces showing horizontal force and sinkage against horizontal movement.
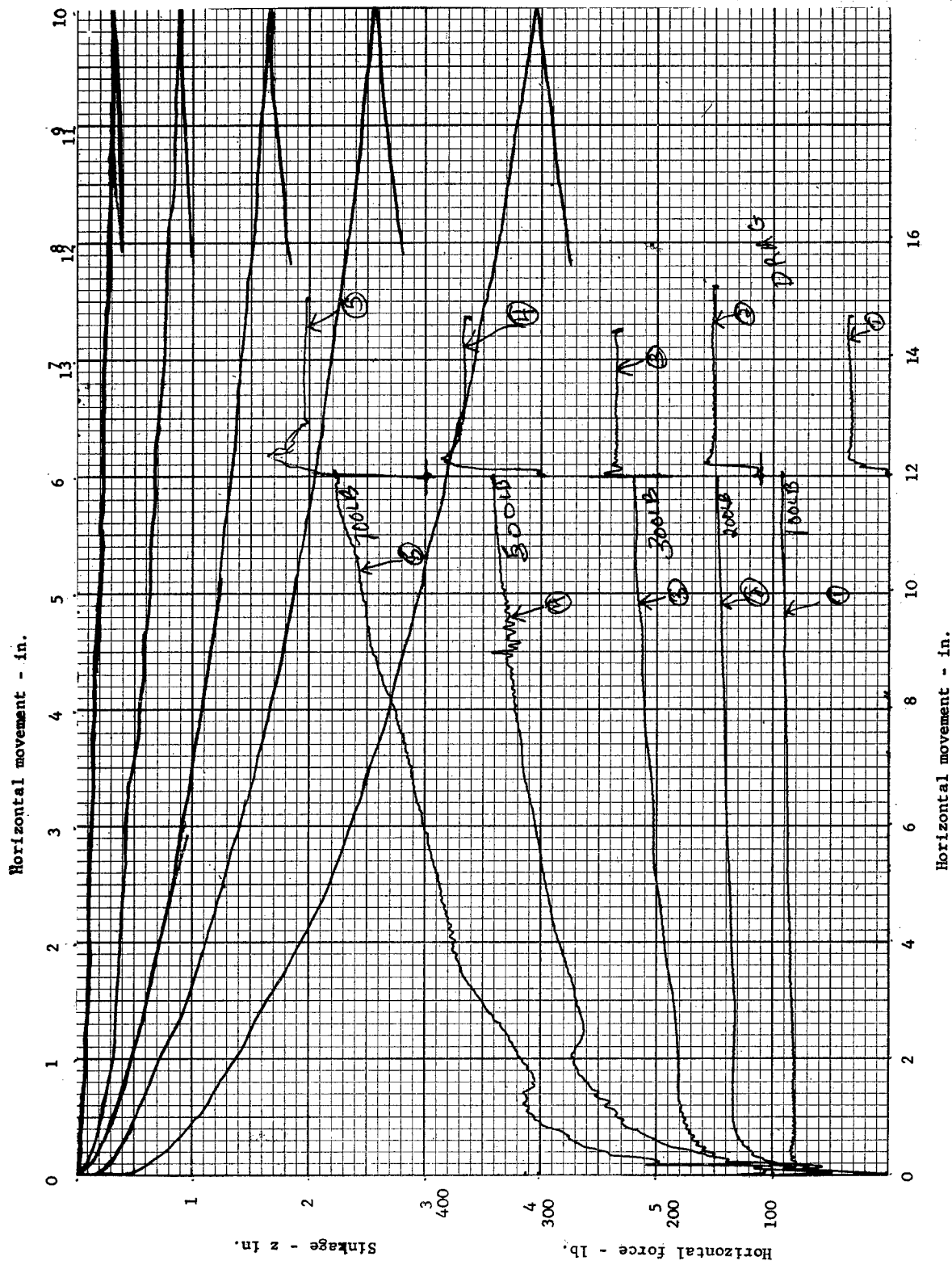
Fig. 5.5.6. Horizontal shear test on a 30" long by 4" wide plate with 2" deep lugs in dry sand. X-Y plotter traces of horizontal force and slip sinkage against displacement for increasing vertical loads.

187

Fig.5.5.7. Horizontal shear test on a 30" long by 4" wide plate with 4" deep lugs in dry sand. X-Y plotter traces of horizontal force and slip sinkage against displacement for increasing vertical loads. Also shows one trace from a single lug bulldozing force test.

188
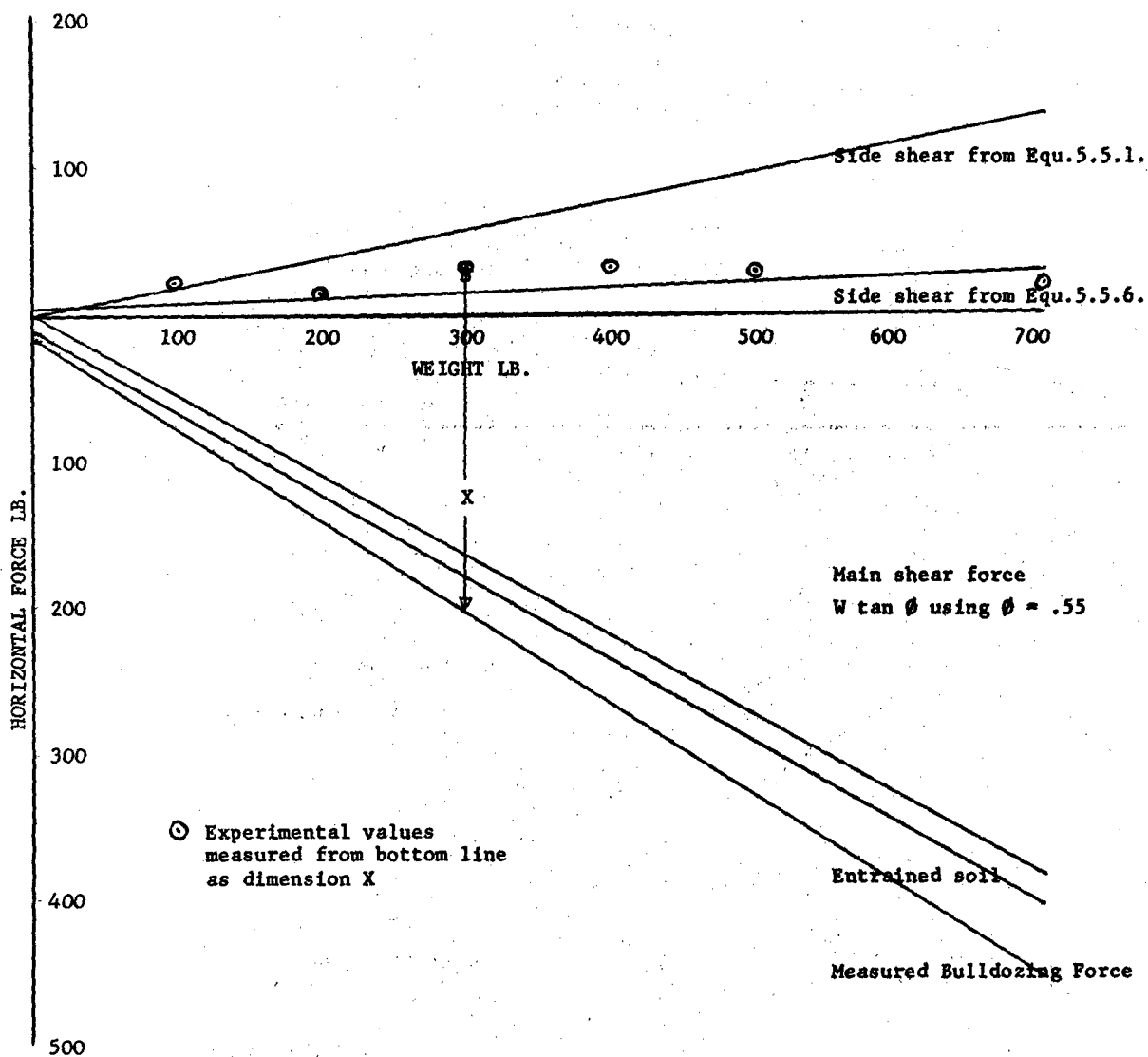
Fig.5.5.8. Analysis of the total horizontal force on a 30" track plate
4" wide with 2" deep lugs.
(Data from table 5.5.1.)

189
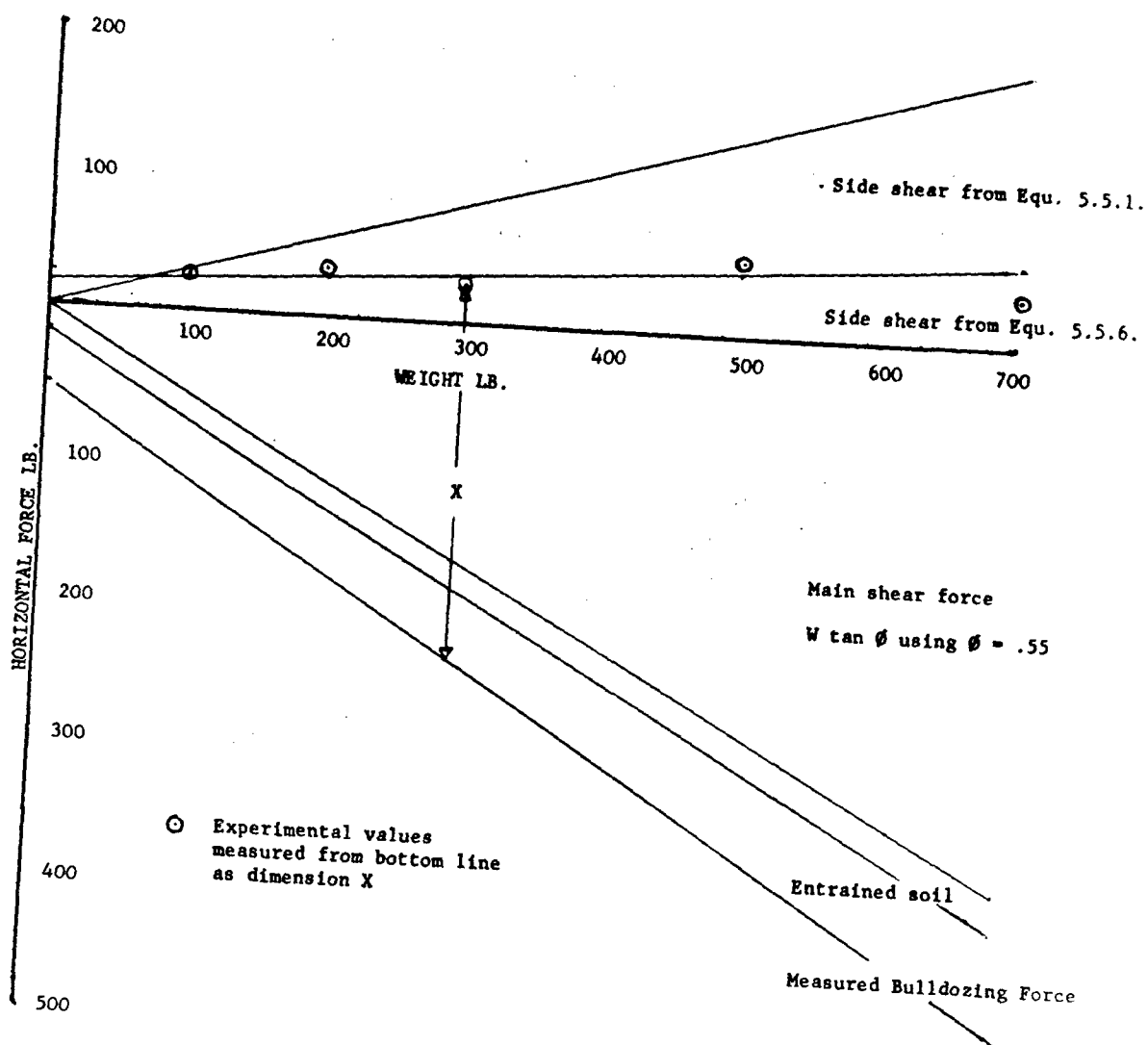
Fig.5.5.9. Analysis of the total horizontal force on a 30" track plate 4" wide with 4" deep lugs. (Data from table 5.5.2.)

190

2" lugs, 2" sinkage

6" lugs, 6" sinkage

Drawbar pull - lb.

E 62
D 200
C 400
B 600

A 2880

0   ¼   ½   ¾   1
Cohesion lb.in.$^{-2}$
3.6   6.6   9.6
Bearing capacity

Drawbar pull - lb.

E 312
D 600

C 1200

B 600

A 2880

0   ¼   ½   ¾   ½
Cohesion lb.in.$^{-2}$
3.6   6.6   9.6
Bearing capacity

5000 lb.

5000 lb.

2"

6"

6"

6"

50"

50"

$O = 8.3$ lb.in.$^{-2}$ $\emptyset = 30^{\circ}$ $= .060$ lb.in.$^{-3}$
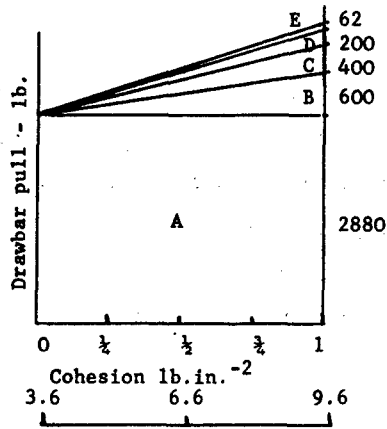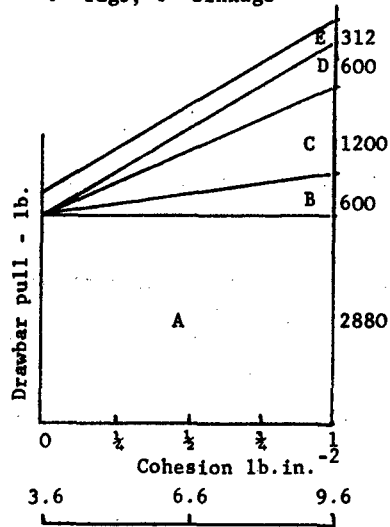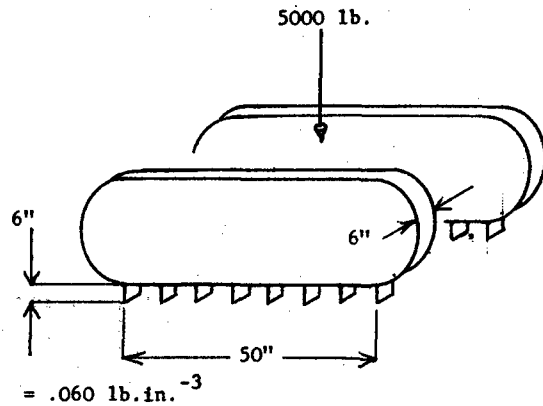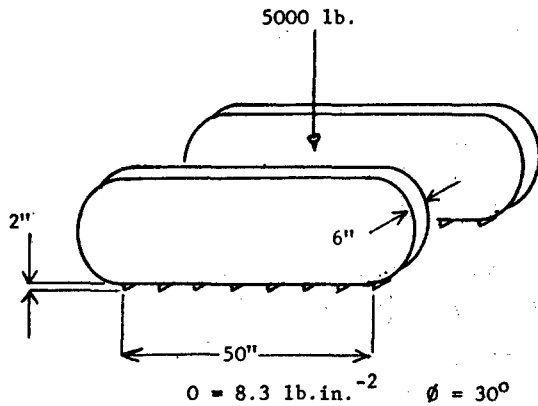
A = Main frictional pull --- $W \tan \emptyset$
B = Base cohesive pull --- $2blc$
C = Lug side cohesive pull --- $4hlc$
D = Lug side cohesive-frictional pull --- $4hlc \left(2 \sin^2 \left(45 + \frac{\emptyset}{2}\right) - 1\right)$
E = Lug side frictional pull --- $4hlz_m \left(\tan \left(45 + \frac{\emptyset}{2}\right) \cos \left(90 - \emptyset\right)\right)$

Fig.5.5.10. A practical example of the effect of lugs on draw bar pull.
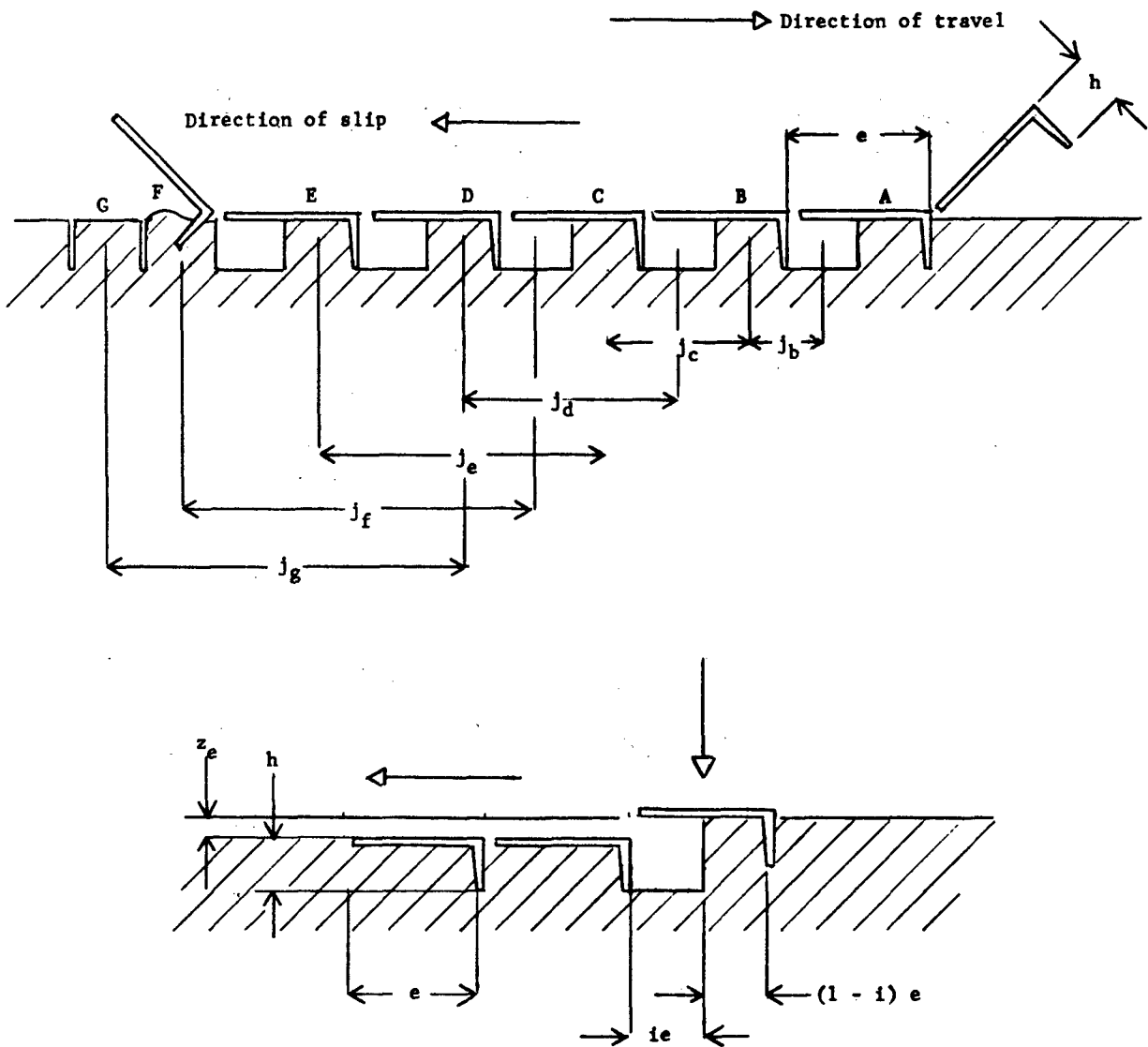
Fig.5.6.1. The process of excavation due to slip of a lugged track.

(a)

(b)
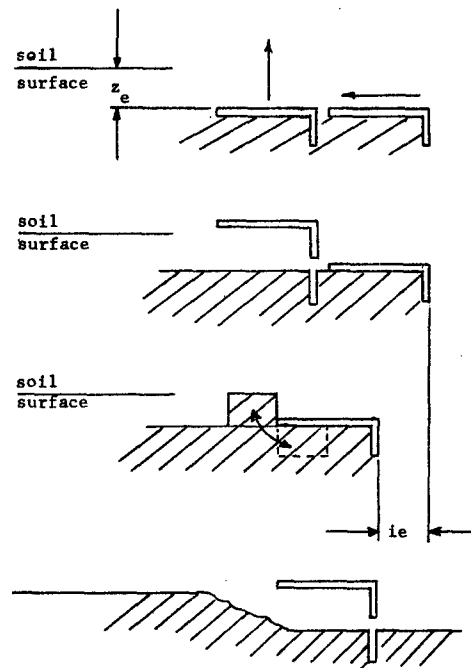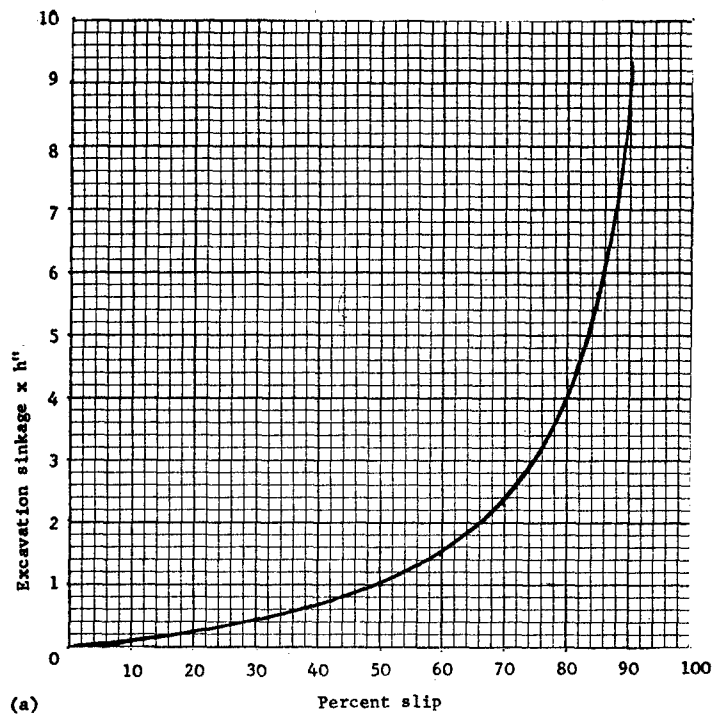
Fig.5.6.2. (a) Relationship between excavation sinkage and slip.
(b) The rut filling process at the rear of a slipping track.

193

Fig.5.6.3. Track print from model tracklayer operating at 50% slip in clay, showing standing sliding blocks beneath each track plate. Some flow has taken place.
σ_m = 5.5 lb.in.$^{-2}$,   c = 3.5 lb.in.$^{-2}$
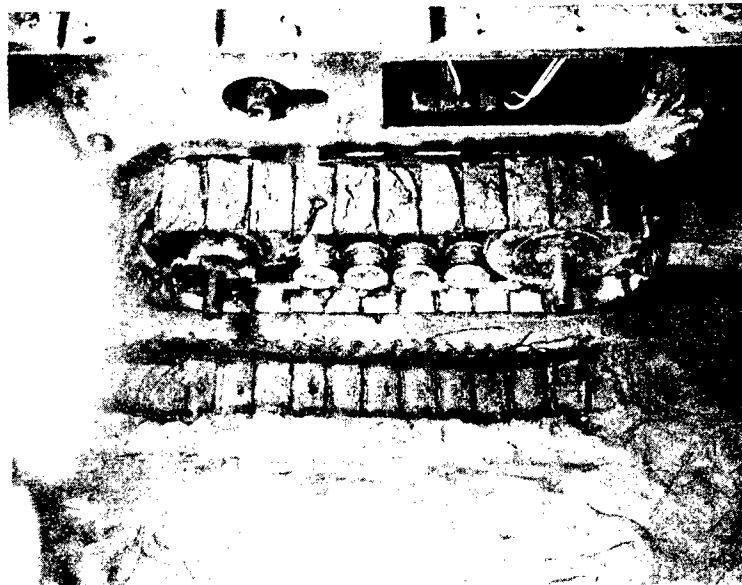
Fig.5.6.4. Track print from model tracklayer operating at 50% slip in clay, showing collapsed blocks filling all the space beneath each track plate.   All test conditions the same as in Fig.5.6.3. except for higher tractor weight.
σ_m = 11.2 lb.in.$^{-2}$,   c = 3.5 lb.in.$^{-2}$
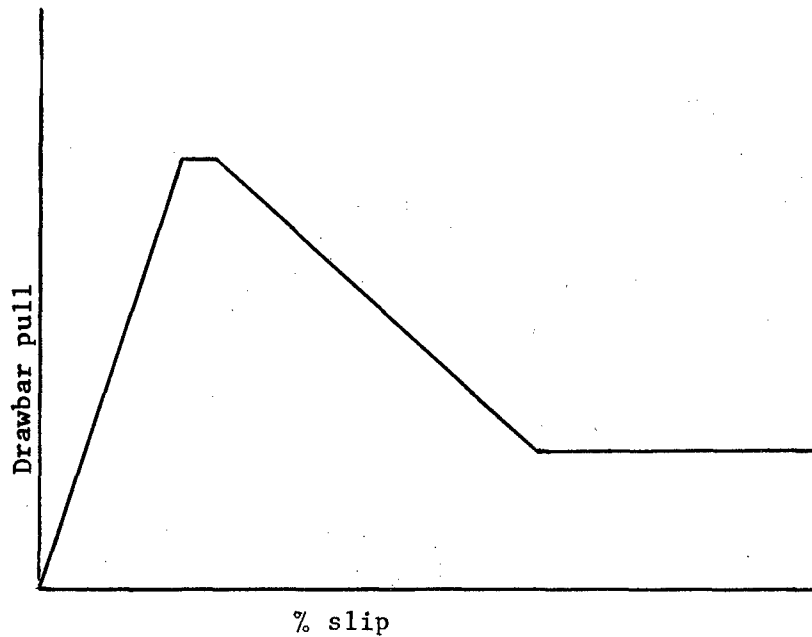
(a)
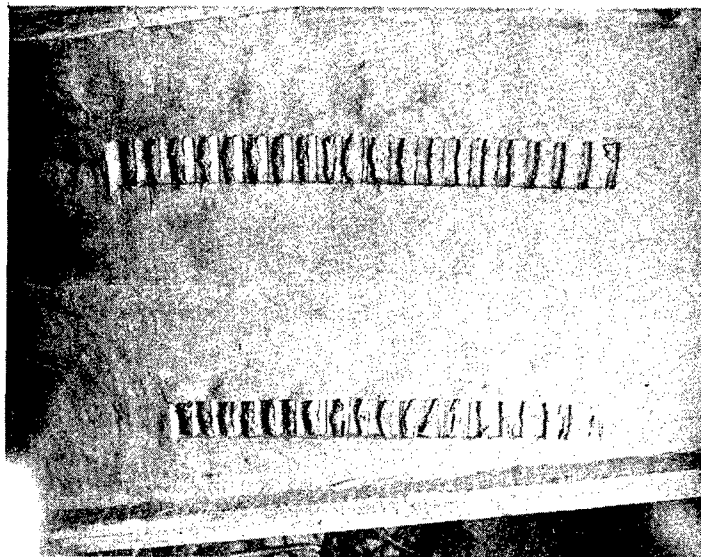
(b)

Fig.5.7.1. (a) Slip pull curve for a tracklayer with contact pressure
considerably less than the surface bearing capacity in
frictionless clay.
(b) The marks made by a crawler tractor with low contact
pressure operating at about 15% slip in clay.   Flow
beneath the lug tips has occurred and the blocks of
clay diminish in size and develop the characteristic
crescent shape towards the rear.
σ_m = 2.6 lb.in.$^{-2}$,cohesion = 2.9 lb.in.$^{-2}$
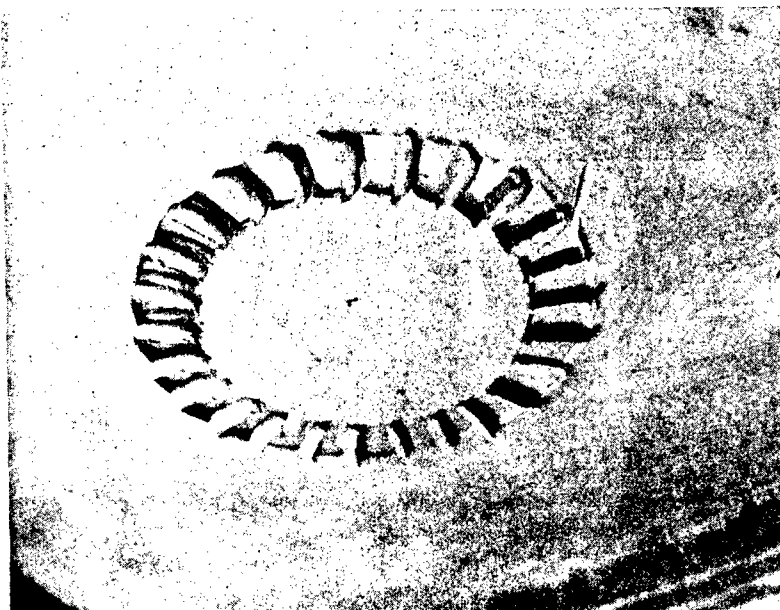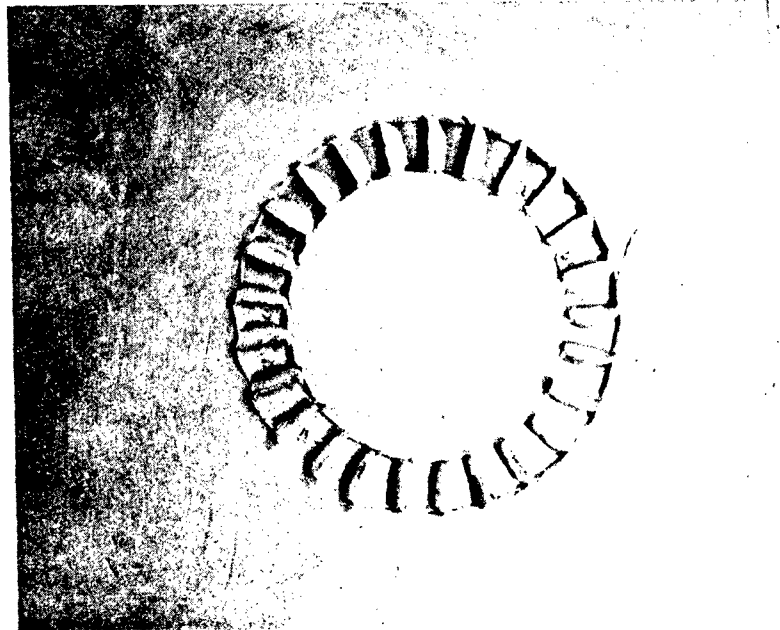
Fig.5.7.2. Bevameter annulus print in clay, showing the effect of clay flow beneath the lug tips. The torque-twist curve for this test is shown on Fig.5.7.3. $O_m = 0.44$ lb.in.$^{-2}$, cohesion = 2.9 lb.in.$^{-2}$
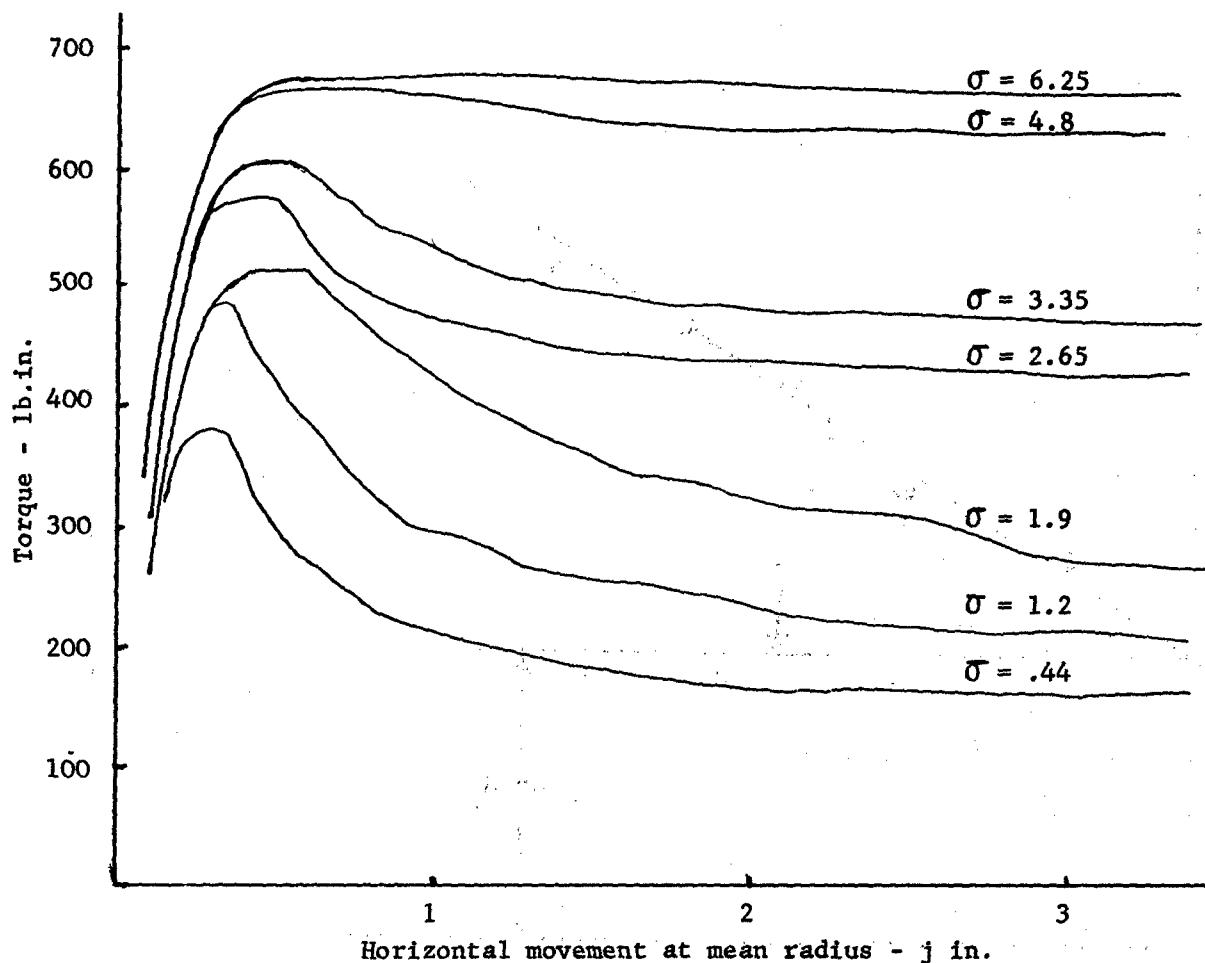
Fig.5.7.3. Typical Bevameter annulus stress-deformation curves in clay.
Annulus 10" o.dia. 7½" i.dia. 5/16" lug height.
Mean radius 4.4". Clay cohesion 2.9 lb.in.
The photograph of Fig.5.7.2. was taken from the $\sigma = .44$
test of this series.
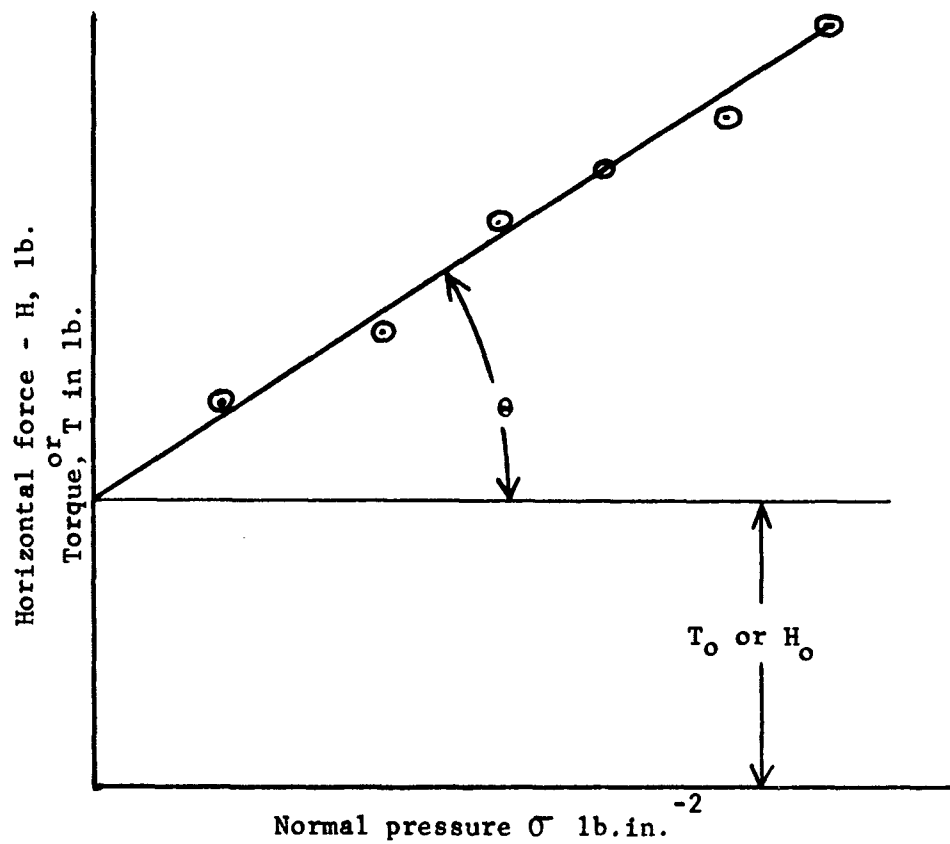
Fig.6.2.1. The determination of c and ∅ from an annular
or linear shear test using shear plates with
lugs of height h.

198

Present Bevameter
measures torque on
all surfaces below
here.

B

A

Proposed to measure
torque on surfaces
below here only.

B

C

D

A
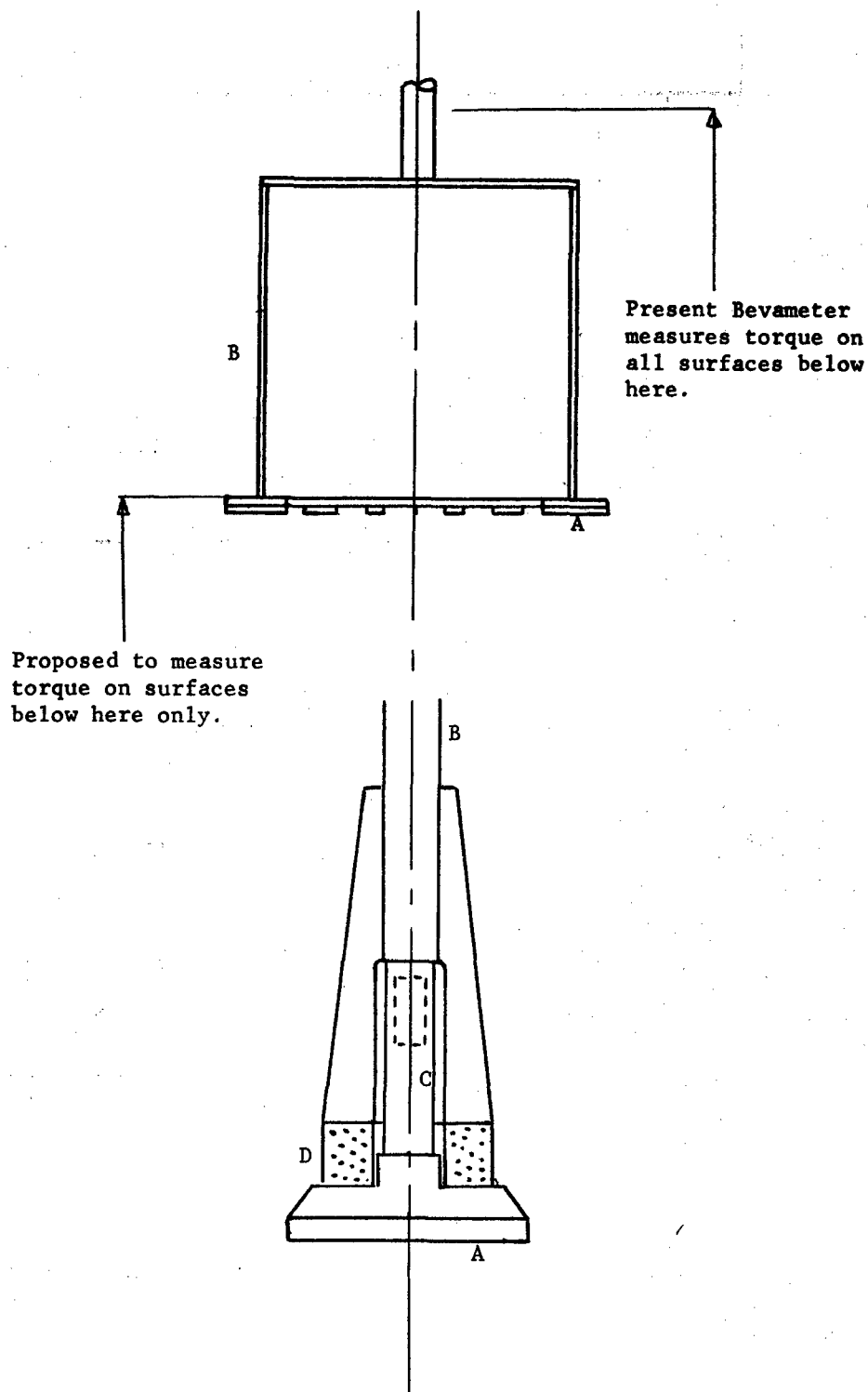
Fig.6.3.1. Proposed new design for annular shear device
to minimize drag.
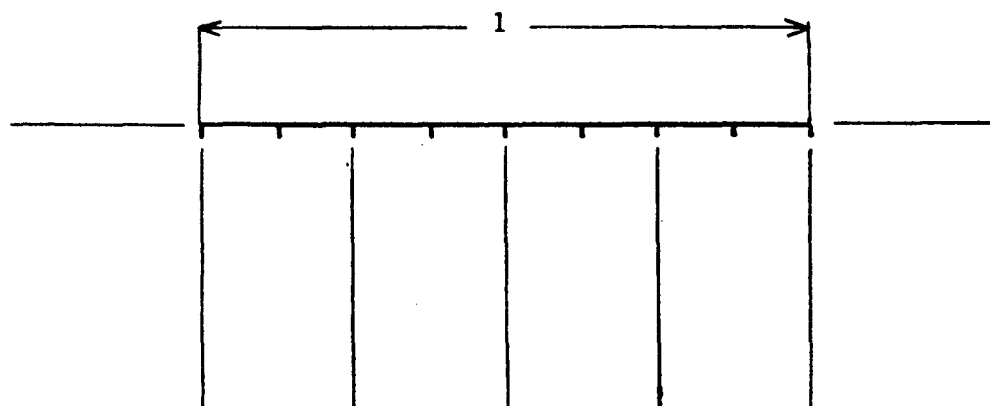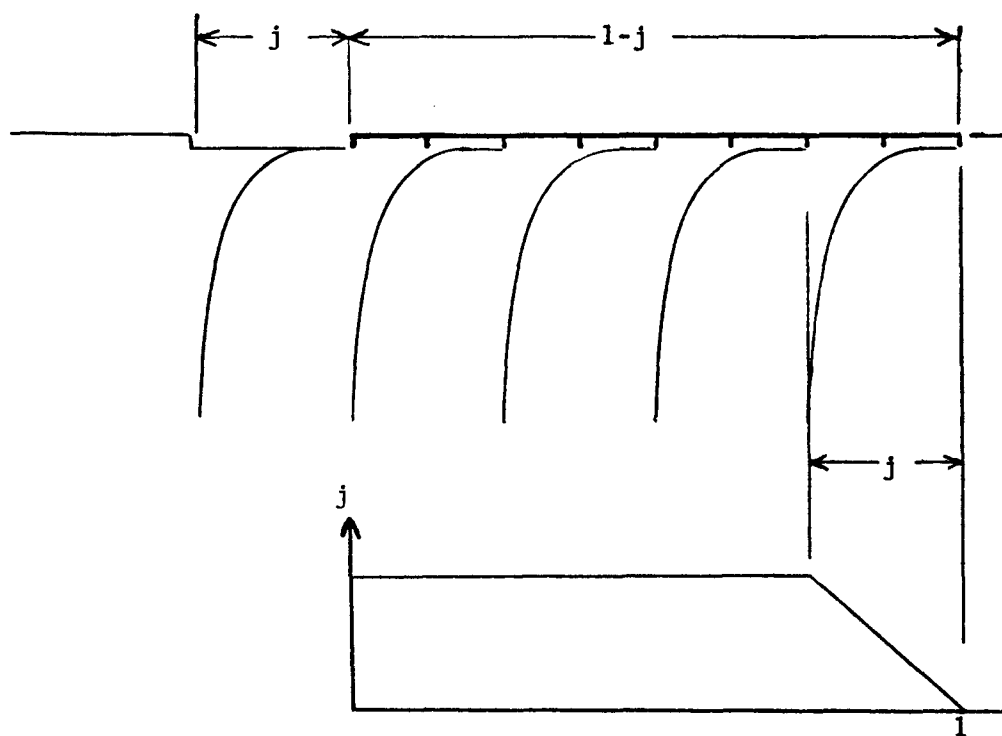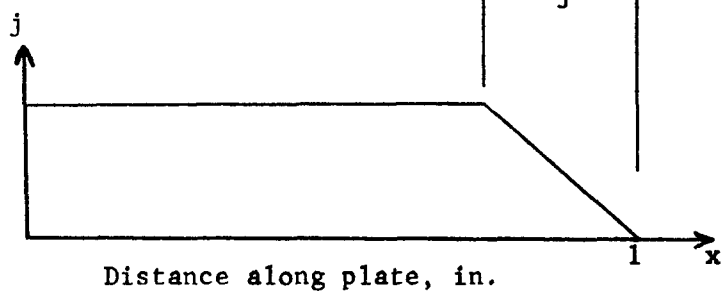
Fig.6.4.1. The kinematics of a linear surface shear plate of finite length.
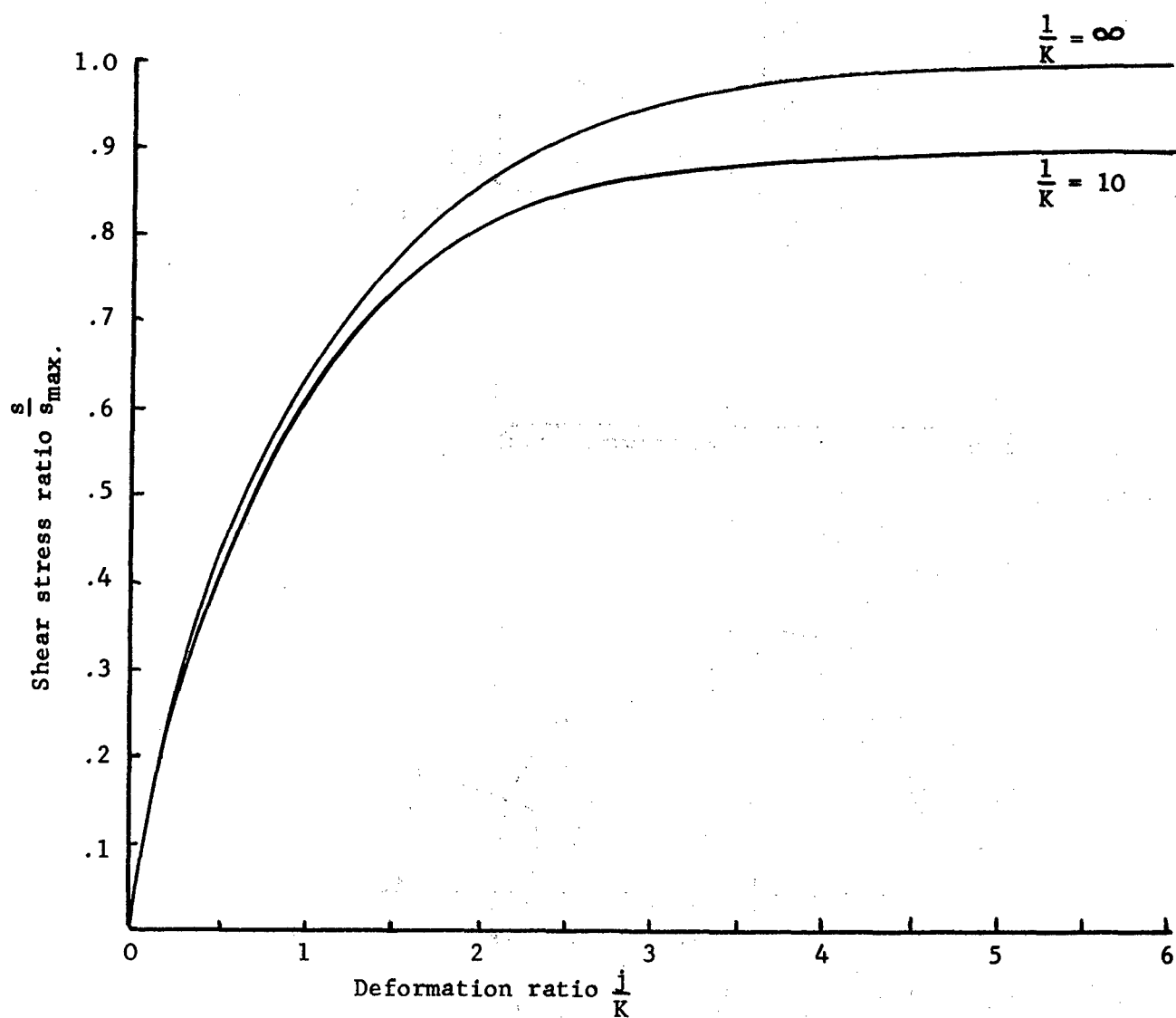
Fig.6.4.2. A comparison in dimensionless co-ordinates of the
shear stress-deformation relation for an infinitely
long shear plate and one with a $\frac{1}{K}$ ratio of 10
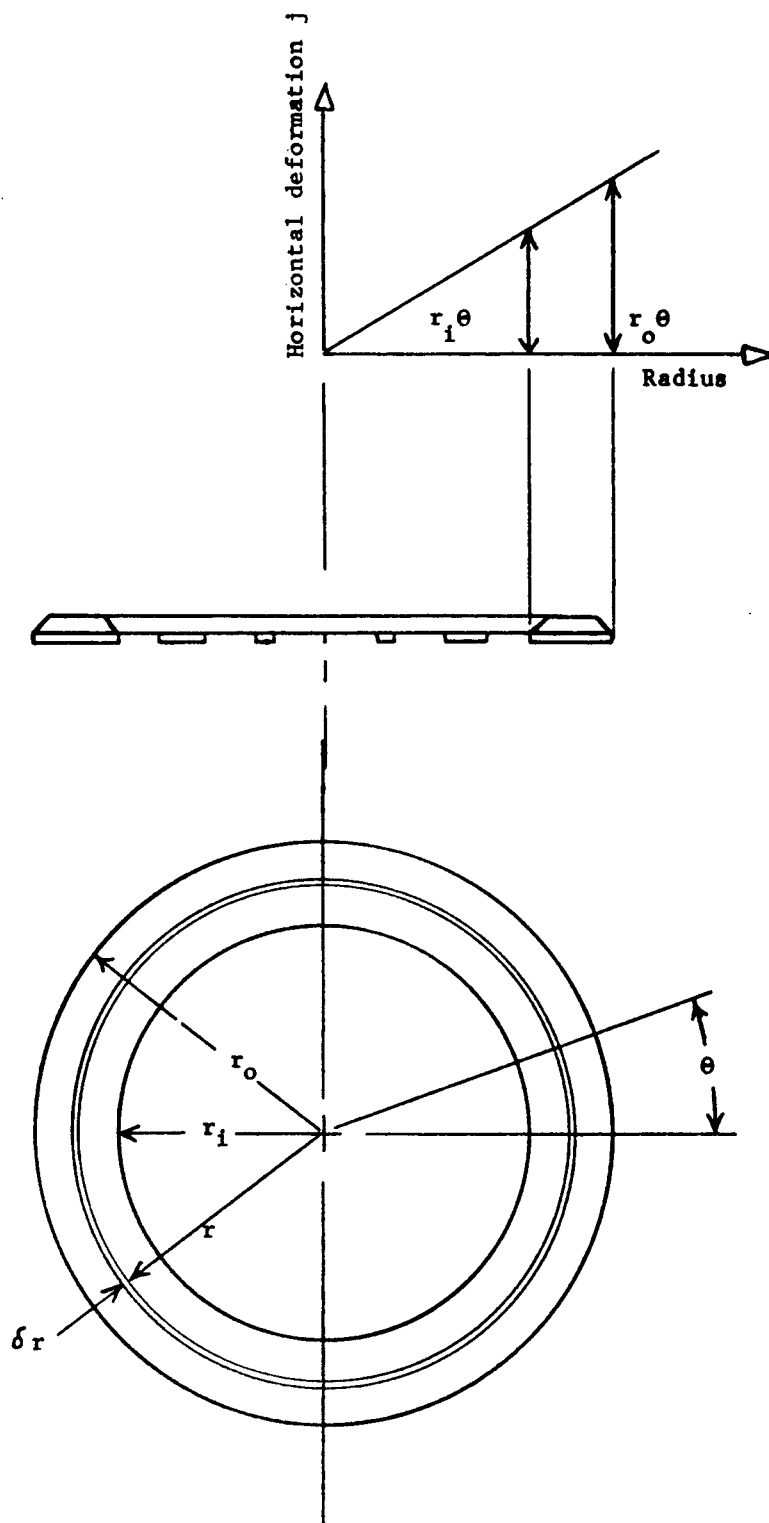
Fig.6.4.3. The kinematics of a circular surface shear plate
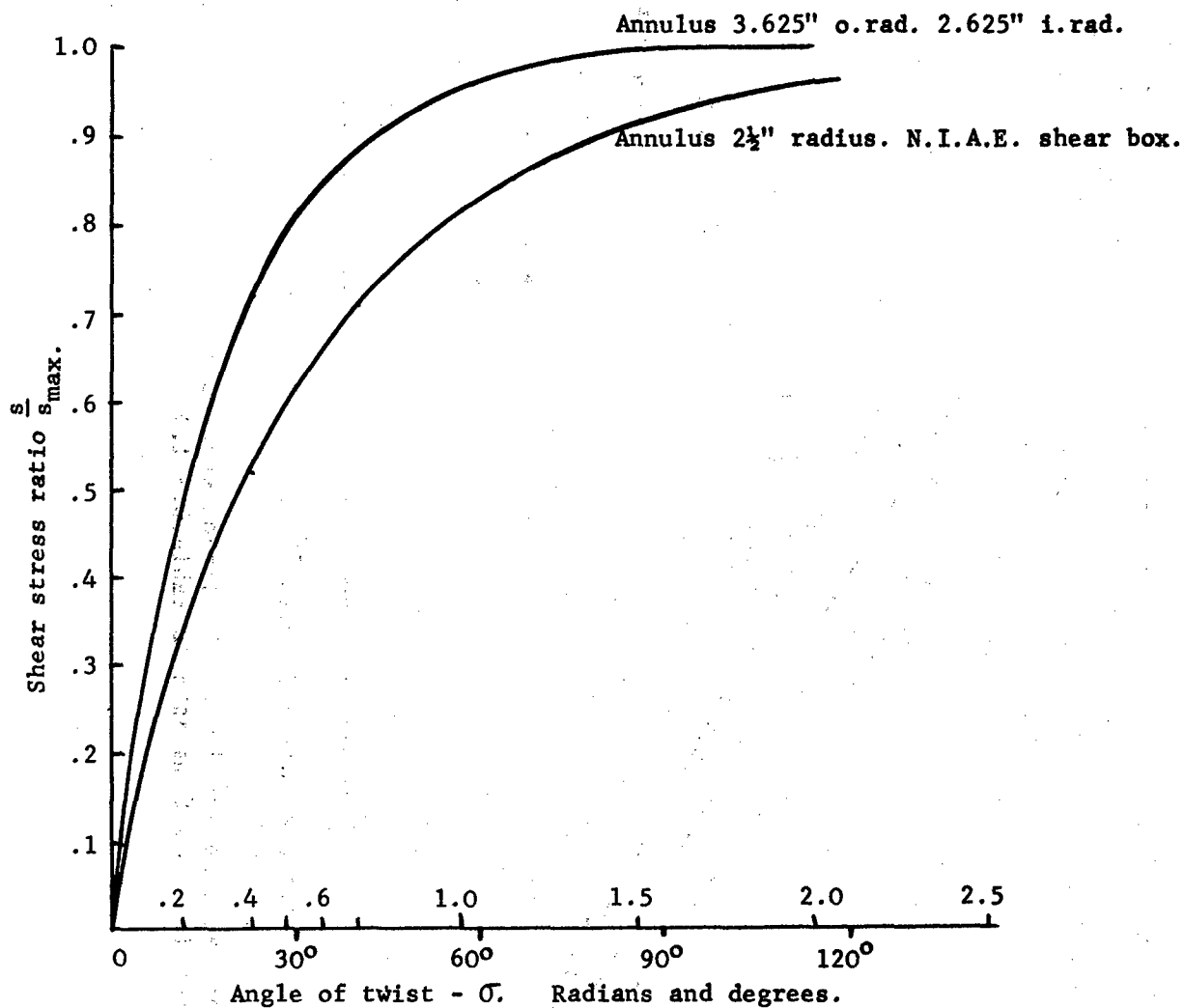
Fig.6.4.4. A comparison of the stress angle of twist relation for
an annular and a circular shear box.   Based on
equation 6.5.4. assuming K = 1.
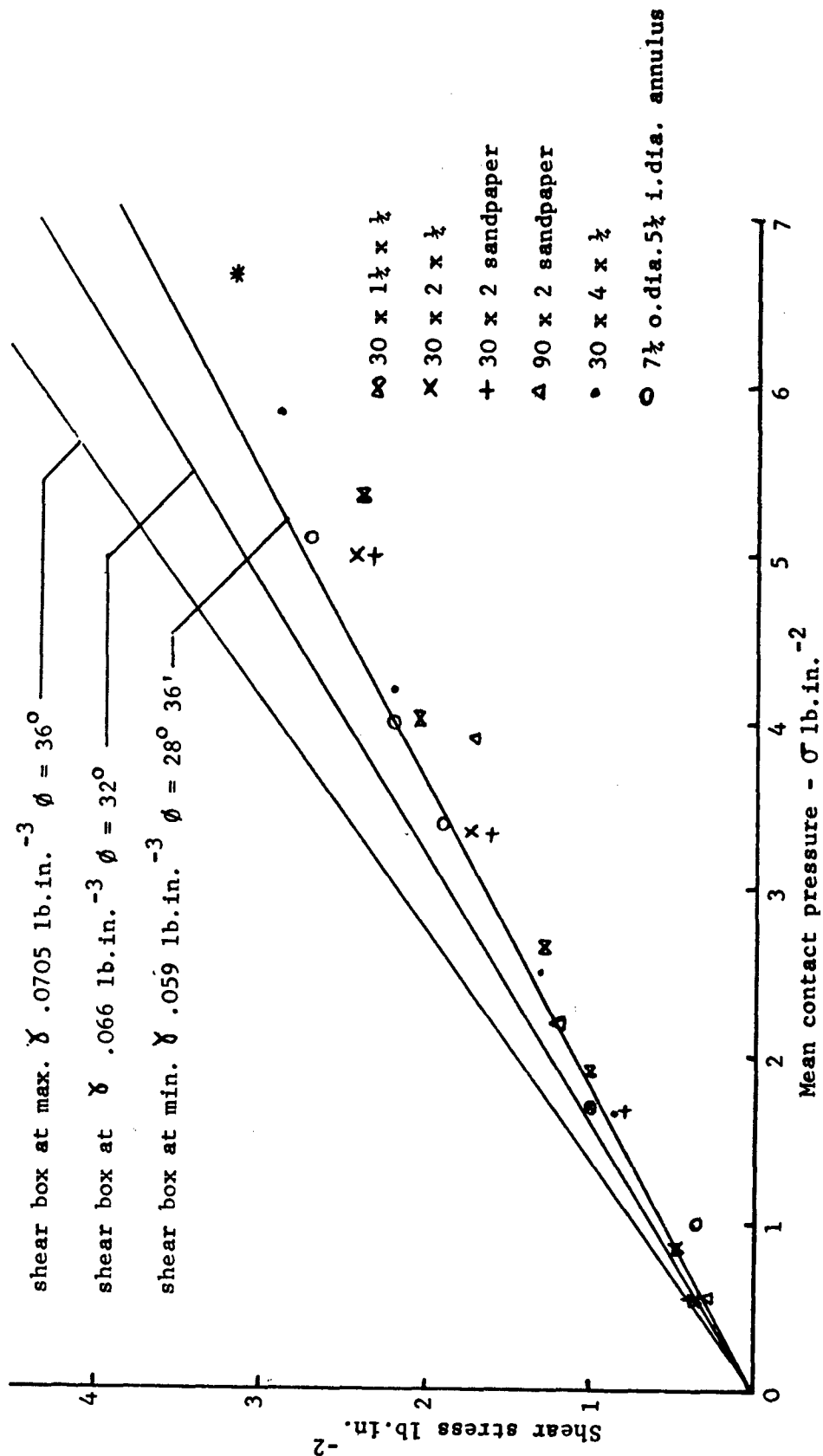
Fig.6.5.1. Comparison between ∅ measured with the linear shear apparatus and the shear box at three densities (plotted from data in Table 6.5.1.)

204
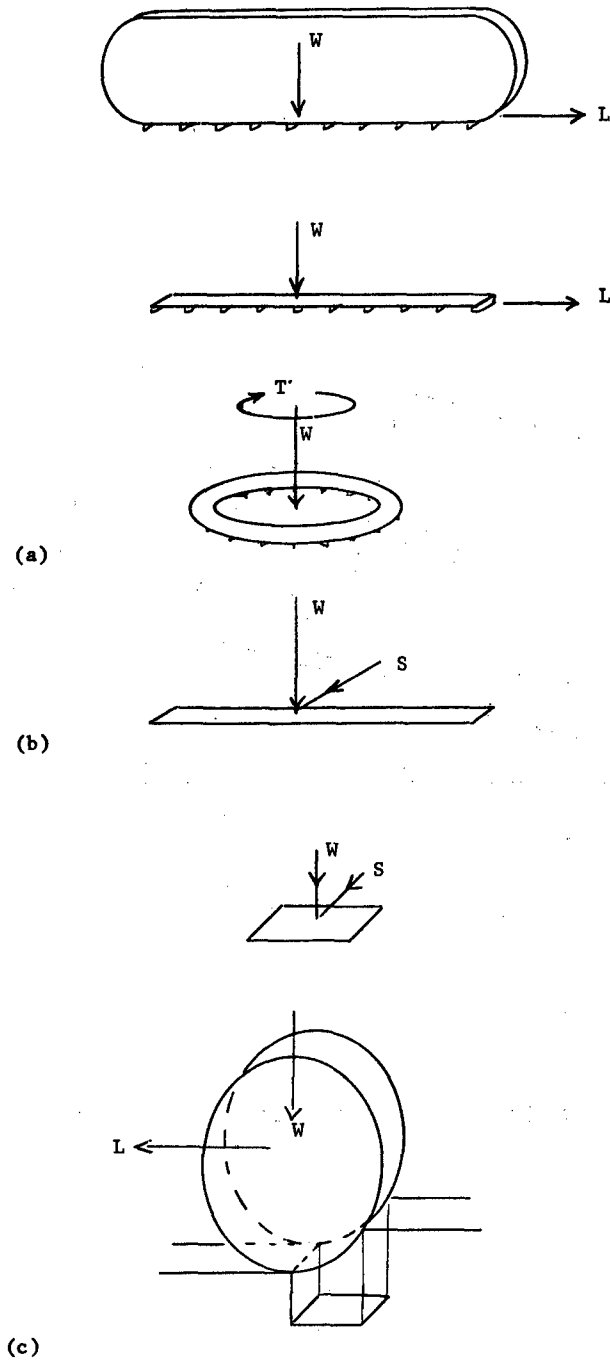
Fig.7.1.1. Vehicle-soil loading systems and corresponding
foundation problems.
(a) Track, bevameter annulus and longtitudinally
loaded strip foundation - an unsolved problem
(b) Laterally loaded strip foundation - a partially
solved problem. No real vehicle equivalent
(c) Wheel and laterally loaded square footing - a
partially solved problem.
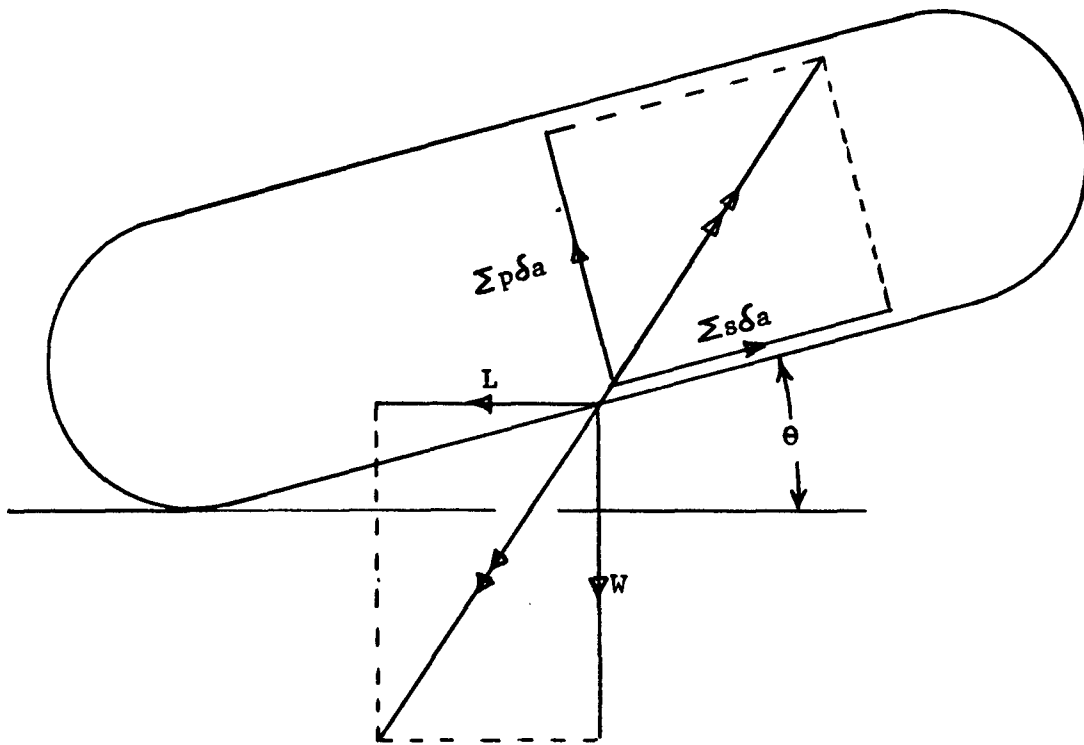
Fig.7.1.2. Forces acting on an inclined tractor, with a trim angle θ
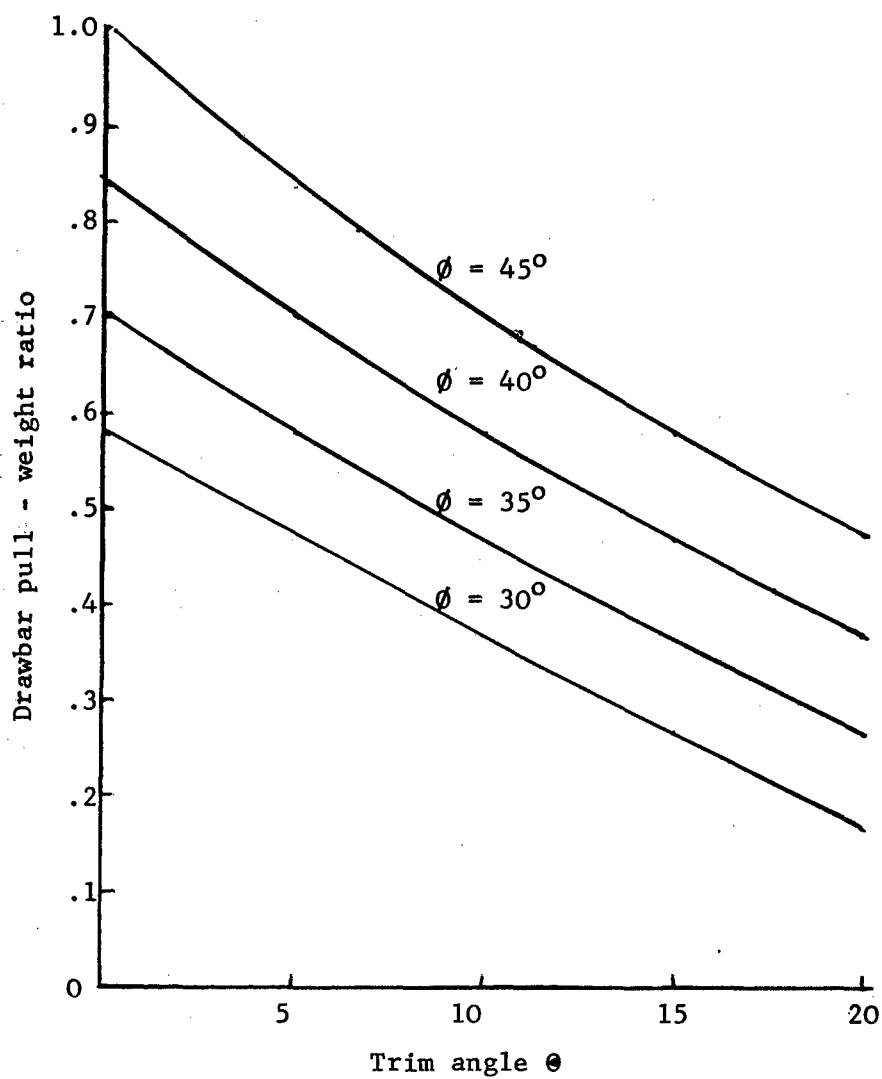
Fig.7.1.3. The reduction in drawbar - pull weight ratio with
increasing trim angle for cohesionless soils with
varying ⌀

207

Fig.7.2.1. X-Y plotter trades showing horizontal force and slip sinkage against horizontal movement. 30" long, 2" wide shear plate with ¼" lugs in clay.

208
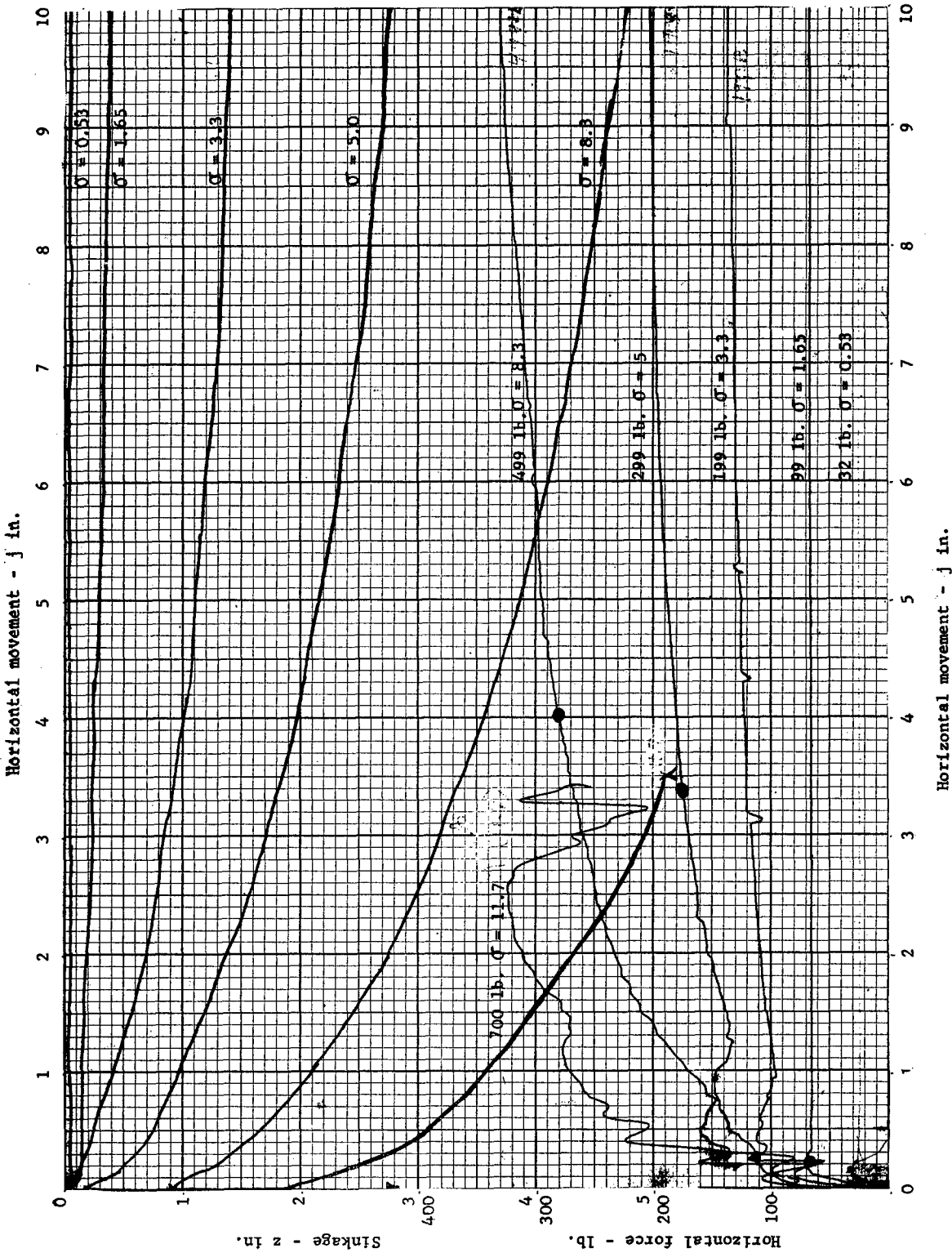
Fig.7.2.2. X-Y plotter traces showing horizontal force and slip sinkage against horizontal motion.
30" long, 2" wide plate with ¼" lugs in wet sand.

209
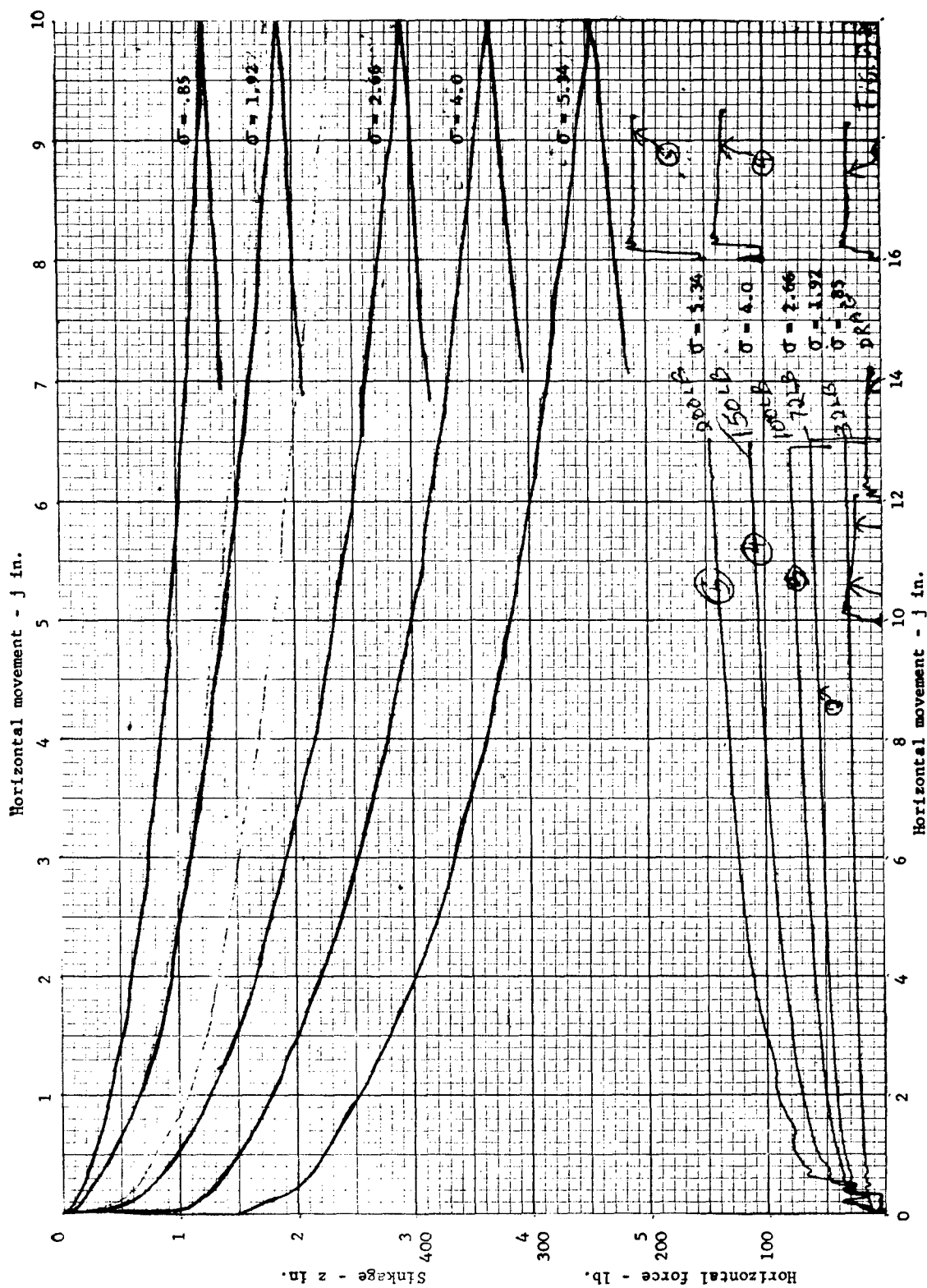
Fig.7.2.3. X-Y plotter traces showing horizontal force and slip sinkage against horizontal motion. 30" long, 1¼" wide plate with ¼" lugs in dry sand.
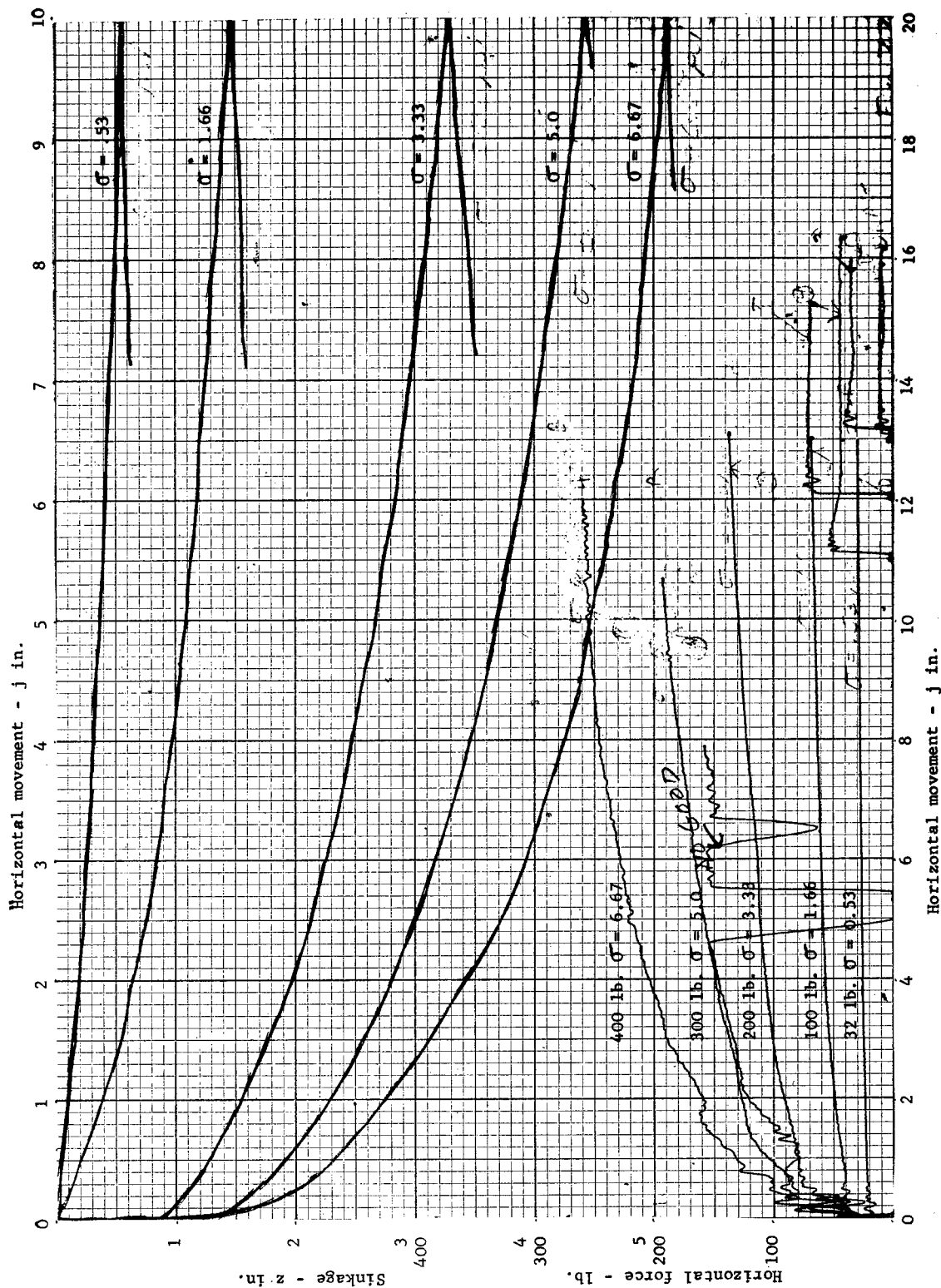
Fig.7.2.4. X-Y plotter traces showing horizontal force and slip sinkage against horizontal motion. 30" long by 2" wide plate with ¼" lugs in dry sand.
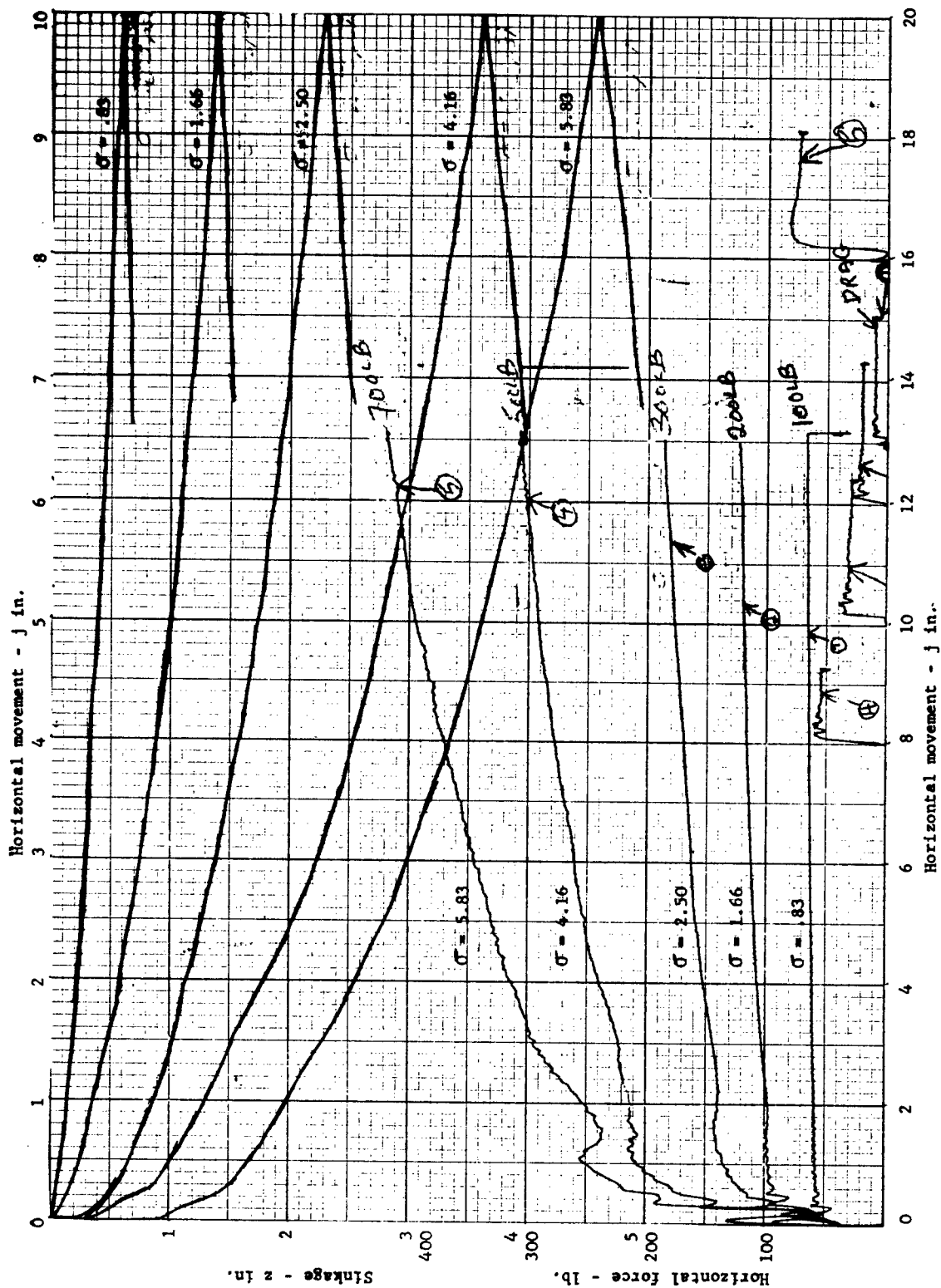
Fig.7.2.5. X-Y plotter traces showing horizontal force and slip sinkage against horizontal motion.
30" long by 4" wide shear plate with ½" lugs in dry sand.

212
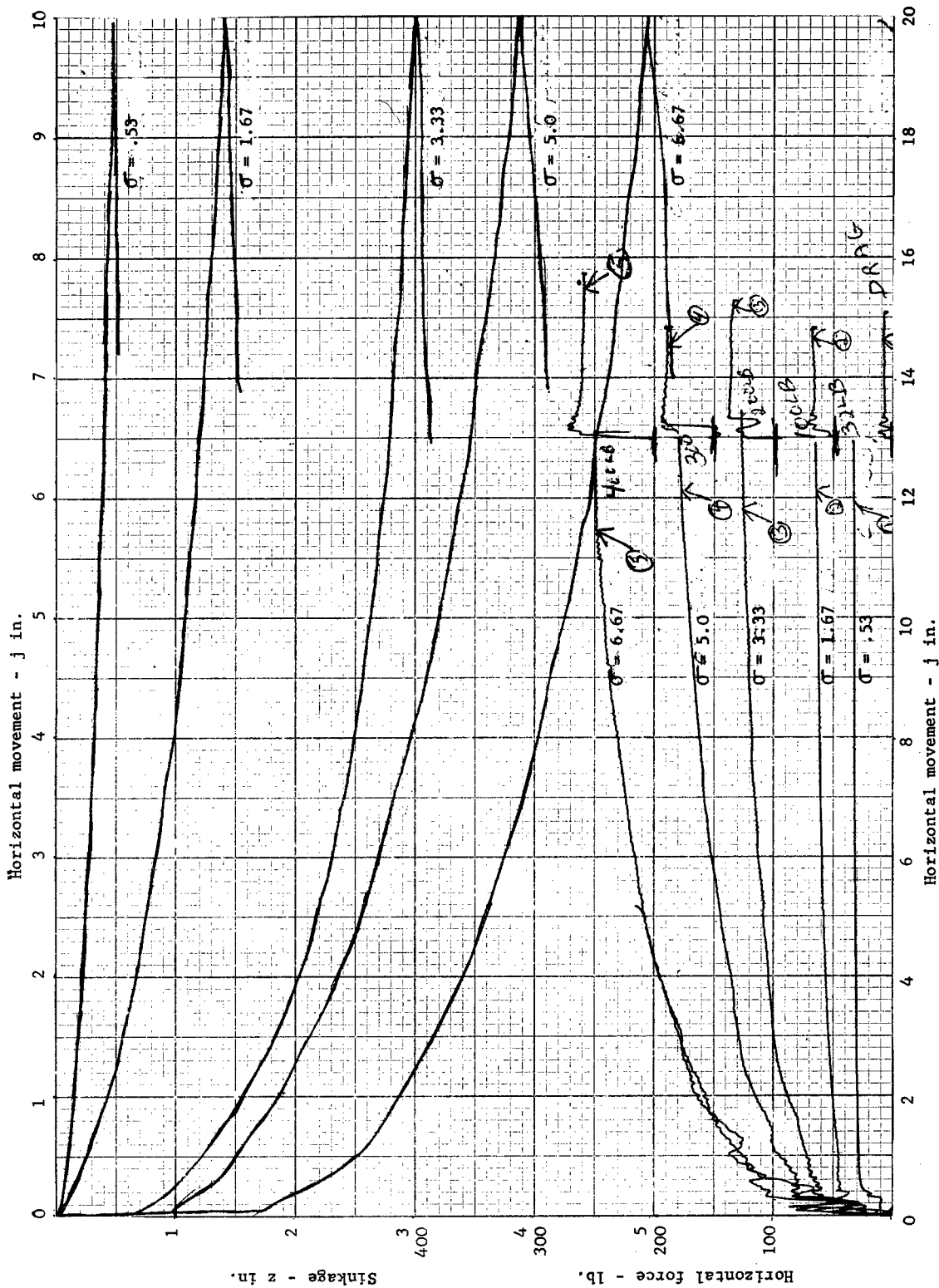
Fig. 7.2.6. X-Y plotter traces showing horizontal force and slip sinkage against horizontal motion. 30" long by 2" wide shear plate covered with coarse sandpaper in dry sand.

213
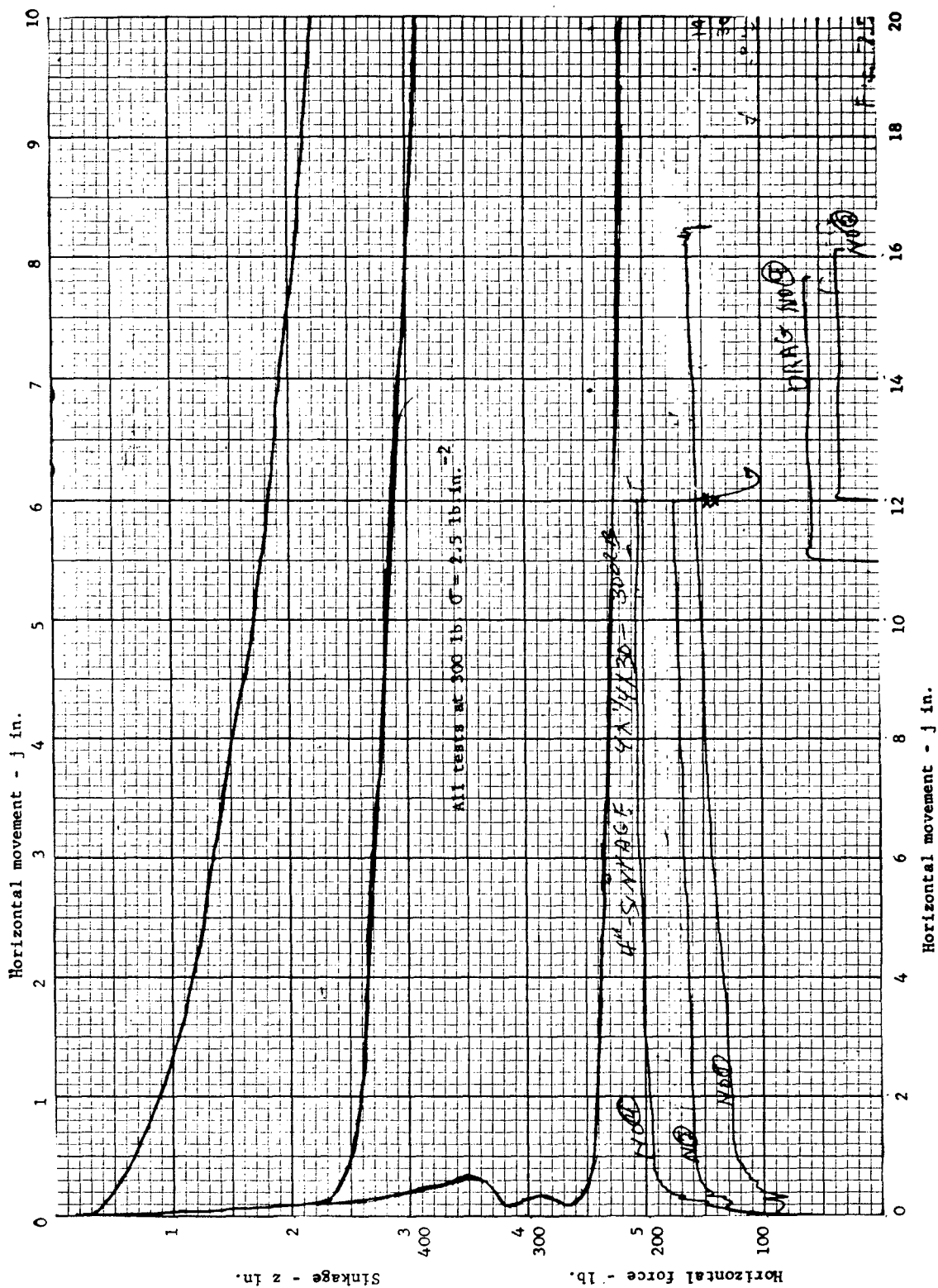
Fig.7.2.7. X-Y plotter traces showing horizontal force and slip sinkage against horizontal motion. 30" long by 4" wide shear plate with ¾" lugs in dry sand showing that slip-sinkage continues to occur even when starting from a considerable initial dug-in sinkage.
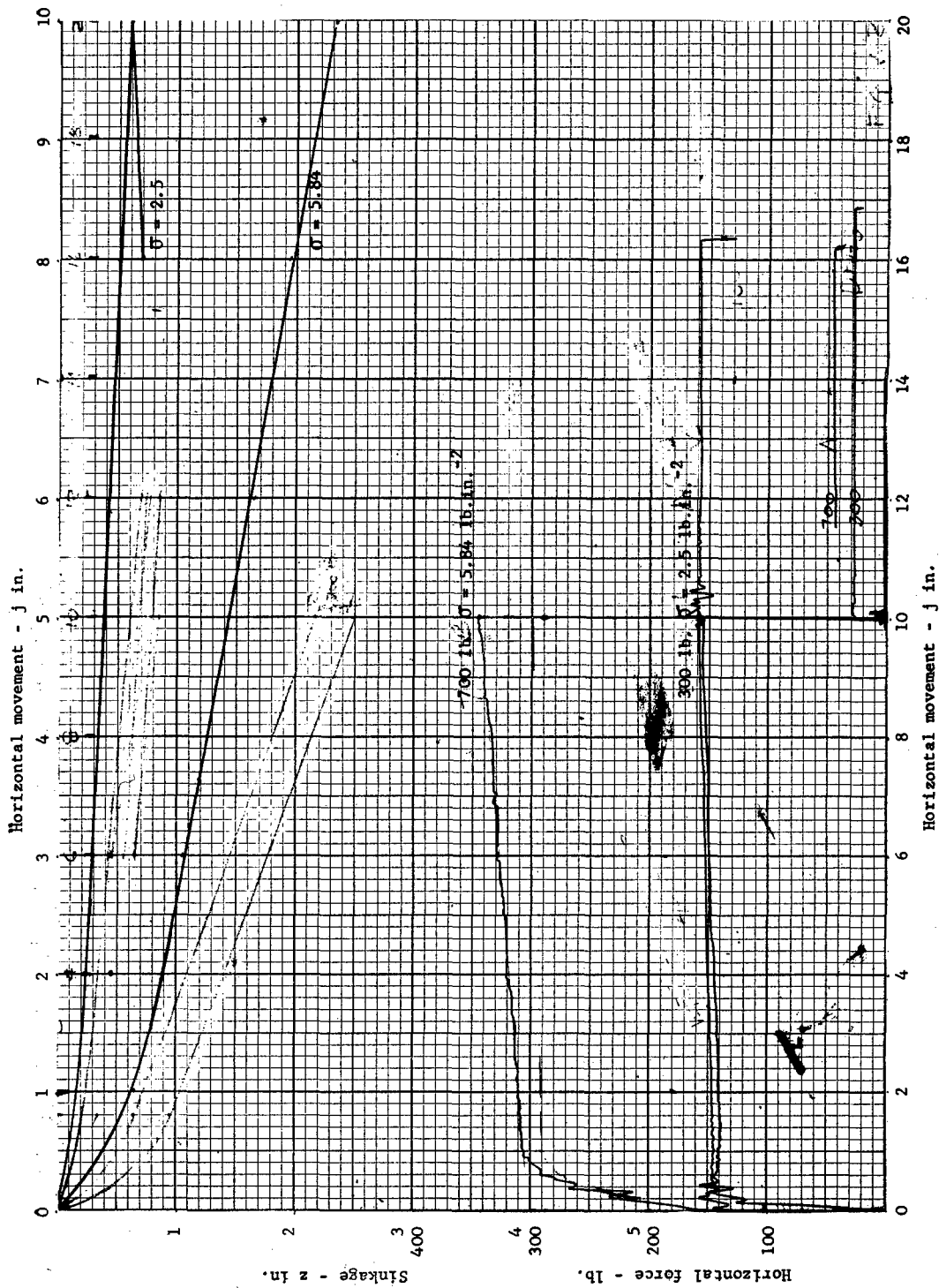
Fig.7.2.8. X-Y plotter traces showing horizontal force and slip sinkage against horizontal motion. 30" long by 4" wide shear plate with ¼" lugs in dry sand. 300 lb. surcharge on sand surface each side of plate showing that slip sinkage continues even when soil is surcharged enough to prevent normal sinkage.
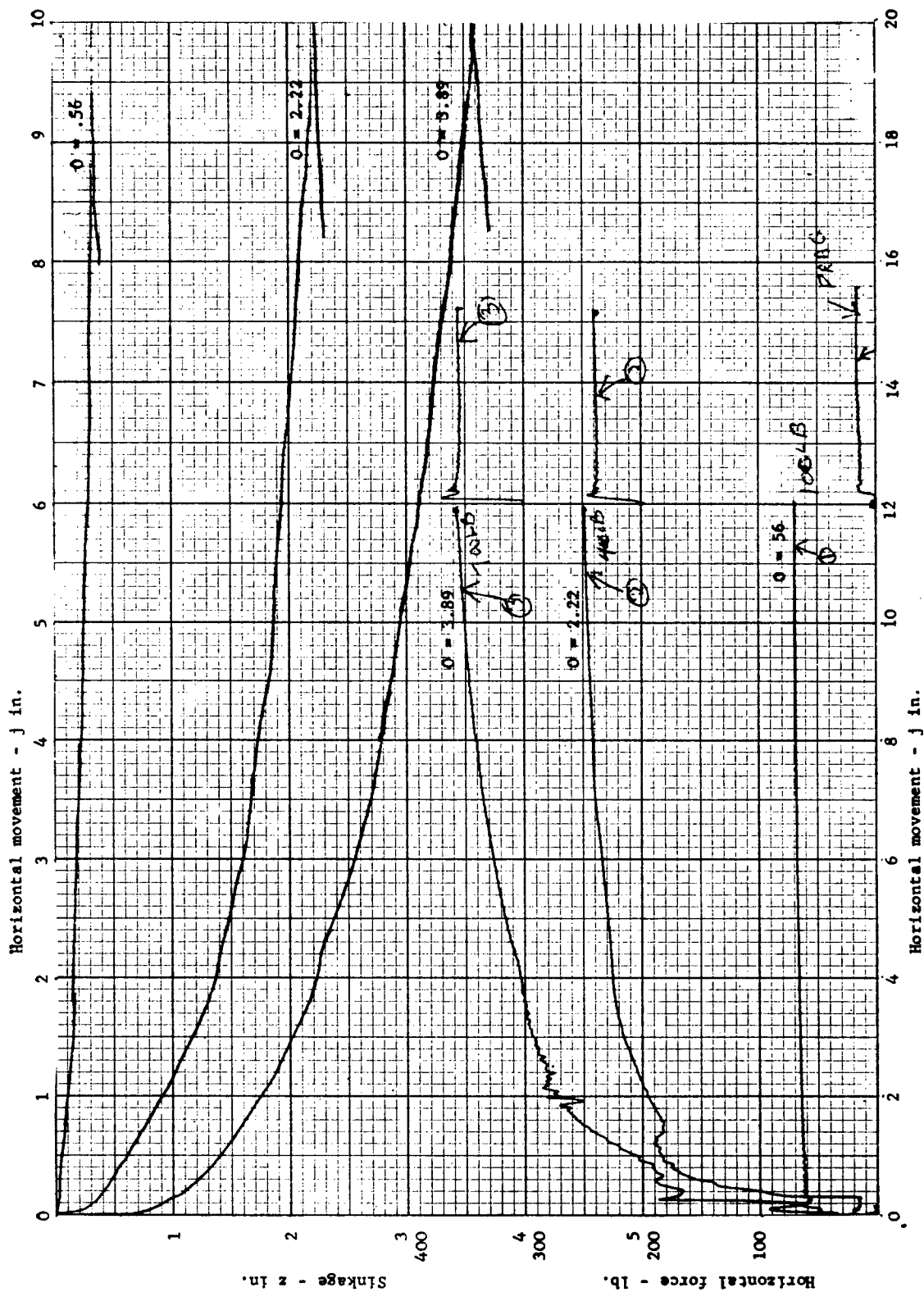
Fig.7.2.9. X-Y plotter traces showing horizontal force and slip sinkage against horizontal motion. 90" long by 2" wide shear plate covered with coarse sandpaper.
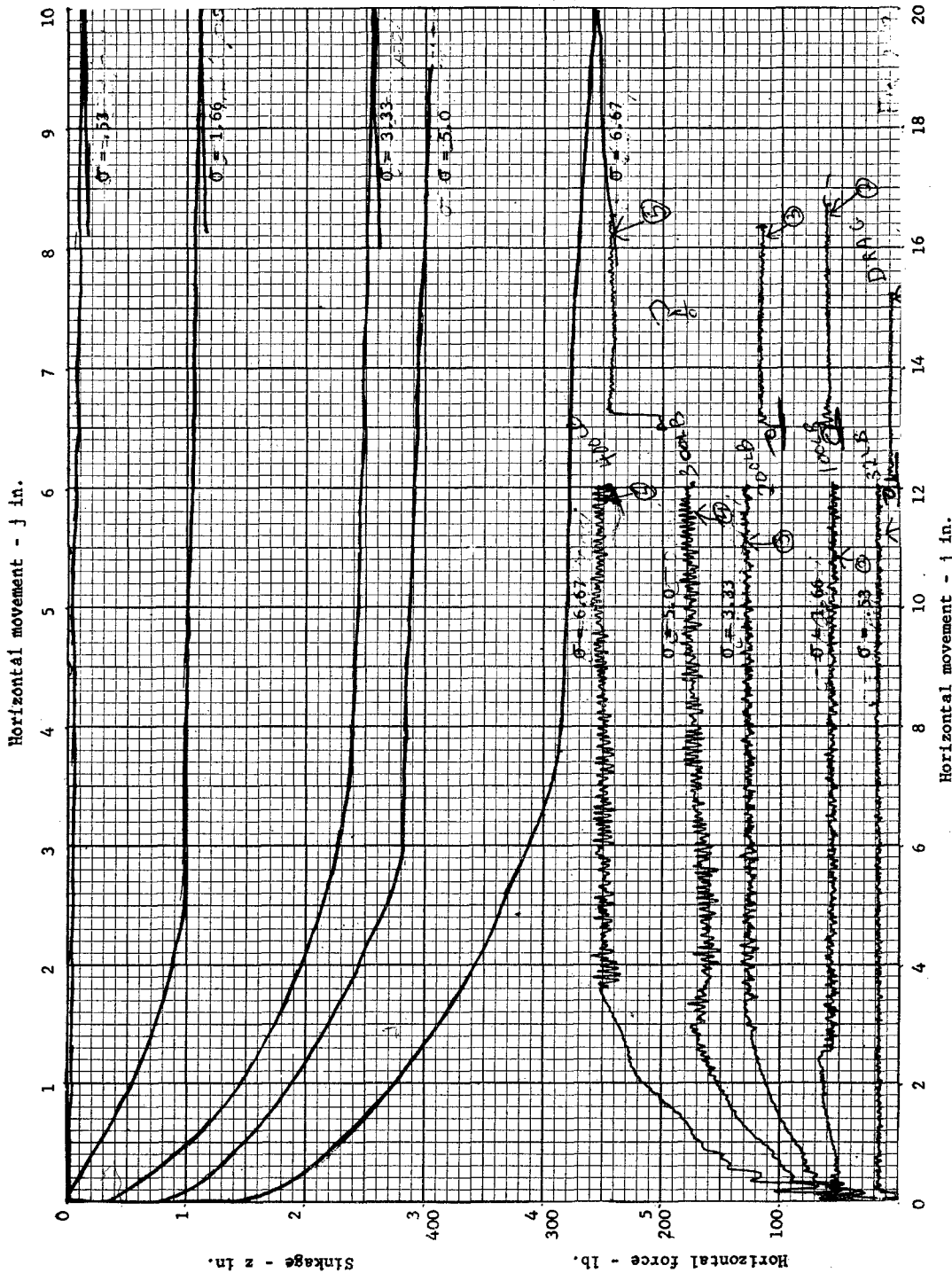
Fig.7.2.10. X-Y plotter traces showing horizontal force and slip sinkage against horizontal motion. 30" long by 2" wide shear plate covered with coarse sand-paper standing on a 60° 2" wide wooden prism covered with the same coarse sand-paper on all three sides.

217
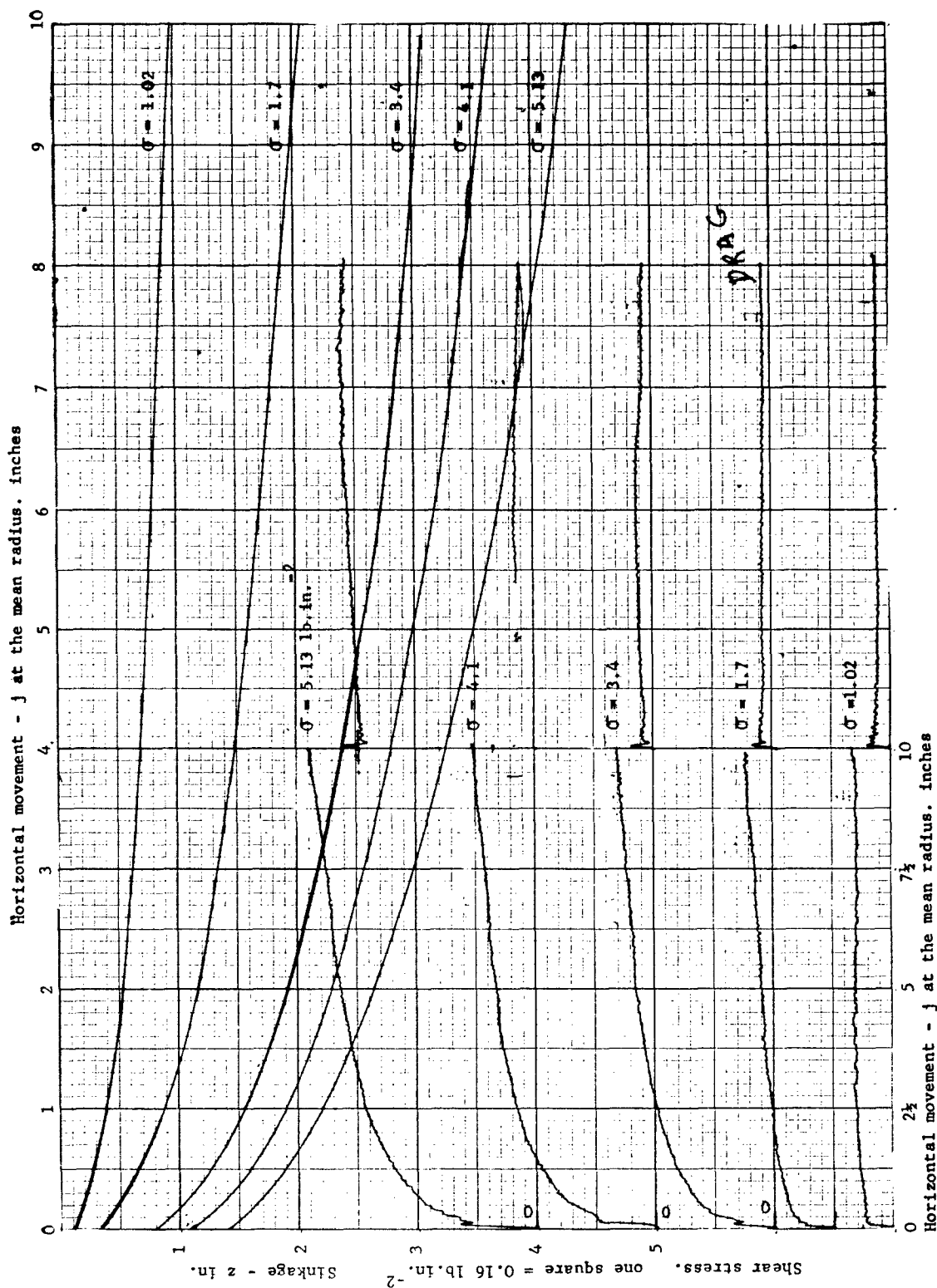
Fig.7.2.11. X-Y plotter traces showing shear stress force and slip sinkage against horizontal motion. Bevameter annular shear ring 7¼" o.dia. 5¼" i.dia. 19.5 in.² area. Mean radius 3.175 in. In dry sand.

218
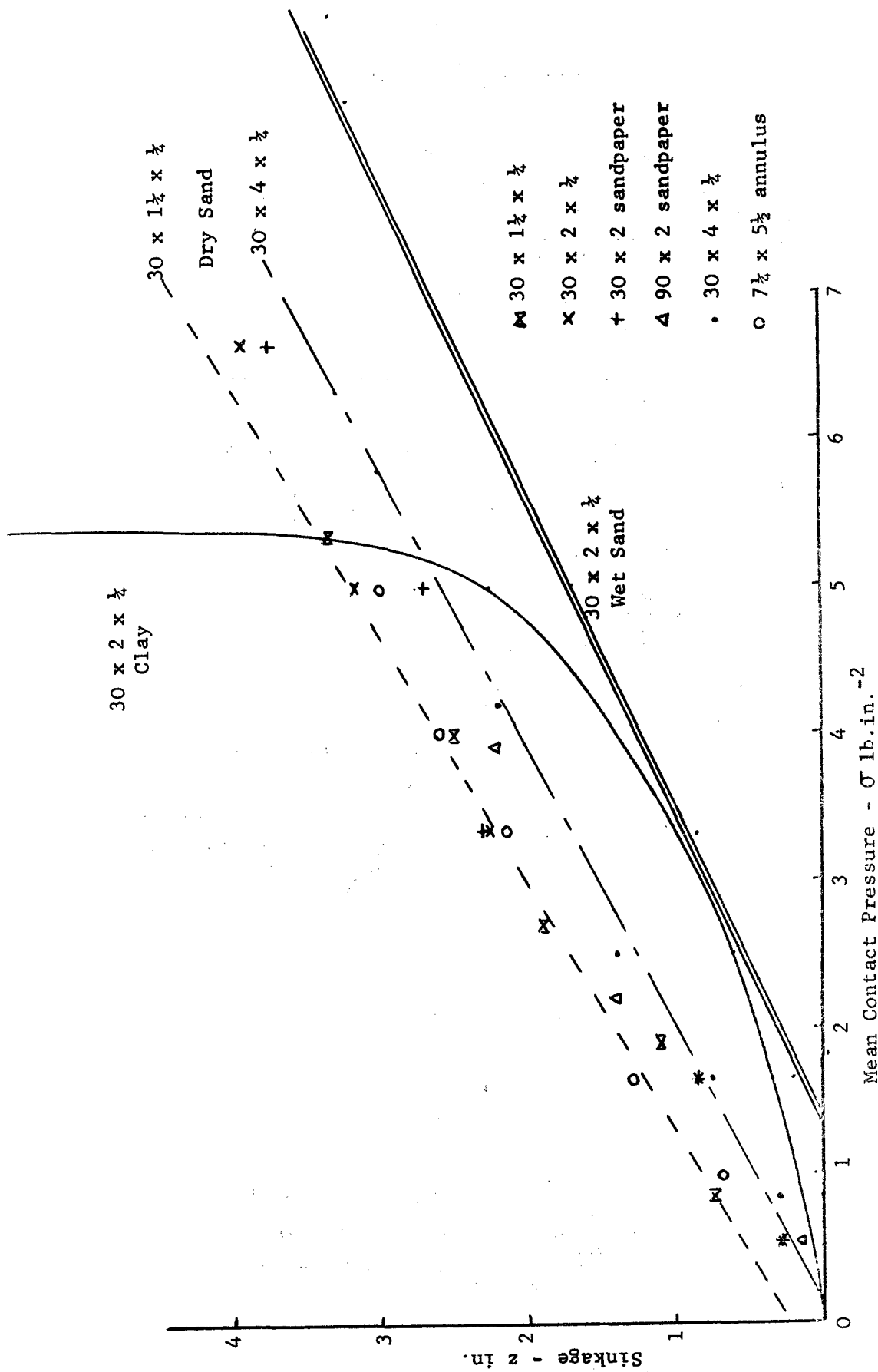
Fig. 7.2.12. Total sinkage after a horizontal movement of ¾ inches as a function of contact pressure for different shear plates in dry sand, wet sand and clay.
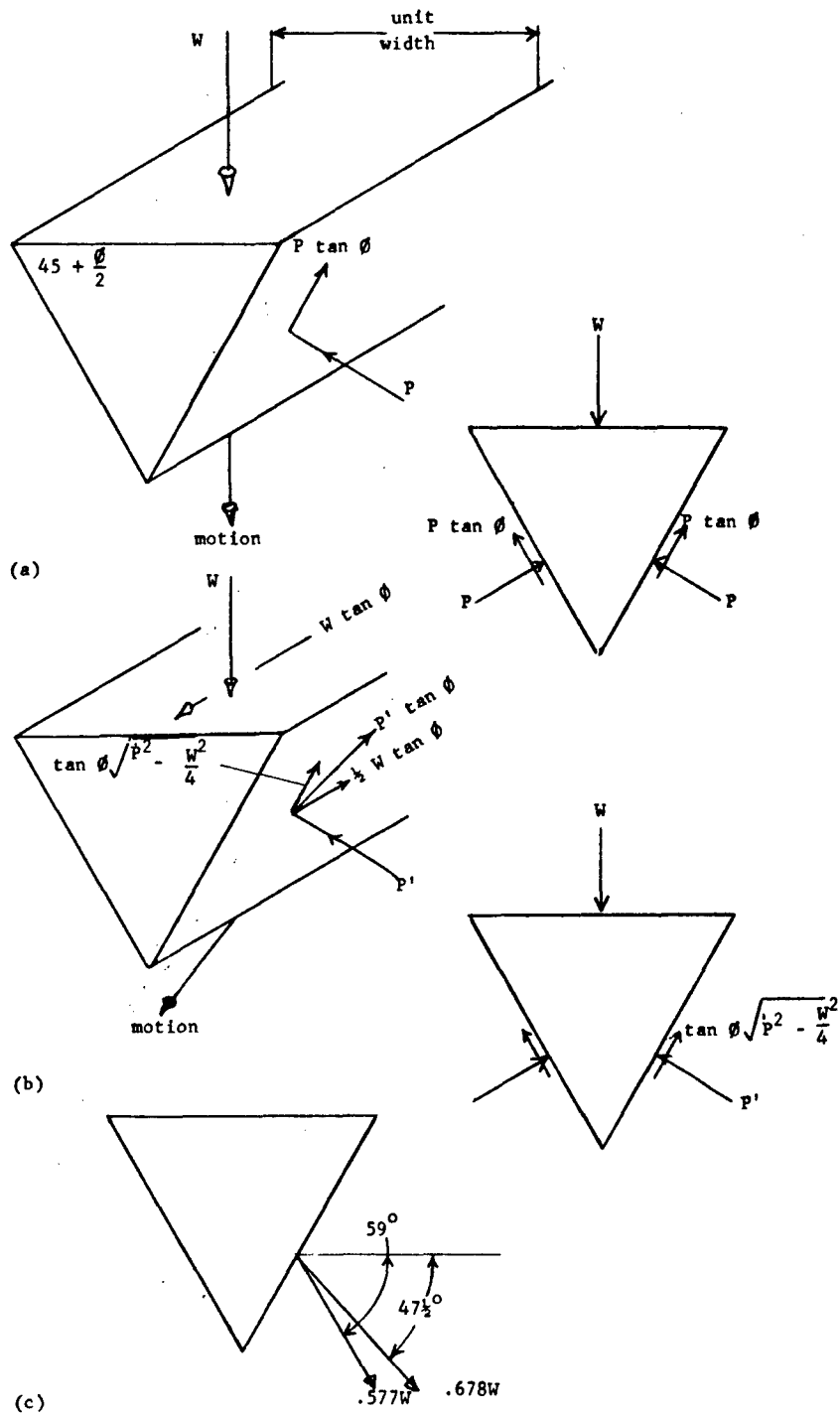
Fig.7.3.1. Forces acting upon the soil wedge beneath a unit length
of an infinitely long shear plate in sand. ($\emptyset = 30^{\circ}$, c = 0)
(a) Under vertical load W
(b) Under the same vertical load W plus the maximum
horizontal load W tan $\emptyset$
(c) Numerical value of the magnitude and direction of
the load applied to the soil

220
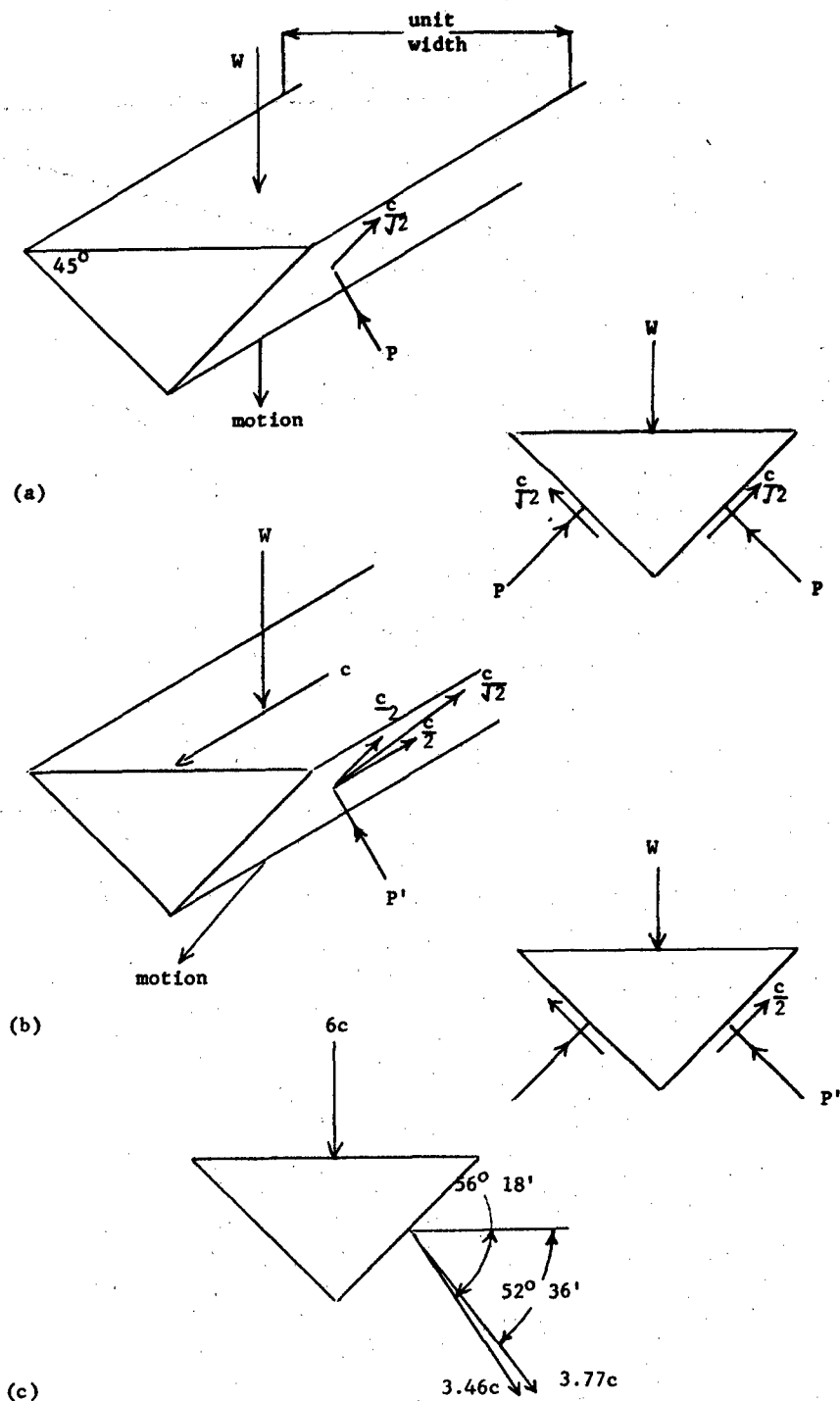
Fig.7.3.2. Forces acting upon the soil wedge beneath a unit length
of an infinitely long shear plate in clay ($\emptyset = 0$, $c = c$)
(a) Under vertical load W
(b) Under the same vertical load W plus the maximum
horizontal load c.
(c) Numerical value of the magnitude and direction of
the load applied to the soil.
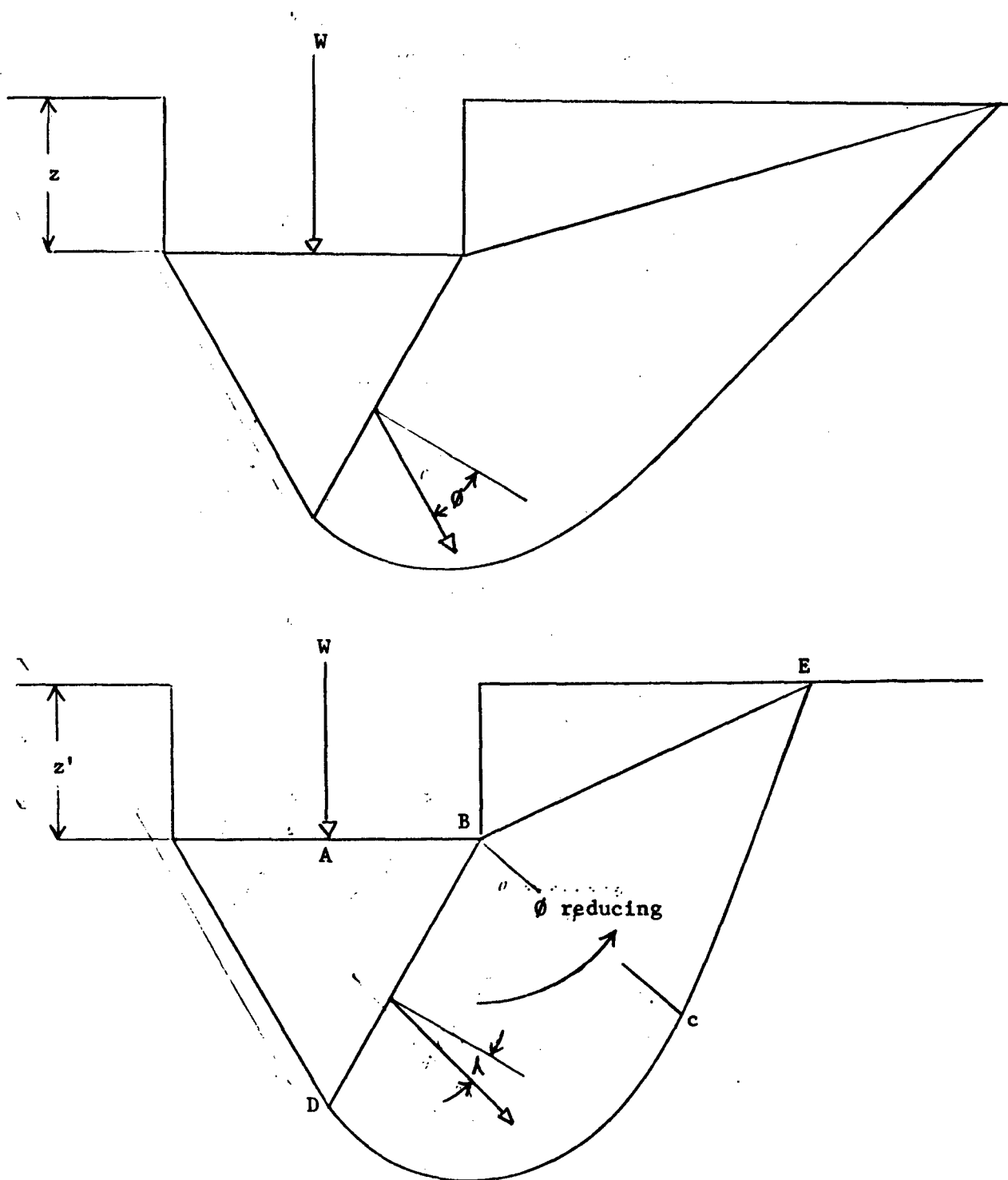
Fig.7.3.3. Failure mechanism to be used in proposed slip sinkage theory.
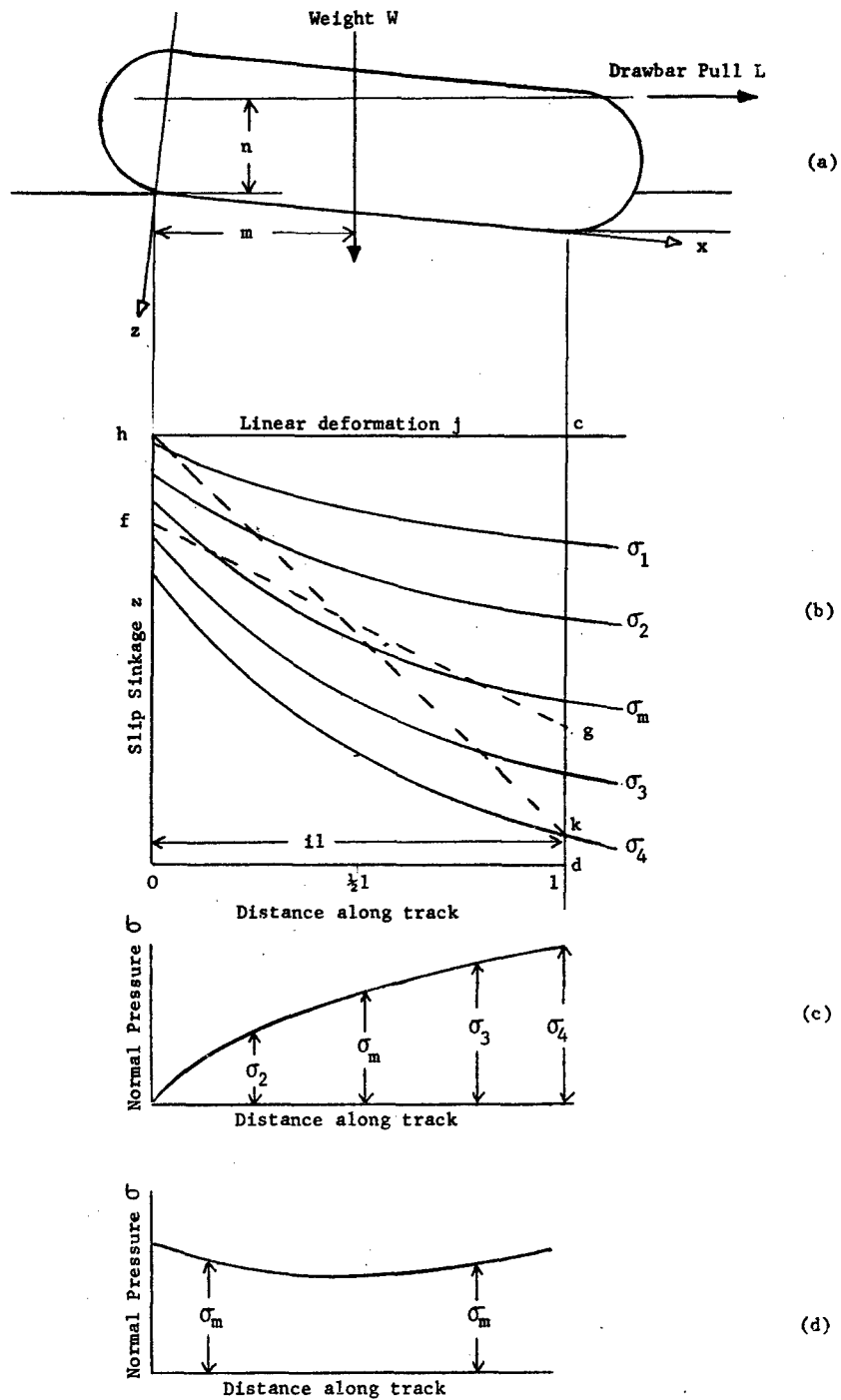
Fig.7.4.1. Prediction of slip sinkage and pressure distribution beneath a tracklayer.
    (a) Vehicle and axes.
    (b) Slip sinkage curves for infinite strips.
    (c) Pressure distribution with load transfer.
    (d) Pressure distribution with zero load transfer.

223

Horizontal deformation - j   in.

0   1   2   3   4

σ = .53

σ = 1.67

σ = 2.2

σ = 3.3

σ = 5

σ = 6.7
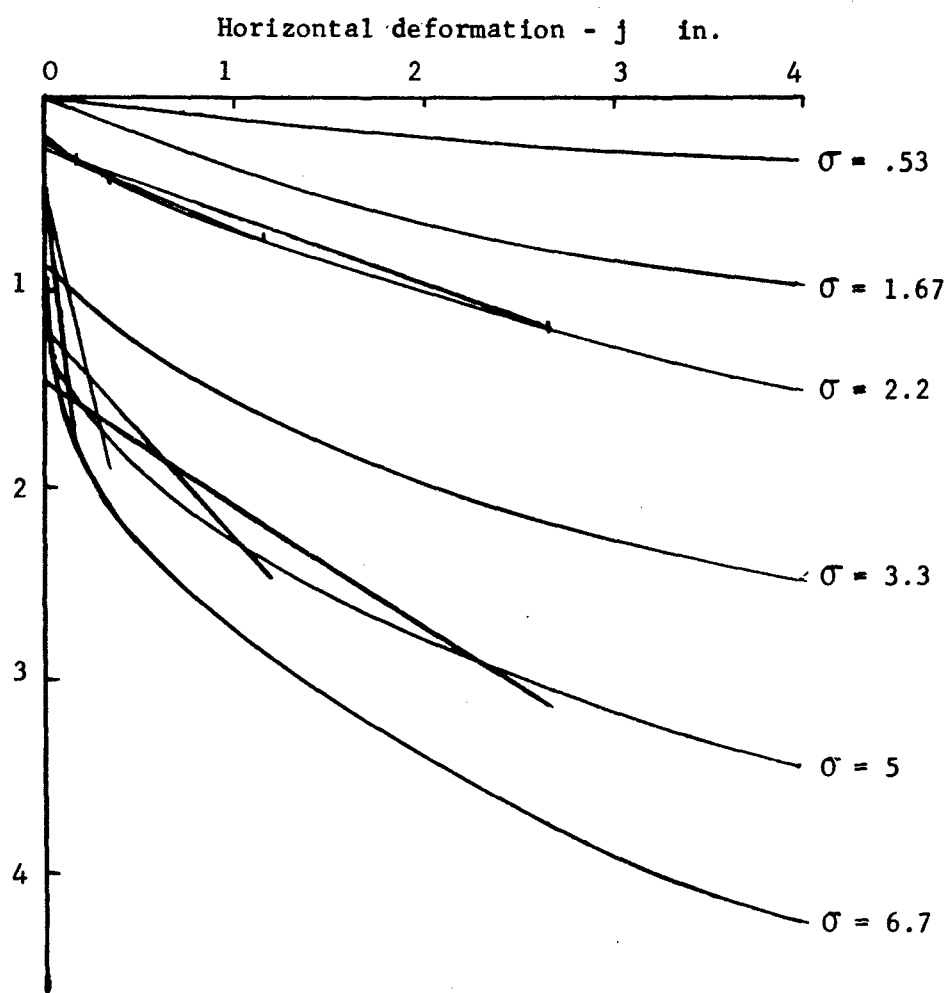
Fig.7.4.2. Slip sinkage curves for a 2 in. shear plate in dry
sand, with lines representing the predicted and
actual sinkages for the four tests of Fig.7.4.3.
The measured sinkages were close to those for a
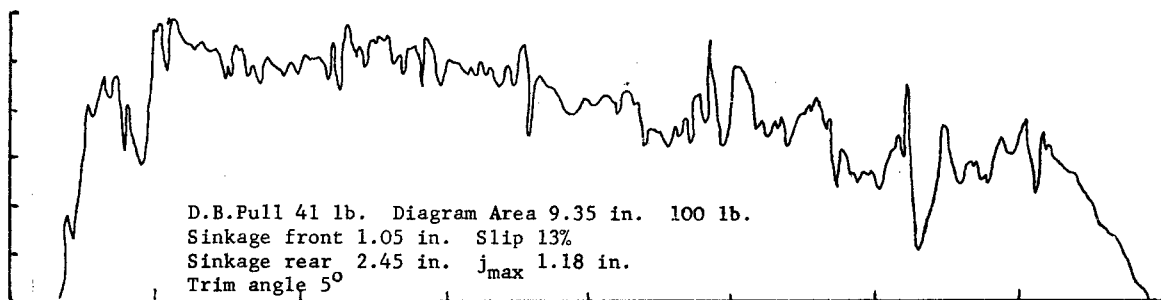contact pressure of 5 lb.in.$^{-2}$ whereas the actual
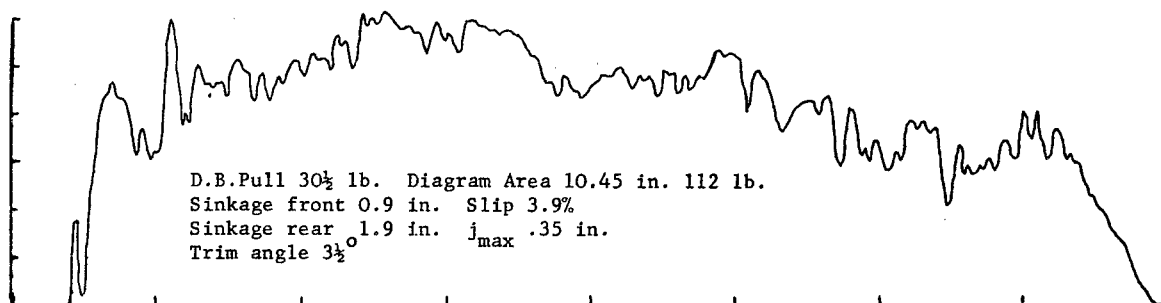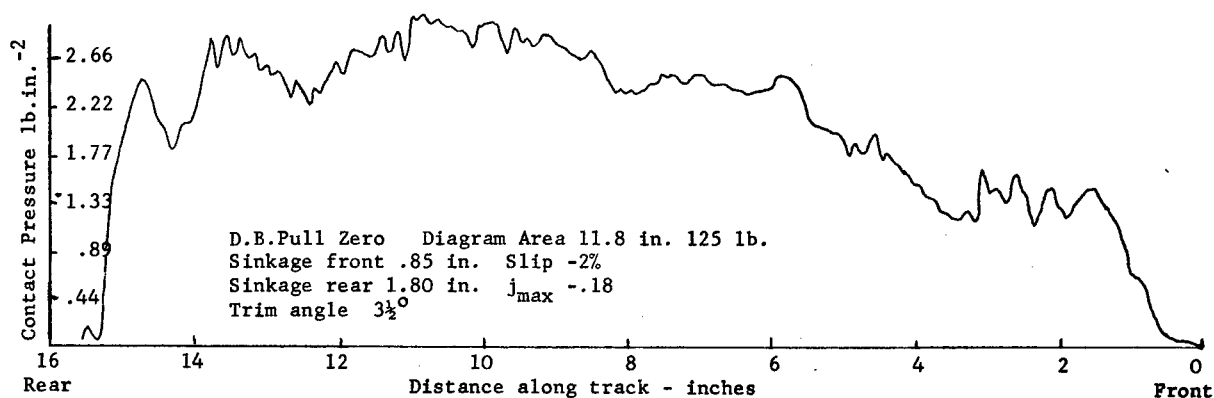mean pressure was 2.2 lb.in.$^{-2}$
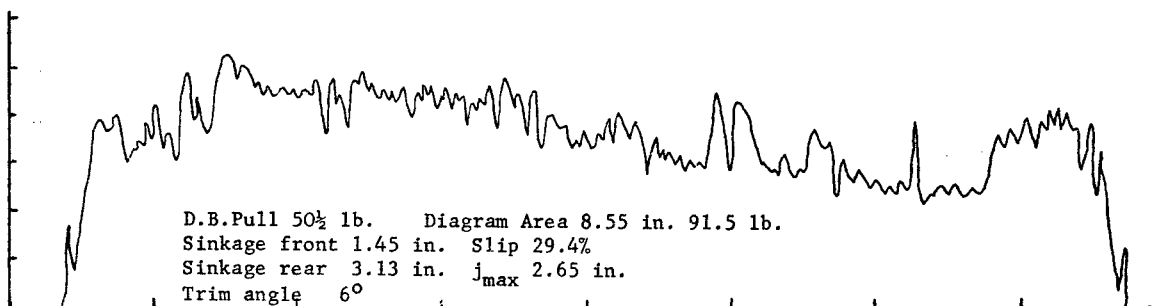
Fig.7.4.3. Pressure distribution records obtained from the track
link dynamometer and results of drawbar pull tests in
dry sand.   Vehicle weight 142 lb.

225

REFERENCES

1. Morin, A., Experiences sur le Tirage des Voitures. Paris, 1842.

2. Reynolds, O., 'On Rolling Friction', Phil. Trans. Royal Soc., London. Vol. 166, Part I. 1875.

3. Bernstein, R., "Probleme Zurexperimentellen Motorpflugmechanik", Der Motorwagen, Vol. 1G, 1913.

4. Gorlatchkin, B. P. (Collective Work), 'Theory and Development of Agricultural Machinery', Moscow, 1936.

5. Micklethwaite, E. W. E., 'Soil Mechanics in Relation to Fighting Vehicles', Military College of Science, Chertsey, 1944.

6. Evans, I., 'The Sinkage of Tracked Vehicles on Soft Ground', Journal of Terramechanics, Vol. 1, No. 2., 1964.

7. Uffelmann, F. L., 'The Performance of Rigid Cylindrical Wheels on Clay Soils', Proc. 1st International Conference, Soil Vehicle Mechanics, Turin, 1961.

8. Bekker, M. G., 'An Introduction to Research on Vehicle Mobility'. Part I, 'The Stability Problem'. Ordnance Tank Automotive-Command, Detroit Arsenal Report No. 22, May, 1957.

9. Bekker, M. G., 'The Theory of Land Locomotion (The Mechanics of Vehicle Mobility)', University of Michigan Press, Ann Arbor, 1956.

10. Bekker, M. G., 'Off the Road Locomotion', University of Michigan Press, Ann Arbor, 1960.

11. 'Trafficability of Soils', Technical Memorandum No. 3-240, and Supplements 1 to 15. U. S. Army Engineer Waterways Experiment Station, Vicksburg, Mississippi. 1947 to 1959.

12. Nuttall, C. J. and R. P. McGowan, 'Scale Models of Vehicles in Soils and Snows.', Proc. 1st International Conf., Soil Vehicle Mechanics, Turin, 1961.

13. Vincent, E. T., H. H. Hicks, E. I. Oktar, and D. K. Kapur, 'Rigid Wheel Studies by Means of Dimensional Analysis', Report No. 79, Army Tank-Automotive Center, Land Locomotion Laboratory, Warren, Michigan, 1963.

14. Reece, A. R. and B. M. D. Wills, 'An Investigation into Validity of Soft Sand Vehicle Mobility Theories', Fighting Vehicles Research and Development Establishment, Chobham, England, 1963. Report No. B. R. 175.

15. Wills, B.M.D., 'The Measurement of Soil Shear Strength and Deformation Moduli and a Comparison of the Actual and Theoretical Performance of a Family of Rigid Tracks', Journal of Agricultural Engineering Research, Vol. 8, No. 2, 1963.

16. Reece, A. R. and J. Adams, 'An Aspect of Tracklayer Performance', A.S.A.E., Paper No. 62-623. Winter Meeting, Chicago, 1962.

17. Rowe, P. W., 'Stress Dilatancy, Earth Pressures and Slopes', Journal of Soil Mechanics and Foundations Division A.S.C.E., May, 1963.

18. Roscoe, K. H., A. N. Schofield, and C. P. Wroth, 'On the Yielding of Soils', Geotechnique, 8.22., 1958.

19. Terzaghi, K., 'Theoretical Soil Mechanics', John Wiley, New York, 1956.

20. Meyerhof, G. G., 'The Ultimate Bearing Capacity of Foundations', Geotechnique, Vol. 2., pp 301-332, 1951.

21. Weiss, S. J., et al, 'Preliminary Study of Snow Values Related to Vehicle Performance'. Land Locomotion Research Laboratory, Detroit Arsenal, 1962.

22. Hanamoto, B., and E. Jebe, 'Size Effects in the Measurements of Soil Strength Parameters", Proc. 8th Conf. on the Design and Development of Experiments in Army Research Development and Testing, December, 1963.

23. Hegedus, E., 'A Preliminary Analysis of the Force System Acting on a Rigid Wheel', Report No. 74, Land Locomotion Laboratory, Detroit Arsenal, 1962.

24. Hanamoto, B. and Z. Janosi, 'Determination of k_c, k_ϕ, n Values by Means of Circular Footings, Modified Procedure', Land Locomotion Laboratory, Detroit Arsenal, Report No. 57, 1959.

25. Hanamoto, B. and Z. Janosi, "Prediction of 'WES Cone Index' by Means of a Stress-Strain Function of Soils", Report No. 46, 1959.

26. Payne, P.C.J., 'The Relationship Between the Mechanical Properties of Soil and the Performance of Simple Cultivation Implements', Journal of Agricultural Engineering Research, 1956. 1, 23-50.

27. Zelenin, A.N., 'Fizicheskie Osnovie Teoru Rezaniya Gruntow', (Basic Physics of the Theory of Soil Cutting). N.I.A.E. Translation.

28. Fountaine, E.R., 'Investigations into the Mechanism of Soil Adhesion', Journal of Soil Science, Vol. t, No. 2., 1954.

29. Fountaine, E.R., and P. C. J. Payne, 'The Mechanism of Scouring for Cultivation Implements', N.I.A.E., Technical Memorandum No. 16. 1954.

30. Meyerhof, G.G. 'The Bearing Capacity of Foundations Under Eccentric and Inclined Loads'. Proc.Third Int. Conf.Soil Mech.Found.Engr.Zurich 1953 Vol.1. 440-445.

31. Vandenberg, G.E. 'Triaxial Measurements of Shearing Strain and Compaction in Unsaturated Soil'. A.S.A.E. Winter Meeting 1962. Chicago. Paper No. 62-648.

32. Reed, I.F.'Measurement of Forces on Track-type Tractor Shoes'. Trans.Amer.Soc.Agric.Engrs. 1958, 1(1) 15.

33. Meyerhof, G.G. 'Discussion of Variation in Bearing Capacity Factors with Shape and Influence of Strength in Triaxial and Plane Strain Tests'. Proc.Fifth Int. Conf.Soil Mech.Found.Eng. Paris 1961 Vol.3. pp 193-194.

34. Kirkpatrick, W.M. 'The Condition of Failure for Sand'. Proc. 4th Int.Conf.Soil Mech.Found.Engr.1, 172, 1957.

35. Haythornthwaite, R.M. 'Stress and Strain in Soils'. Reprint from "plasticity" Pergamon Press.

36. Payne, P.C.J. 'Method of Measuring the Shear Strength of Topsoils'. J.Soil Science 1952 3 136-144.

37. Cohron, G.T. 'The Soil Sheargraph'. A.S.A.E. Paper No. 62-133 Washington Meeting June 1962.

38. Hafiz, M.A. 'Shear Strength of Sands and Gravel'. Ph.D. thesis London University 1950.

39. Rajput, M.A. 'The Shear Strength of Sands'. Unpublished M.Sc.thesis.Dept.Agric.Eng. University of Newcastle upon Tyne 1960.

40. Osman, M.S. 'The Mechanics of Soil Cutting Blades' Unpublished Ph.D. thesis. University of Newcastle upon Tyne 1964.

TECHNICAL REPORT DISTRIBUTION LIST

Title: Problems of Soil Vehicle Mechanics   Report No.
                                                    8470

Address	Copies
Director, Research and Engineering Directorate (SMOTA-R) 1	

Components Research and Development Laboratories
ATTN: Administrative Branch (SMOTA-RCA) 2

Components Research and Development Laboratories
ATTN: Materials Laboratory (SMOTA-RCM) 1

Systems Requirements and Concept Division
ATTN: Systems Simulations Branch (SMOTA-RRC). 1
ATTN: Systems Concept Branch (SMOTA-RRD) 1
ATTN: Economic Engineering Study Branch (SMOTA-RRE) 1
ATTN: Systems Requirements Branch (SMOTA-RRF) 1
ATTN: Foreign Technology Section (SMOTA-RTS.2). 1
ATTN: Technical Information Section (SMOTA-RTS) 2

Commanding General
U. S. Army Mobility Command
ATTN: AMSMO-RR 1
ATTN: AMSMO-RDC 1
ATTN: AMSMO-RDO 1
Warren, Michigan   48090

USACDC Liaison Office (SMOTA-LCDC) 2

Sheridan Project Office (AMCPM-SH-D) 1

U. S. Naval Civil Engineering
Research and Engineering Laboratory
Construction Battalion Center
Port Hueneme, California 1

Commanding Officer
Yuma Proving Ground
Yuma, Arizona 85364 1

Harry Diamond Laboratories
Technical Reports Group
Washington, D. C. 20025 1

Address	No. of Copies

Defense Documentation Center
Cameron Station
ATTN: TIPCA
Alexandria, Virginia 22314 20

Commanding General
Aberdeen Proving Ground
ATTN: Technical Library
Maryland 21005 2

Commanding General
Hq, U. S. Army Materiel Command
ATTN: AMCOR (TW). 1
ATTN: AMCOR (TB). 1
Department of the Army
Washington, D. C. 20025

Land Locomotion Laboratory 2

Propulsion Systems Laboratory 5

Fire Power Laboratory. 1

Track and Suspension Laboratory 6

Commanding General
U. S. Army Mobility Command
ATTN: AMCPM-M60
Warren, Michigan 48090. 3

Commanding General
Headquarters USARAL
APO 949
ATTN: ARAOD
Seattle, Washington 2

Commanding General
U. S. Army Aviation School
Office of the Librarian
ATTN: AASPI-L
Fort Rucker, Alabama 1

Plans Officer (Psychologist)
PP&A Div, G3, Hqs, USACDCEC
Fort Ord, California, 93941. 1

Commanding General
Hq, U. S. Army Materiel Command
Research Division
ATTN: Research and Development Directorate
Washington, D. C. 20025 1

Address	No. of Copies

Commandant
Ordnance School
Aberdeen Proving Ground, Md. 1

British Joint Service Mission
Ministry of Supply
P. O. Box 680
Benjamin Franklin Station
ATTN: Reports Officer
Washington, D. C. 2

Canadian Army Staff
2450 Massachusetts Avenue
Washington, D. C. 4

British Joint Service Mission
Ministry of Supply Staff
1800 K Street, N. W.
Washington, D. C. 6

Director
Waterways Experiment Station
Vicksburg, Mississippi 3

Unit X
Documents Expediting Project
Library of Congress
Washington, D. C.
   Stop 303 4

Exchange and Gift Division
Library of Congress
Washington, D. C. 20025. 1

Headquarters
Ordnance Weapons Command
Research & Development Division
Rock Island, Illinois
   Attn: ORDOW-TB. 2

Army Tank-Automotive Center
Canadian Liaison Office, SMOTA-LCAN. 4

United States Navy
Industrial College of the Armed Forces
Washington, D. C.
   Attn: Vice Deputy Commandant 10

Continental Army Command
Fort Monroe, Virginia 1

Address	No. of Copies

Dept. of National Defense
Dr. N. W. Morton
Scientific Advisor
Chief of General Staff
Army Headquarters
Ottawa, Ontario, Canada 1

Commanding Officer
Office of Ordnance Research
Box CM, Duke Station
Durham, North Carolina 3

Chief
Office of Naval Research
Washington, D. C. 1

Superintendent
U. S. Military Academy
West Point, New York
   Attn: Prof. of Ordnance 1

Superintendent
U. S. Naval Academy
Anapolis, Md. 1

Chief, Research Office
Mechanical Engineering Division
Quartermaster Research & Engineering Command
Natick, Massachusetts 1

AD
Accession No.
Components Research and Development Laboratories, U. S.
Army Tank-Automotive Center, Warren, Michigan
PROBLEMS OF SOIL VEHICLE MECHANICS by Alan R. Reece

Report No. 8470, March 1964, 225 pp., 10 tables, 85
figures Unclassified Report

The theory of soil vehicle mechanics is developed into a
more accurate tool for the design and evaluation of cross-
country vehicles. Several suggestions for improving the
basic soil mechanics are made, including a new sinkage
equation and a method for dealing with slip sinkage. It
is concluded that soil vehicle mechanics theory must be
based on the static equilibrium theory for incompressible
soils which is used in foundation engineering.